

March 2009

Diploma Thesis

Analyzing and Resolving Electric Power
Supply Quality Problems in Ship Electric
Grids due to Large Power Machine
Operation

Author: Panagiotis Mouzakis

Examination Board:

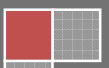
Prof. John Prousalidis (Assistant Professor)
(Supervisor)

Prof. Gerasimos Politis (Associate Professor)

Prof. Lambros Kaiktsis (Assistant Professor)



National Technical University of Athens
School of Naval Architecture and Marine Engineering
Athens, March 2009



This page has been left intentionally blank.

This page has been left intentionally blank.

Diploma Thesis

Dedicated to the scientists unfulfilled targets in all
over the world, the passion for creation
for the benefit of the community.

Diploma Thesis

Acknowledgements

*The following gratitude expressions can be expressed **in any order**:*

I would like to express my gratitude to **Prof. John Prousalidis** not only for his prompt offer to supervise my degree dissertation but also for his contribution to my attempt to express my passion as well as my creativity for marine electrical engineering. I would also like to thank him for his sustain to my effort to built up my skills in science and to tolerate the very tiring way I would like to work on.

I also think that I cannot express my gratitude in any sufficient good way to **Maran Gaz Maritime inc. (Angelicoussis Shipping Group)** for his prompt offer to give me whatever was need for the purposes of this degree dissertation. In detail, I would like to thank personally, **Dr. Stavros Hatzigrigoris, Steve Mavrakis and Stamatis Adrianou.**

I would like to express my thanks to **Prof. Gerasimos Politis** not only for his prompt offer to supervise my degree dissertation but also for his absolutely helpful notifications regarding propeller hydrodynamic behavior. The lack of his contribution would be sufficient to make the completion of this degree dissertation unachievable.

I think that I cannot express my gratitude in any sufficient good way to **Prof. Lambros Kaiktsis** for his uncountable valuable contribution to my studies in NTUA, for his offer to enter me to the wonderful world of science and research, to teach me the basic principles of research methodology, to give me the opportunity to get in touch with the magic world of fluids, to tolerate the very tiring way I would like to work on and for his prompt reply to supervise my degree dissertation.

I would also like to thank very much **Prof. Bill Zisis** for his uncountable valuable contribution to my studies in NTUA as well as for his very valuable advices for the rest of my life.

I would also like to thank very much **Prof. Christos Papadopoulos and Dr. Evangelos Boulougouris** for their contribution to my studies in NTUA, to my ship design project as well as to the limited research I have done so far.

Diploma Thesis

I would like to thank my parents (**Spyros and Stefany Mouzakis**) as well as my brother (**Odysseas Mouzakis**) for their invaluable help not only during my studies in NTUA but also for their unaccountable contribution throughout my life. I think that I cannot express my gratitude in any sufficient good way. I thank them so much.

Last but not least, I would like to thank the **School of Naval Architecture and Marine Engineering** and **NTUA** in general for their sustain to my effort to express my love as well as my passion for creativity and to built up my skills regarding research and science in general. In addition, I thank them very much for their prompt reply to recognize the possible value of my efforts throughout my studies in NTUA by giving me prizes and awards.

Diploma Thesis

Table of Contents

Acknowledgements	5
Table of Contents	71
Contents of Current Thesis	9
Chapter01 (All Electric Ship – The State of the Art)	11
All Electric Ship Research	12
All Electric Ship: a Clean and Environmentally – Friendly Vessel	13
All Electric Ship : a Safe Vessel	13
All Electric Ship : an Efficient Vessel.....	14
All Electric Ship : Electric Power Supply Quality Problems in ship grids due to extensive electrification	15
Chapter02 (Bow Thruster driven by Squirrel Cage Asynchronous Motor)	16
Introduction	17
Thruster Electric Asynchronous Motor Starting Up	19
Starting-Up of Thrusters driven by Induction Motors.....	26
Relevant Standards	27
Approximation of Bow Thruster Propeller Torque Variance During Pitch Ratio Change	32
Case Studies	36
Conclusions	81
Chapter03 (Bow Thruster driven by Wound Rotor Asynchronous Motor)	82
Introduction & Study Cases A,B	83
Data Representation	86
Further Approximation Case Study C.....	96
Conclusions/Comments	102
Chapter04 (Podded Propulsors driven by Electric Motors)	104
Introduction	105
Pod Propulsion and Characteristics	106
Failure Statistics	108
Hydrodynamic Considerations	110
Pod Hydrodynamic Behavior during Turning Maneuvers (Cases A,B,C,D,E,F)	112
Conclusions	134

Diploma Thesis

Chapter05 (Short Circuits)	135
Introduction	136
Data Tables and Graphs	137
Conclusions	148
Chapter06 (Dynamic Response Full Generator Model: Approximation Formula)	150
Voltage and Speed Response System Approximation Analysis	151
Steam Generator Response Approximation	154
Diesel Generator Response Approximation	155
Steam Generator Response Approximations Graphs and Steam System Stability.....	156
Diesel Generator Response Approximations Graphs and Steam System Stability	162
Steam System Further Investigation	168
Conclusions.....	172
Future Possible Issues	173
Appendix A (Paper: “On Studying the Power Quality problems due to Thruster Start-ups”)	175
Appendix B (Technical Manuals)	177
Appendix C (LNG on Board Inspection Pictures)	193
Appendix D (Typical Diesel Engine Configuration)	196
Appendix E (Typical Steam engine Configuration)	198
Appendix F (Typical Pod Configuration)	200
Appendix G (Typical Short circuit Configuration)	202
Appendix H (Typical Diesel / Steam Approximation Configuration)	204
Bibliography	206

Diploma Thesis

Contents of the current thesis:

This dissertation involves a multi-scale investigation on electric power quality problems, large power thruster starting-up methods, electric motors driving podded propulsors, electric power system behavior in short circuits as well as steam and diesel generator system response approximation methods. For these purposes, a Ro-Ro passenger ferry, as well as a LNG vessel was examined.

The simulation results do not concern only voltage and frequency variations, but also the entire examined system transient response, i.e. not only the electric power motor contribution to the examined phenomenon but also the contribution of the generator, the exciter, the speed governor as well as the steam turbine or diesel engine (it depends on the examined study case).

In **chapter01**, a short but coherent review of the most important technical advantages and great difficulties regarding the forthcoming AES vessels has been done.

In **chapter02**, the case of bow thruster system driven by an asynchronous AC motor of squirrel cage type and the use of controllable pitch propeller are presented. In detail, numerous starting up methods have been investigated on bow thruster motor, taking into consideration its effect on vessel power grid, making in this way more clear the need for rules and regulations. In this case, the study of the interaction between the motor and the two steam generators is also included, providing significant conclusive points regarding the system stability as well as the finite power capability system response.

In **chapter03**, the case of a bow thruster system driven by an asynchronous AC motor with wound rotor, rather than a squirrel cage is presented power in the cases of ideal electric power source and diesel generator. These simulations also include the use of fixed and controllable pitch propeller. However, two of the three main simulation cases refer to hypothetical scenarios.

In **chapter04** an initial but very promising approach of the pods behavior from the electric power point of view during three different types of maneuvering has been done. This approach also concerns the use of two different types of motor (synchronous and asynchronous machine), making in this way more clear the fact that the choice of the optimum type of motor for this case is of great importance.

Diploma Thesis

In **chapter05**, the system response under short circuit condition is investigated. In detail, this limited approach reveals the cases in which during the fault application the bow thruster due to its pre-fault rotating condition can act as electric power source helping in this way the whole system to recover sooner. The examined scenarios contain three different kind of faults as well as two different types of loading conditions.

In **chapter06**, it is attempted successfully that the steam and diesel system response are approximated for specific type of loading (step loading) by the use of second order transfer function.

In **APPENDIX A** an academic paper by Prof. John Prousalidis and Panagiotis Mouzakis, mainly summarizing chapter 02 is presented, regarding large electric motor starting up processes, their impact on the electrical grid and power supply quality problems.

In **APPENDIX B** the technical manuals of the most important electric devices are presented.

In **APPENDIX C** photos of the onboard inspection on the LNG examined vessel are presented.

In **APPENDIX D** a typical diesel engine configuration is presented.

In **APPENDIX E** a typical steam engine configuration is presented.

In **APPENDIX F** a typical pod configuration is presented.

In **APPENDIX G** a typical short circuit configuration is presented.

In **APPENDIX H** a typical Diesel/Steam approximation configuration is presented.

In **BIBLIOGRAPHY** there are referred all the used bibliographical resources thank to them the present diploma thesis has been achieved.

CHAPTER 01

All Electric Ship – The State of the Art

All Electric Ship Research

The AES concept exemplifies the rapidly increasing trend in the marine industry to move from mechanical to electrical systems. This is motivated by the additional flexibility that such systems offer. More specifically, propulsion systems comprise electric motors driven by associated power electronic converters, acting as their gear boxes. This combination results in several advantages as increased manoeuvrability, precise and smooth speed control, reduced machinery space, low noise and pollutant emission levels. Furthermore, AES results in savings in running and maintenance costs. In addition, in podded propulsion schemes (in which the propeller and its driving electric motor are both located in a compact unit underneath the vessel's hull), the vessel's shaft system is completely eliminated. In AES, considering that all sub-systems are controlled via electronic control units, an overall control centre can be established, offering increased Monitoring and Control capabilities. This function is enabled by a central electric Power Management System (PMS), often referred to as Electric Power Management And Control System (EPMACS). Thus, the manufacturers of the electric power system (or even of key components) become the "system integrators" for the entire vessel. As a consequence of the development of ship design concepts, marine electrical networks are becoming very different from those previously encountered ashore or aboard. In the framework of AES design, the power generation units (marine Diesel engines, gas turbines and possibly fuel cells in the future), optimized to operate for maximum fuel economy and minimum pollutant emissions, are still crucial for the overall propulsion efficiency.

The advantages offered by AES, i.e. a **clean, safe and efficient** means of waterborne transportation, as discussed subsequently.

AES: a Clean and Environmentally-friendly Vessel

The marine Diesel engines, currently used in most vessels for both propulsion and electric power generation, are exploited in AES only as prime movers in generator sets. In AES applications, due to the larger electric power demand, generator sets are characterized by increased size and power output, compared to those of traditional vessels. In the AES approach, significant progress in terms of reduced fuel consumption and pollutant emissions of Diesel engines can be realized by operating them at optimum steady-state conditions. The approach is particularly interesting for closed seas, where transients correspond to a significant part of the ship operation. As all machinery is electrical, the total electric load can be managed and controlled in an easier and more effective manner via the Electric Power Management And Control System (EPMACS).

AES: a Safe Vessel

AES is an inherently safe vessel due to:

- Increased vessel survivability with multiple energy supplying scenarios, especially for critical loads, e.g. propulsion motors in conjunction with a central Power Management System.
- Increased flexibility in managing power redundancy (optimum exploitation of synchronized generators sharing their energy between the propulsion and the auxiliary systems).
- Increased reliability of equipment (electrical/electronic components have high reliability indices, higher than any other mechanical equivalent device).
- Increased manoeuvrability (resulting in lower collision probability) due to either installed pod propulsion systems or thruster systems, both allowing for a 0°-360° of vessel manoeuvring, resulting in shorter response times. The decrease in accidents also corresponds to reduced environmental pollution.

AES: an Efficient Vessel

The AES concept offers several advantages in terms of construction and maintenance:

- The initial building cost of an AES is comparable to that of conventional ships, provided that electric propulsion has been selected from the early pre-design stage. In this case, the increased expenses due to the cost of electronic components are compensated by savings in steel and building man-hours (resulting from reduced machinery space requirements).
- In comparison to conventional designs, AES is characterized by lower maintenance costs, owing to extensive use of non-rotating electrical equipment. Furthermore, the entire power system becomes modular, which enables reduced maintenance times and costs.
- The AES is characterized by lower operational costs (lower fuel consumption, lower lubrication oil demands, reduced personnel for operation due to increased automation). Furthermore, due to its environmentally friendly character, AES is expected to be subject to smaller penalties and fees.
- The AES can be overall faster than conventional ships due to smaller size and the increased flexibility in hull design. Savings can also be achieved by increased manoeuvrability capabilities (e.g. decrease in sailing tugs costs).

Currently, electric propulsion is applied mainly in the several ships such as: cruise vessels, ferries, dynamically positioned (DP) drilling vessels, thruster assisted moored floating production facilities, shuttle tankers, cable layers, pipe layers, icebreakers and other ice going vessels, supply vessels. There is also a significant on-going research and evaluation of using electric propulsion in new vessel designs for existing and new application areas. An important candidate is the recently developed sector of Liquefied Natural Gas (LNG) carriers, currently comprising a fleet of approximately 300 vessels, driven by steam power plants.

Electric Power Supply quality problems in ship grids due to extensive electrification

One of the challenges emerged and have to be faced consists in the electric power supply quality problems due to the extensive electrification. These Power Quality problems comprise among others the following:

- Strong interference among large power electric loads installed aboard,
- power electronic device operation and harmonic distortion,
- problems during electrification of large power electric loads (e.g. motor starting-up)
- voltage disturbances (dips, swells, transients and spikes) in the entire electric network

On the other hand, the status of standards and rules is not sufficient at all especially in the cases of transients during starting-up of large power electric motors such as those of maneuvering thrusters or main propulsion.

This dissertation mainly deals in depth with investigating power quality problems provoked by either the operation in transient starting-stage of large power maneuvering thruster motor drives or in the maneuvering-state of pod propulsion systems driven by electric motors. Moreover, an effort is made to offer solutions and recommendations in the standardization domain.

CHAPTER 02

Bow Thruster driven by Squirrel Cage Asynchronous Motor

Diploma Thesis

Bow Thrusters Starting Up Procedures – Problems and Difficulties

I. Introduction

The last two decades, auxiliary propulsion systems (well known as thrusters) have been installed in the aft or stern part of various ship types improving their maneuverability and collision avoidance capabilities. Nowadays, bow thrusters are the most preferable kind of thrusters, while it is a common practice that rotation is provided by an electric motor. In most cases this demand is covered by an asynchronous alternative current motor.

The required power of bow thruster motor varies between (0.5-2.5) MW which increases considerably the electric power demands that the electric power generation set has to meet. In addition, the application of this huge electric load often encounters great difficulties especially on starting up condition when the system is not only forced to cover the motor steady states needs but also to meet its requirements regarding a transient “inrush current” of high values (varying, in general, between 4-7 times the rated current [1-3]). Consecutively, during the inrush phenomenon (i.e. for approximately up to 15-20 s after its time zero) the thruster motor power demands in terms of active and reactive power are high, too. During this procedure, the power factor is fairly low, which means that the reactive power demands are greater than those in steady-state operating condition.

This high energy demand, in most cases, cannot be easily covered by the vessels electric power system leading to generator overloading or even tripping. Furthermore, these large transient inrush currents are accompanied by large voltage drops introducing “symmetrical” voltage dips to all three phases. In the case of bow thrusters applications, this large power load is located far away from the vessels engine room so that the intervention of cables impedance cannot be avoided leading to further voltage dips to all three phases. All these factors according to both simulations and experimental data- increase the difficulty of motor starting up, especially in the case of repetitive operation of thruster motor.

In most large scale applications, the thruster propeller is a controllable pitch one and during starting-up the blade pitch is set to 0^0 in order to minimize the electric power demands. In this way, it is ensured that blades are closed during starting up, reducing the polar inertia moment of the propeller down to the minimum possible value. Still, the resultant total inertia moment of the rotating masses is considerable worsening even more the starting up procedure.

Diploma Thesis

These starting up difficulties stress even more the importance of voltage and frequency drop during this procedure. Coming back to this case, the actual ship maneuvering operating mode begins by varying the thruster's blade angle, as soon as the starting-up transients of the driving electric have decayed. Still considering the possible behavior of the thruster unit during maneuvering, the variations in the propeller's pitch can result to significant power fluctuations in the power demands. Therefore, it can be argued that the thruster unit operation resembles that of a pulsed load, a load that has large power demand for a very short interval followed by small power demand for fairly longer intervals. However, the existing standards regarding modulation concern only voltage and frequency fluctuations.

II. Thruster Electric Asynchronous Motor Starting Up

It is well known that there are two different types of asynchronous motors, the squirrel cage and the wound rotor ones. The main difference between these types of motor are the rotor resistance (variable or not) and, hence, the motor performance during starting-up and steady-state condition. The motor behavior strictly depends on the rotor resistance as described in the chapter dealing with asynchronous motor architecture and technical characteristics.

The figures below indicate the starting up procedure of an asynchronous motor for a range of different starting up procedures.

i) D.O.L operation

This method can be proved as very harmful for entire electric system due to the high transient inrush current on starting up. Eventually the speed is growing up until it reaches its nominal speed. Due to the adverse transient phenomena, DOL starting up cannot be applied for motors above 3kW. Transient inrush current is due to low impedance of the motor during its starting up and mainly due to the slip rotor resistance.

Eventually, as speed grows-up close to its nominal value, slip decreases and hence total motor impedance increases to its steady state value. Moreover, it can be observed that during the high value current, a voltage dip occurs in the electric system of approximately 20% of the nominal value.

An improved version of the DOL method is the “Wye/Delta” (Y/D) starter. According to this method, initially the motor windings are connected in wye-connection resulting in smaller currents –but lower electromagnetic torque too, while as soon as steady-state speed has been reached, the winding connection changes into delta. It is worth noting that neither the Y/D starter is easily applicable to high power motors.

ii) Starting up via autotransformer

The motor starts via the intervention of an autotransformer connected in series to the motor. The autotransformer has a tap changer in order to change each time its transforming ratio.

On starting up, the motor which is connected to the secondary side of the autotransformer is supplied by high current and low voltage. In this case due to motors low impedance and high rotors slip a voltage dip is observed at motor bus-bar. The problem worsens even further due to low voltage level. According to this method, the transforming ratio tends to unity, when the motor reaches its nominal speed by changing its tap changer.

Anyhow, the main problem of this approach is that the high-valued starting current entails a large voltage drop at the autotransformer impedance, worsening even further the voltage dip problem, which, in turn, delays even longer the motor to reach steady-state. Thus, for the same motor as before, starting-up time has increased by 450% compared to DOL. However, the required time duration for the motor to reach its nominal speed strictly depends on the change rate of transforming ratio.

iii) Starting up via autotransformer and capacitor

The problems by using autotransformers can be overcome by using autotransformers along with capacitors. A capacitor acts as a reactive power source. It is recommended that the capacitor rating is approximately 30% of the motor rated power. Anyway, steady-state condition is reached almost at the same time as by using Direct on Line Operation.

It is worth noting that when steady-state is reached, towards 12s, a current spike is observed in current waveform due to autotransformer tap changing, see (Waveform Group 1).

However, this solution is not appealing in terms of both cost and space requirements considering the two auxiliary components (autotransformer and capacitor) needed only during the critical period of starting-up.

It is worth noting that the large power capacitor installed can provoke other fast electromagnetic transients during switching on and off, endangering the whole equipment. More specifically, during circuit breaker making, a capacitor absorbs large high frequency inrush

Diploma Thesis

currents while during breaking voltage escalation problems with multiple circuit breaker restriking can occur.

iv) Soft starting via power electronic devices

This method is based on soft starters and power converters. The voltage which is applied to the motor input varies from the initial value V_0 and the rated voltage value. The progressively increasing voltage level at the input of the motor manages to achieve low inrush current accompanied by long time duration in order to reach its nominal speed. On the other hand this method is not noisy and characterized by small space requirements. However, these devices are pretty costly, especially in the case of high power applications.

v) AVR (Automatic Voltage Regulator) soft starting

This method is based on progressively increasing the output voltage of the generator by changing its excitation current value. This proportional increment of its voltage value is controlled by an AVR system. The supplying generator with the controllable AVR must be dedicated, i.e. a standalone gen-set feeding only the motor.

AVR's are more advantageous compared to:

- a) AVR devices concern only the output power from the generator and not the input power to the load.
- b) Before any installation, a demagnetization procedure must be done first in order to eliminate any remanence flux in the air gap, which is able to spoil the initialization of the AVR.
- c) By using AVR soft starting system the input power to the motor does not contain any pollutant power harmonics.
- d) The generator RMS terminal voltage can be set during the motor start up by the following mathematical form.

Diploma Thesis

$$V_{RMS}=V_0, \text{ if } t<0$$

$$V_{RMS}= V_0+k_v t, t>0$$

Where:

T: motor starting up term

k_v : voltage gradient

V_0 : initial rms terminal voltage

It is quite common that the initial terminal RMS voltage is approximately 30.0% of the rated voltage level.

To sum up, the AVR soft starting method can be equally if not more technically advantageous rather than other methods due to i) nor noisy characteristics ii)small space requirements iii)safe operation iv) low cost

The table1 as well as the figures1-7 summarize the results from the previous applications.

Soft-Starting Data Summarizing Index						
	DOL	Autotransformer	Autotr.+Capacitors 375KVAR	AVR $K_v=5e-3$	AVR $K_v=3.5e-3$	AVR $K_v=2e-3$
Qgen[MVAr]	0.93	0.53	0.41	0.57	0.54	0.51
Pgen[MW]	0.81	0.35	0.30	0.55	0.48	0.50
Power Factor [-]	0.66	0.55	0.59	0.69	0.66	0.70
Voltage Dip[p.u]	0.43	0.22	0.12	-	-	-
Starting Time [sec]	4.50	46.00	11.00	32.50	43.00	81.00
Starting Current [p.u]	2.23	1.43	1.54	1.25	1.22	1.19
Thermal Energy in Motor Airgap [MJ]	0.014	0.770	0.058	0.382	0.654	1.700

Table 1

Diploma Thesis

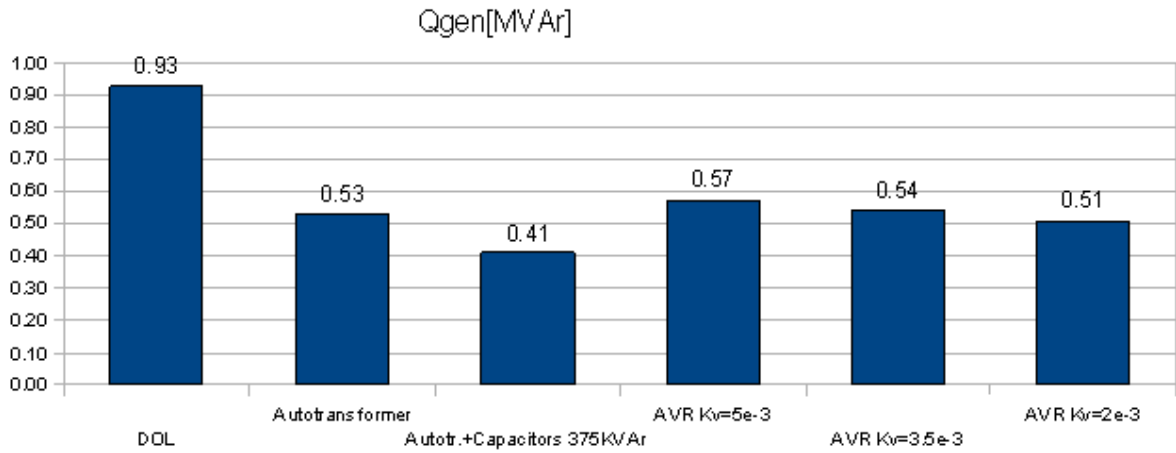


Figure 1

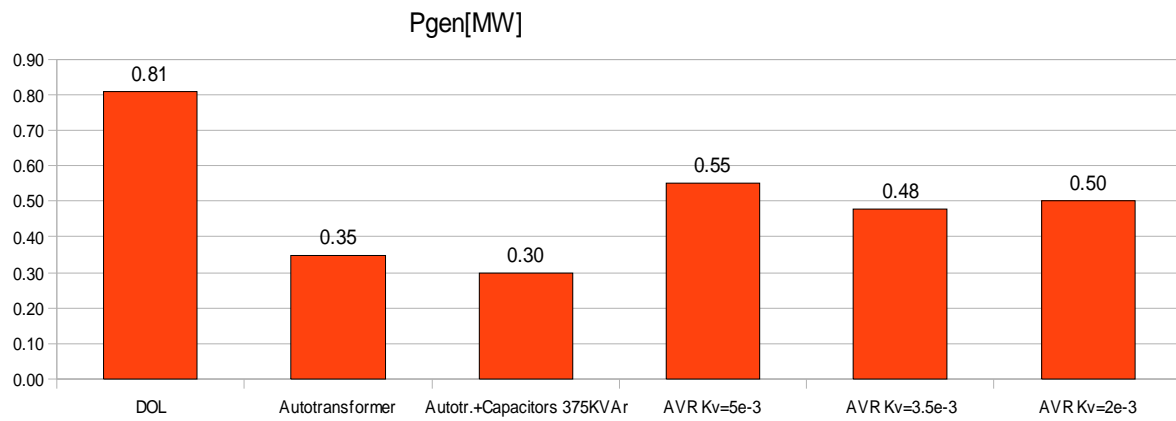


Figure 2

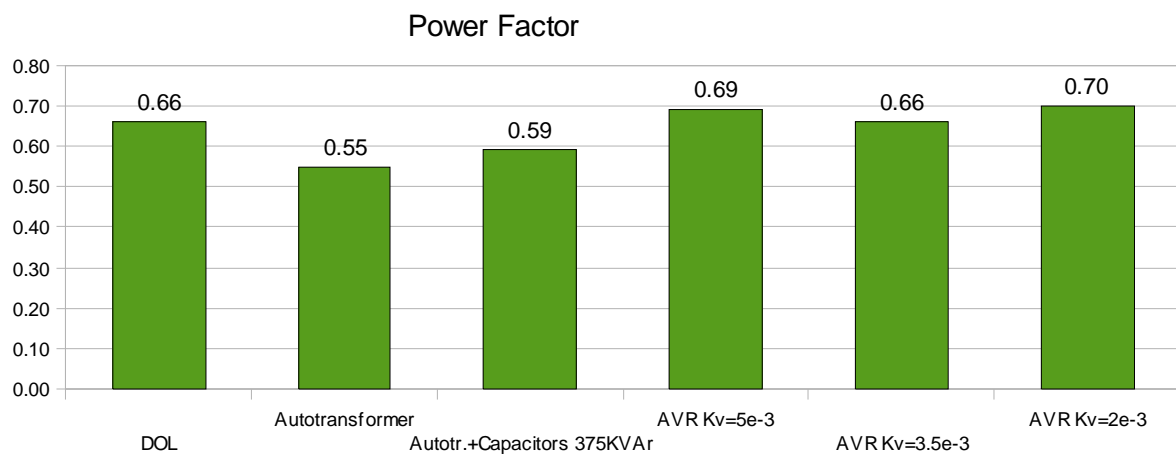


Figure 3

Diploma Thesis

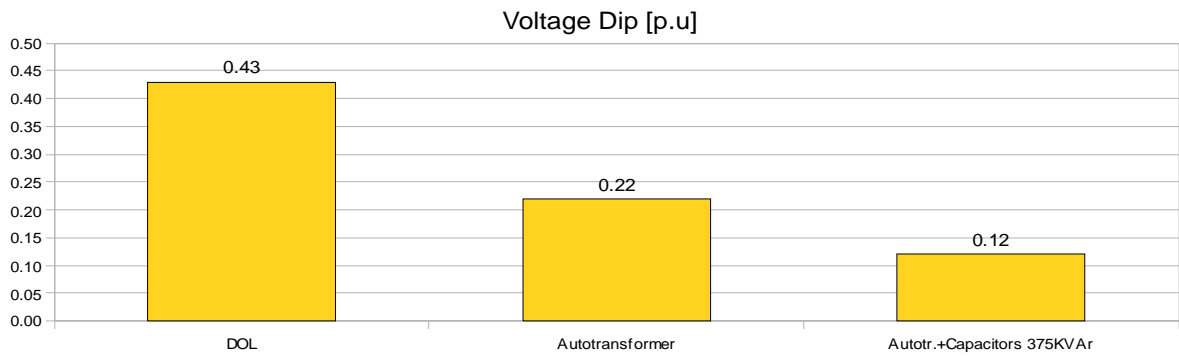


Figure 4

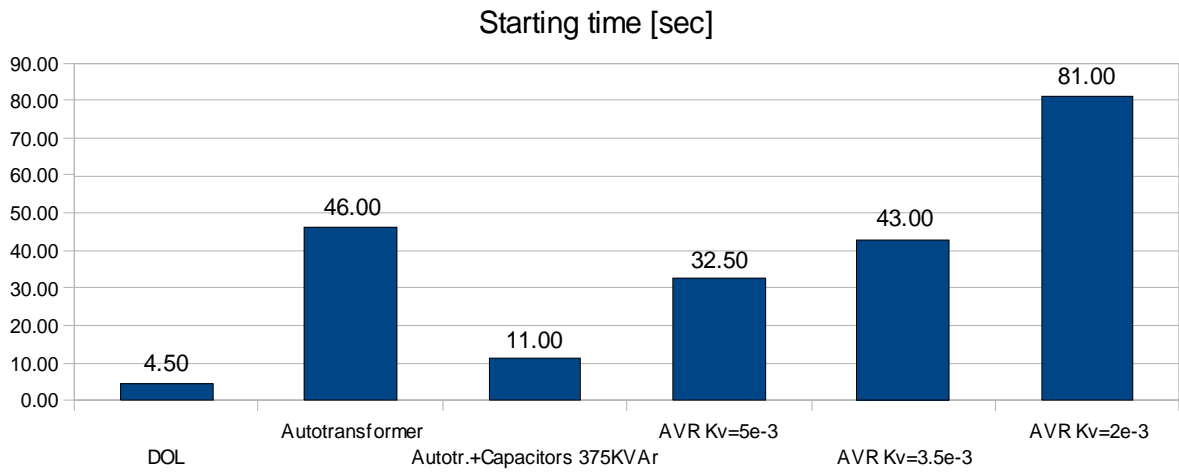


Figure 5

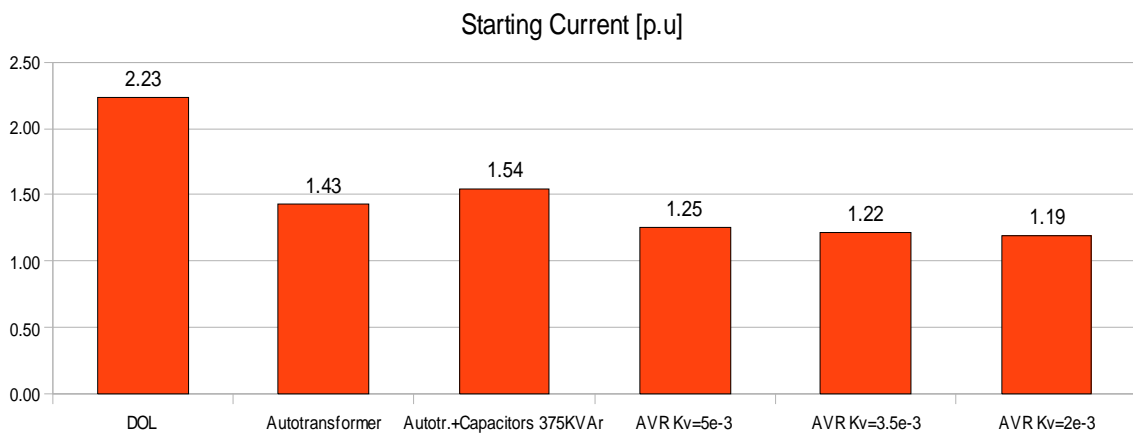


Figure 6

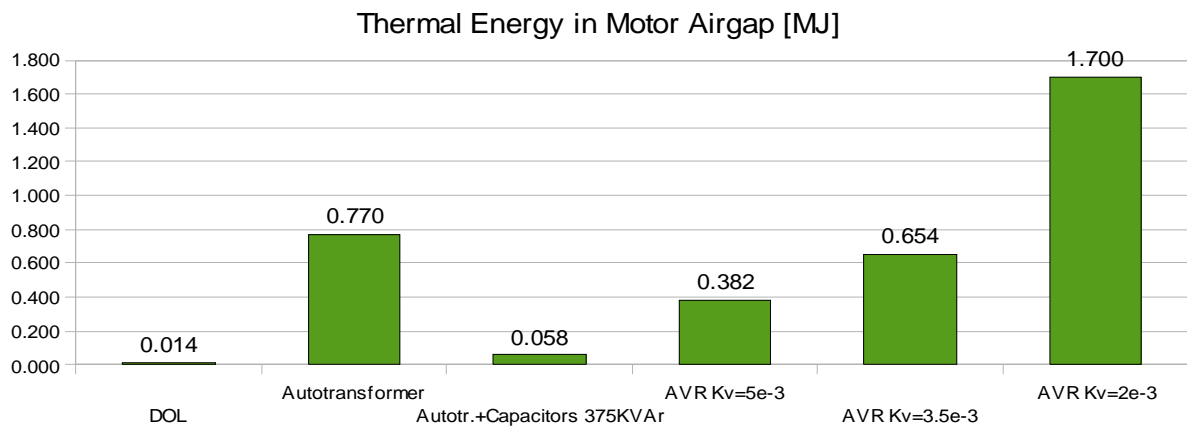


Figure 7

III. STARTING –UP OF THRUSTERS DRIVEN BY INDUCTION MOTORS

Taking into account the previous soft starting methods, two main alternative configurations are used for starting up an electric motor driven thruster unit.

The first alternative enables the combination of a squirrel cage motor along with controllable pitch propeller. In this case, initially the pitch is set to 0.0 so that the total inertia moment of the system is as minimum as possible. This pitch ratio is kept constant until the motor reaches its nominal angular speed. Moreover manoeuvring is achieved by varying at each time the propeller pitch.

In this way, motor starting up procedure is not repeated; it is reminded that repetitive starting up is forbidden in this case, in order to prevent equipment overheating.

On the other hand, the second alternative enables a wound rotor induction motor along with variable resistors and a fixed pitch propeller. As already mentioned, in the case of wound rotor application, the inrush transient current can be limited (the current is controlled so that its rated value is not exceeded). In addition, maneuvering is achieved via repetitive switching-on / switching-off the electric motor, as in this case, the starting current does not exceed its rated value, so no overheating is endangered.

Diploma Thesis

IV. RELEVANT STANDARDS

Several Power Supply Quality related issues appeared as a result of ships extensive electrification without taking into consideration the need of the forthcoming All Electric Ships. The problems during thruster starting-up can be included in this category too, as explained in the following.

In detail, the phenomenon of large power motor starting-up is usually observed as a voltage dip which is partially covered by the standardized limits of transient voltage fluctuations, i.e. the maximum permissible voltage dip along its corresponding duration within a fundamental period, see Table 2. Taking into account that the most significant problem which is caused by the thruster motor starting-up is the voltage dip resulting to a series of other equipment malfunction, the related standards are a fairly good starting point of discussion. The majority of the standards set limits regarding the time duration as well as the fluctuation maximum value with respect to the rated value.

Thus, according to [IEEE Standard 45-1998]: “A *voltage transient is a sudden but temporary change in the peak amplitude of the voltage, which exceeds the user voltage tolerance limits. Typical time duration for voltage transients is between a fraction of a cycle and 2 seconds for both 60Hz and 400Hz systems. Transients are usually the result of changes in load. The reaction of the prime mover, alternator and associated controls to that change defines the recovery time. Voltage recovery times can be shorter than the original disturbance that caused the transient. A typical example of this is voltage recovery during the start of a large motor load.*”

According to this approach, no restrictions on the transient peak load current, neither on the corresponding power demands (in terms of active and reactive power) are cited.

On the other hand, compliance with these voltage norms is verified as described in the following[[IEEEStandard45-1998]]:

“when the generator is running at no load, at nominal voltage, and the specified sudden load is switched on, the instantaneous voltage drop at the generator terminals shall not be more than 15% of the generators nominal voltage. The generator voltage shall be restored to within $\pm 3\%$ of the rated voltage within 1.5 sec. Concerning the sudden load applied, although not officially written it is 60% of the generator capacity”.

Diploma Thesis

Standard/rule	VOLTAGE TRANSIENT*	VOLTAGE SPIKE
ABS (2005) BV(2003) DNV(2001) GL(2004) PRS (2002) RINA(2005)	$\pm 20\%$ (1.5s)	No
(LRS) (2001)	+20%. -15% (1.5s)	No
IEEE 45-1998	$\pm 12\%$ (2s)	$\pm 2500V$ (380V – 600V) 1000V (120V- 240V)
STANAG 1008 (Ed.9). USA MIL- Std-1399	$\pm 16\%$ (2s) [$\pm 22\%$ (2s)] 18-35V. 24Vdc	2.5kV. 440V 1kV. 115V 0.6kV. 24Vdc

* Permissible transient frequency variation is $\pm 10\%$ (5s) in all rules

Table 2 Comparison of shipboard Standards regarding transients and spikes

Diploma Thesis

In accordance with the authors' suggestion, the best choice of "a sudden load" for assessing this generator set transient response would be the thruster electric motor. Taking into account that in most cases, this is the largest motor installed onboard, being of equivalent capacity to that of the ship generators. Furthermore, taking also into account that the starting-up procedure (followed by a corresponding stopping) could be repeated more than once during manoeuvring operation, it can be considered that in this case the thruster operation is close to pulsed load characteristics (figure 8).

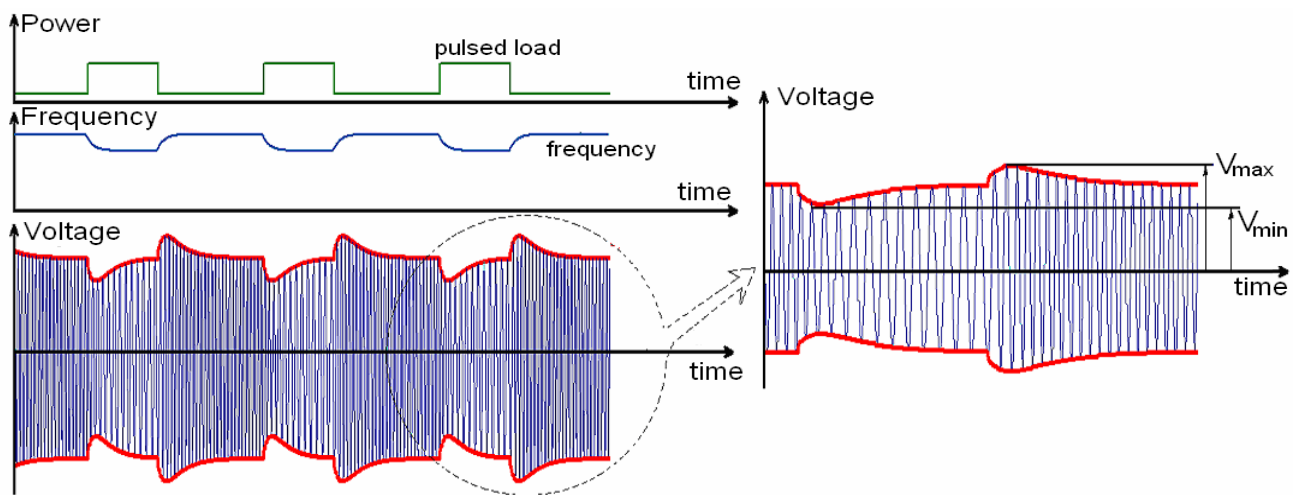


Figure 8

The thruster as a pulsed – load. Standardization issues

According to STANAG 1008 definition, pulsed load is "a repetitive random or cyclic load that imposes time-varying power requirements on the system that result in amplitude modulation in voltage and frequency". From the same source it is concluded that voltage or frequency modulations are periodic or quasi periodic variations such as might be caused by regularly or randomly repeated loading with frequency less than the nominal. It should be mentioned that the term refers either to certain navigation systems (e.g. sonars or radars) or to sophisticated weapon systems. However its definition as mentioned above does not exclude any other load with the features noted (i.e. "repetitive high power"). This means that the occasionally repetitive starting-up procedure of a thruster motor can be considered to be a specific-type pulsed load. In addition, the resemblance is improved considering that like the other pulsed loads, thruster motors are supplied with electric power via auxiliary power interface units so that in this case the starting up problems are minimized.

Diploma Thesis

Nevertheless, what is important is that for this type of loads there are certain standards, which can be used as the grounds for further discussion. Therefore, a brief citation of the standards on pulsed loads is made followed by a case study. During the pulsed load operation, the limits below (Equation1) must not be exceeded otherwise voltage and/or frequency modulation will be appeared endangering not only the power supply quality but also the stability of the system.

If such a load cannot be avoided, the power supply design authority is to be consulted so corrective action can be determined.” [STANAG 1008 and USA MIL-STD-1399].

Voltage and Frequency modulation limits:

$$Q_{pulse} < 0.065 * S_{supply} \quad \text{and} \quad P_{pulse} < 0.25 * S_{supply} \quad \text{Equation 1}$$

Where P_{pulse} • Q_{pulse} = active, reactive power of the pulsed load respectively, while S_{supply} = full rated apparent power of the supply during pulsed load operation.

$$Q_{pulse} \leq 0.065 S_{supply} \quad \text{and} \quad P_{pulse} \leq 0.25 S_{supply}$$

According to the complex power definition:

$$(P_{pulse}^2 + Q_{pulse}^2)^{1/2} = S_{pulse} \quad \text{Equation2}$$

The power factor is defined as:

$$P.F = \frac{P_{pulse}}{S_{supply}} \quad \text{Equation3}$$

It is concluded that:

$$P.F * x < 0.25 \quad \text{and} \quad P.F > [1 - (0.065 / x)^2]^{1/2} \quad \text{where} \quad x = \frac{S_{pulse}}{S_{supply}} \quad \text{Equation4}$$

It is known that $(P_{pulse}^2 + Q_{pulse}^2)^{1/2} = S_{pulse}$ and the power characteristics defined as

$$P.F = \frac{P_{pulse}}{S_{supply}}$$

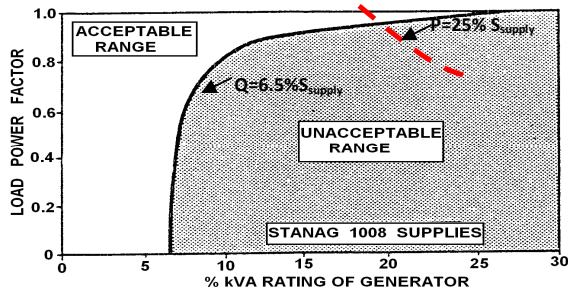


Figure 9

Limit-curve for pulsed load operation according to [STANAG 1008 and USA MIL-STD-1399] (load power factor vs. % pulsed power supplying generator rated apparent power)

The previous pulsed load active and reactive limitations can also be written as voltage and frequency modulation limitations as below:

$$\Delta V/N_{\text{ominal}} \leq \pm 2.5\% \text{ and } \Delta f/n_{\text{ominal}} \leq \pm 0.5\% \text{ Equation 5}$$

, which are stricter than the transient fluctuations tabulated in Table 2, as they refer to the quasi-steady-state modulation phenomenon.

Provided that the thruster motor is to be considered a pulsed load, it should be more appropriate to consider P_{Pulse} and Q_{Pulse} equal to its transient rather than steady state power demands.

Depending on the configuration discussed in induction motor characteristics, the transient demands are expected to be many times the rated values (in case of squirrel cage rotor with single starting-up followed by propeller pitch variations) or almost equal to the rated thruster motor power (in case of the wound rotor, where repetitive starting-up during maneuvering occurs).

From the power generation point of view, the generator sets must have the capacity to meet the motor demands withstanding any related problems e.g. frequency or voltage stability problems.

V. Approximation of Bow Thruster Propeller Torque Variance During Pitch Ratio Change

For the purposes of this degree dissertation, podded propulsion and bow-thruster propeller applications will be examined. Both of them are of great interest regarding their increasing required torque in function of increasing speed range.

Below typical Wagenigen Series-B propeller (FPP) open flow diagram (figure 10) and ducted propeller (CPP) open flow diagram (figure 11, 12) represent how the torque as well as trust coefficient change in function of various parameters.

The most representative propeller parameters should be the following:

$$J = \frac{V_0}{nD}, k_T = \frac{T}{\rho n^2 D^4}, k_Q = \frac{Q}{\rho n^2 D^5}, n_0 = \frac{V_0 T}{\omega Q} = \frac{V \frac{T}{\rho n^2 D^4}}{\omega D \frac{Q}{\rho n^2 D^5}} = \frac{V}{2\pi n D} \frac{k_T}{k_Q} = \frac{J}{2\pi} \frac{k_T}{k_Q}$$

$$\omega = 2\pi n \quad \text{Equation Group 6}$$

Where:

n : propeller rotating speed [rps]

D: propeller diameter [m]

V₀: open flow propeller speed [m/sec]

T: open flow propeller thrust [N]

Q: open flow propeller torque [Nm]

K_T: thrust coefficient

K_Q: torque coefficient

Diploma Thesis

Open Flow Wagenigen series-B4-85 propeller (Fixed Pitch Propeller) (for propulsion)

The diagram (figure10) below represent the behavior of the propeller Wagenigen Series-B4-85 operating in open flow.

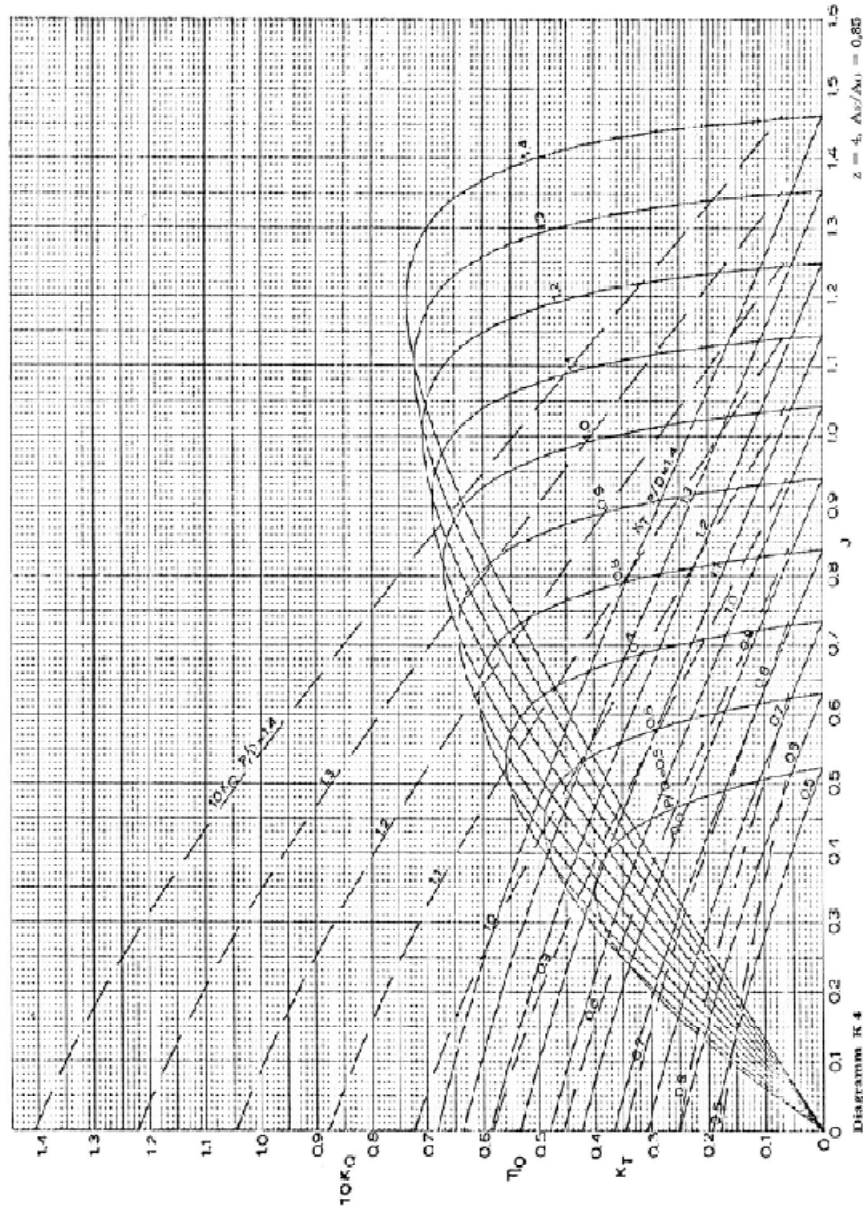


Figure 10

Diploma Thesis

Despite the fact that podded propulsion systems are not equipped with Wagenigen Series B propellers, the just referred diagrams can represent the typical behavior of podded propulsion propellers regardless the values of the diagram magnitudes.

It is generally accepted that the requested torque from the open flow propeller provided that the pitch ratio are kept constant, increases proportionally to the square of the rotating speed while the propeller open flow speed increases proportionally to the propeller rotating speed. On the top of that, the propeller requested power increases proportionally to the cube of the propeller rotating speed.

Ducted Propellers

The LNG vessel which is examined for the purposes of this degree dissertation is also equipped with a bow-thruster. The propeller behavior of the bow thruster can be considered similar to the ducted propeller behavior.

Figure11 and figure12 represent the ducted propeller behavior under static bollard condition.

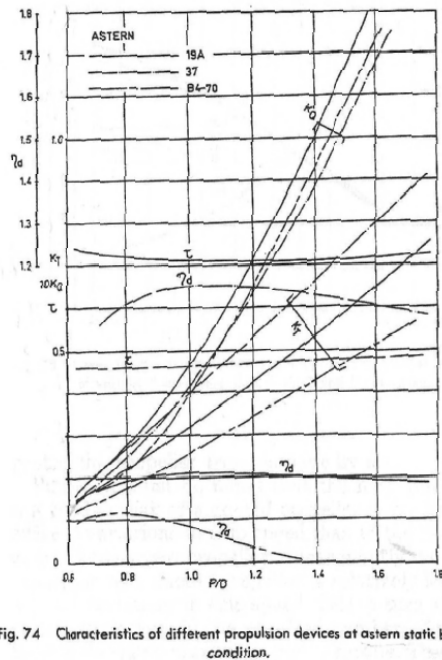
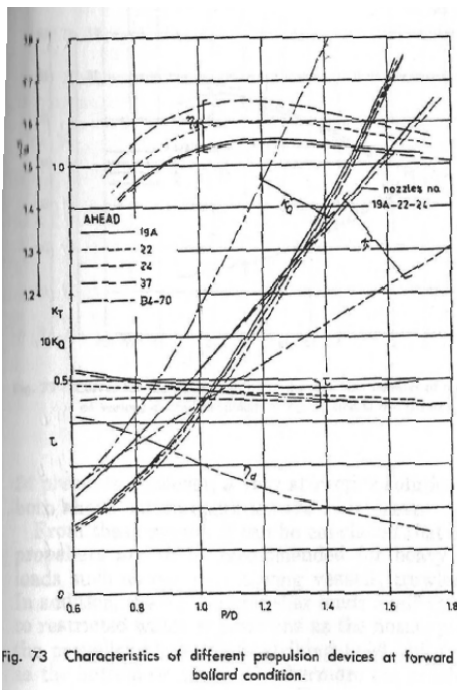


Figure 11

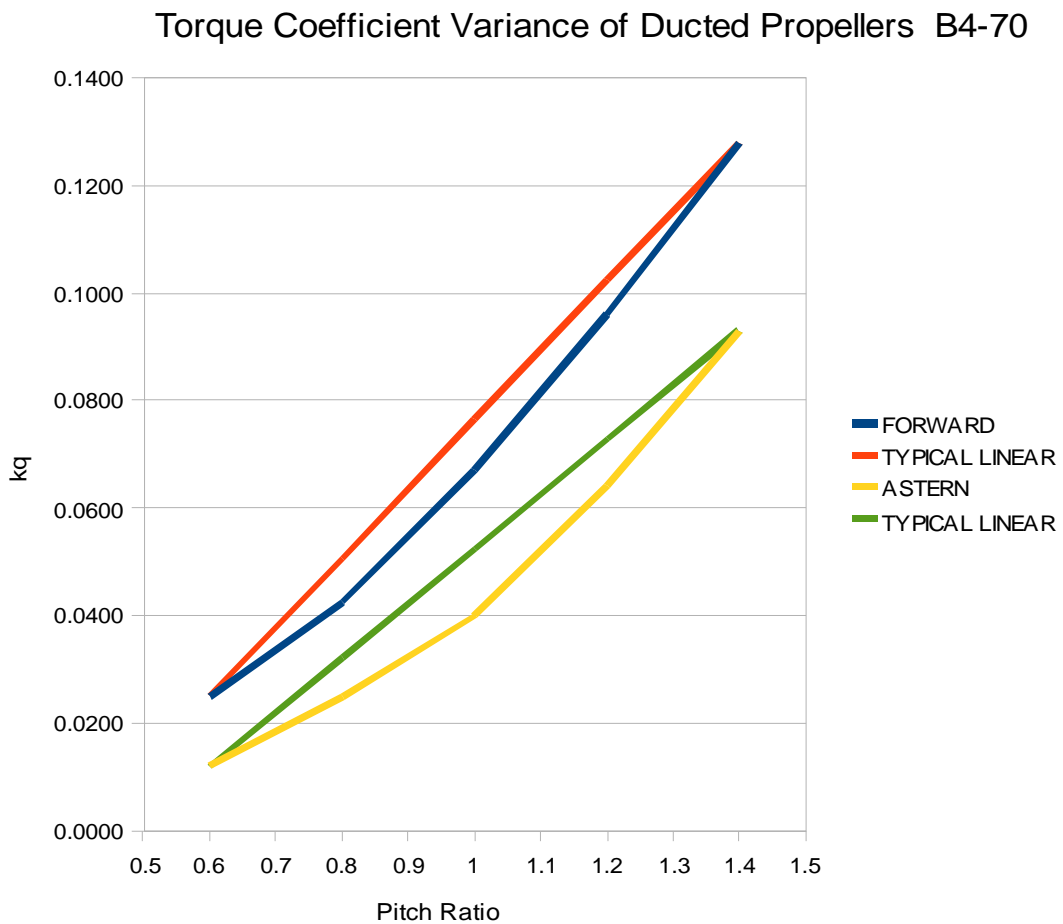


Figure 12

It can be observed that the linear approximation of the torque coefficient variance in conjunction with propeller pitch ratio as well as making the assumption that the static bollard condition of the problem remains, seems to be adequate for the purposes of the present research work.

The simulation results which are expressed in study case B, contain the assumption that the requested active power from the propeller increases proportionally to the propeller pitch ratio. The pitch ratio, in turn, increases proportionally with time.

Diploma Thesis

VI. Case Studies

The rules which have been discussed regarding the bow thruster as pulsed load have been examined into two different case studies:

A. A Car/passenger ferry with a bow-thruster motor of 1.0 MW/440V (power factor=0.9 inductive), induction motor of squirrel cage type, supplied by a dedicated shaft generator 1.4 MVA/440V.

B. An LNG carrier with a bow-thruster motor of 1875 kW/6.6 kV (power factor=0.8 inductive), induction motor of squirrel cage type, supplied by two synchronized steam- and one stand-by generator of 4312.5 kVA /6.6 kV each.

In these two cases, power quality problems during starting-up have been noticed and alternative configurations have been investigated. These alternatives include generator combinations, as well as auxiliary starting up interfaces, such as capacitors and autotransformers.

In all cases, the criteria regarding the ratios of active and reactive power in comparison with the generators capability both for steady state and transient thruster power demands have been used.

All simulations are performed in PSCAD computer program.

Specifically, with regards to case study A/ (waveform group 1), a representative comparison between several starting methods is made.

In this case study, four alternative power starting-up interfaces have been considered for investigation. Namely:

A1. Direct On Line Operation case, which evidently could not be applied due to the too high motor rated power,

A2. Power Supply via an autotransformer with two-step tap changer (50%-100%).

A3. Power supply via the combination of an autotransformer (as before) with a capacitor bank,

A4. The dedicated shaft generator operates in AVR-soft starting system mode.

Diploma Thesis

Table3 presents the thruster power demands with respect to the operating generators rated capacity. They are divided into two different pairs of columns. In the first pair of columns, it represents the worst power demand at (nominal) steady-state conditions, i.e. rated motor power along with any interface power supply (i.e. capacitor) is compared to the rated generator power. In the second pair of columns, it is represented the corresponding transient power demands of the thruster, as obtained from the simulations are presented. The corresponding transient power demands focus on the power demands on starting up process.

The inappropriate selection of the generator capacity is emerged in all sub-cases, regardless if interest is focused on steady-state rated values of the thruster or transient-state ones. The limits of equation1 are exceeded; hence the grid suffers from a significant voltage dip which the generator cannot compensate. On the other hand, the motor succeeds in starting up only in sub-cases A3 and A4. In particular, sub-case A2 is proven marginally unsuccessful as the motor reaches its nominal speed slightly after 48 s, i.e. when its thermal limits have been exceeded and the over-current relay should trip.

In contrast, sub-case A4, is marginally successful from the motor thermal limits point of view.

With regards to case study B (Waveform Group 2-21), seven alternative scenarios with synchronized generators (modeled with their complete dynamic model along with their speed governors and AVR's), as well as starting-up interfaces have been considered (autotransformers and capacitive loads):

Regarding the study case B, it should be pointed out that before starting up process begins, the capacitive loads have already been charged so that no inrush capacitive charging current is noticed.

B1: One steam turbine generator 4312.5 kVA, along with an autotransformer with two-step tap changer.

B2: Two steam turbine generators (2x4312.5 kVA), along with an autotransformer with two-step tap changer.

B3i: Two steam turbine generators (2x4312.5 kVA), along with an autotransformer with three-scale tap changer.

B3ii: Two steam turbine generators, along with autotransformer with two-step tap changer and a capacitive load of 500 kVAr.

Diploma Thesis

B3iii: Two steam turbine generators 2x4312.5 kVA, along with an autotransformer with three-step tap changer and a capacitive load of 300 KVA.

B3iv: Two steam turbine generators 2x4312.5 kVA, along with an autotransformer with two-step tap changer and a capacitive load of 300 KVA.

B4: Two steam turbine generators synchronized and one stand-by generator (3x4312.5 kVA) along with an autotransformer with two-step tap changer. The stand-by unit is to be synchronized prior to thruster starting-up.

	Nominal power demands from the generator (motor rated values 1000 KW. 436 kVA)		Transient State power demands from the generator (motor maximum demands during starting-up: 0.35 MW. 0.5 MVA)	
	Active Power $P_{\text{thruster}} / S_{\text{supply}}$	Reactive power $Q_{\text{thruster}} / S_{\text{supply}}$	Active Power $P_{\text{thruster}} / S_{\text{supply}}$	Reactive power $Q_{\text{thruster}} / S_{\text{supply}}$
A1:Single-dedicated shaft generator (unsuccessful)	<u>71.43>25%</u>	<u>31.14%>6.5%</u>	<u>314.29%>25%*</u>	<u>547.6%>6.5%*</u>
A2:Shaft generator and autotransformer (marginally unsuccessful)	<u>71.43>25%</u>	<u>31.14%>6.5%</u>	25%*	<u>59.5%>6.5%*</u>
A3:Shaft generator. autotransformer and capacitor banks 300 kVA	<u>71.43>25%</u>	<u>9.71%>6.5%</u>	25%	<u>53.57%>6.5%</u>
A4. AVR–soft-starting and shaft generator (marginally successful)	<u>71.43>25%</u>	<u>31.14%>6.5%</u>	25%	<u>53.00%>6.5%</u>

Table 3 Case study A (car/passenger ferry) (figures underlined exceed the limits of equation (a))

* The electric motor does not succeed in starting rotating as the generator is not capable of providing the energy required. The exact power demands of the motor are determined by considering the generator to be ideal sources in the simulations.

Diploma Thesis

	Active Power $P_{thruster}/S_{supply}$	Reactive power $Q_{thruster}/S_{supply}$	Active Power $P_{thruster}/S_{supply}$	Reactive power $Q_{thruster}/S_{supply}$	Minimum Voltage and Voltage Dip at generator terminals (in % of rated value)	Minimum frequency and Maximum frequency Dip (in % of rated value)
B1: 1 steam-turbine generator 4312.5 kVA +autotransformer with 2-step tap changer (unsuccessful)	<u>43.48%>25%</u>	<u>32.61%>6.5%</u>	<u>80%>25%*</u>	<u>60%>6.5%*</u>	-	-
B2: 2 steam-turbine generators 2x4312.5 kVA+autotransformer with 2-step tap changer	21.73%	<u>16.30%>6.5%</u>	7.54%	<u>20.29%>6.5%</u>	88.48% (Dip DV=11.52%)	96.18% (Dip Df=3.82%)
B3i: 2 steam-turbine generators 2x4312.5 kVA+autotransformer with 3-step tap changer	21.73%	<u>16.30%>6.5%</u>	5.10%	<u>14.26%>6.5%</u>	94.39% (Dip DV=5.61%)	98.61% (Dip Df=1.39%)
B3ii: 2 steam-turbine generators 2x4312.5 kVA+autotransformer with 2-step tap changer+capacitor 500 KVAR	21.73%	<u>10.50%>6.5%</u>	8.12%	<u>18.55%>6.5%</u>	89.63% (Dip DV=10.37%)	97.45% (Dip Df=2.55%)
B3iii: 2 steam-turbine generators 2x4312.5 kVA+autotransformer with 3-step tap changer+capacitor 300 KVAR	21.73%	<u>12.80%>6.5%</u>	5.22%	<u>13.33%>6.5%</u>	94.70% (Dip DV=5.30%)	98.61% (Dip Df=1.39%)
B3iv: 2 steam-turbine generators 2x4312.5 kVA+autotransformer with 2-step tap changer+capacitor 300 KVAR	21.73%	<u>12.80%>6.5%</u>	8.12%	<u>19.36%>6.5%</u>	89.34% (Dip DV=10.66%)	97.37% (Dip Df=2.63%)

Diploma Thesis

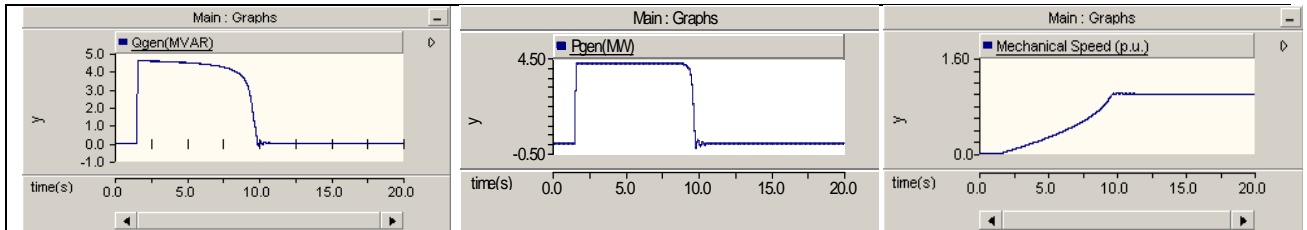
B4:2-steam-turbine generators + 1 stand-by generator (3x4312.5 kVA)+autotransformer with 2-step tap changer	14.49%	<u>10.86%</u> >6.5%	5.02%	<u>15.30%</u> >6.5%	94.09% (Dip DV=5.91%)	97.71% (Dip Df=2.29%)

Table 4 Case study B (LNG vessel) (figures underlined exceed the limits of equation (a))

** The electric motor does not succeed in starting rotating as the generator is not capable of providing the energy required. The exact power demands of the motor are determined by considering the generators to be ideal sources in the simulations.*

Diploma Thesis

Waveform Group 1

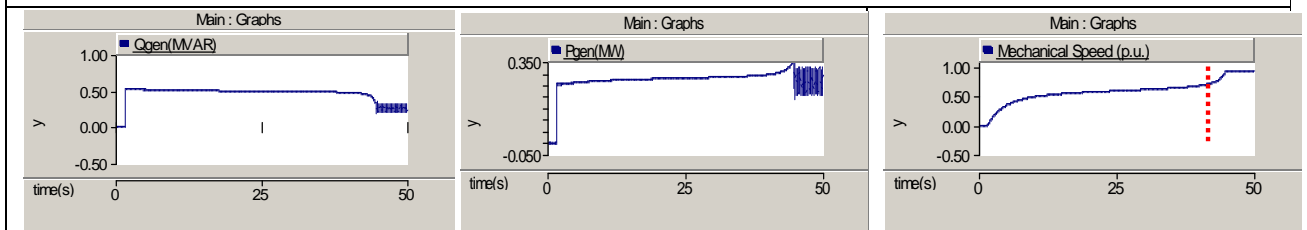


(a) Reactive Power vs time

(b) Active Power vs time

(c) Mechanical speed vs time

Evolution of Reactive Power. Active Power and Mechanical Speed during DOL starting

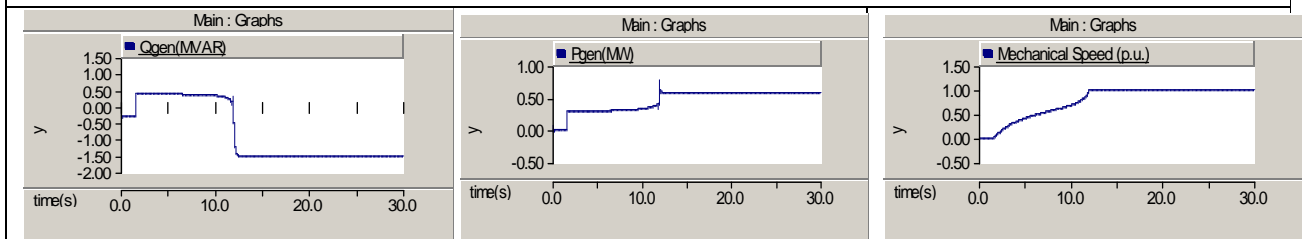


(d) Reactive Power vs time

(e) Active Power vs time

(f) Mechanical speed vs time

Evolution of Reactive Power. Active Power and Mechanical Speed during starting via Autotransformer

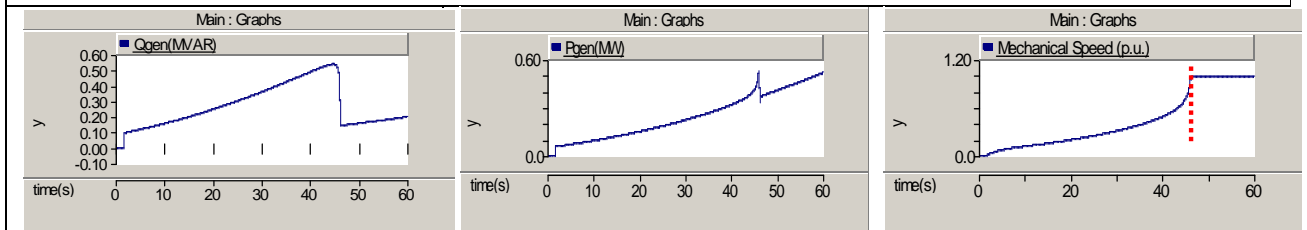


(g) Reactive Power vs time

(h) Active Power vs time

(i) Mechanical speed vs time

Evolution of Reactive Power. Active Power and Mechanical Speed during starting via Autotransformer-Capacitor combination



(j) Reactive Power vs time

(k) Active Power vs time

(l) Mechanical speed vs time

Evolution of Reactive Power. Active Power and Mechanical Speed during AVR-soft-starting

Diploma Thesis

The corresponding simulation results are tabulated in Table4. Like in case A, the first column includes the comparison of rated power demands of the thruster system along with any capacitor power supply with respect to the operating generator apparent power. The second column presents the corresponding transient power demands of the thruster motor, as provided by the simulations. The last two columns correspond to the worst voltage and frequency dips occurred during the starting-up procedure and they are measured at the main generator bus-bar.

It can be observed that like in case A, even if the rated power of the thruster is used, the problematic operation is deduced. Hence, in all cases, where divergences of power demands from the limits of equation1 are noticed, significant voltage and frequency dips occur endangering the stability of the system. With the exception of sub-case B1, where the thruster motor fails to start-up due to insufficient power redundancy on behalf of the (only in this sub-case) generator, the active power restriction is met in all cases, whereas the reactive power one is not. Hence, it is plausible to argue that numerical limits in equation1 need some reconsideration. Further, the limits of voltage and frequency dips in Equation5 are violated in certain cases, but not the limits of Table2. It is also noted that the ratios of thruster power demands over the supplying generator rated capacity, can be used as classification indices, indicating how effective each alternative solution is. Considering that the optimum solution is the one resulting in minimum values of voltage and frequency dips, several combinations between the transient power demands are sought see Table 5. Thus, in Table 5, it is proven that ranking according to the “**sum**” or the “**product**” of transient power demands coincides with that of the dips. It is underlined, that while these transient power demands of the thruster motors are provided by their manufacturer, the dips are accessed via simulations of the entire ship grid operation.

Regarding the alternatives investigated, further conclusions can be drawn. Thus, power redundancy does not necessarily lead to the optimum solution. More specifically, synchronizing an extra generator (sub-case B4) can be less favorable solution than that of the combination of two generators along with an auto-transformer with 3-step tap changer (sub-cases B3i and B3iii).

In the same way, an alternative with a large capacitor bank which in most cases is more expensive and more space demanding, can be less appealing than a combination of an autotransformer with increased step number in its tap changer along with a smaller capacitor unit (sub-case B3iii versus B3ii).

Diploma Thesis

Ranking	Cases	Active Power	Reactive power	$(P_{thruster} / S_{supply}) +$	$(P_{thruster} / S_{supply}) *$	Voltage Dip DV	Frequency Dip Df
		$P_{thruster} / S_{supply}$	$Q_{thruster} / S_{supply}$	$(Q_{thruster} / S_{supply})$	$(Q_{thruster} / S_{supply})$		
1	B3iii	5.22%	13.33%	18.55%	0.70%	5.30%	1.39%
2	B3i	5.10%	14.26%	19.36%	0.73%	5.61%	1.39%
3	B4	5.02%	15.30%	20.32%	0.77%	5.91%	2.29%
4	B3ii	8.12%	18.55%	26.67%	1.51%	10.37%	2.55%
5	B3iv	8.12%	19.36%	27.48%	1.57%	10.66%	2.63%
6	B2	7.54%	20.29%	27.83%	1.53%	11.52%	3.82%
7	B1	80.00%	60.00%	140.00%	48.00%	-	-

Table 5 Classification of alternative starting-up methods

The Table 5 compares the seven different alternatives regarding the power ratios, their sum and product as well as voltage and frequency dips.

It can be also observed that with the exception of active power ratio all the other indexes lead to the same optimum solution.

In accordance with Table 5, the plots below represent how the capacitive load as an interface to the motor as well as the transient active and reactive bow thruster motor power demand in accordance with the generators capacity affect voltage and frequency dip.

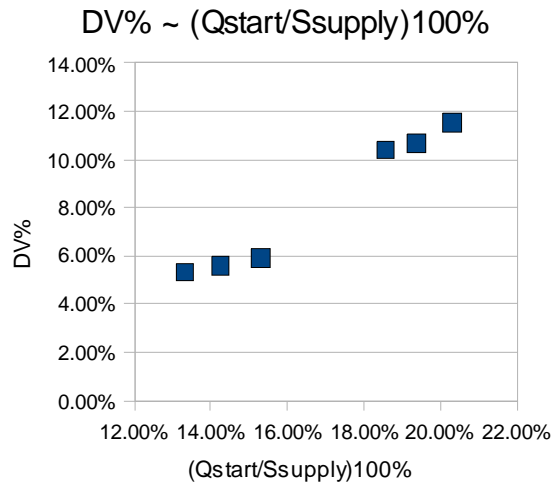


Figure 13

According to the figure 13, it is evident that voltage dip strictly depends on the motor reactive power demand in comparison with generator capacity during starting up procedure.

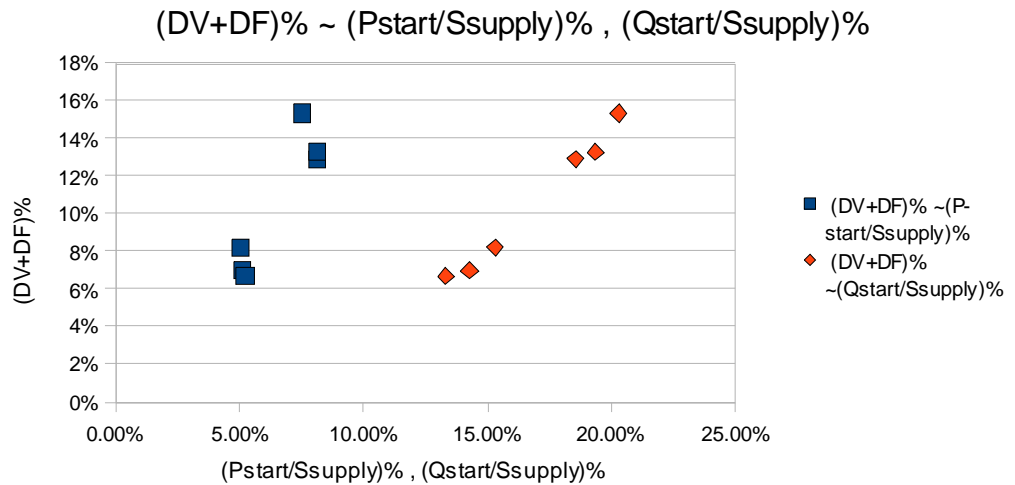


Figure 14

From the figure 14 it is concluded that specific values of the amount $(DV+DF)\%$ are appeared for larger amounts of $(Q_{start}/S_{supply})\%$ rather than for $(P_{start}/S_{supply})\%$. This means that the amount $(P_{start}/S_{supply})\%$ affects more the amount $(DV+DF)\%$ than the amount $(Q_{start}/S_{supply})\%$ does.

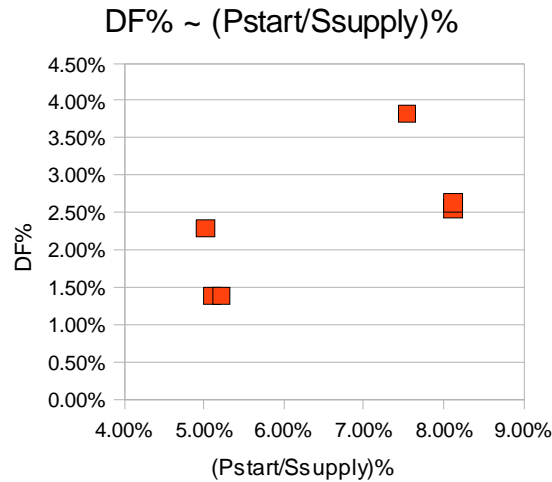


Figure 15

According to the figure 15, it is evident that frequency dip strictly depends on the motor active power demand in comparison with generator capacity during starting up procedure.

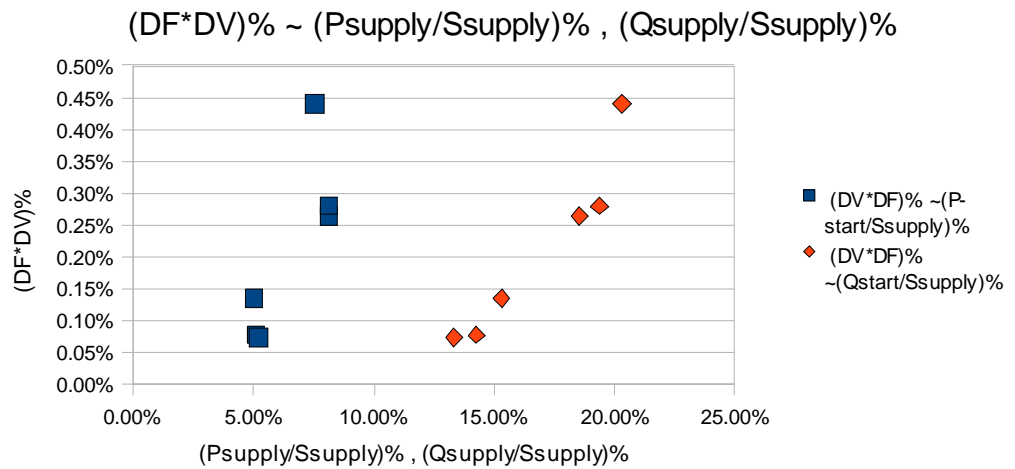


Figure 16

From the figure 16, it is concluded that specific values of the amount $(DV*DF) \%$ appear for larger amounts of $(Qstart/Ssupply) \%$ rather than for $(Pstart/Ssupply) \%$. This means that the amount $(Pstart/Ssupply) \%$ affects more the amount $(DV+DF) \%$ than the amount $(Qstart/Ssupply) \%$ does.

The figure 17 indicates the variance of the values $(P_{start}/S_{supply})\%$ and $(Q_{start}/S_{supply})\%$ for each study case.

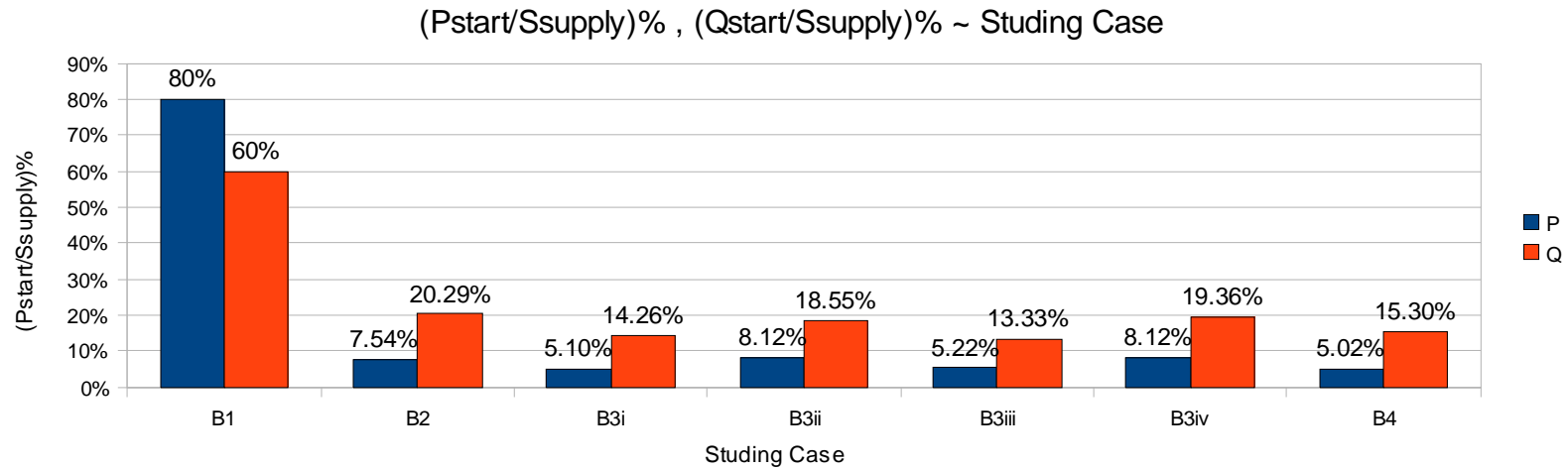


Figure 17

Diploma Thesis

Capacitive Load Cases								
		Cap[kVAr]	Pmotor(nominal) /Sgen [%]	Qmotor(nominal) /Sgen [%]	DV [%]	DF [%]	Cap/[Pmotor /Sgen]	Cap/[Qmotor/S gen]
2g-2s-500	B3ii	500	21.74%	16.30%	10.37%	2.55%	2299.91	3067.48
2g-2s-300	B3iv	300	21.74%	16.30%	10.66%	2.63%	1379.94	1840.49
2g-2s-150		150	21.74%	16.30%	10.74%	2.50%	689.97	920.25
2g-3s-300	B3iii	300	21.74%	16.30%	5.30%	1.39%	1379.94	1840.49
2g-3s-150		150	21.74%	16.30%	5.35%	1.39%	689.97	920.25

Table 6 Classification of alternative starting-up methods with two more adds of capacitive load of 150kVAr.

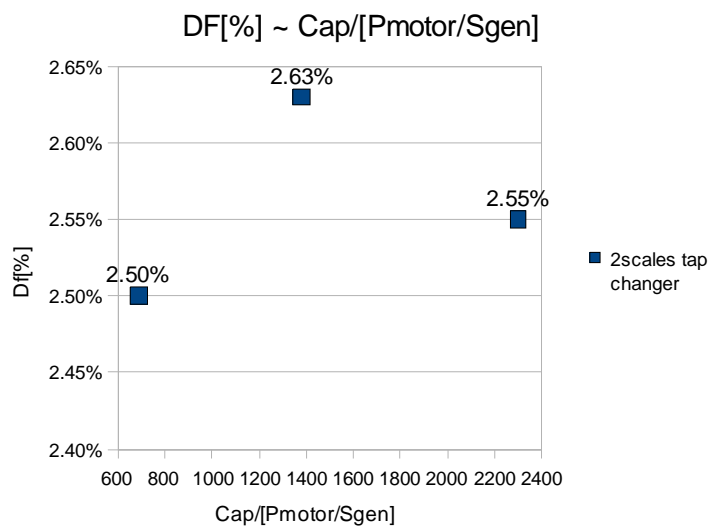


Figure 18

Diploma Thesis

According to the figure 18, the frequency dip depends on the capacitive load interface; however no qualitative estimations can be done in advance in accordance with the simulations, increasing the applied capacitive load, the frequency dip appears maximum and minimum value. The just referred simulations concern only two scales tap changer autotransformer application.

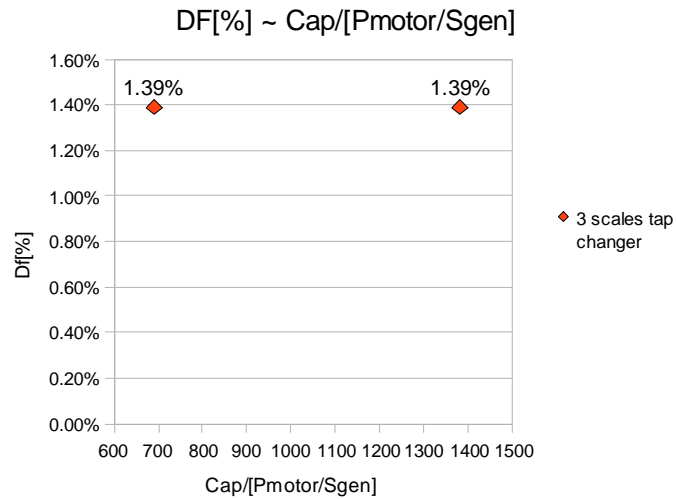


Figure 19

According to the figure 19, the frequency dip does not depend on the capacitive load interface. The just referred simulations concern only three scales tap changer autotransformer application.

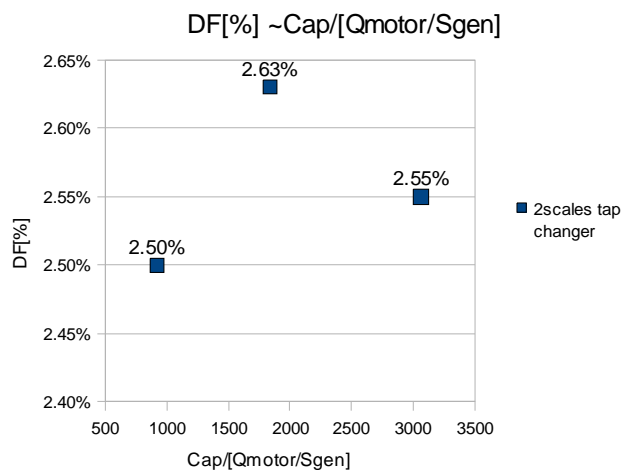


Figure 20

Diploma Thesis

According to the figure 20, the frequency dip depends on the capacitive load interface; however no qualitative estimations can be done in advance in accordance with the simulations, increasing the applied capacitive load, the frequency dip appears maximum and minimum value. The just referred simulations concern only two scales tap changer autotransformer application.

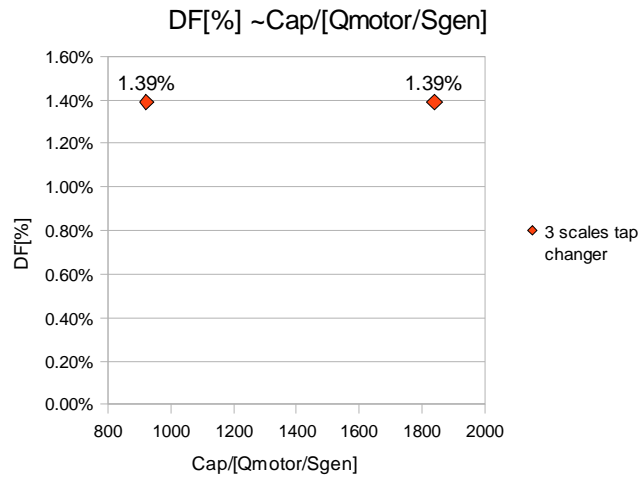


Figure 21

According to the figure 21, the frequency dip does not depend on the capacitive load interface. The just referred simulations concern only three scales tap changer autotransformer application.

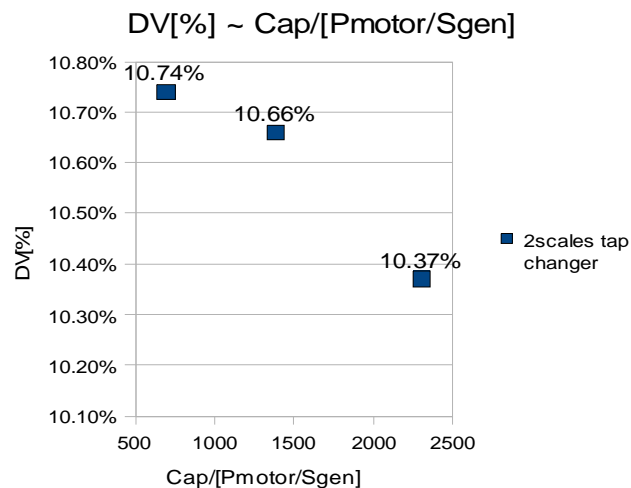


Figure 22

Diploma Thesis

Figure 22 indicates how the voltage dip decreases by increasing the capacitor load interface of the bow thruster induction motor. However, it can be seen that even if the capacitive load varies between 10.67% and 35.6% of the motor nominal reactive power, the reduction of the voltage dip is fairly slow. This means that taking into consideration that the capacitive interface is in most cases a costly as well as a high space requirement solution, it is not as favorable improving solution as the addition of further tap changers to the existing autotransformer .In other words, capacitive loads should be accompanied by autotransformer.

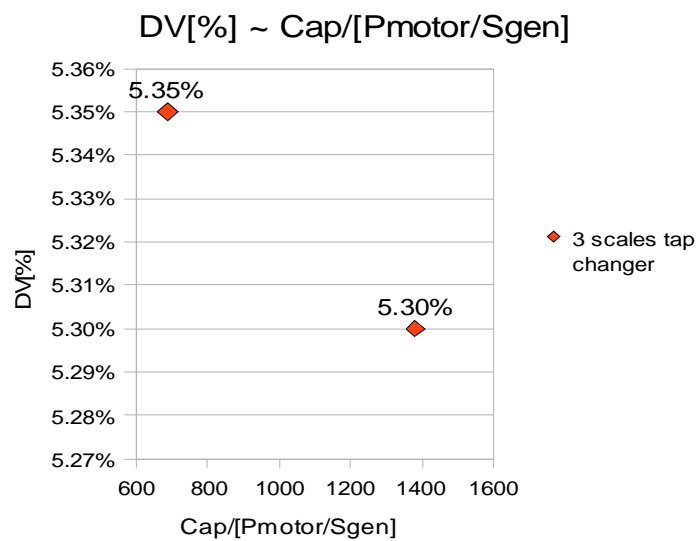


Figure 23

Figure 23 indicates how the voltage dip decreases by increasing the capacitor load interface of the bow thruster induction motor. However it can be seen that even if the capacitive load varies between 10.67% and 35.6% of the motor nominal reactive power, the reduction of the voltage dip is fairly low. This means that taking into consideration that the capacitive interface is in most cases costly as well as high space requirement solution, it is not as favorable improving solution as the addition of further tap changers to the existing autotransformer or in other words capacitive loads should be accompanied by autotransformer.

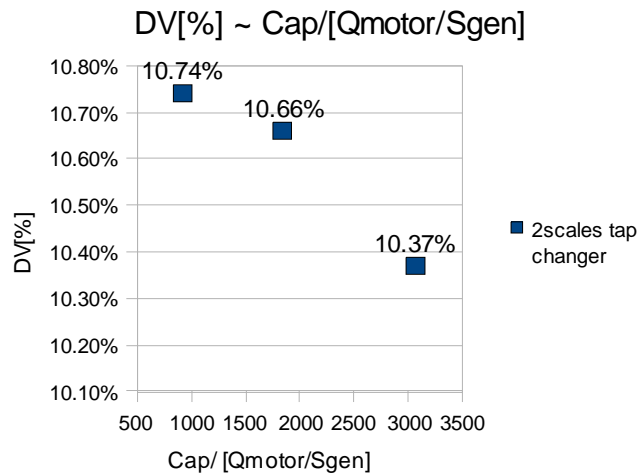


Figure 24

Figure 24 indicates how the voltage dip decreases by increasing the capacitor load interface of the bow thruster induction motor. However it can be seen that even if the capacitive load varies between 10.67% and 35.6% of the motor nominal reactive power, the reduction of the voltage dip is fairly low. This means that taking into consideration that the capacitive interface is in most cases costly as well as high space requirement solution, it is not as favorable improving solution as the addition of further tap changers to the existing autotransformer or in other words capacitive loads should be accompanied by autotransformer.

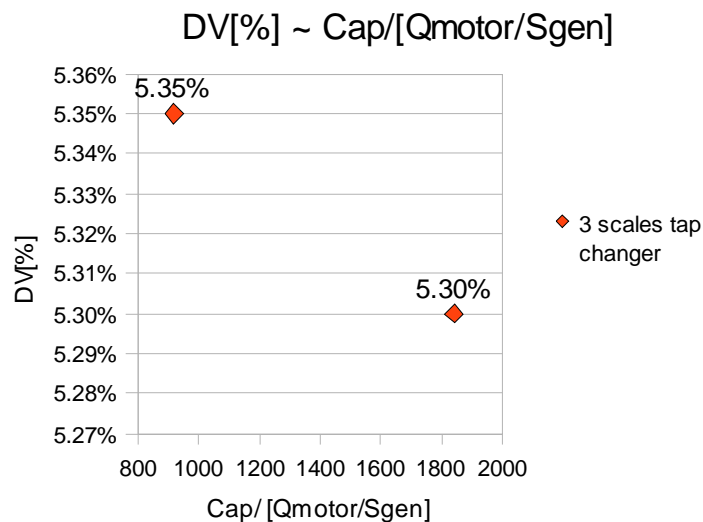


Figure 25

Diploma Thesis

Figure 25 indicates how the voltage dip decreases by increasing the capacitor load interface of the bow thruster induction motor. However, it can be seen that even if the capacitive load varies between 10.67% and 35.6% of the motor nominal reactive power, the reduction of the voltage dip is fairly low. This means that taking into consideration that the capacitive interface is in most cases costly as well as high space requirement solution, it is not as favorable improving solution as the addition of further tap changers to the existing autotransformer or in other words capacitive loads should be accompanied by autotransformer.

It should be pointed out that because of the fact that the simulations refer to the same motor, which means that the values $[Q_{\text{motor}}/S_{\text{gen}}]$ and $[P_{\text{motor}}/S_{\text{gen}}]$ are kept constant the amounts $\text{Cap}/[Q_{\text{motor}}/S_{\text{gen}}]$ and $\text{Cap}/[P_{\text{motor}}/S_{\text{gen}}]$ should be taken into consideration as Cap only, i.e. the reference .

A feasible solution was to readjust the voltage reference point to a light increase value by 1.5% (6700V) instead of 6600V. This slight increase does not have any harmful effect on the equipment regarding insulation stressing or premature aging.

In addition to the previous simulations, eleven and nine more simulations were run for nominal voltage value 6600V and 6700V respectively. Regarding the following cases which contain capacitive load motor interface it should be noted that in comparison with the previous study case B simulations, the capacitive loads are charged at the same time, when the bow thruster motor is connected to the electric network.

In case B, the tabulated results and the results which are expressed in bar charts refer to the maximum or minimum value of each index concerning that the simulation results strictly be taken into consideration after 90.0sec. In case B, the valid recordings refer to recordings after 90.0sec.

In wave form graphs, instantaneous waveform values herring after called as NO RMS values.

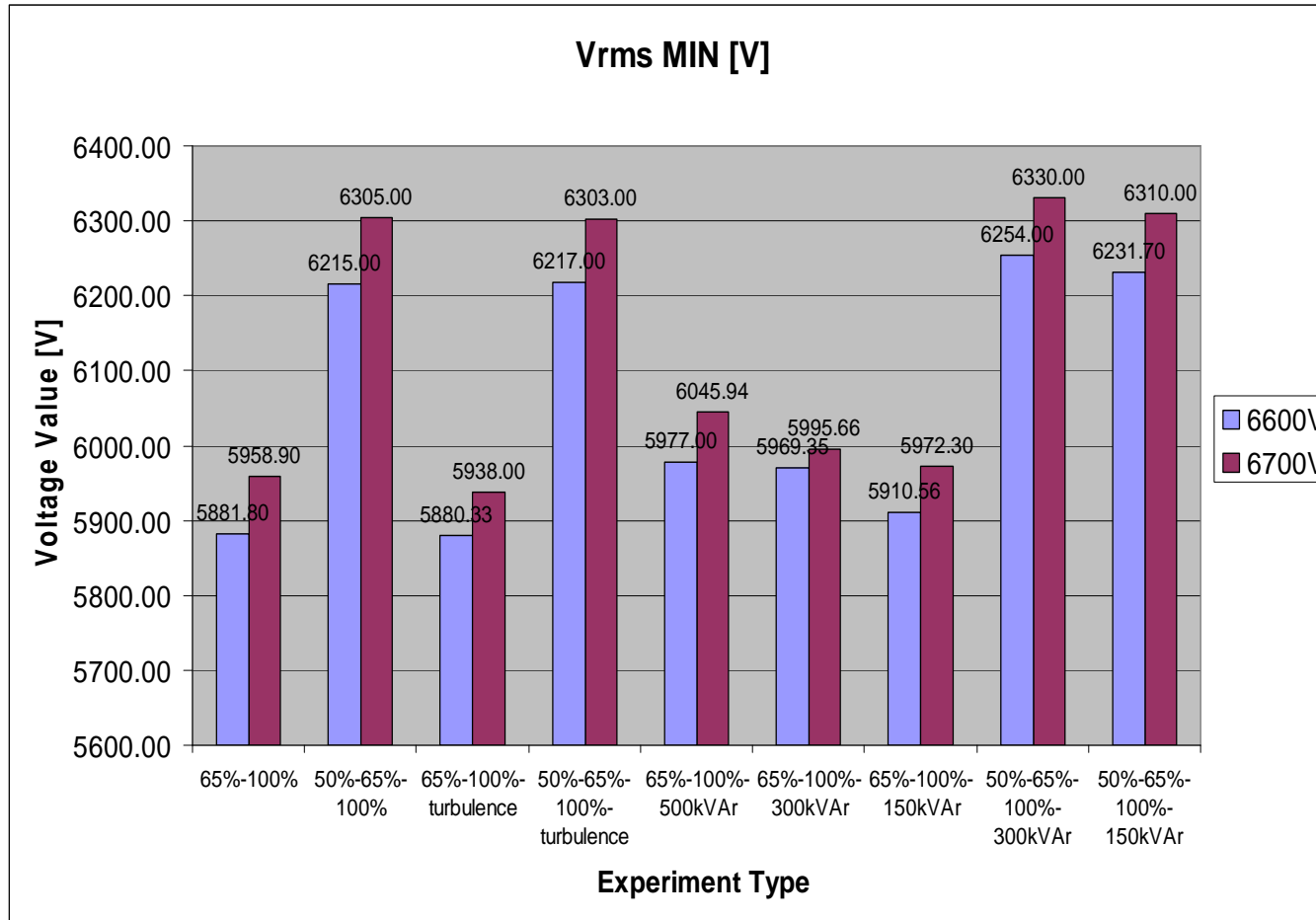


Figure 26

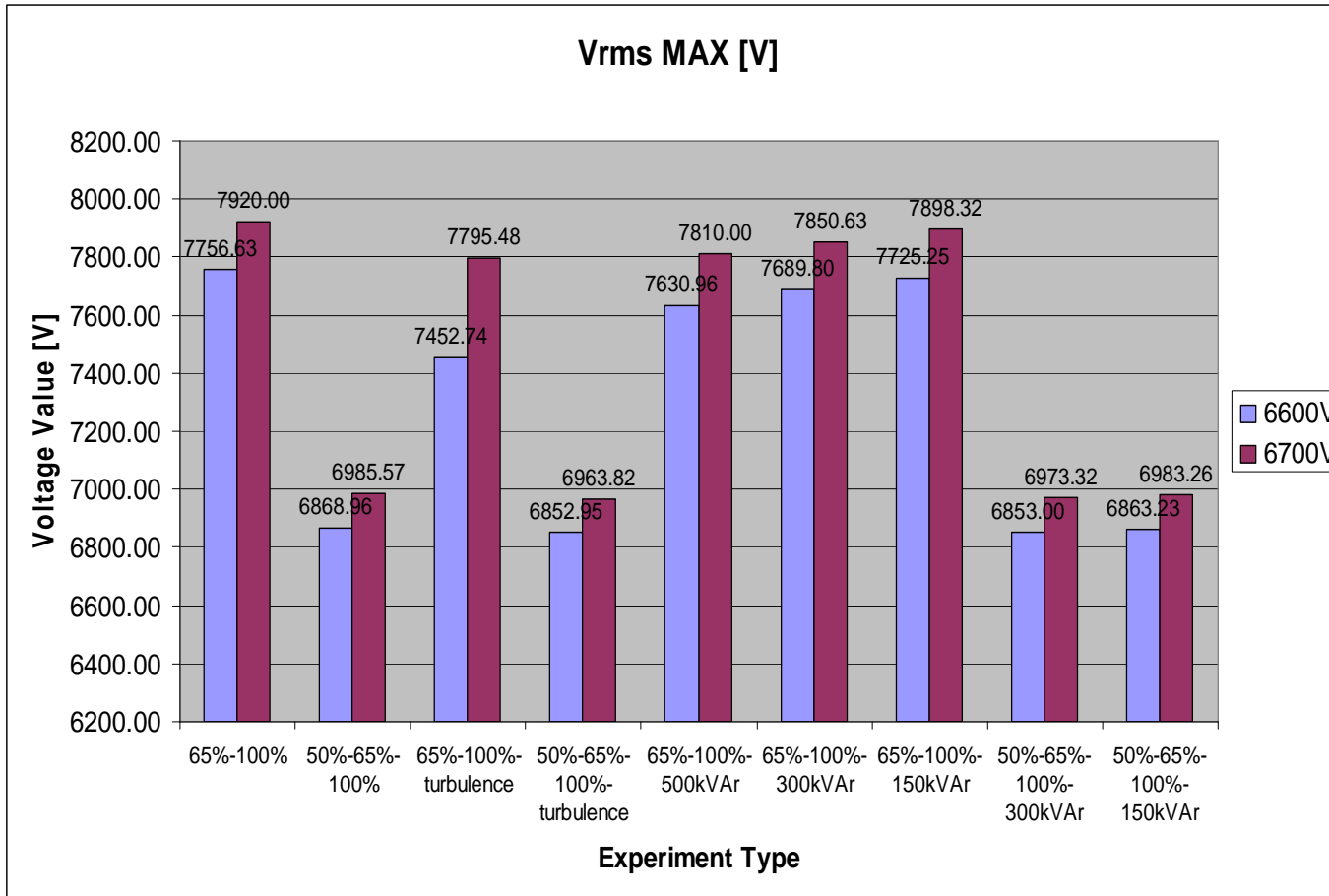


Figure 27

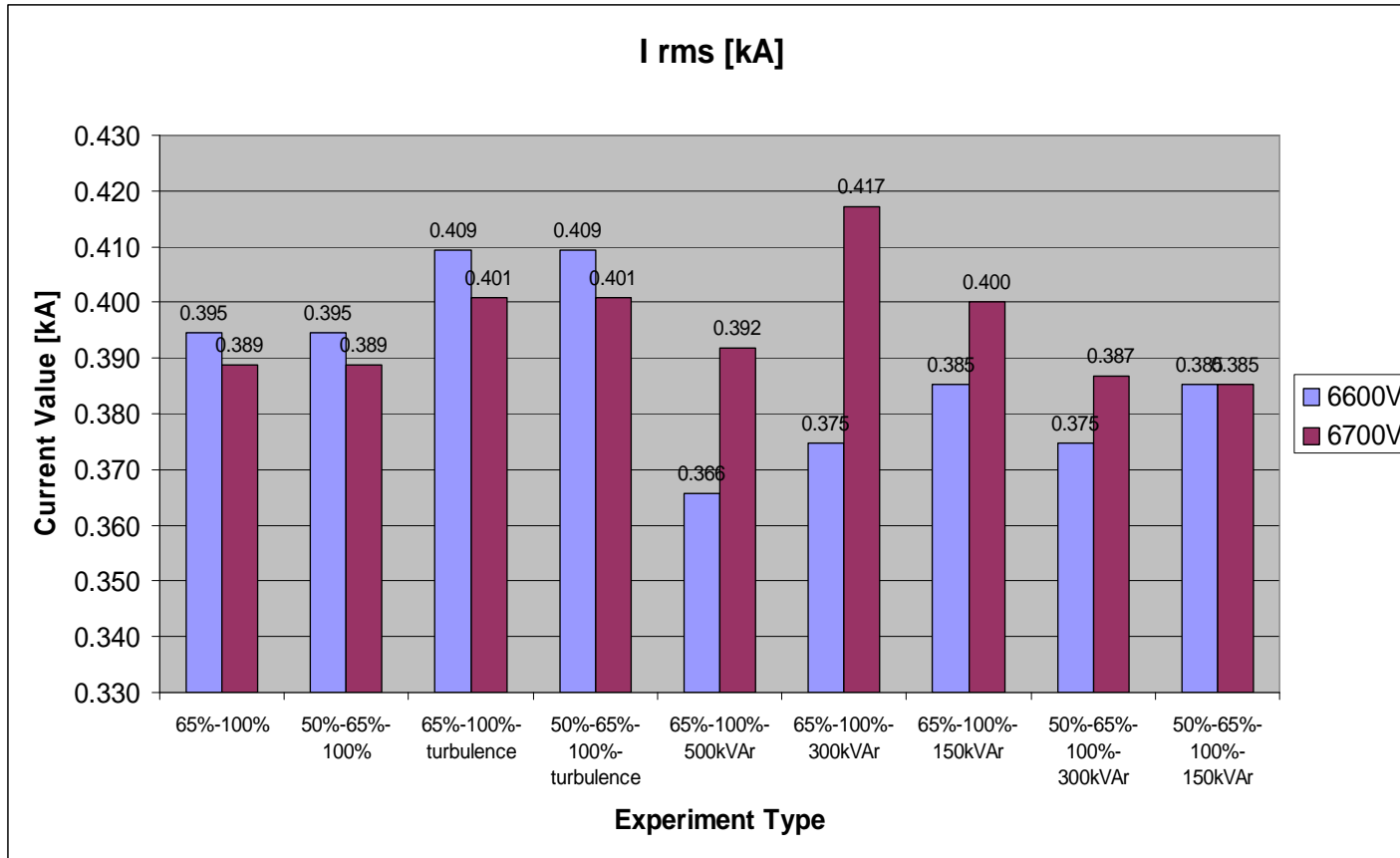


Figure 28

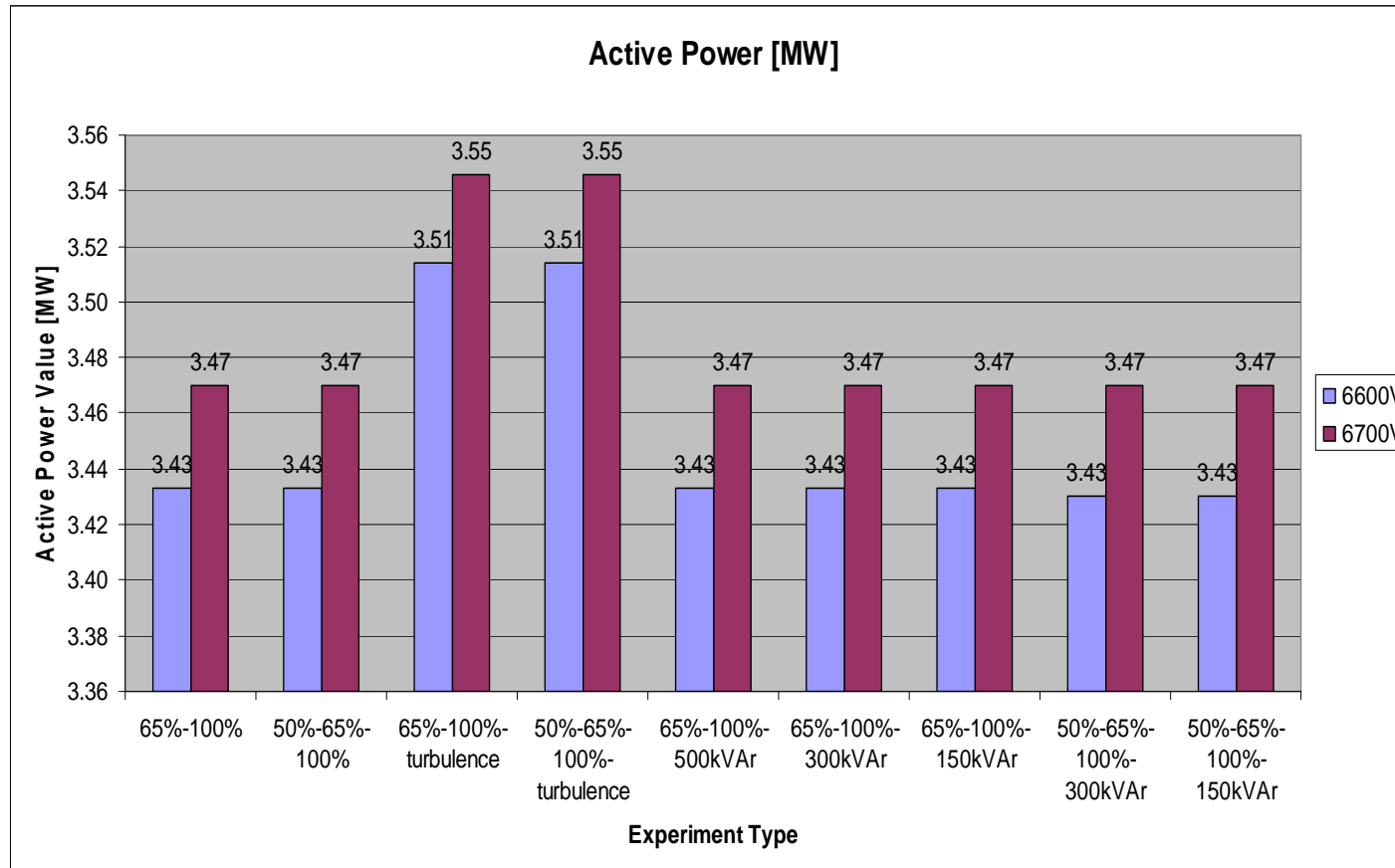


Figure 29

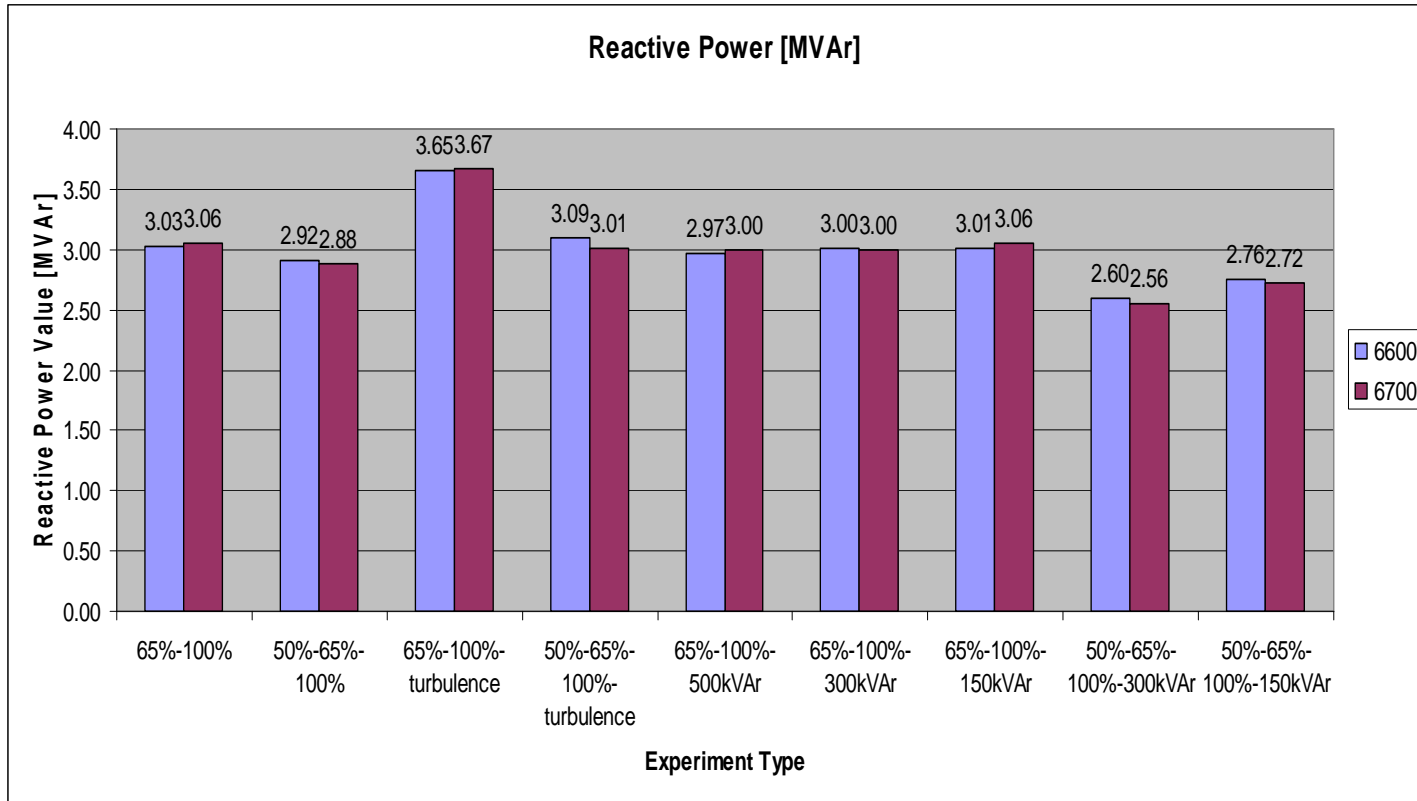


Figure 30

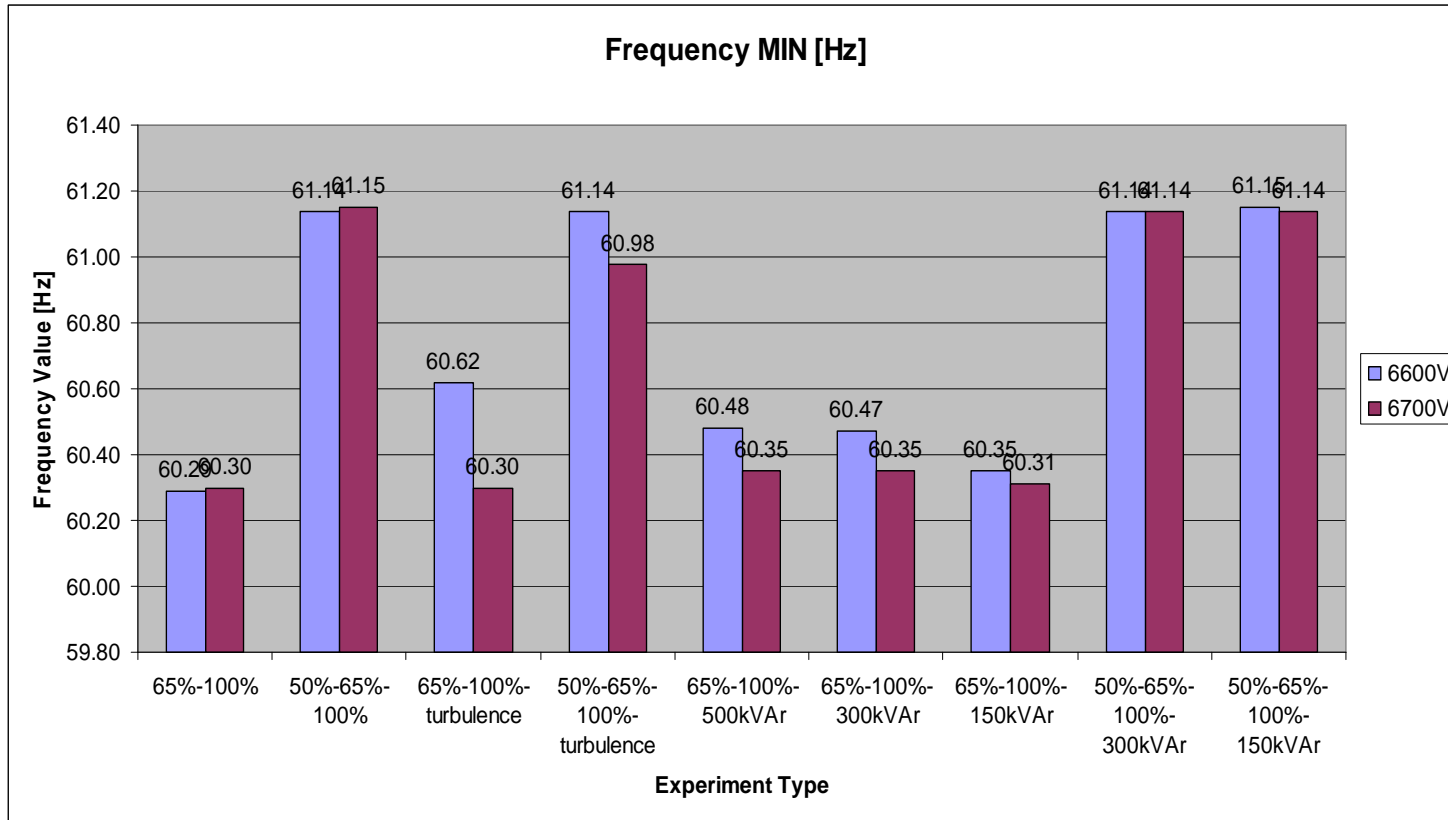


Figure 31

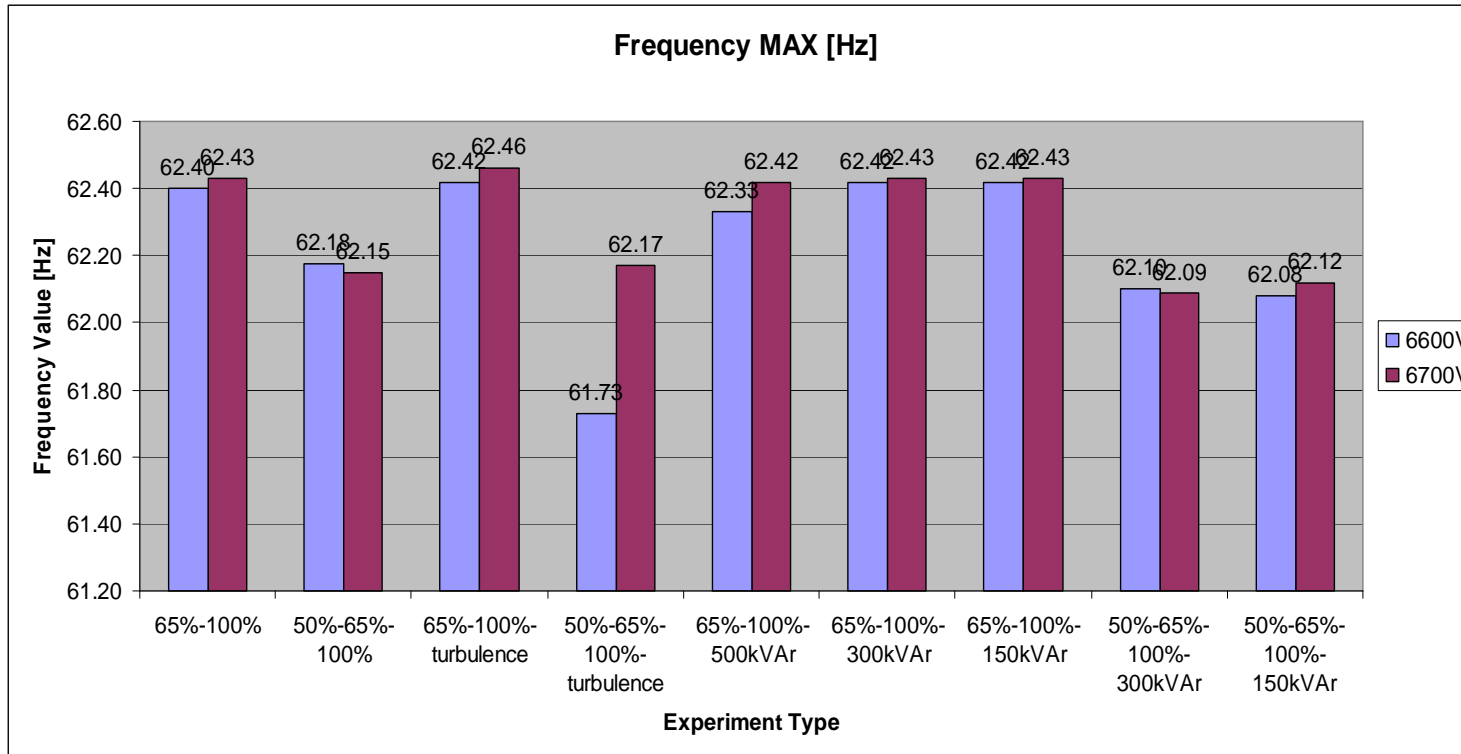
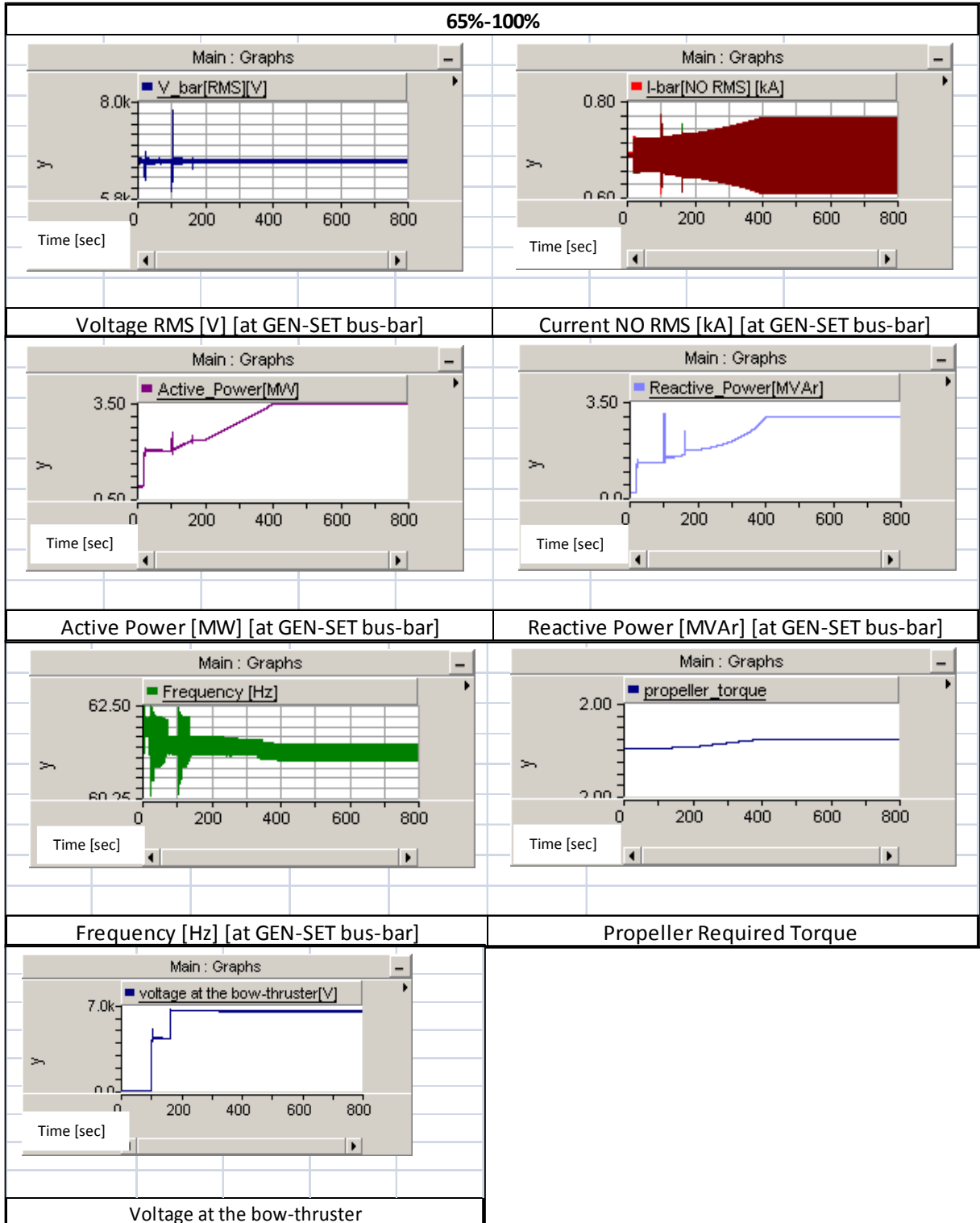


Figure 32

Diploma Thesis

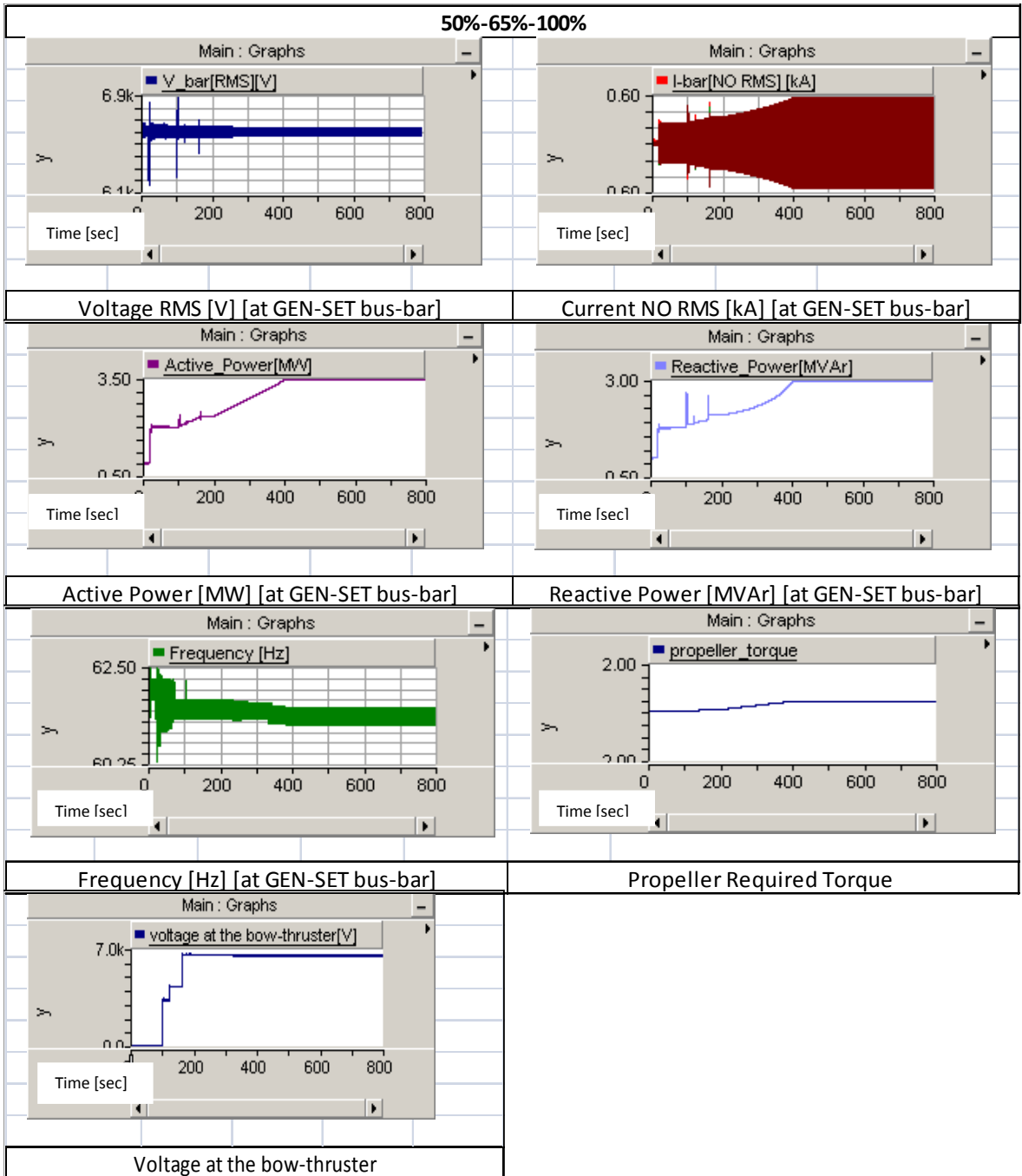
- Waveforms representation regarding simulations applied to 6600V generator bus-bar

Waveform Group 2



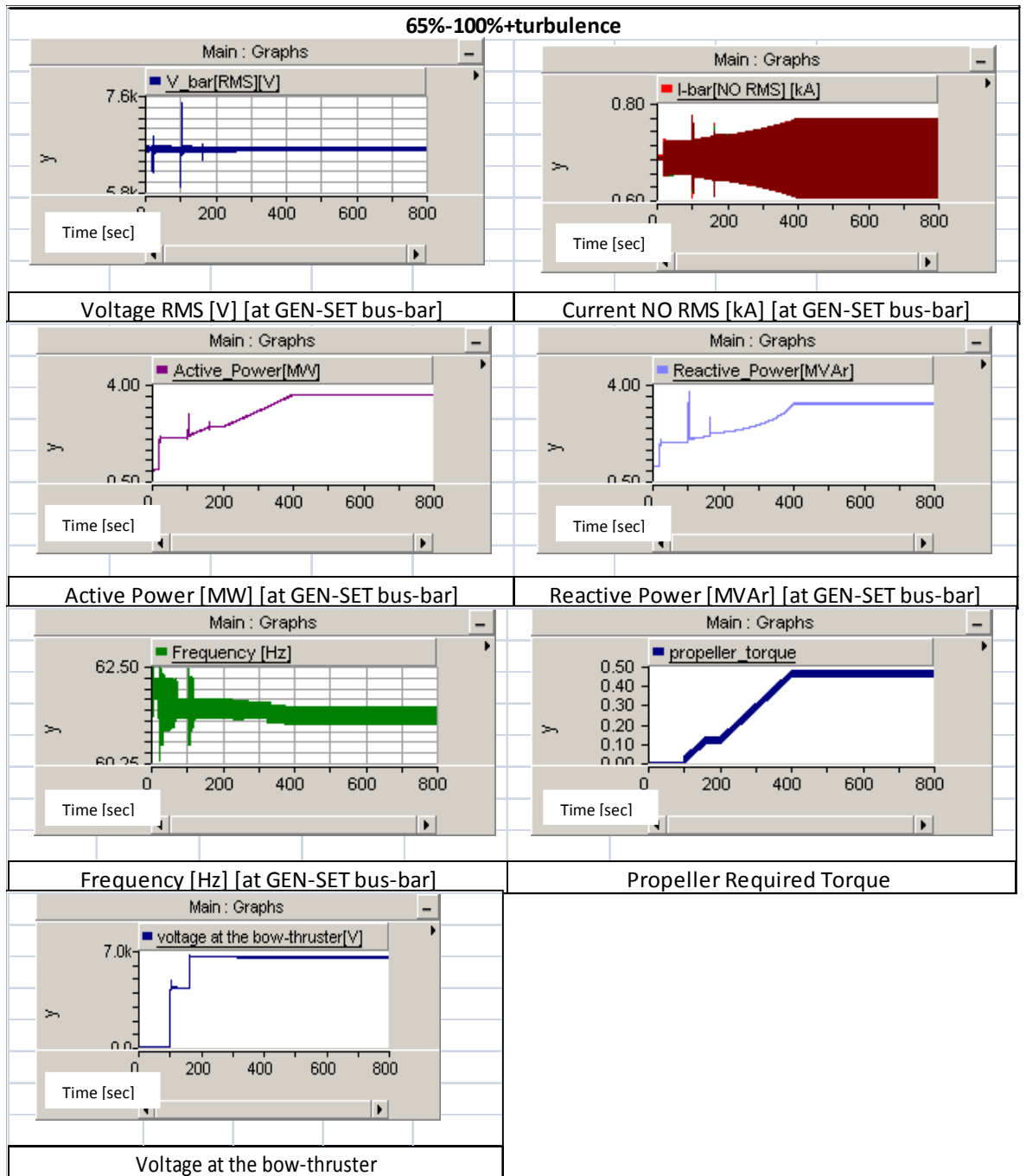
Diploma Thesis

Waveform Group 3



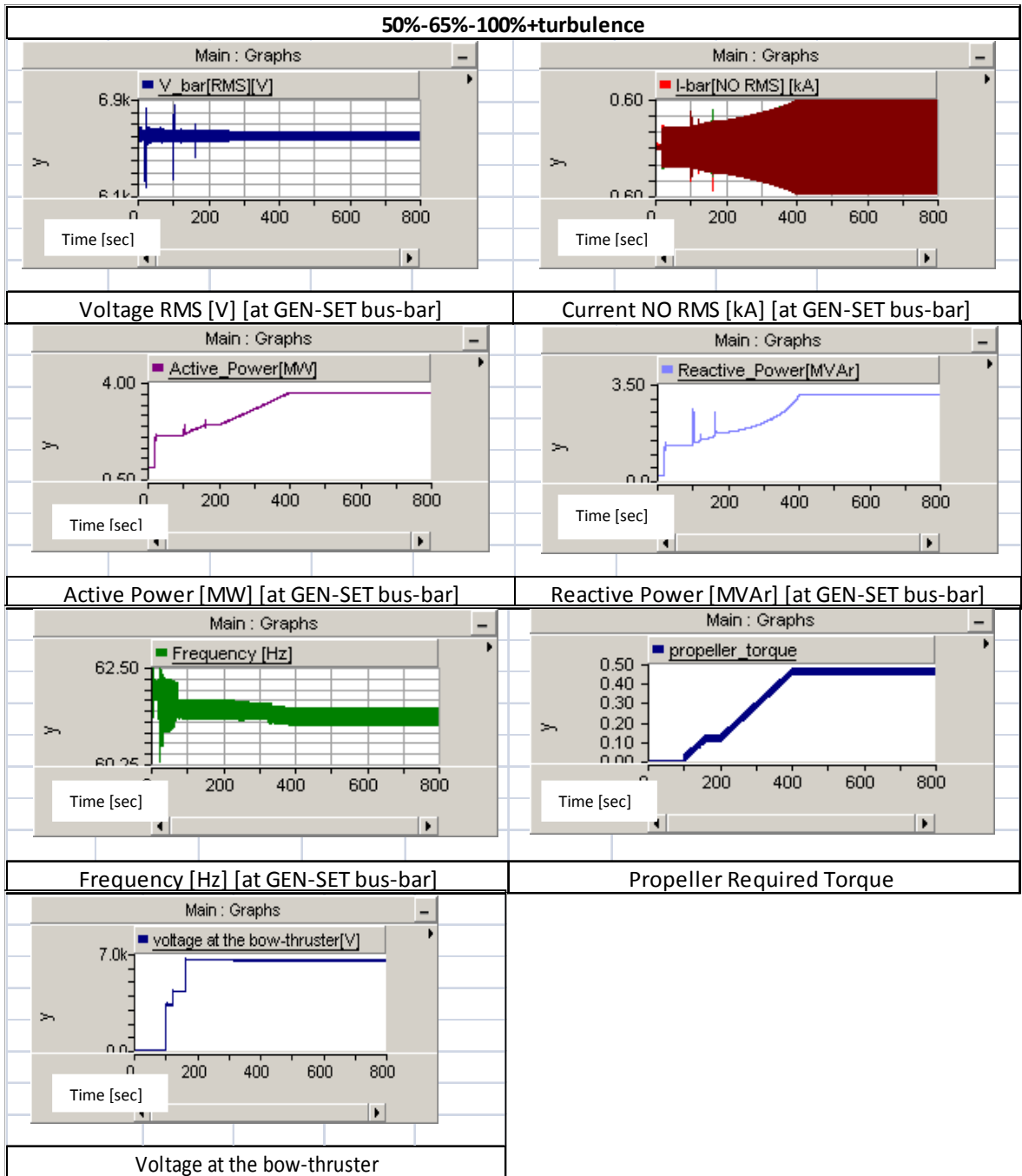
Diploma Thesis

Waveform Group 4



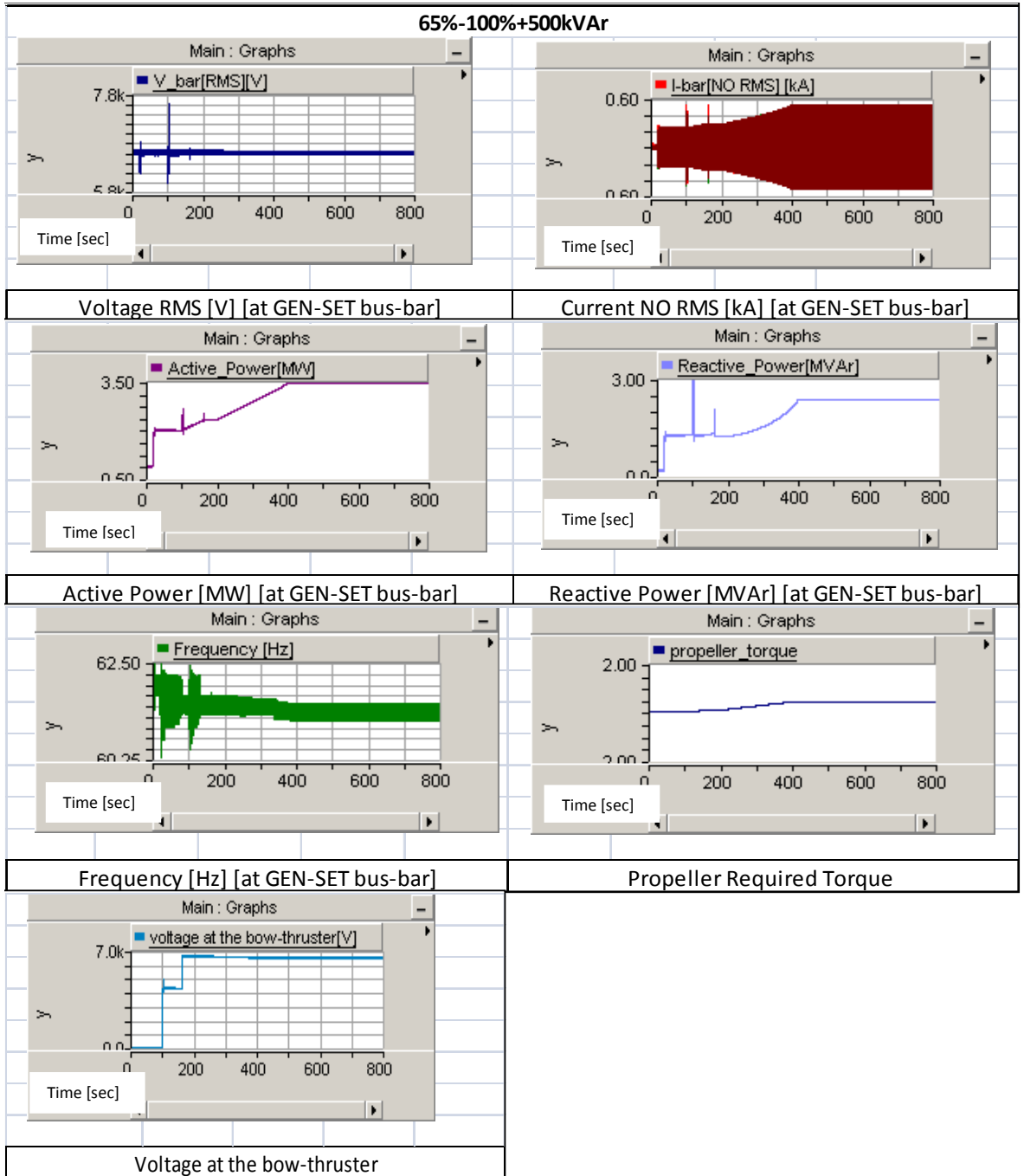
Diploma Thesis

Waveform Group 5



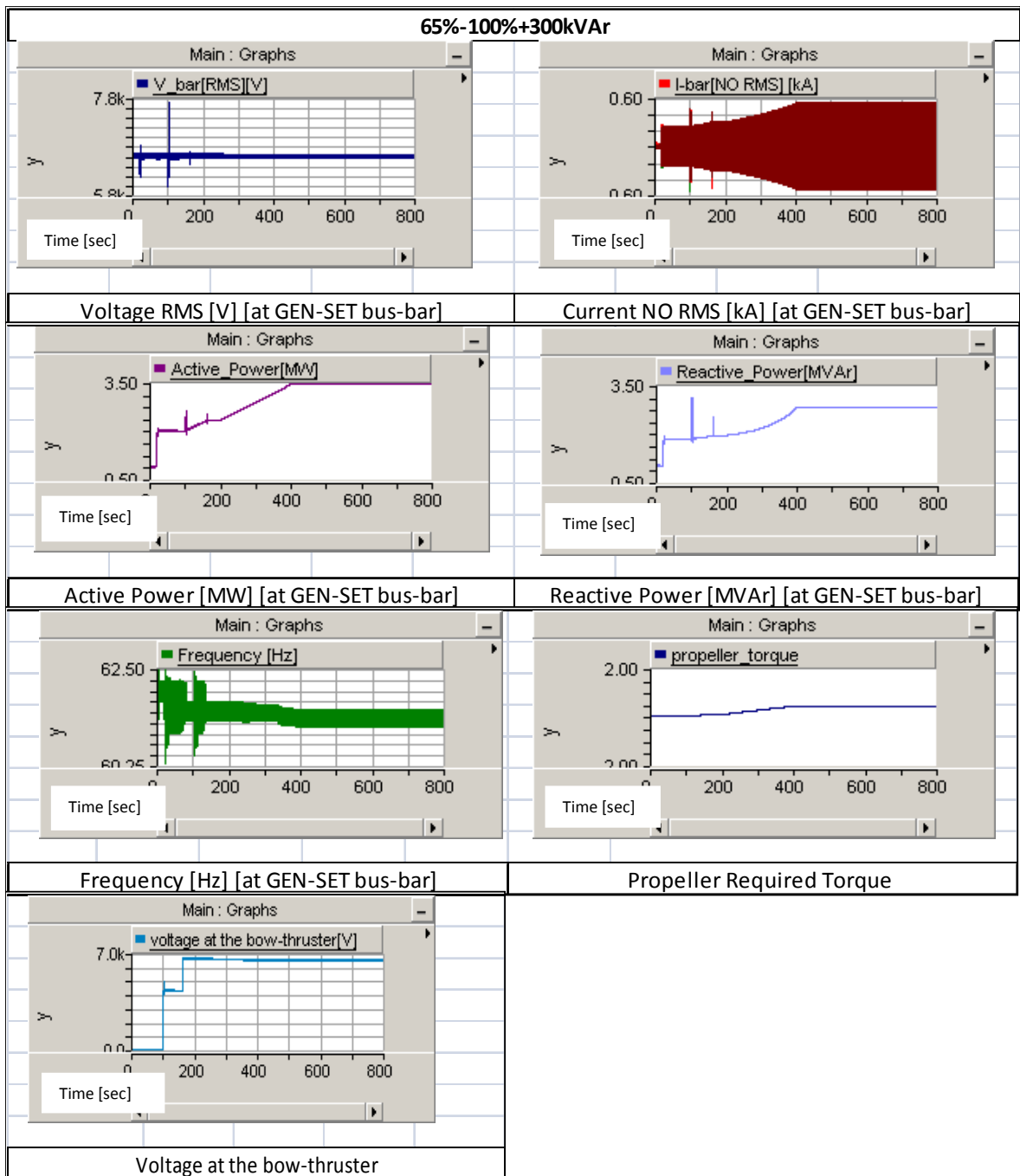
Diploma Thesis

Waveform Group 6



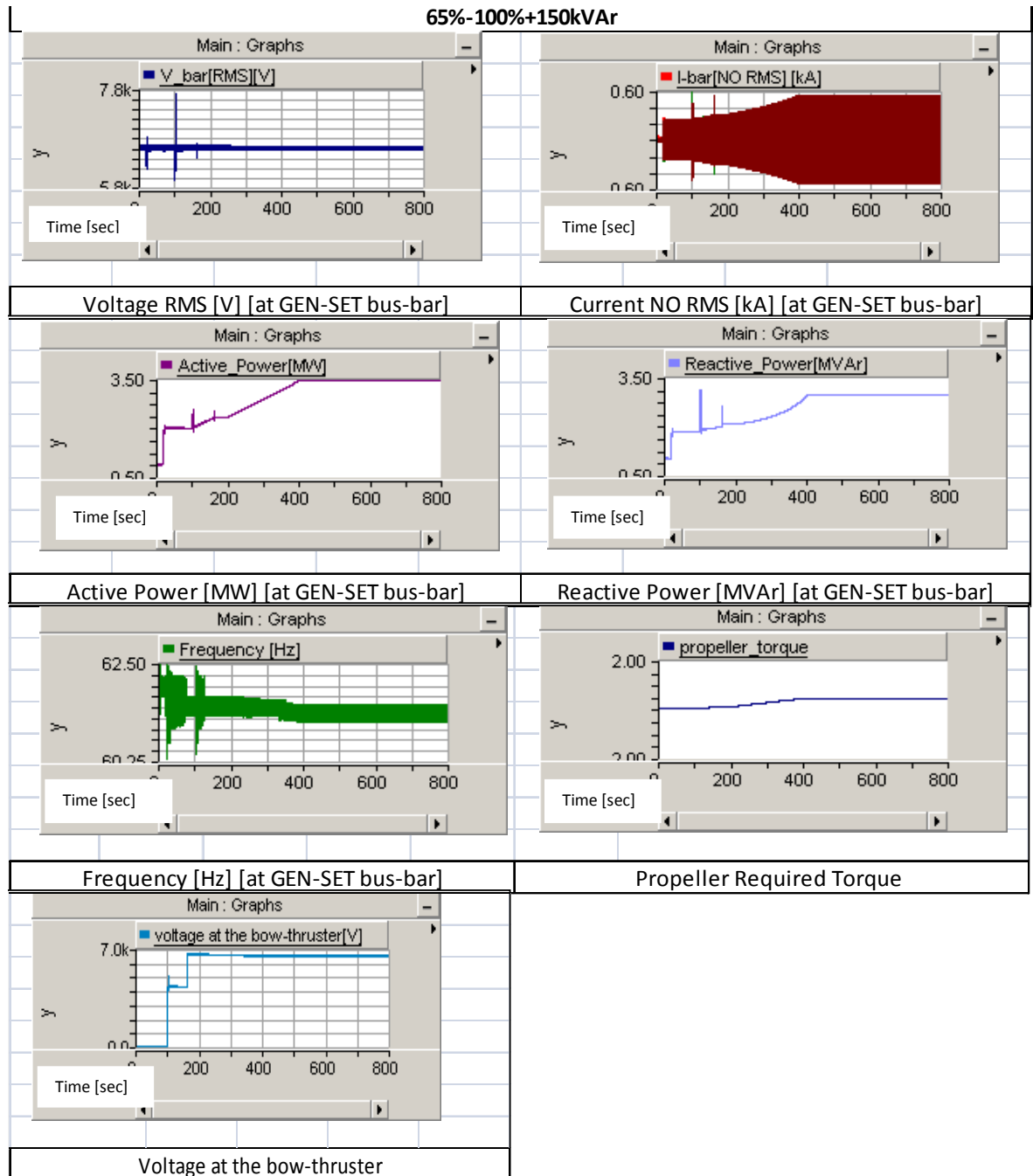
Diploma Thesis

Waveform Group 7



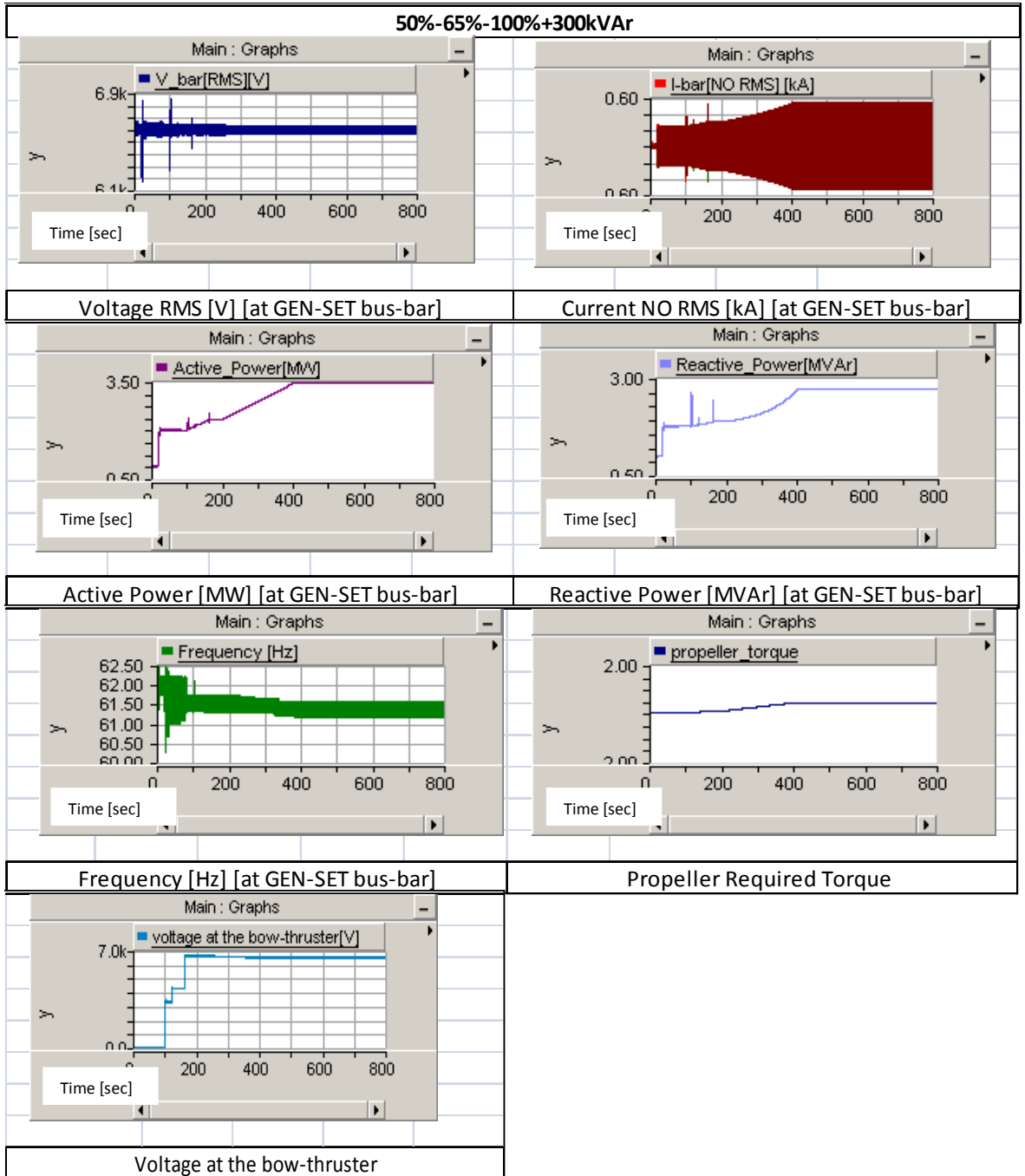
Diploma Thesis

Waveform Group 8



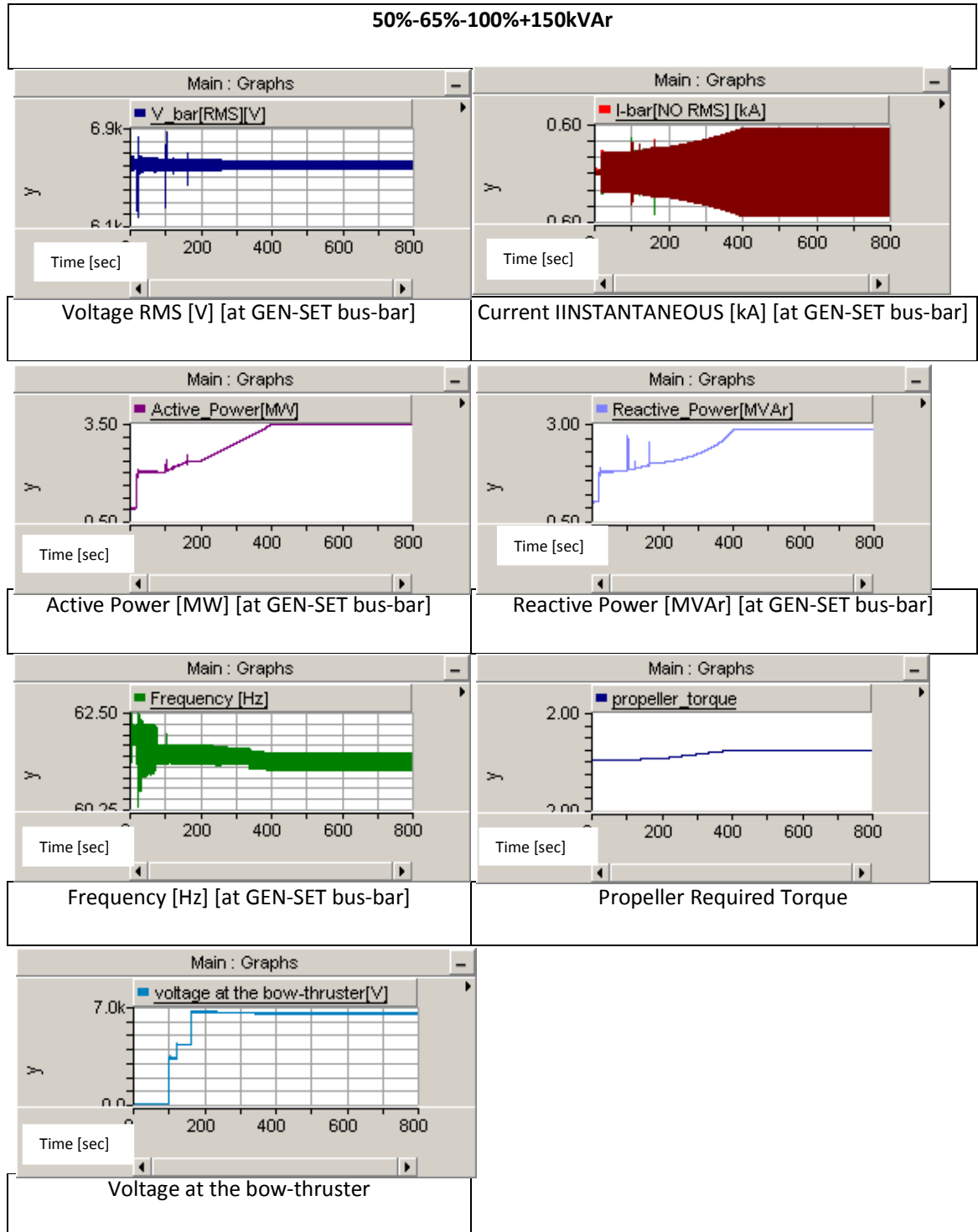
Diploma Thesis

Waveform Group 9



Diploma Thesis

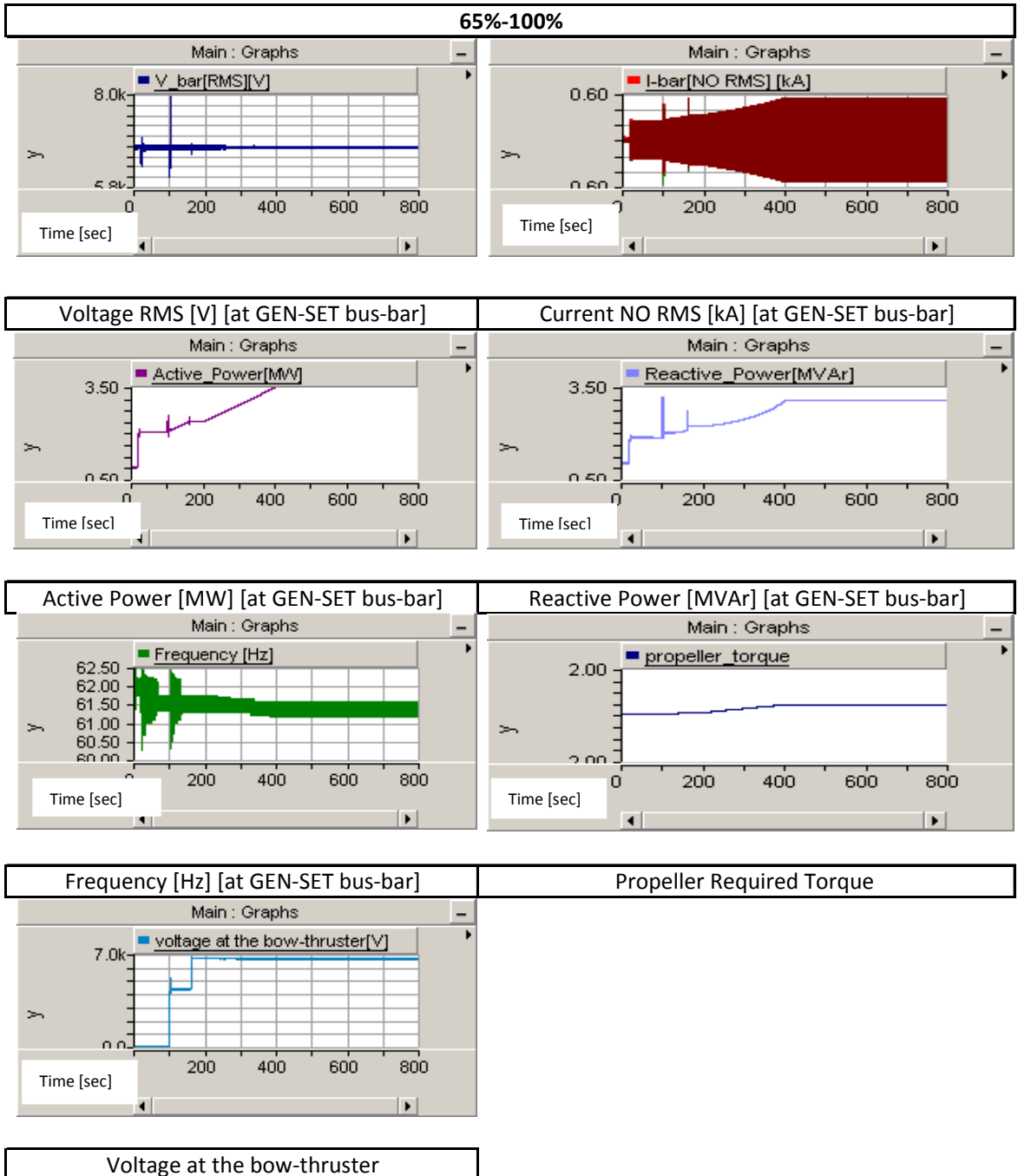
Waveform Group 10



Diploma Thesis

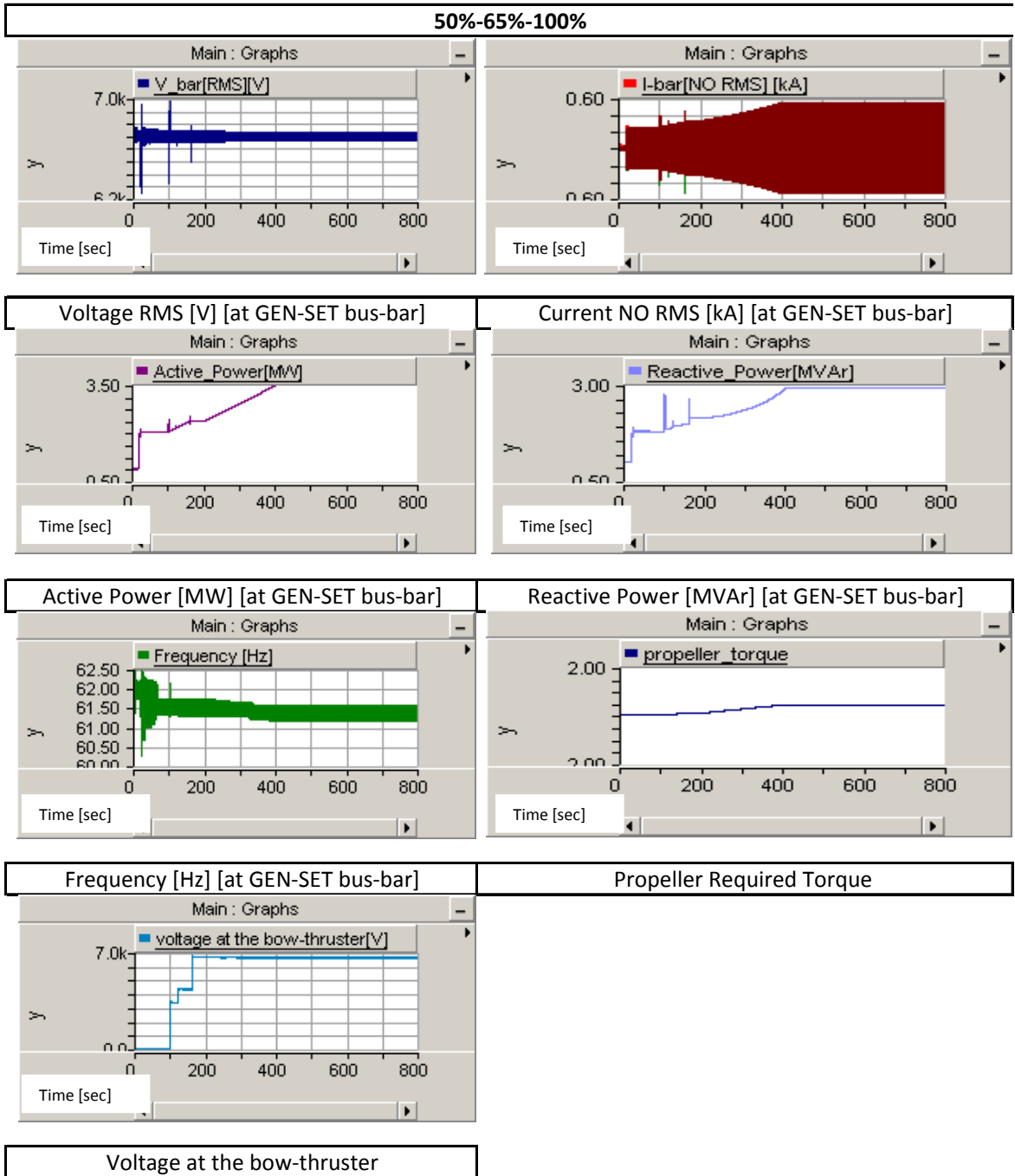
- Waveforms representation regarding simulations applied to 6700V generator bus-bar.

Waveform Group 11



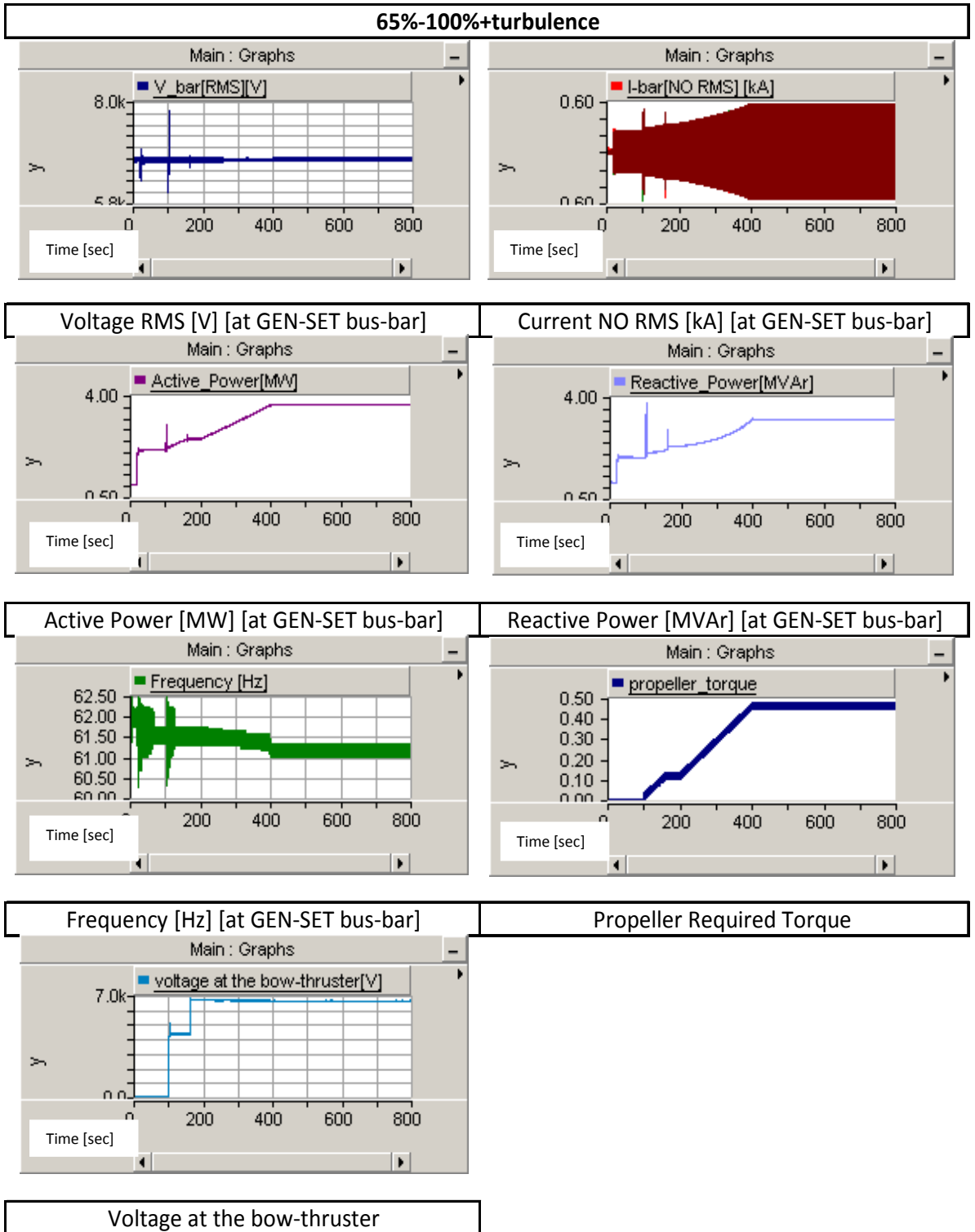
Diploma Thesis

Waveform Group 12



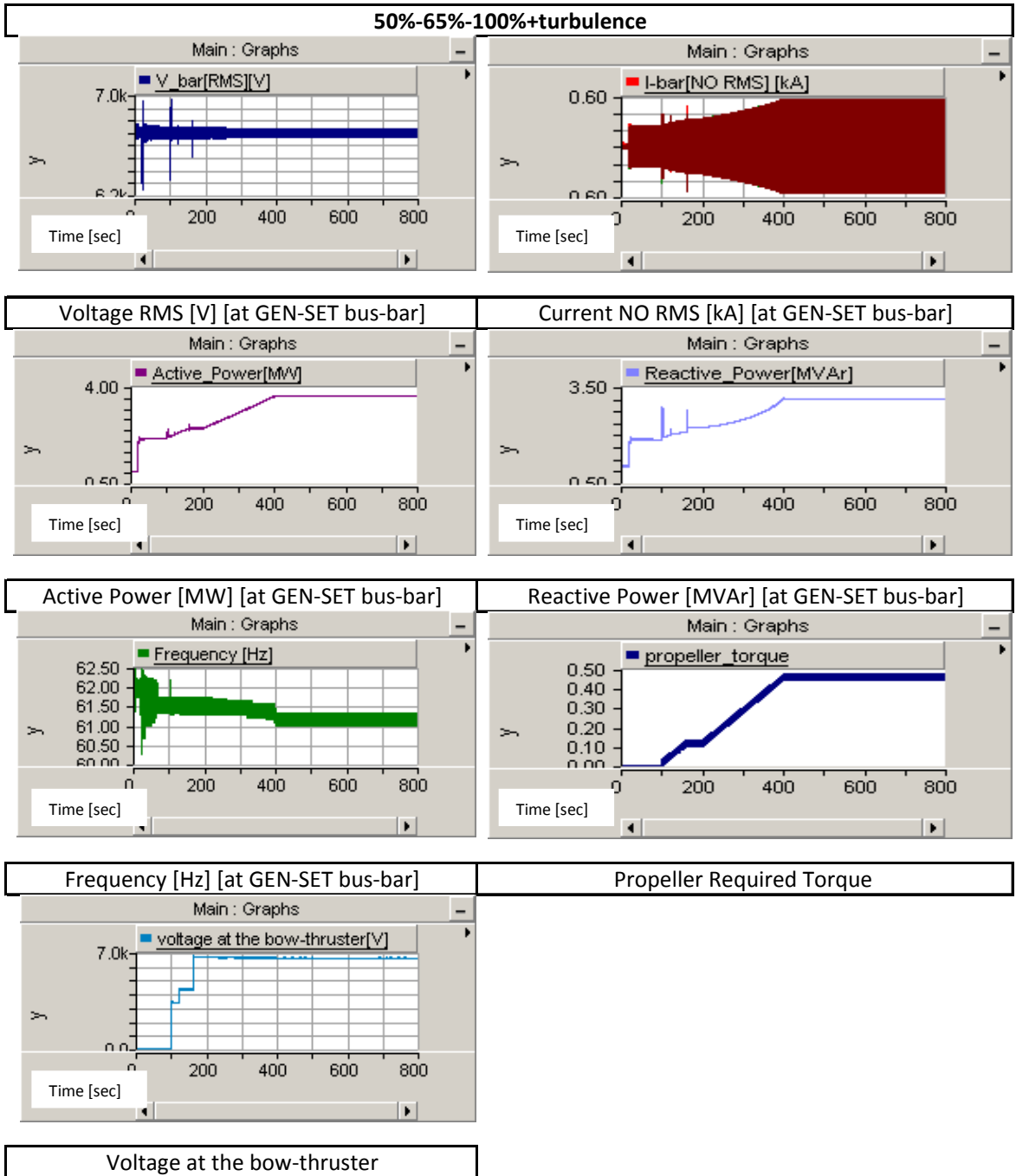
Diploma Thesis

Waveform Group 13



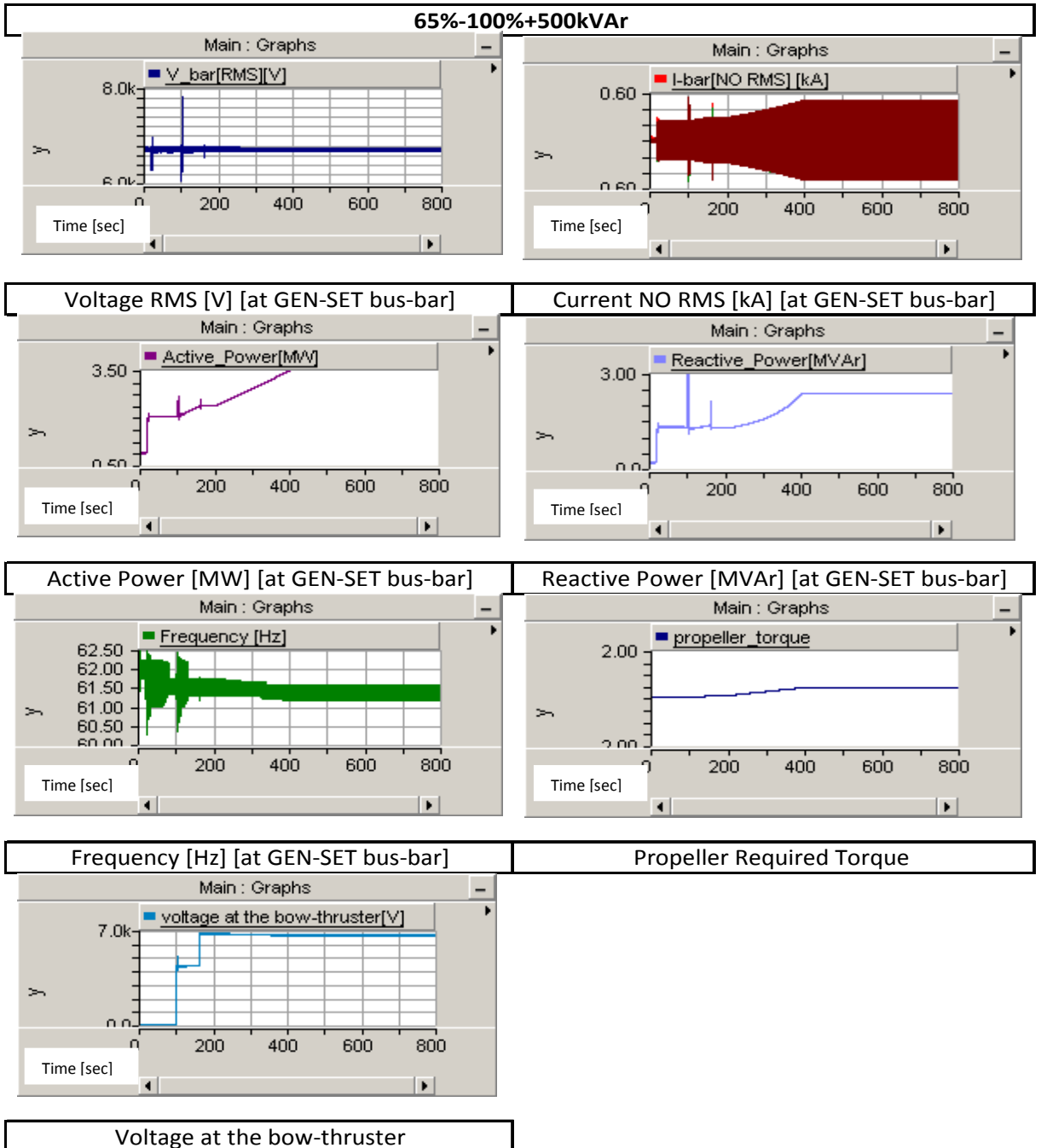
Diploma Thesis

Waveform Group 14



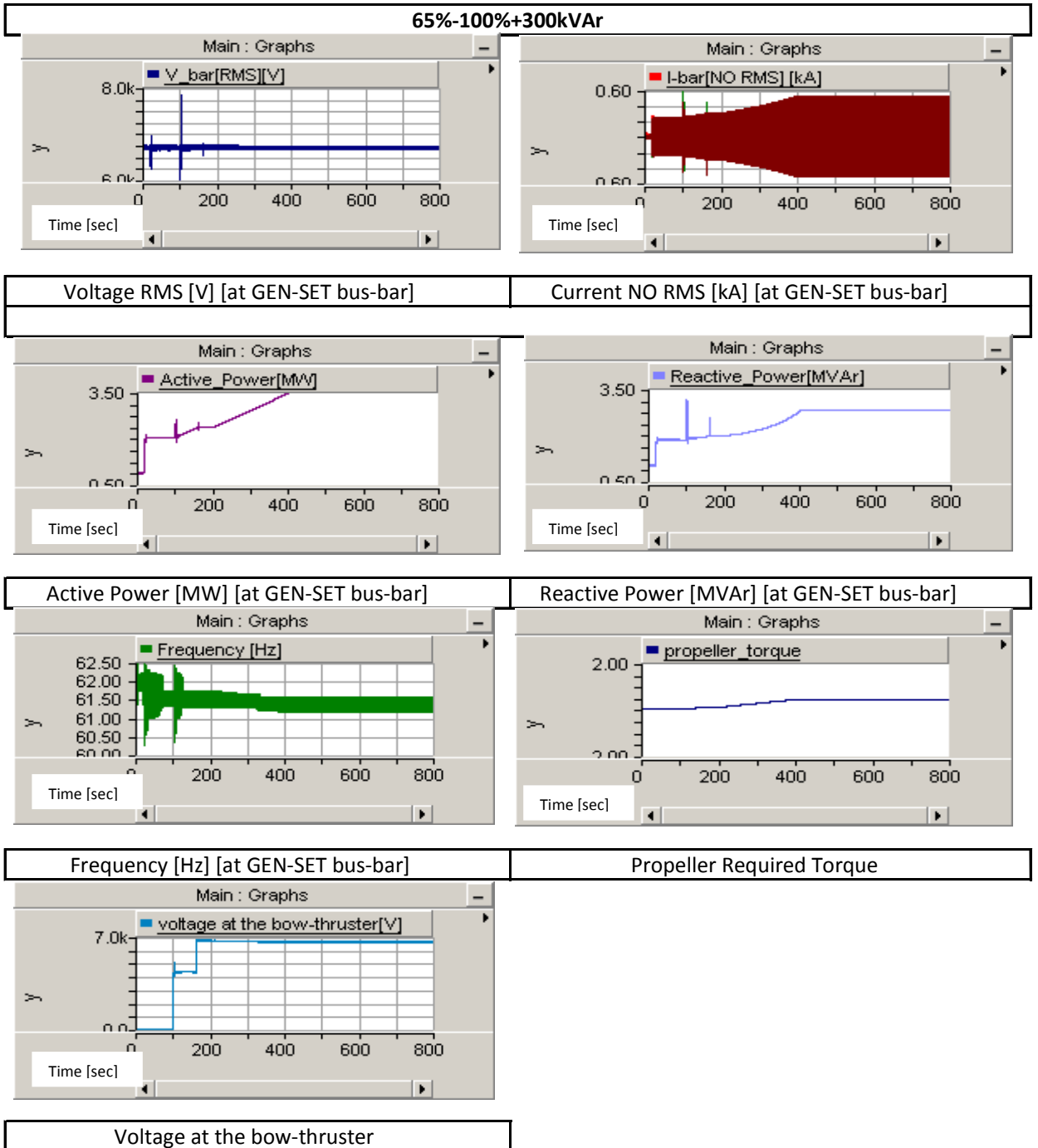
Diploma Thesis

Waveform Group 15



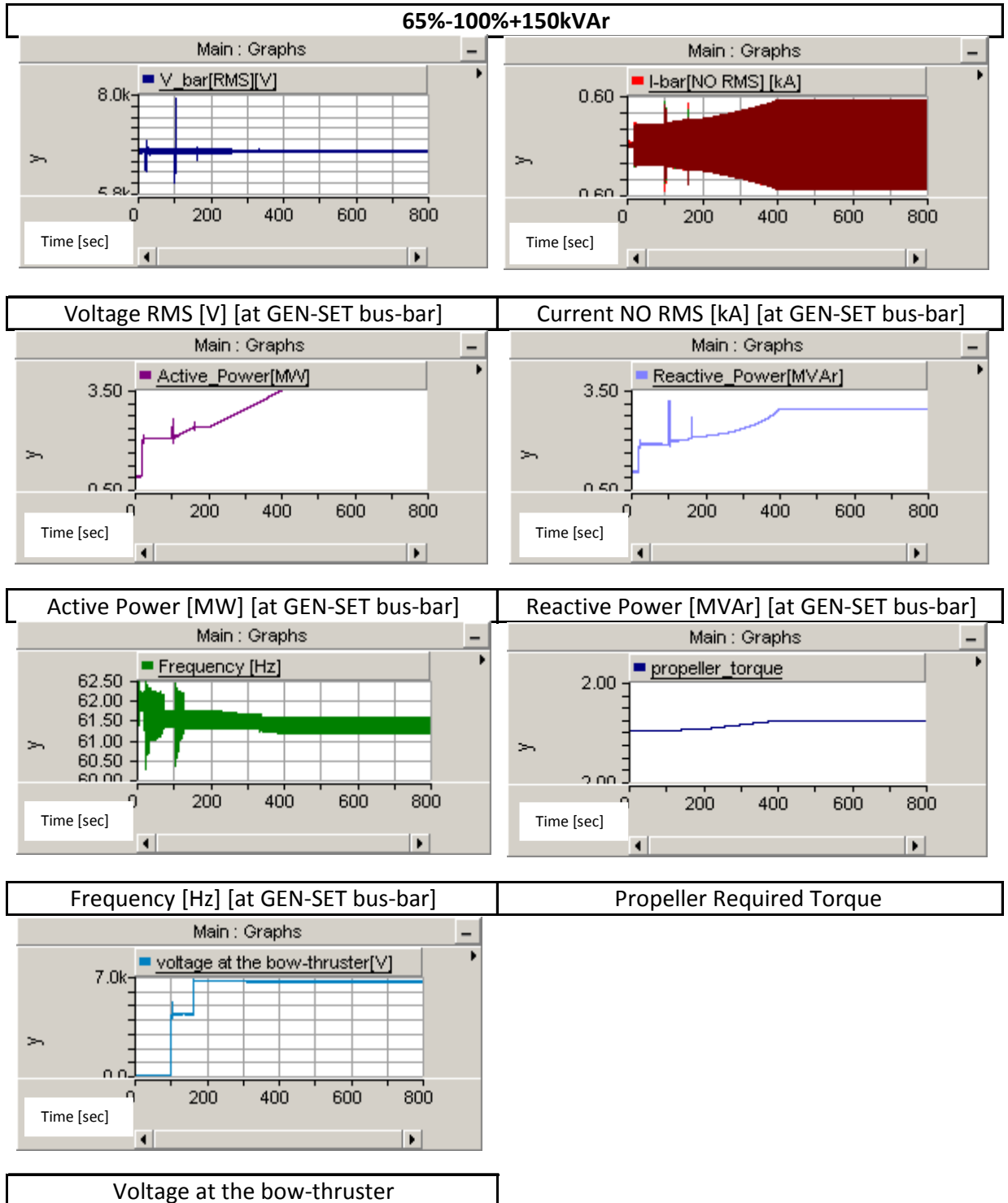
Diploma Thesis

Waveform Group 16



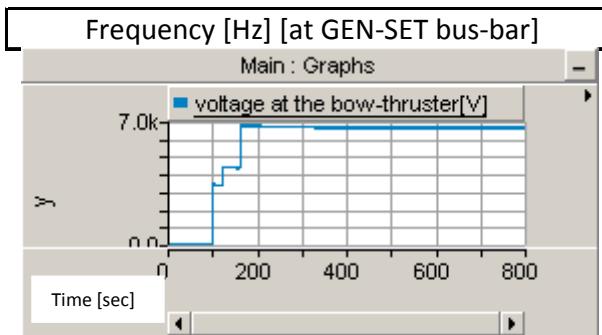
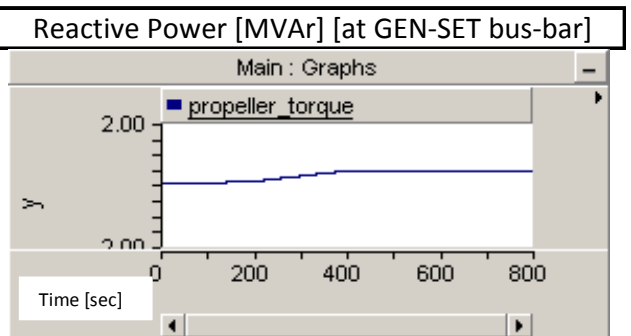
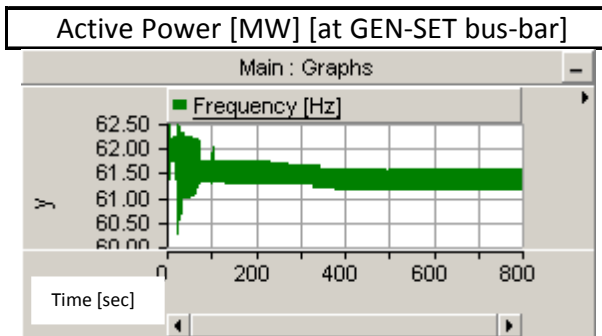
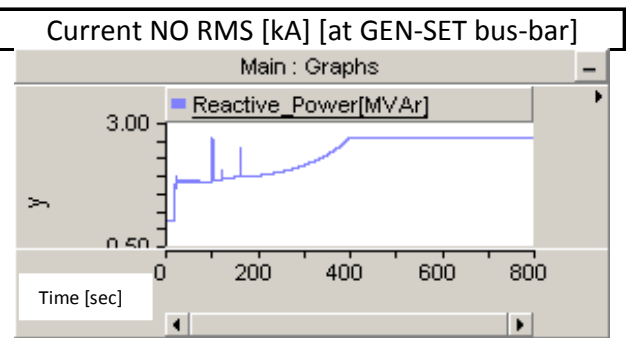
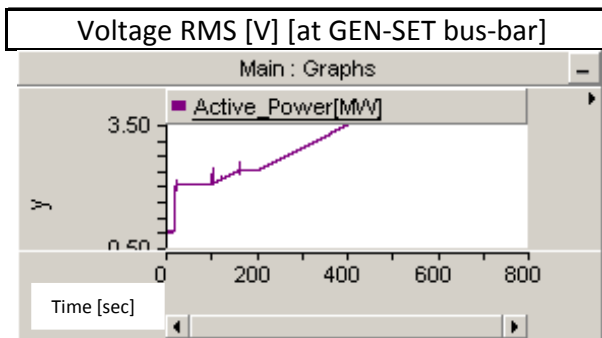
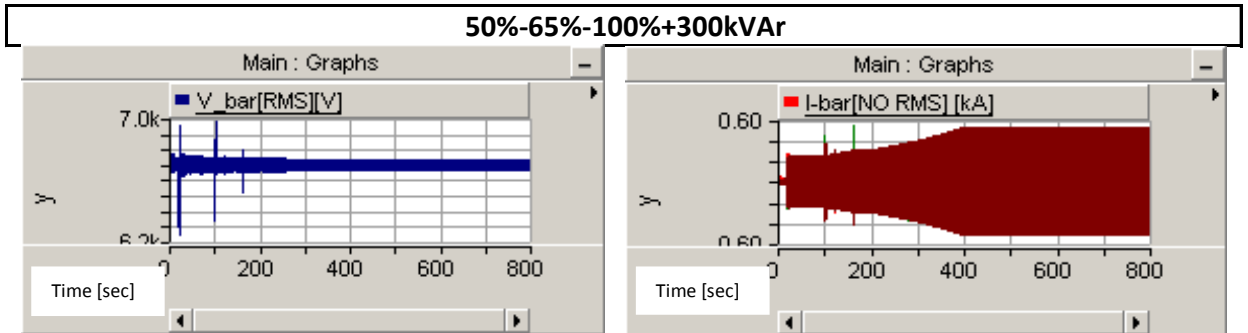
Diploma Thesis

Waveform Group 17



Diploma Thesis

Waveform Group 17

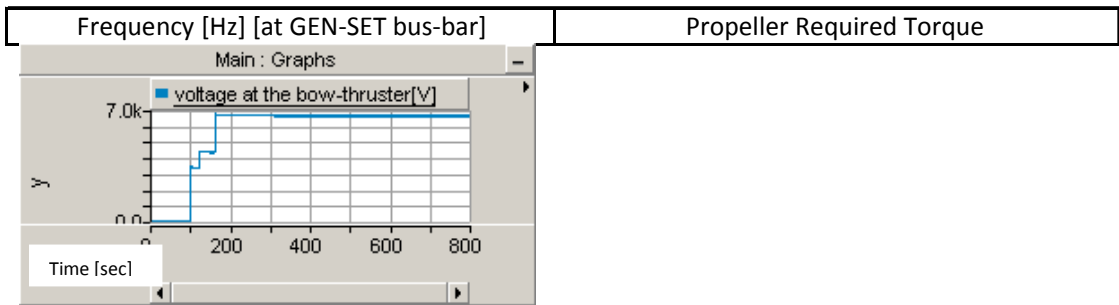
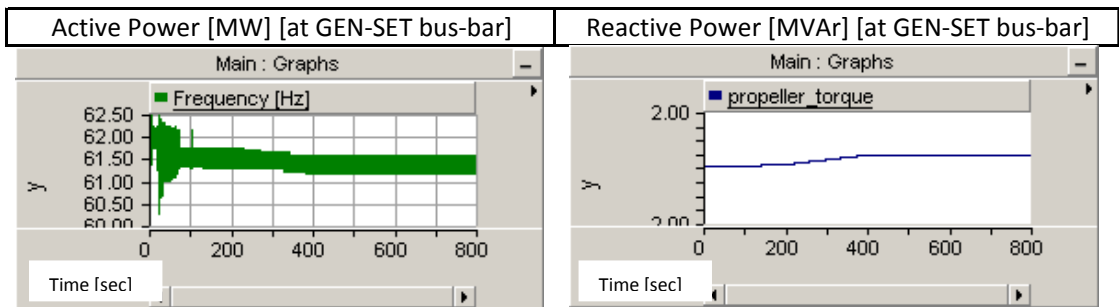
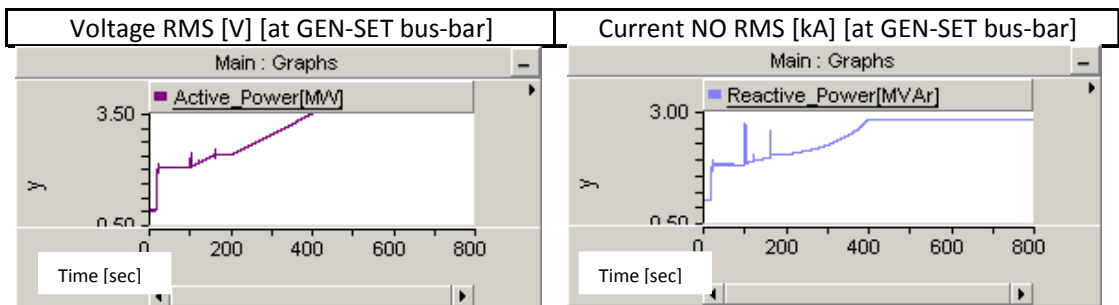
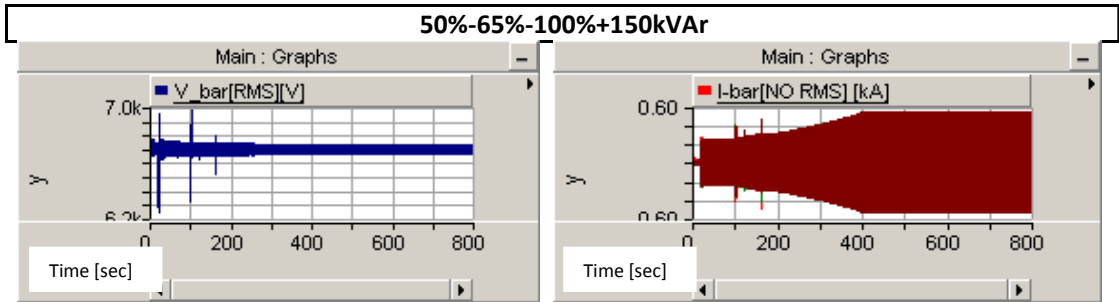


Propeller Required Torque

Voltage at the bow-thruster

Diploma Thesis

Waveform Group 18



Voltage at the bow-thruster

Diploma Thesis

In addition to the previous simulations, regarding the 6600V study cases as well as the three scale autotransformer application (50%-65%-100%) two more simulations were run for 5.0sec and 10.0 sec time period repetitive switching.

The tables below indicate the waveforms of the RMS phase-to-phase voltage, instantaneous value current, active and reactive power, and frequency measured at the common bus-bar of the two generators.

In this case it should also be mentioned that the repetitive switching takes place during the starting up procedure of the motor and not while the motor has reached its nominal speed. This happens because it is highly possible to be used by the captain for emergency maneuvering requirements when he may not be aware, if the motor has reached its nominal speed or not. In this case, the simulations results are on the safe case of the problem.

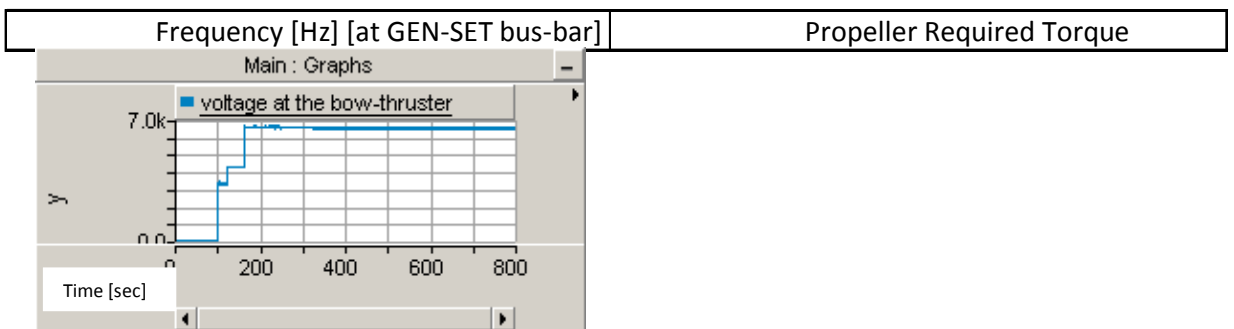
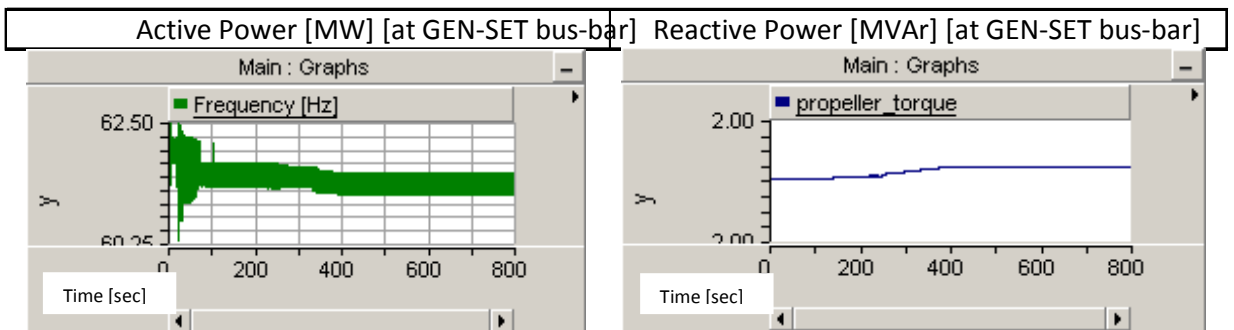
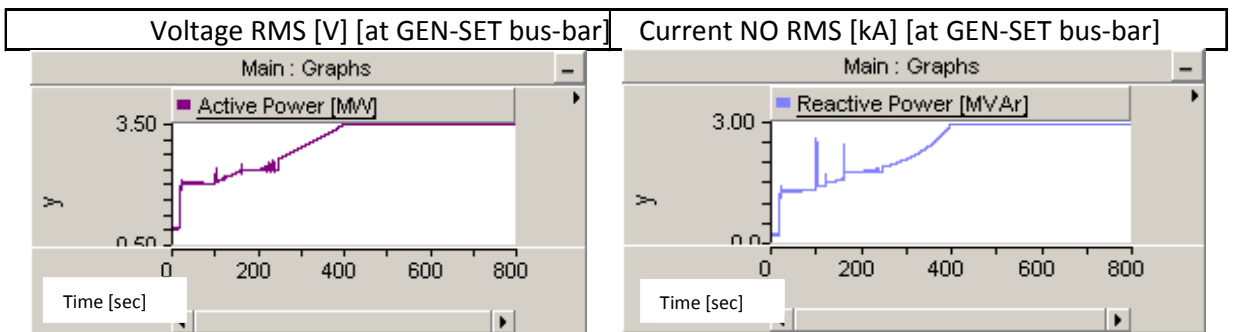
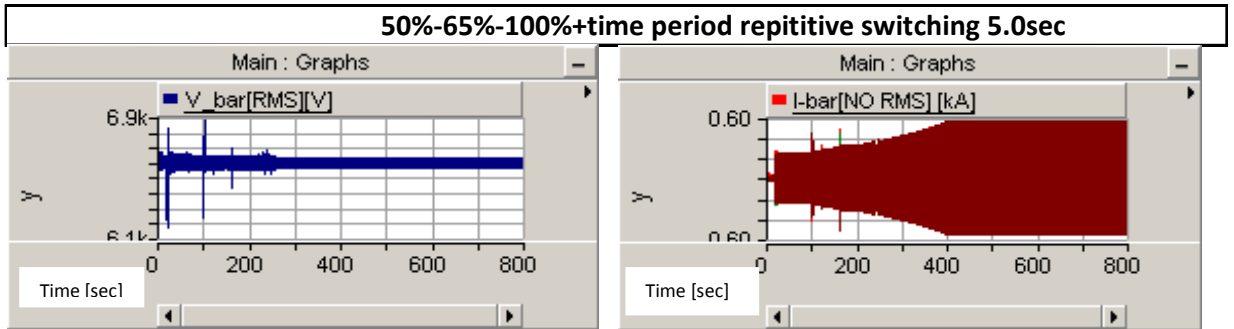
The tabulated results refer to the maximum or minimum value of each index concerning that the simulation results must strictly be taken into consideration after 90.0sec.

	50%-65%-100%	
	time period repetitive switching 5.0sec	time period repetitive switching 10.0sec
Vrms(min)(V)	6216.00	6217.00
Vrms(max)(V)	6868.96	6868.96
linstant.(max)(kA) [INSTANTANEOUS]	0.56	0.56
Pmax(MW)	3.43	3.43
Qmax(MVAr)	2.92	2.92
fmin(Hz)	61.14	61.00
fmax(HZ)	62.17	62.17

Table 7

Diploma Thesis

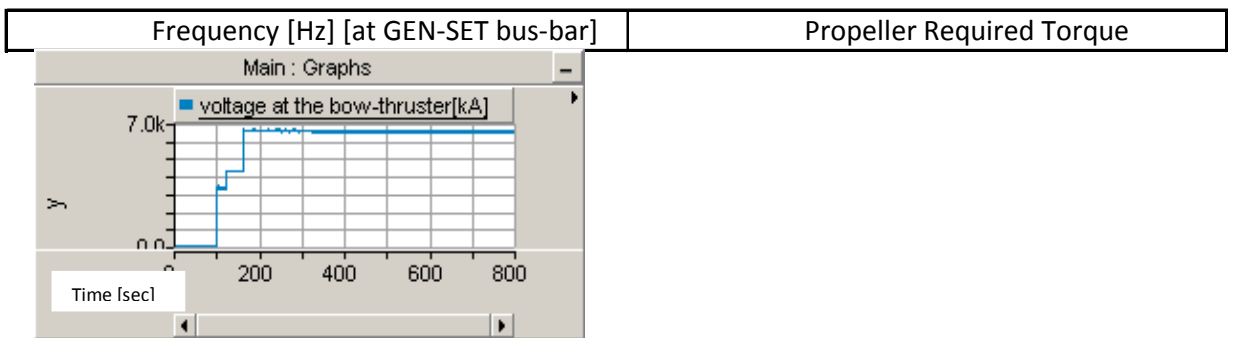
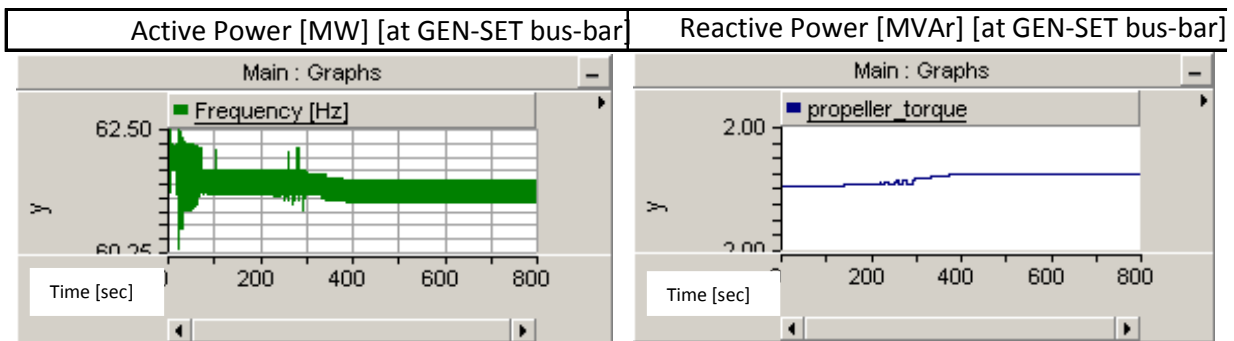
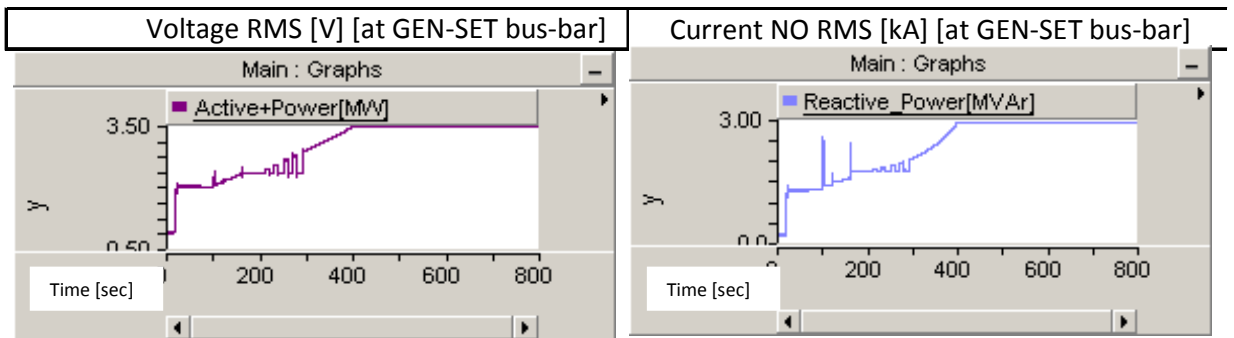
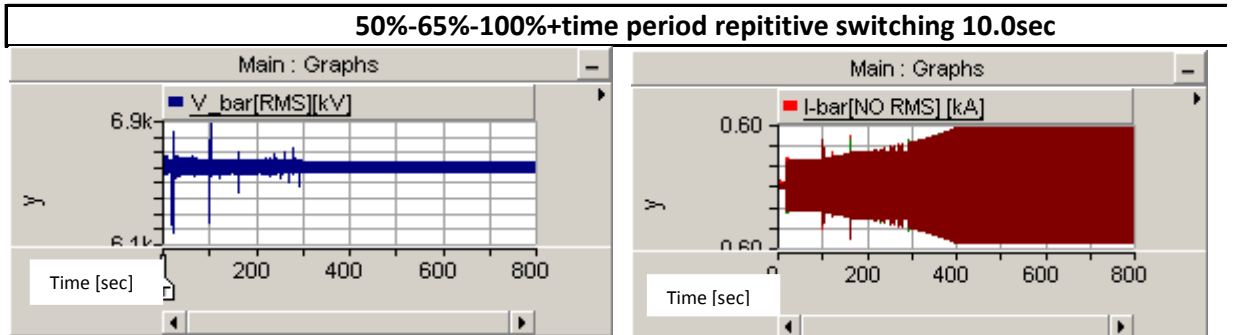
Waveform Group 20



Voltage at the bow-thruster

Diploma Thesis

Waveform Group21



Voltage at the bow-thruster

VI. Conclusions

This chapter deals with stressing the importance of the maneuvering thruster start-ups in the electric power quality of the entire ship grid. It is further shown that the existing standardization status is not sufficient and has to be improved. This argumentation is enriched by presenting the analysis results of two actual ship case studies with troublesome thruster operation, namely a car-passenger ferry and an LNG carrier.

Thus, on the one hand, it is recommended that the voltage-transient recovery test of the generators is performed by considering a thruster start-up to be the sudden-load specified by the standards.

On the other hand, it is recommended to exploit the experience on pulsed loads standardization where numerical limits of the load power demands with respect to supplying generator capacity exist. These power ratios compared to the corresponding limits can be used as a means of qualitative assessment that a problematic operation of the entire grid is expected. Although, it is shown that thruster units and pulsed loads have similarities and hence these limits could be the same still their numerical values could be modified to thruster units.

Moreover, the ratios of the load power demands with respect to supplying generator capacity could be used as an index for quantitative evaluation of the adverse effect the thruster load provokes on the normal operating condition of the ship grid. Through this approach alternative power supplying schemes could be evaluated and compared, too.

CHAPTER 03

Bow Thruster driven by Wound Rotor Asynchronous Motor

Diploma Thesis

Wound Rotor

I. Introduction & Case Study A,B

In this section, an alternative configuration compromising FPP and wound rotor is investigated.

According to this consideration, variable rotor resistances lead to low inrush currents on starting up process, accompanied by high efficiency and low slip at steady-state condition. This flexibility gives the opportunity to achieve the nominal current on starting-up (by changing the rotor resistance), so in this way there is no need for controllable pitch propeller. In most cases, the rotor resistance change is performed by connecting/disconnecting external resistances, which is highly possible to be regulated.

For the purposes of these academic studies, there are three sets of wound rotor applications. The first one concerns ideal source supply while the second one, a diesel generator driving controllable pitch propeller. The third one refers to ideal source supply, but in this case the motor drives fixed pitch propeller. All of them include cases of normal operation as well as repetitive torque switching of 5.0sec and 10.0sec.

Regarding the previous simulations (squirrel cage motor driving ducted propellers), the assumption that the propeller pitch ratio increases proportionally to the time allows us to consider that the propeller torque increases proportionally to the time.

According to what it has been said, in most cases wound rotor motor is accompanied by fixed pitch propellers. However, for study cases A & B, the assumption that the propeller used is the propeller of the previous simulations (controllable pitch propeller) is made. In addition, the study cases A & B, refer to the HYPOTHETICAL (these cases do not happen in fact) scenario that the propeller required torque increases proportionally to the motor angular speed. Regarding study case C, the driven propeller is supposed to be a fixed pitch one, thus, the required torque increases proportionally to the square of the motor angular speed.

Diploma Thesis

As it has been said, the behavior of the motor can be controlled by attaching variable resistances to the rotor windings controlling in this way the behavior of the motor.

The profile of the external connected variable resistances for this study case (study cases A & B) is shown in figure 33:

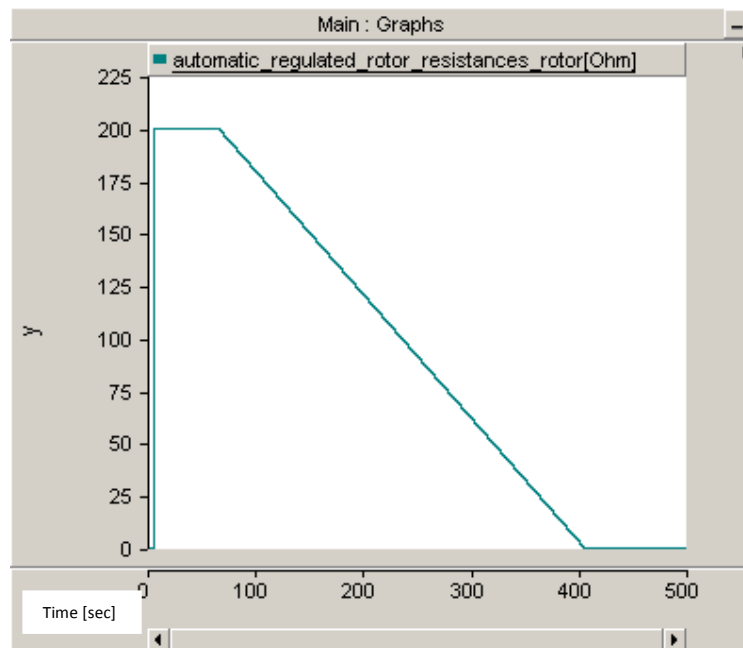


Figure 33

It should be noticed that according to the following current profiles, the starting current is not equal to the nominal despite the fact that all the wound rotor applications include external connected resistances.

Below the tabulated data as well as the represented waveforms of each study case explain how the motor behaves for three loading types (normal loading, torque switching with time period (5.0sec , 10.0sec)).

Diploma Thesis

<i>Case Studies</i>	<i>Characteristics</i>				
	<i>Motor type</i>	<i>Power Supplier</i>	<i>Propeller</i>	<i>Resistance Time Period Regulation</i>	<i>Required Torque</i>
<i>Case Study A</i>	Wound Rotor	Ideal Source	CPP	340.0 sec	$T \sim n^*$
<i>Case Study B</i>	Wound Rotor	Diesel Generator	CPP	340.0 sec	$T \sim n^*$
<i>Case Study C</i>	Wound Rotor	Ideal Source	FPP	20 sec	$T \sim n^2$

* HYPOTHETICAL scenarios.

Table 8

Before any attempt to present simulation results, the followings should be mentioned (**They refer to study cases A & B**):

- Regarding three phase currents, the current waveform graphs refer to instantaneous values, while the tables in the areas which contain three phase current values refer to RMS values.
- The simulation results, which are included in the table 9 refer to the maximum or minimum value of specific magnitudes as they have been recorded throughout the whole time duration of the simulation and not necessarily at the instance, starting up begins.
- In the same way as in squirrel cage application, the switching operation concerns the propeller pitch ratio and not the voltage supply to the motor.
- The high resistance application lasts 60.0sec as well as the external connected resistance reduction lasts 340.0sec (study case A & B). Moreover, the motor is supposed to be equipped with its own cooling system independent from its fan rotation.

II. Data Representation

Ideal/Continuous Source (Study case A)		Ideal/Continuous Source repetitive switching time period 5.0sec. (Study case A)	Ideal/Continuous Source repetitive switching time period 10.0sec. (Study case A)
Vrms(min)(V)	6600	6600	6600
Vrms(max)(V)	6600	6600	6600
I RMS(max)(kA)	1.00	1.00	1.00
Pmax(MW)	1.8704	1.8704	1.871
Qmax(MVAr)	1.407	1.407	1.407
fmin(Hz)	59.95	59.95	59.95
fmax(HZ)	60.05	60.05	60.05

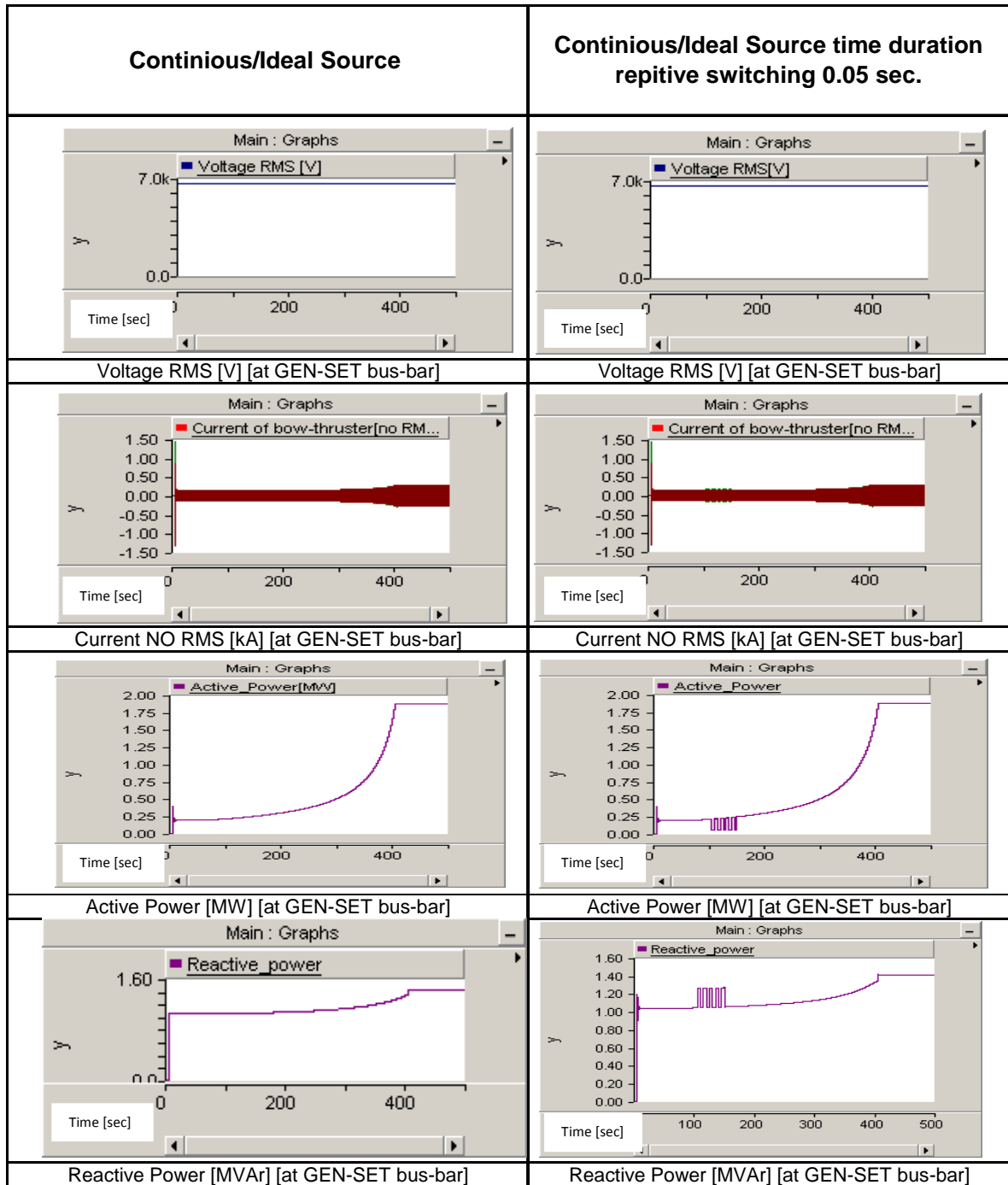
Diploma Thesis

Diesel Generator Source (<i>Study case B</i>)		Diesel Generator Source repetitive switching time period 5.0sec. <i>(Study case B)</i>	Diesel Generator Source repetitive switching time period 10.0sec. <i>(Study case B)</i>
Vrms(min)(V)	4689.07	4756	4760
Vrms(max)(V)	7537.66	7698.23	7700
I RMS (max)(kA)	0.52	0.29	0.29
Pmax(MW)	2.42	2.695	2.695
Qmax(MVAr)	2.91	2.871	2.871
fmin(Hz)	56.34	56.5	56.5
fmax(HZ)	71.11	70.92	70.92

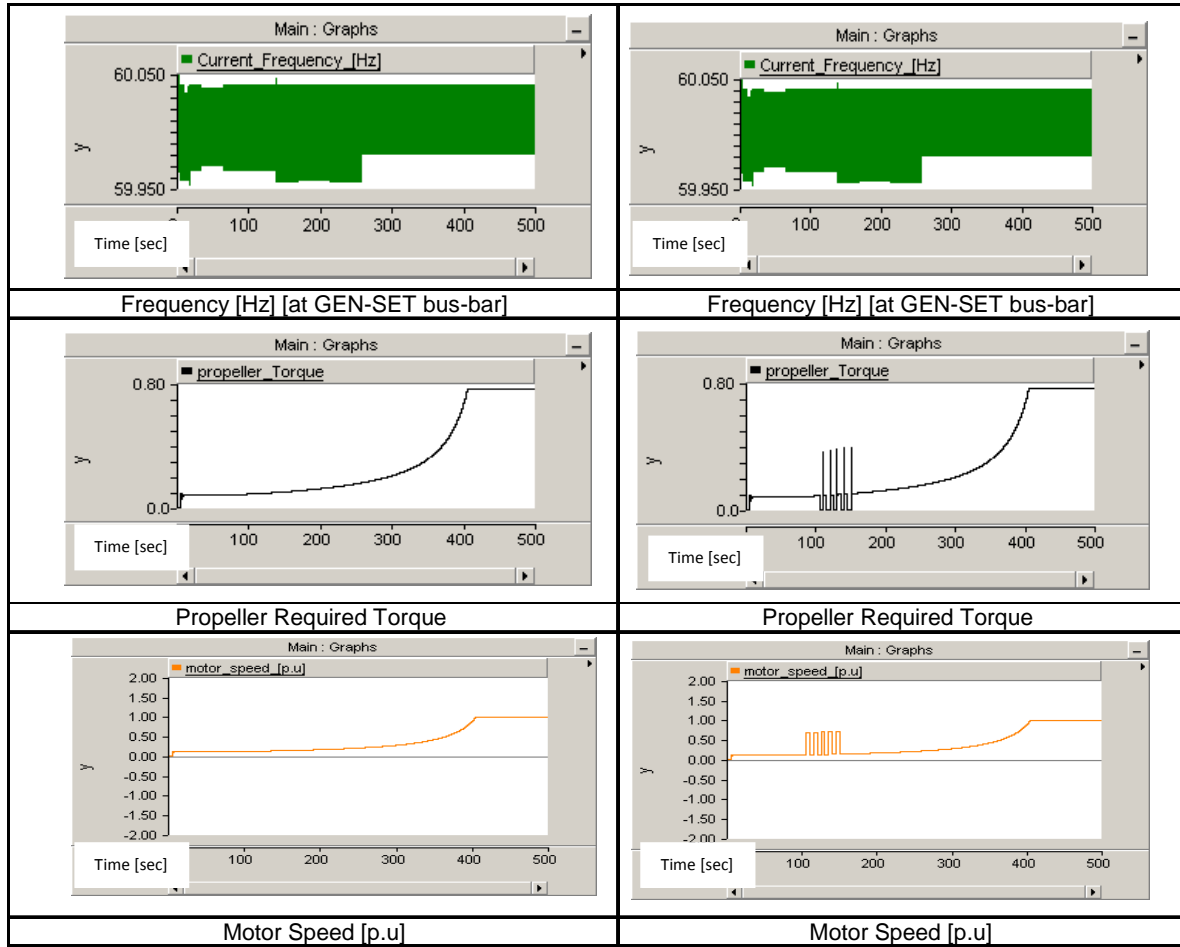
Table 9

Diploma Thesis

Waveform Group 22 (Study Case A)



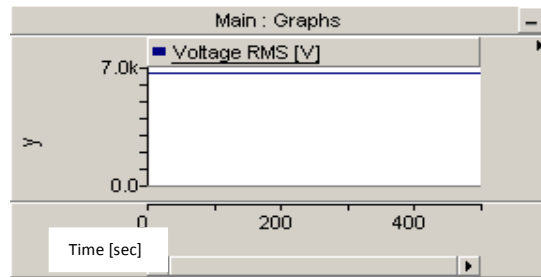
Diploma Thesis



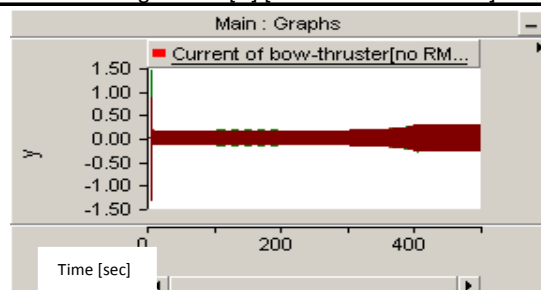
Diploma Thesis

Waveform Group 23 (Study Case A)

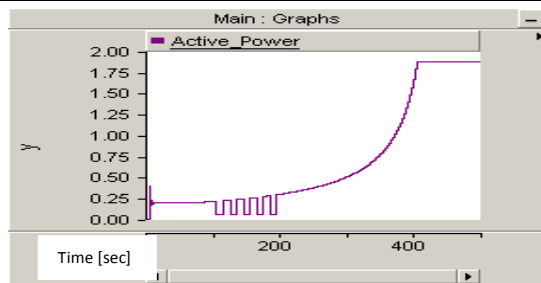
**Continious/Ideal Source time duration
reptive switching 1.0 sec.**



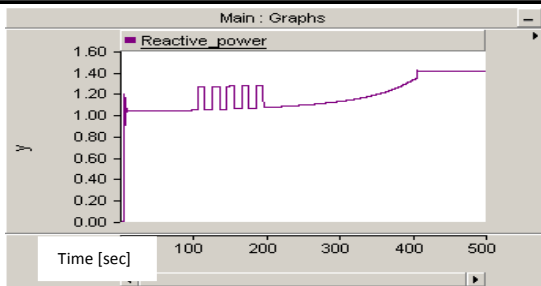
Voltage RMS [V] [at GEN-SET bus-bar]



Current NO RMS [kA] [at GEN-SET bus-bar]

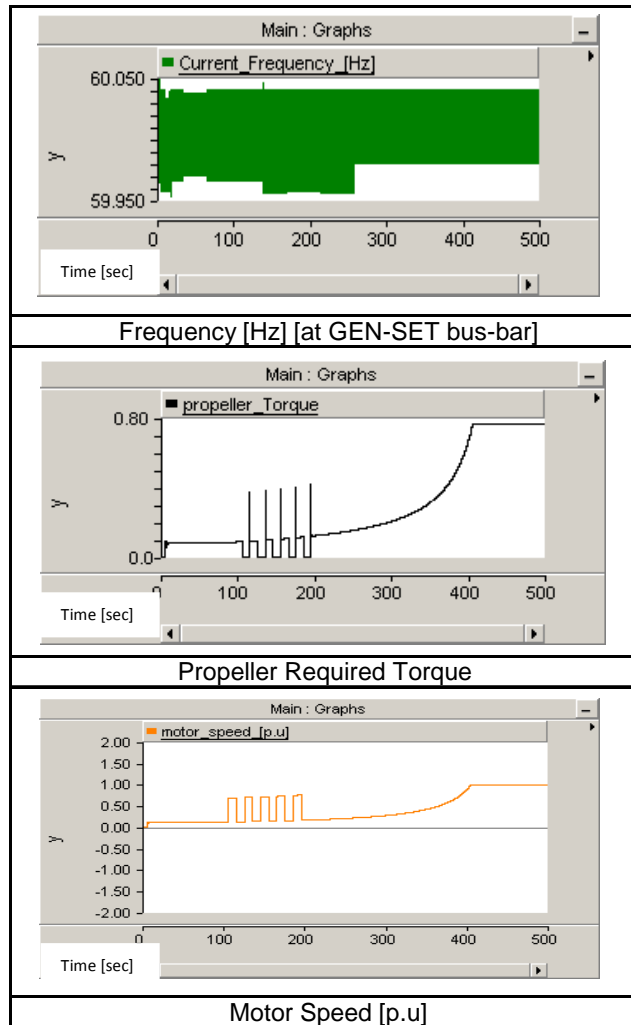


Active Power [MW] [at GEN-SET bus-bar]



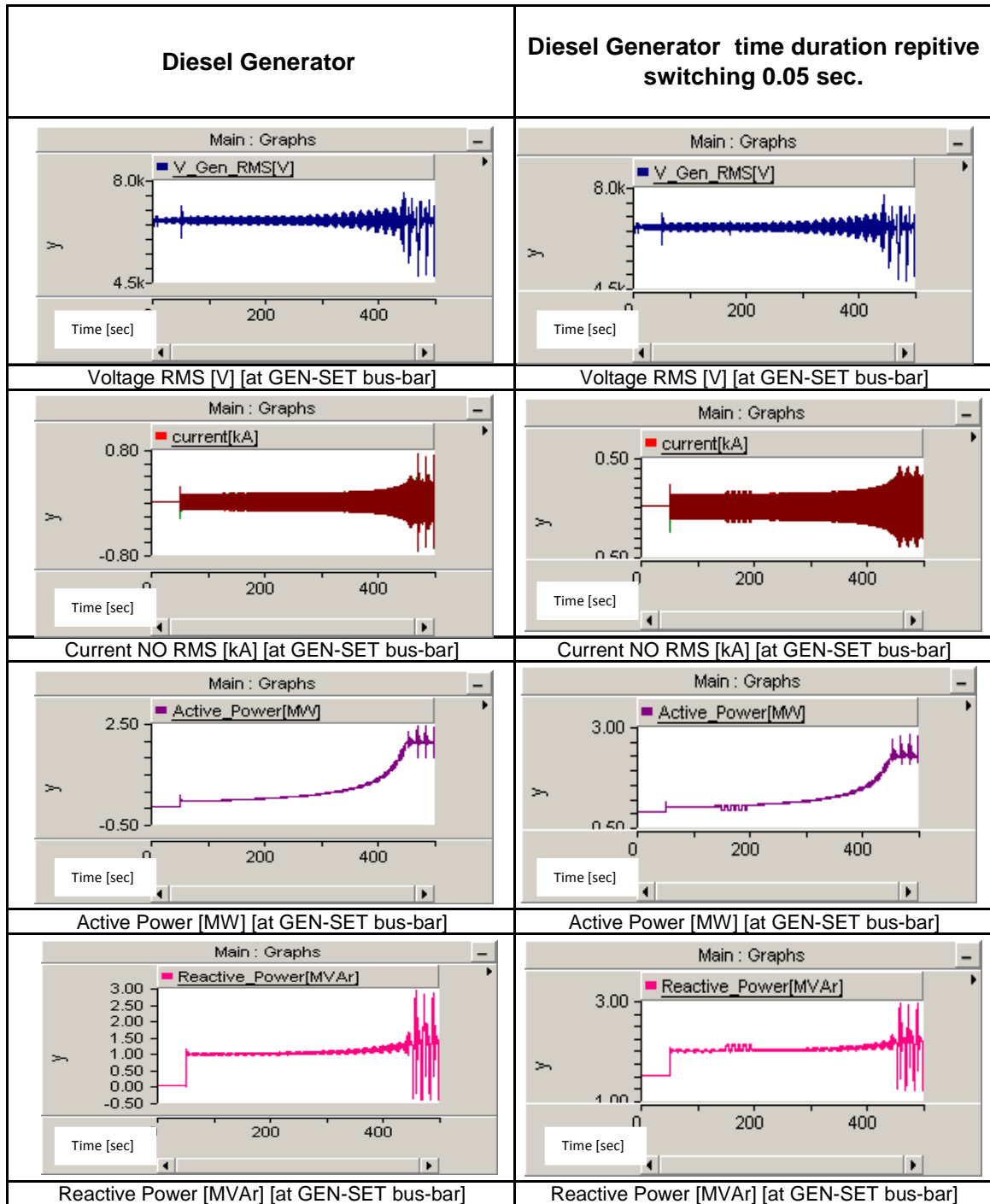
Reactive Power [MVar] [at GEN-SET bus-bar]

Diploma Thesis

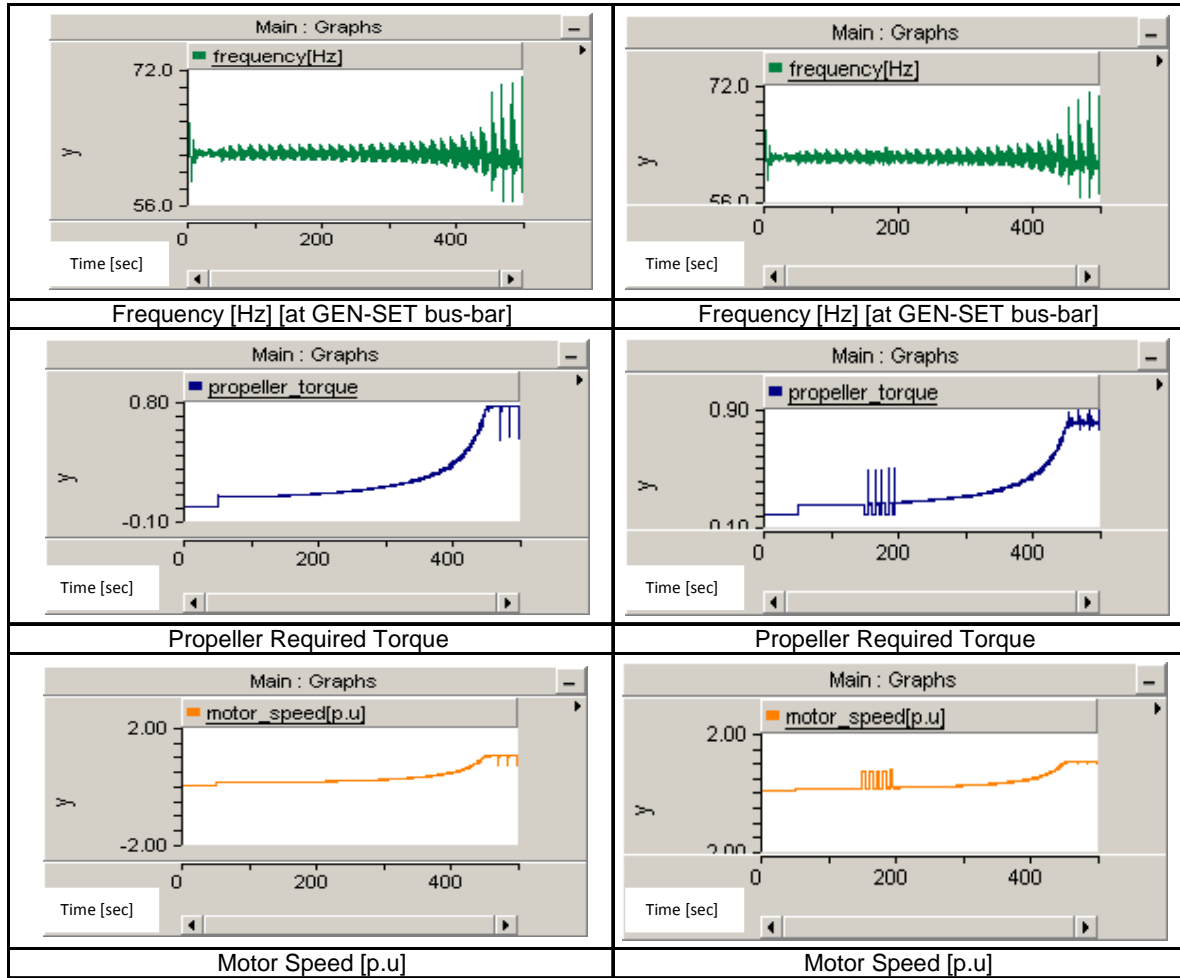


Diploma Thesis

Waveform Group 24 (Study Case B)



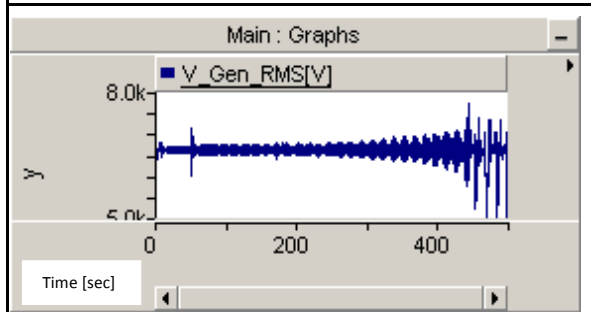
Diploma Thesis



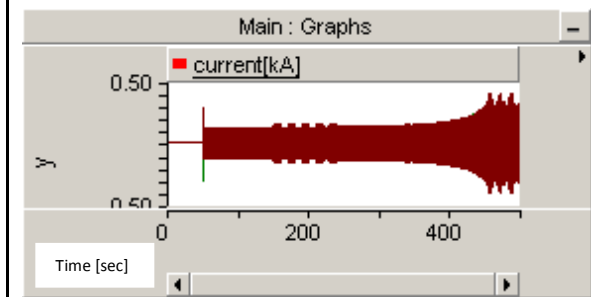
Diploma Thesis

Waveform Group 25 (Study Case B)

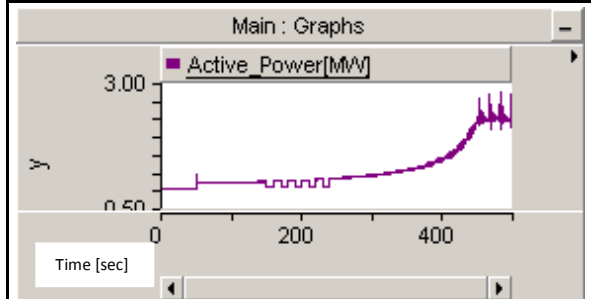
Diesel Generator time duration repetitive switching 1.0 sec.



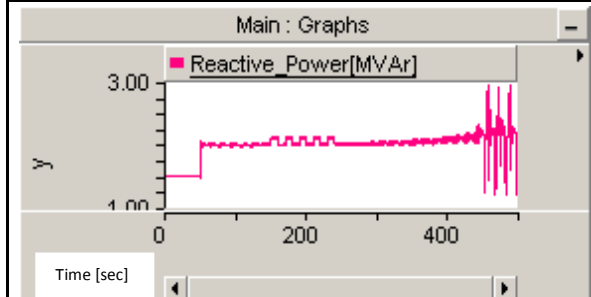
Voltage RMS [V] [at GEN-SET bus-bar]



Current NO RMS [kA] [at GEN-SET bus-bar]

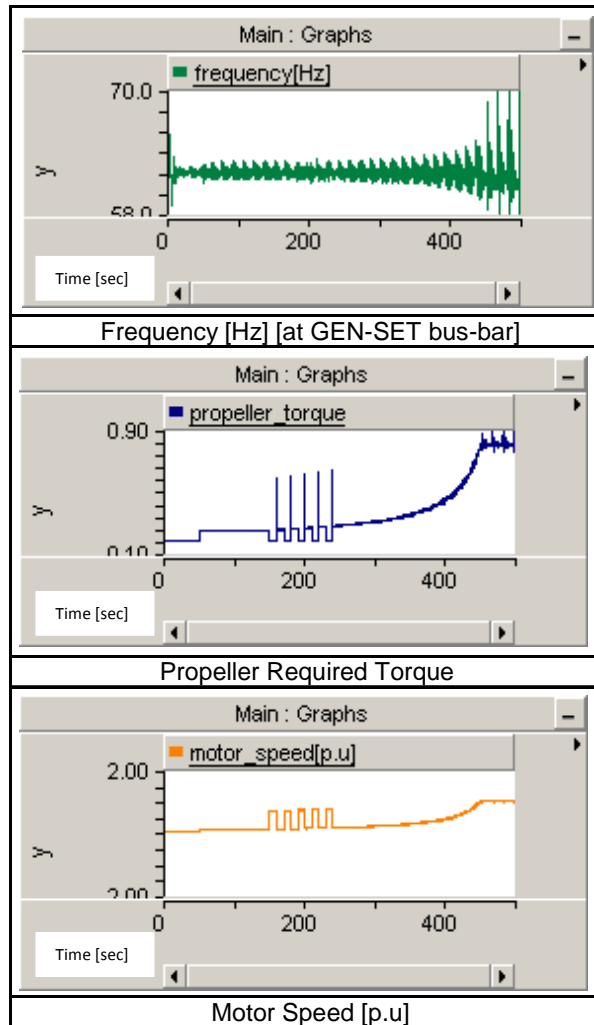


Active Power [MW] [at GEN-SET bus-bar]



Reactive Power [MVar] [at GEN-SET bus-bar]

Diploma Thesis



Diploma Thesis

III. Further approximation of the problem (Study Case C)

In addition, to the previous simulations, one more set of simulations was added to the simulation range referring to ideal source supply (*Study case C*). In detail, in this case the propeller required torque increases proportionally to the square of the motor rotating speed. This means that the wound rotor motor drives fixed pitch propeller. As it has also been said, even though the application of high rotor resistances lasts 60.0sec as before, the reduction of them to rotor nominal value lasts only 20.0sec in comparison with both sets of previous simulations according to which this lasts 340.0sec. In any case there is not thermal overloading problem as these resistances are externally connected to the motor.

The rotor resistance decrease profile for study case C is illustrated in figure 34:

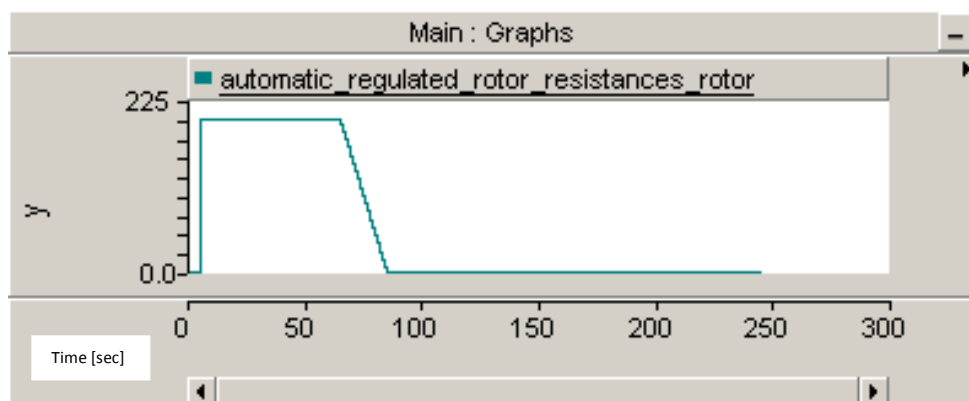


Figure 34

- Regarding three phase currents, the current waveform graphs refer to instantaneous values while the tables in the areas which contain three phase current values refer to RMS values.
- The simulation results which are contained to the table refer to the maximum or minimum value of specific magnitudes as they have been recorded throughout the whole time duration of the simulation and not necessarily at the instance starting up begins.
- For this study case only, the switching operation does not concern the propeller pitch ratio but the voltage supply to the motor.

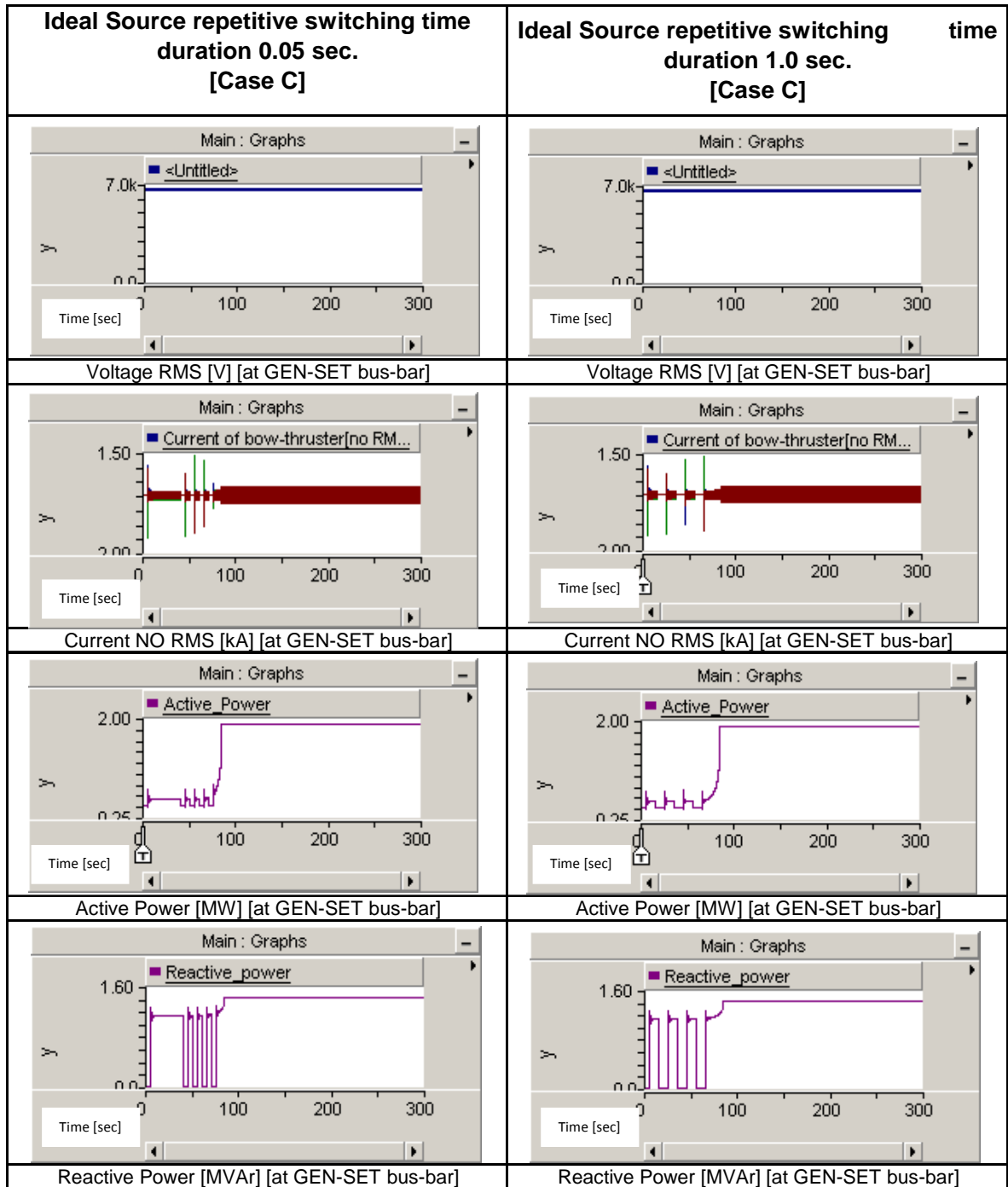
Diploma Thesis

	Ideal/Continuous Source (Study case C)	Ideal/Continuous Source repetitive switching time period 5.0sec. (Study case C)	Ideal/Continuous Source repetitive switching time period 10.0sec. (Study case C)
Vrms(min)(V)	6600	6600	6600
Vrms(max)(V)	6600	6600	6600
I RMS(max)(kA)	1.0	1.07	1.07
Pmax(MW)	1.8704	1.8704	1.807
Qmax(MVAr)	1.407	1.407	1.407
fmin(Hz)	59.95	59.95	59.95
fmax(HZ)	60.05	60.05	60.05

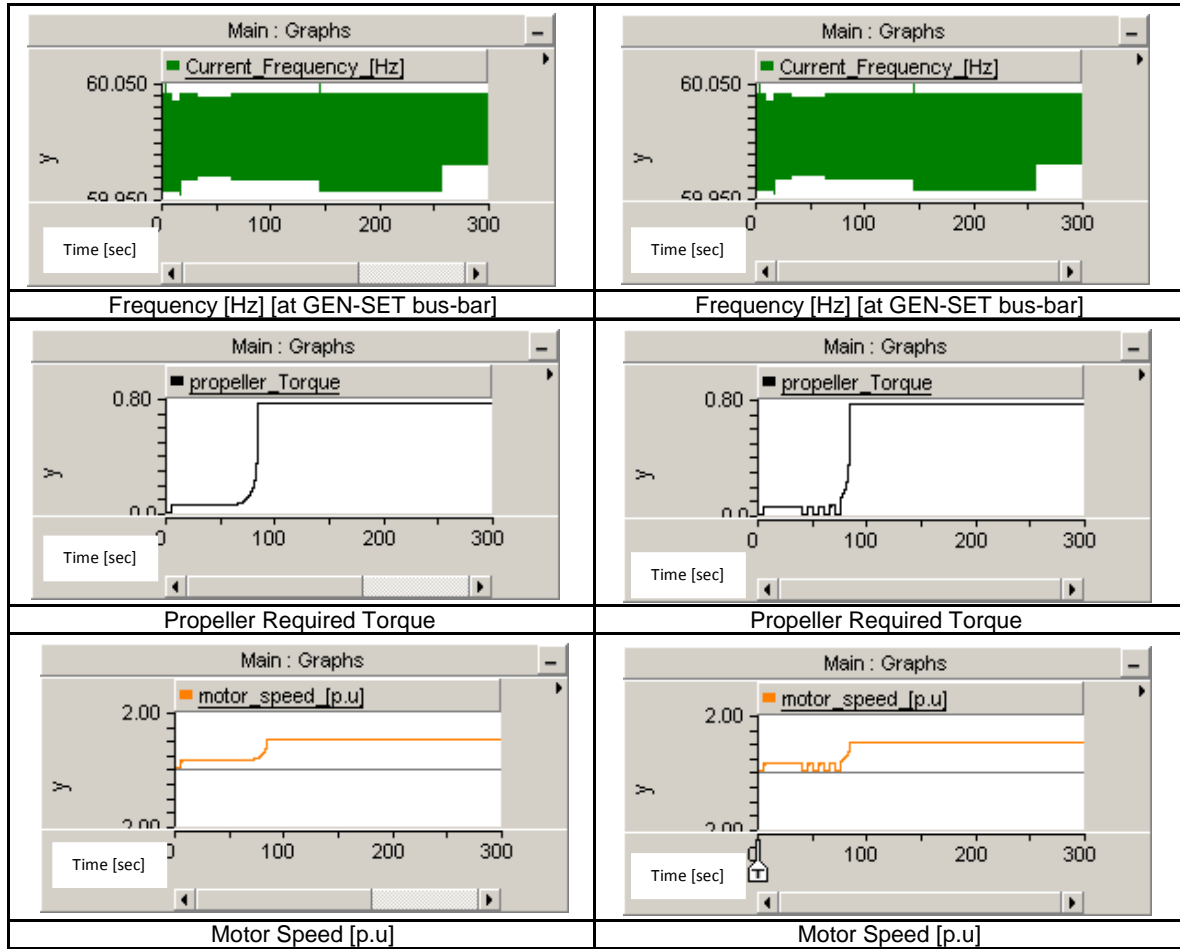
Table 10

Diploma Thesis

Waveform Group 26



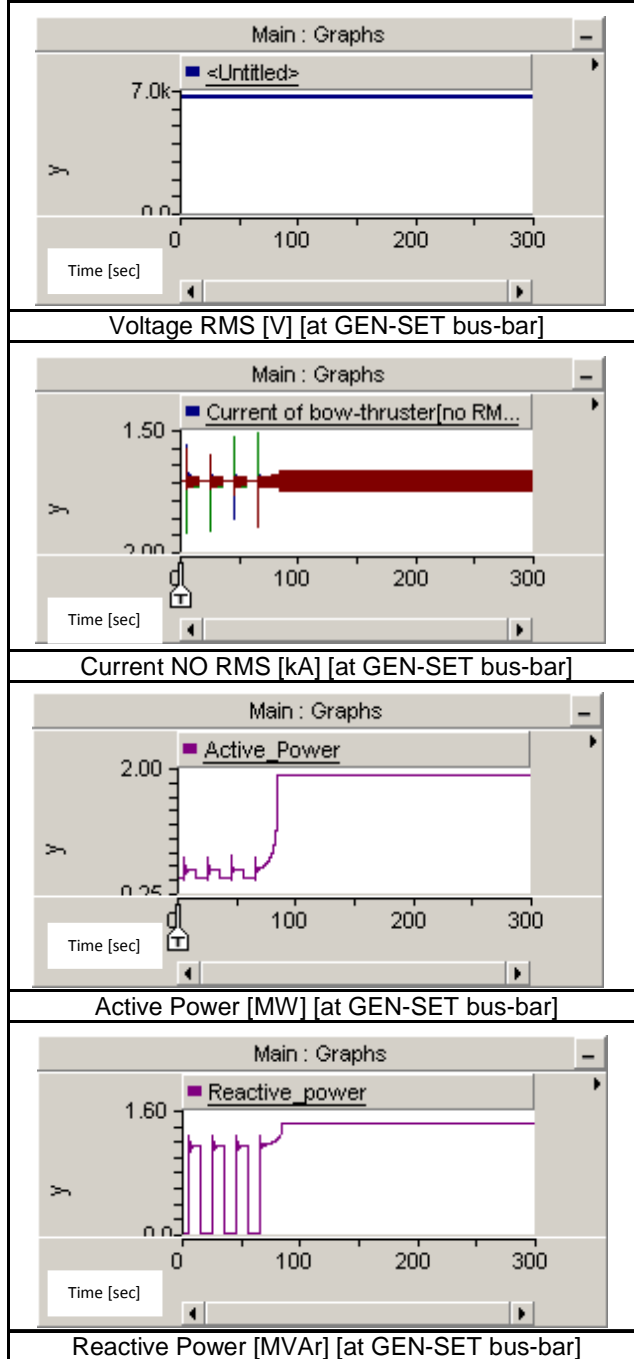
Diploma Thesis



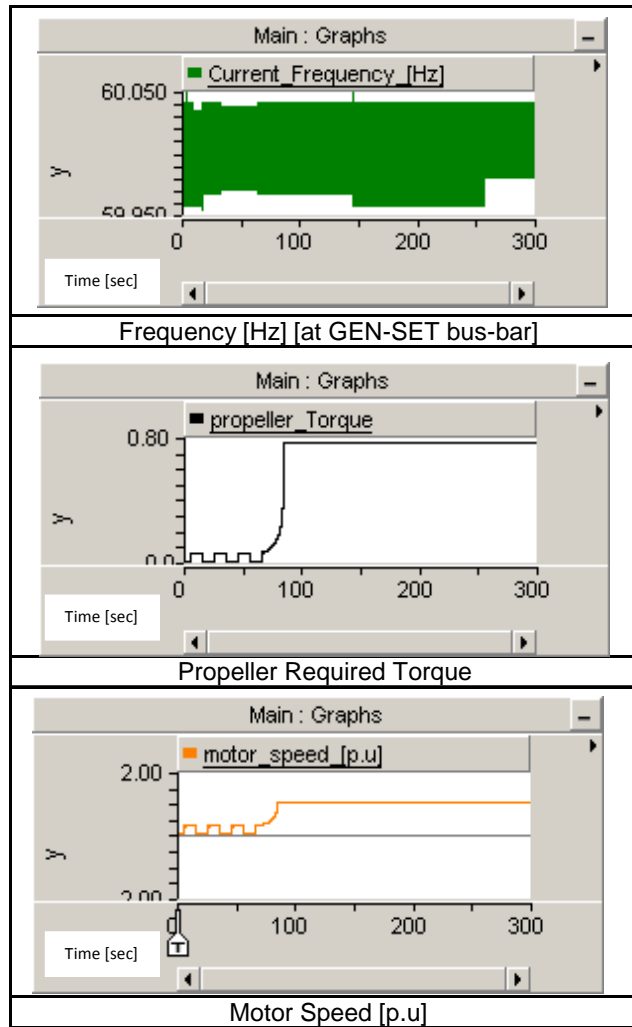
Diploma Thesis

Waveform Group 27

Ideal Source repetitive switching time duration 1.0 sec. [Case C]



Diploma Thesis



Diploma Thesis

IV. Conclusions/Comments

Taking into consideration the simulation results, the following notes are made.

Study cases A & B:

- Regarding diesel generator application, the frequency variance due to motor operation is much higher than in the case of steam generators and ideal source supply. This can be justified due to the fact that diesel engine is well known for its angular speed pulsations coming from its torque ripples. However it is highly possible that diesel engine speed governor settings need to change.
- Wound rotor motor starting current in ideal source supply application is much higher than the value of the same index in diesel generator application. This happens because ideal source is able to supply the motor with much higher amounts of active and reactive power than diesel generator does.
- During torque switching (by varying the propeller pitch ratio) the decrease in active power demand is accompanied by an increase in reactive power demand at the same time. This may happen due to the fact that closing the propeller blades, motor load condition tends to light load condition (low power factor). In addition, as the motor has not reached yet its nominal speed, it has also been recorded a step increase in motor angular speed.
- During switching on condition, a spike torque transient demand has been recorded except for the step increase.
- Regarding the diesel generator application, the simulation results are compatible to what has been observed on board. In detail, regarding squirrel cage application, even if the bow thruster starting up process includes two scale autotransforming (65%-100%), one single steam generator is not adequate to cover the motor transient needs. By using wound rotor, according to current, active and reactive power waveforms, (referring to simulations with diesel generator application), the transient (on starting up process) demand for these magnitudes are fairly lower than in the case of squirrel cage application with two steam generators by connecting the external resistors. However, once again it must be pointed out that wound rotor applications which involve the assumption that the propeller required

Diploma Thesis

torque increases proportionally to the motor angular speed are purely HYPOTHETICAL.

Study cases A & B:

- The results concerning study case C, seems to be similar to those of study case A. Thus, no great differences are observed as the source supply in this case is ideal.

CHAPTER 04

Podded Propulsors driven by Electric Motors

Pods

I. Introduction

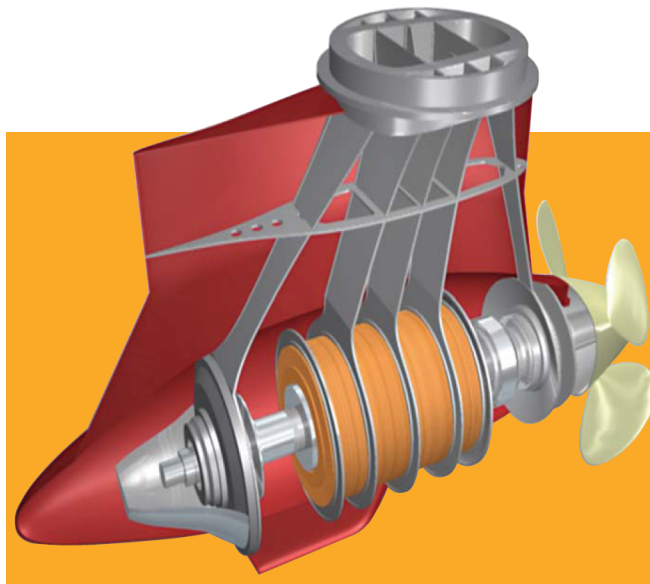
Throughout the 20th century, the knowledge as well as the applied techniques in ship hydrodynamics have been considerably changed leading to great improvements regarding vital parts of ship hull.

Some of them should be the following:

- Hull form
- Bulbous bow
- Rudders

In addition, the increase of propeller efficiency, the improvement of ship maneuverability and the increase of stabilizing fins efficiency are considered as some of the most difficult challenges in ship hydrodynamic behavior.

The last decade of 20th century, in particular early in 1990, Pods made their commercial debut bringing to foreground in great flexibilities in vessel maneuvering and propulsion efficiency accompanied by requests for further investigation and research on it.



II. Pod Propulsion and Characteristics

A podded propulsor is defined as a propulsion or maneuvering device that is external to the ship's hull and houses a propeller powering capability. This therefore, distinguishes them from azimuthing thrusters which have their propulsor powering machinery located within the hull and commonly drive the propeller through a system of shafting and spiral bevel gearing. Consequently, in outline terms, the mechanical system of a podded propulsor consists of a short propulsion shaft in which the electric motor is mounted on, as well as a system of rotating elements, radial and thrust bearings. The electric power supply of the podded propulsor motor is achieved by cables connected to the inboard system via slip rings, which are the interface between the hull of the ship and the propulsor.

The podded propulsor is suspended below the hull by an airfoil shaped fin. Podded propulsors can be either tractor or pusher units. Some designs have a system of tandem propellers. According to this design, tandem configurations contain two propellers each connected at each end of propulsor body.

In most cases, propulsion is achieved by means of fixed pitch propellers powered by an AC synchronous electric motor or permanent magnet motor fitted inside the pod.

Podded propulsion devices comprise the following sub-systems:

- Inside the propulsion pod:
 - Fixed Pitch propeller
 - Exciter
 - Electric Motor
 - Bearings (thrust & radial)
 - Bilge pumps
 - Monitoring and control equipment
 - Propeller shaft
 - Shaft propeller brake

- Outside the propulsion pod:
 - Lubricating oil equipment
 - Ventilation and air cooling system
 - Steering unit

Some of the most significant advantages of podded propulsors are the following:

- ✚ Fuel savings and low exhausted gas emissions due to improved hydrodynamic characteristics.
- ✚ Excellent maneuvering characteristics (also at low speed operation)
- ✚ Low Noise and vibration level thanks to propeller operation in uniform wake field.
- ✚ Flexibility in machinery arrangement
- ✚ Space saving in general arrangements
- ✚ Minimized crash stop distance

On the other hand, in most cases, pods suffer from the following disadvantages:

- ✚ Higher capital costs
- ✚ Limitations in power per screw (5-30 MW)
- ✚ Power losses due to electric propulsion

On the top of that, regarding pod installation on existing conventional vessels, podded propulsors cannot be fitted on two stroke diesel engine power vessels. However, this is not of great importance as, in this case, podded propulsion would be of lower propulsion efficiency.

Diploma Thesis

III. Failure Statistics

According to experience up-to-date, podded propulsors use has brought into foreground various types of failure making, in this way, more clear the need for further research. An analysis from Lloyds Register of Shipping shows that the incidence of failure (electrical and mechanical) throughout the past ten years, confirms even more this need.

Figure 35 and figure 36 represent the relative incidence of electrical and mechanical failures.

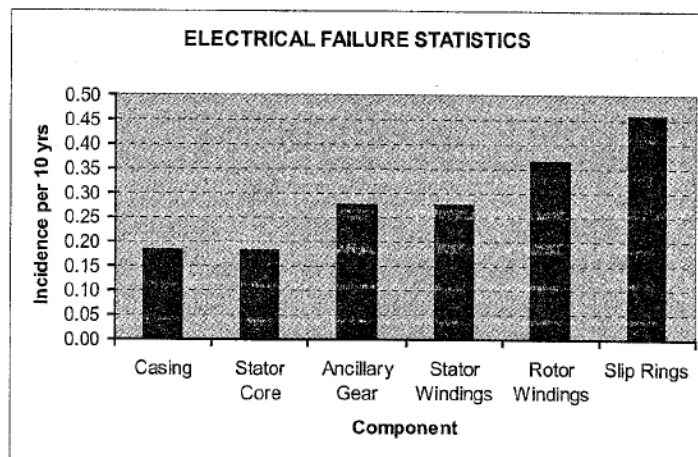


Figure 35

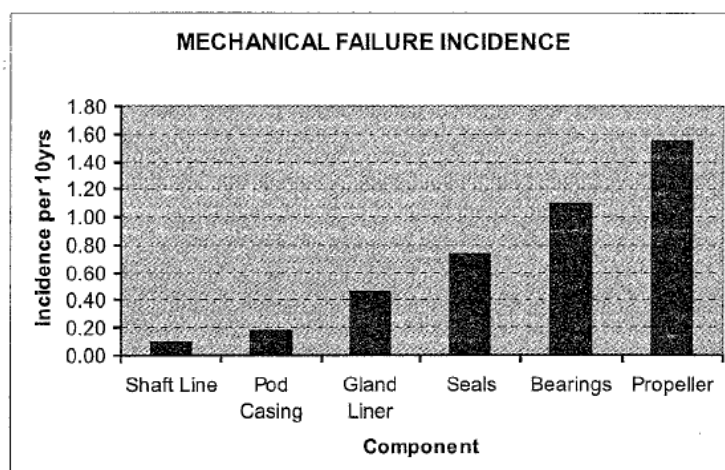


Figure 36

Diploma Thesis

Taking into consideration that pods are not an innovative product but an innovating packaging of systems and components used for many years both on the industrial and marine field, they have been affected by:

- ✚ Shaft seals failures
- ✚ Electrical failures
- ✚ Thrust and support bearing failures
- ✚ Lubricating failures

In most cases according to failure recordings, electrical failures are caused by high temperature in windings. Lower temperature can be achieved by low inductive currents such as might be caused by using permanent magnet motors, as well as, by adequately dimensioning the windings and the cooling flows.

According to a brief, but coherent research based on bibliographical resources, it can be concluded that the life time of electric devices and protective switching gears is expected to be about 30000-40000 hours.

In the case of mechanical failure distribution propeller failures, in detail blade failures seem to be the most common type of failure due to the contact with underwater objects. Furthermore, the repetitive collision with underwater items may lead to the failure of other podded propulsor components such as the rolling element bearings or shaft line. Thrust and support bearing failures strictly depend on their improper choice during design stage regarding arrangement, type and size. Whirling and gyroscopic loads have to be correctly accounted for an initial stage design. However it should be mentioned that the construction of podded propulsors is still at the first level of their existence. This means that due to the lack of the required experience, periodical failure appearing can be higher in these early development periods.

Diploma Thesis

IV. Hydrodynamic Considerations

For a start, let's assume the use of a tractor podded propulsor in its twin screw configuration; these propulsive devices will operate in relatively uniform flow far away from the hull boundary layer. This is in contrast to a conventional twin screw propulsion arrangement in which the incident wake field is distributed by the shafting and its supporting brackets. Alternatively, a pusher pod twin screw configuration has to operate in the boundary layer generated by the pod body and strut. This means that the use of podded tractor propulsors even if the hull design is not optimized should be better for ahead free running mode of operation rather than the case of twin screw ship.

However according to the bibliography, it has been found that podded propulsors, in general, seem to be sensitive to small changes regarding to its relatively location on the hull in comparison with conventional propulsion devices. The optimum podded azimuth angle for ahead free running operation seems to be strictly dependent on the flow stream lines of the hull.

The loadings generated by the pod are extremely complex due to the fact that a large number of factors and parameters should be taken into consideration (the flow around the fin, the strut, as well as the helicoidal propeller slipstream). In addition, the interaction between the propeller, the pod body and the pod bodies in twin screw configuration must be taken definitely into account.

The forces and the moments need to be calculated as accurately as possible for a range of different loading/operating conditions. Otherwise, the induced loads to bearings and to the shaft will not be well estimated, leading to premature failure of the involved components.

These induced loads strictly depend on the pod azimuth angle. At each azimuth angle, the thrust and the torque of the pod should be contrasted with thrust and torque at zero azimuthing angle.

The pod body design is of great importance as, in this way, the hull boundary layer, as well as developed vorticity can be minimized.

Diploma Thesis

The pod hydrodynamic characteristics strictly depend on its shape. This means that the pod body should be designed with the smallest possible diameter as well as with the greatest possible length. This, in turn, from the hydrodynamic point of view, means that the ratio of pod radius to pod body length must be as minimum as possible. These requirements can only be met by the use of permanent magnet motors or high temperature superconducting motors [source: American Superconductor Society, Carlton].

The great maneuvering abilities thanks to podded propulsive devices can be represented by the figures 37 & 38.

Turning circle test at full speed

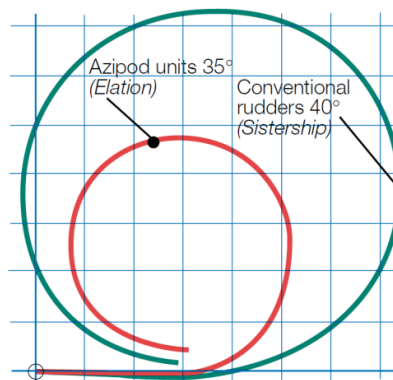


Figure 37

Source: [ABB]



Shuttle tanker *M/T Ulkku*

Figure 38

Source: [ABB]

V. Pod Hydrodynamic Behavior during Turning Maneuvers

In the case of twin screw configurations, undertaking a turn, the resulting forces and moments produced by the propellers located on the port and on the starboard side of the sides of the hull, are different.

This difference strictly depends on the side boundary layers and on the flow field in the way of the propellers.

Figure 39 represents these differences measured on the starboard pod propeller for different pod azimuth angles provided that the propeller angular speed remains constant.

(The graph data have been withdrawn from Lloyds Register of Shipping relevant research).

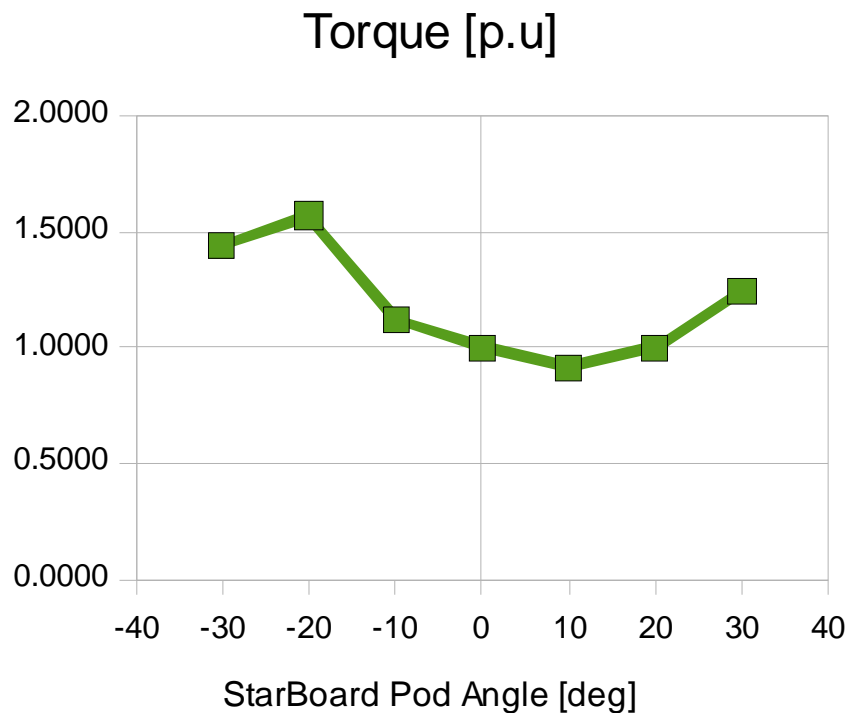


Figure 39

Diploma Thesis

It should be mentioned that regarding the LRS starboard pod experiment [Carlton], positive angles refer to turns to open sea, while negative angles refer to turn to hull side. On the other hand, regarding port pod operation, positive angles refer to turns to hull side, while negative angles refer to turns to open sea. In other words, in general, positive angles indicate pod turn from the port side to the starboard side, while negative angles indicate pod turn from the starboard side to the port side of the vessel.

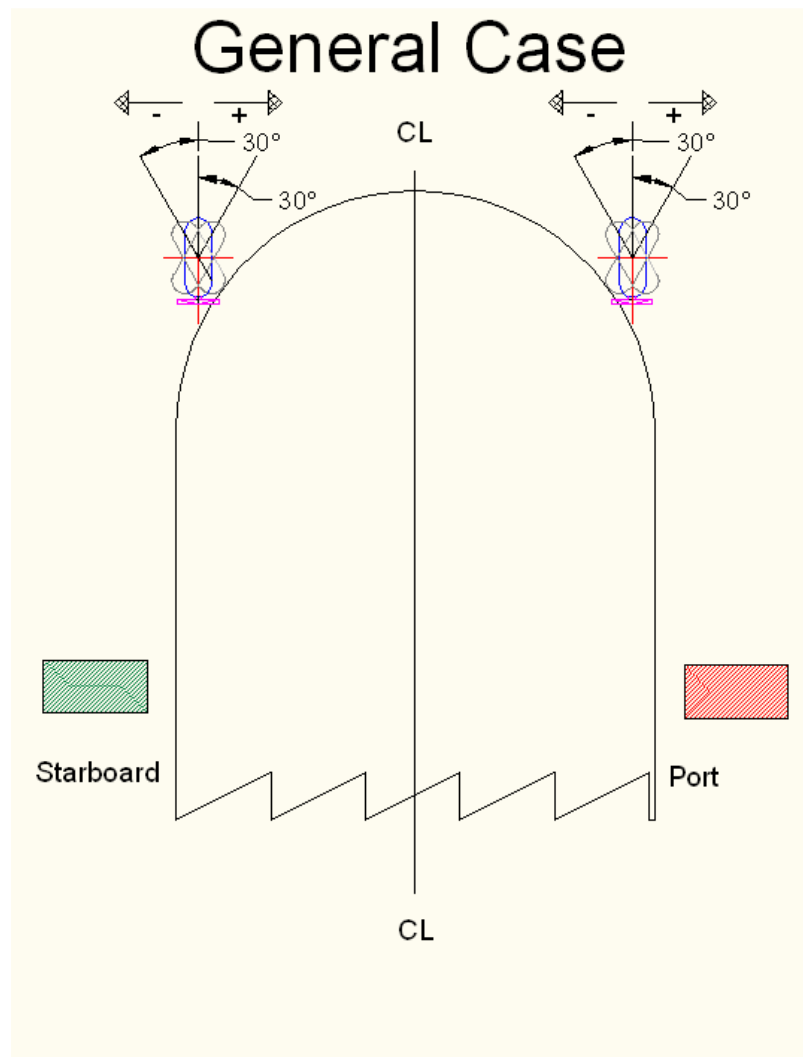


Figure 40

Diploma Thesis

With this assumption (starboard motor angular speed constant), during the turn to port, the starboard motor would be in danger of being overloaded. This means that the propeller, the shaft and the bearings face the risk of premature aging or failure.

For the purposes of this degree dissertation, simulations of pod synchronous motor behavior were conducted organized into six different study cases as presented to Table 11.

Pod Study Cases		From	To	Pod Driver
Case Study A	Star Board Pod	x	P	S
	Port Pod	-	-	-
Case Study B	Star Board Pod	x	P	S
	Port Pod	x	P	S
Case Study B	Star Board Pod	x	P	S
	Port Pod	x	S	P
Case Study D	Star Board Pod	x	P	S
	Port Pod	-	-	-
Case Study E	Star Board Pod	x	P	S
	Port Pod	x	P	S
Case Study F	Star Board Pod	x	P	S
	Port Pod	x	S	P

Table 11

Regarding twin screw configurations, the following assumptions are made:

The curve which represents the required torque from the pod for different azimuth angles (provided that its angular speed remains constant) remains unchanged for twin screw configuration. This means that it is assumed (due to lack of further data regarding pod hydrodynamic behavior) that there is no interaction between these two propulsive devices.

Diploma Thesis

For the purposes of these simulations, regarding *the three first cases*, A-C the pod motor is supposed to be a *synchronous AC machine* with the following technical characteristics (Table 12):

Pod Motor Technical Characteristics	
<i>Nominal Active Power</i>	25 MW
<i>Nominal Reactive Power</i>	18.75 MVAR
<i>Nominal Power Factor</i>	0.8
<i>Speed at full load</i>	120 RPM
<i>Line Voltage</i>	6600 V
<i>Efficiency at Full Load</i>	97.5 %
<i>Structure Born Noise</i>	< 60 dB
<i>Design Life</i>	30 years

Table 12

In detail, the input and output power flows of the motor are described in the table 13:

SYNCHRONOUS MACHINE		
NOMINAL CHARACTERISTICS		
	INPUT	OUTPUT
P [MW]	25.64	25
Q [MVAR]	19.23	-
P.F	0.8	-

Diploma Thesis

EFFICIENCY: 0.975

PERFORMANCE		
	INPUT	OUTPUT
P [MW]	25.11	-
Q [MVAR]	19.49	-
P.F	0.8	-

Table 13

On the other hand, for the rest of the simulations, the pod motor is supposed to be an *asynchronous AC squirrel cage induction machine* with the following technical characteristics (Table 14):

Pod Motor Technical Characteristics	
<i>Nominal Active Power</i>	24.64 MW
<i>Nominal Reactive Power</i>	14.90 MVAR
<i>Nominal Power Factor</i>	0.855
<i>Speed at full load</i>	120 RPM
<i>Line Voltage</i>	6600 V
<i>Efficiency at Full Load</i>	97.5 %
<i>Structure Born Noise</i>	< 60 dB
<i>Design Life</i>	30 years

Table 14

Diploma Thesis

The input and output power flows of the motor are described in the table 15:

SQUIRREL CAGE ASYNCHRONOUS MACHINE		
NOMINAL CHARACTERISTICS		
	INPUT	OUTPUT
P [MW]	25.20	24.64
Q [MVAR]	15.27	-
P.F	0.855	-

EFFICIENCY: 0.975		
--------------------------	--	--

PERFORMANCE		
	INPUT	OUTPUT
P [MW]	25.20	-
Q [MVAR]	15.27	-
P.F	0.855	-

Table 15

It must be mentioned that for the figures 42,45,48,50,53,56, the non dimensional expressed values are referred to the nominal characteristics of each type of motor (it depends on the examined case).

Regarding *the time analysis* of the simulations, for the three first simulations (powered by the synchronous machine) (Cases A, B &C), the motor(s) starts directly when the starboard motor azimuth angle is equal to -30.0 degrees (towards the hull). Due to the fact that there is a huge transient phenomenon throughout the angle range [-30.0, -25.0] the recorded data refer to the angle range [-25.0 , +30.0] degrees. In addition, the angle range [-30.0 +30.0] is covered in 60.0 seconds.

Diploma Thesis

On the other hand, for the last three simulations, (powered by the squirrel cage asynchronous machine) (Cases D, E & F), it is considered that the motor(s) starts at azimuth angle 0.0 and then it turns to the starting azimuth angle (-30.0 or 30.0 degrees). In addition, the angle range [-30.0 , +30.0] is covered in 60.0 seconds.

■ Case Study A:

According to this case (figure 41), the simulation contains the operation of the starboard pod only. The starboard pod turns from the port side of the hull to the open sea (starboard). The pod is powered by ideal electric power source.

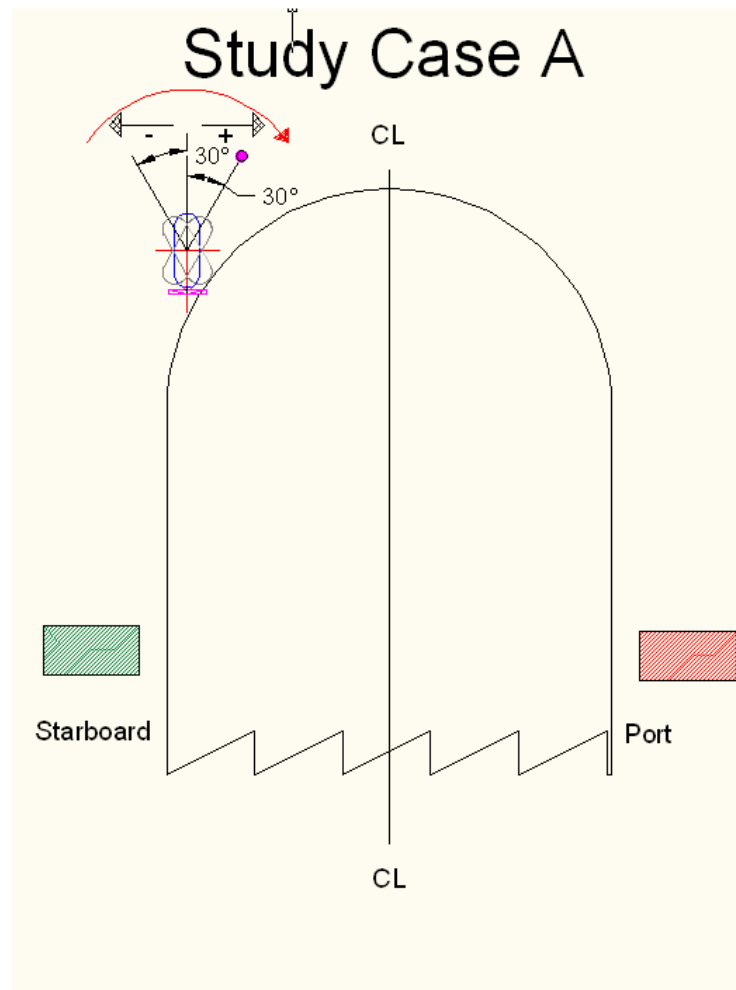


Figure 41

Diploma Thesis

The motor power demands (regarding active and reactive power as well as three phase current) are represented to the figure 42:

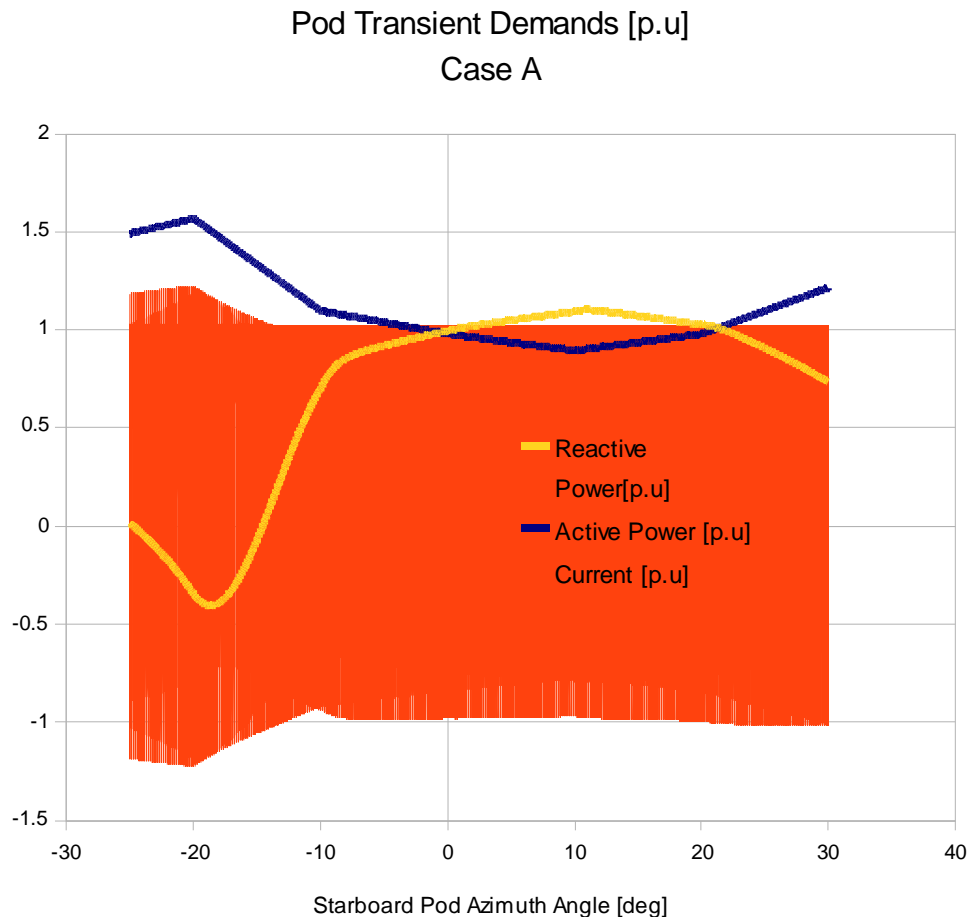


Figure 42

It can be observed that the active power curve strictly depends on the propeller required torque (figure 39) while the motor line current response is affected from both active and reactive power demand.

In addition, the starboard pod active power demand reaches its lowest ever rate 10 degrees starboard (toward the open sea), while at the same point reactive power reaches its highest ever rate. On the other hand, active power reaches its highest rate at 20 degrees port (towards the hull), while at the same point, reactive power stands at its lowest ever rate.

It also must be pointed out that the pod requirements in azimuth angle 22.6 degrees are equal to those in zero azimuth angle.

■ Case Study B:

In this case, the simulation concerns the operation of the starboard and port pod. The starboard pod turns from the hull side to the open sea, while the port pod turns from the open sea to the hull side. The pods are powered with ideal electric power source. It can be seen that there is different loading between these two motors at the same time, as the first one turns from the hull side to the open sea, while the second one turns from the open sea to the hull side.

In this case (figure 43,44), the required torque for different azimuth angles for each pod is described from the following diagram.

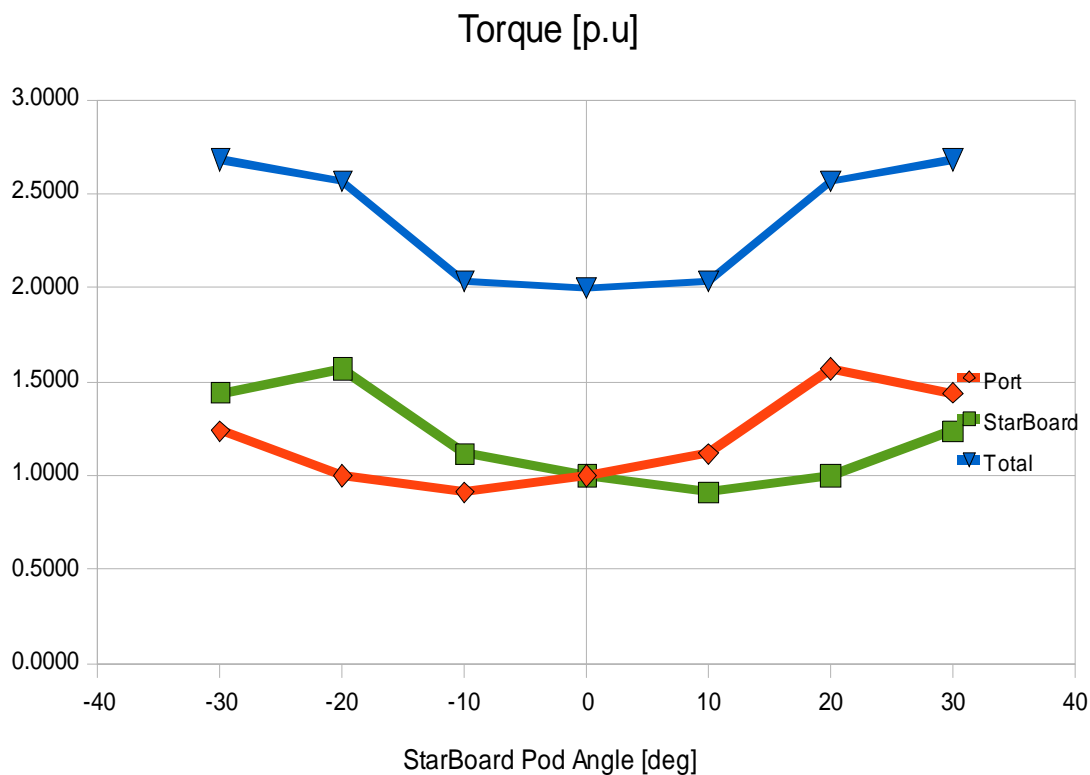


Figure 43

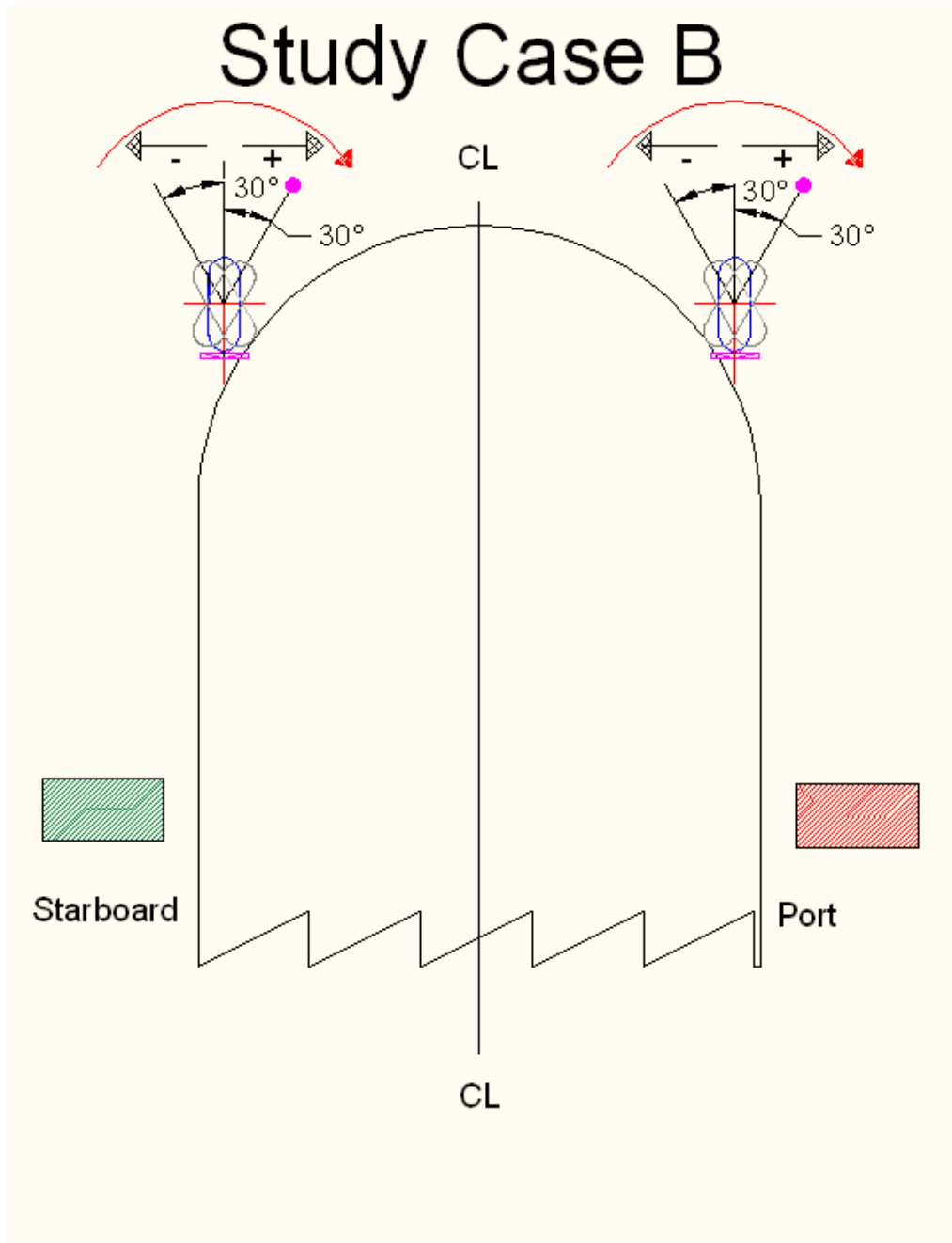


Figure 44

Diploma Thesis

The total motor power demands (regarding active and reactive power as well as three phase current) are presented to the figure 45:

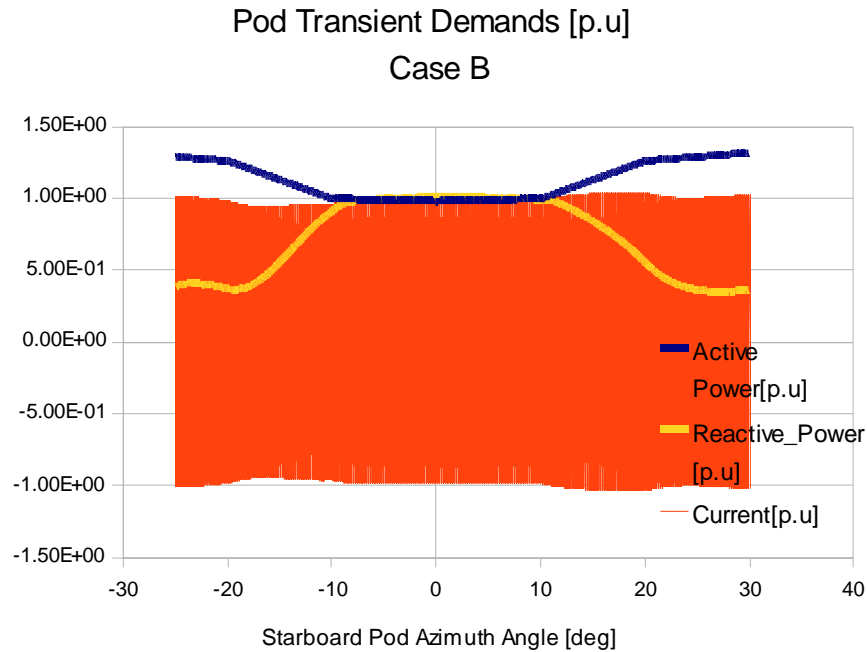


Figure 45

It is noticed, as in the case A, that the active power curve strictly depends on the total propeller required torque, while the motor line current response is affected from both active and reactive power demand.

It must be also mentioned that at zero azimuthing angle for both pods, the total active power requirements stands at its lowest ever rate, while the requirement for reactive power stands at its highest rate.

It must be pointed out that the total pod requirements depend on the azimuth angle regardless the angle direction.

Diploma Thesis

■ Case Study C:

In this case, the simulation contains the operation of the starboard and port pod. Both of them turn from the hull side to the open sea. The pods are powered by ideal electric power source. It can be seen that there is no different loading between these two motors at the same time, as both of them turn from the hull side to the open sea.

In this case, the required torque for different azimuth angles for each pod is presented in the figures 46,47.

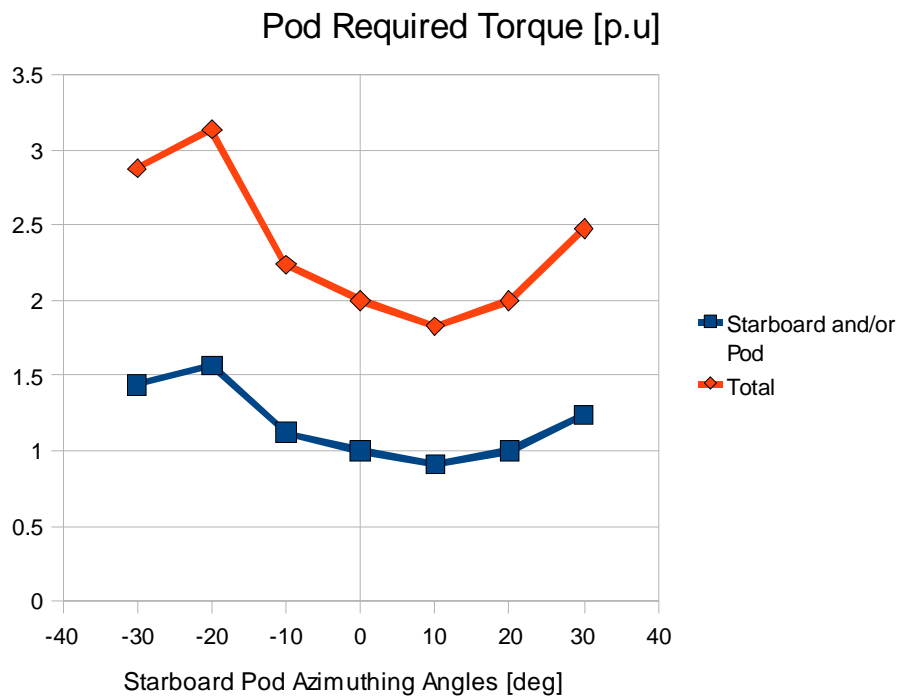


Figure 46

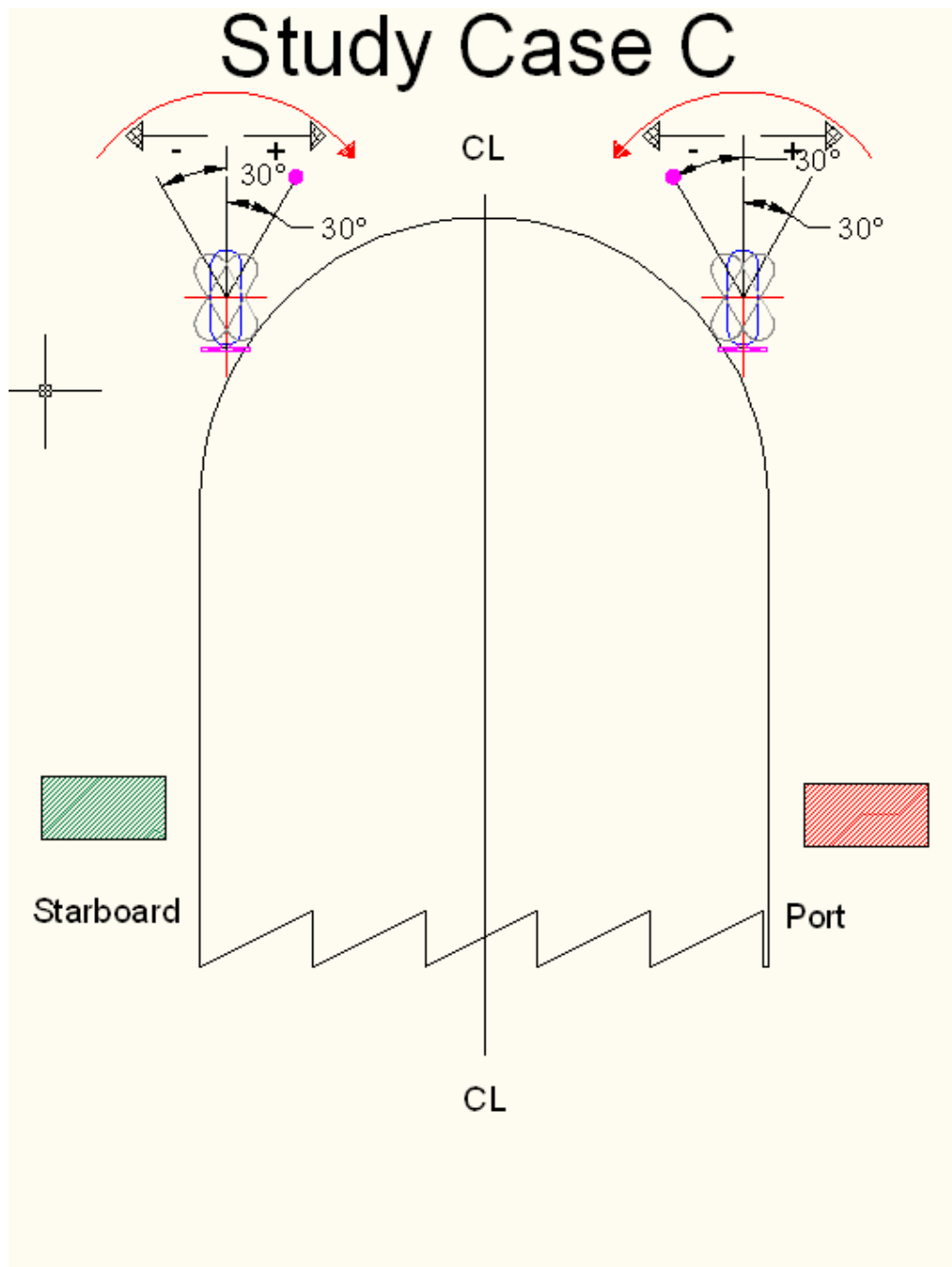


Figure 47

Diploma Thesis

The total motor power demands (regarding active and reactive power, as well as three-phase current) are presented in the figure 48:

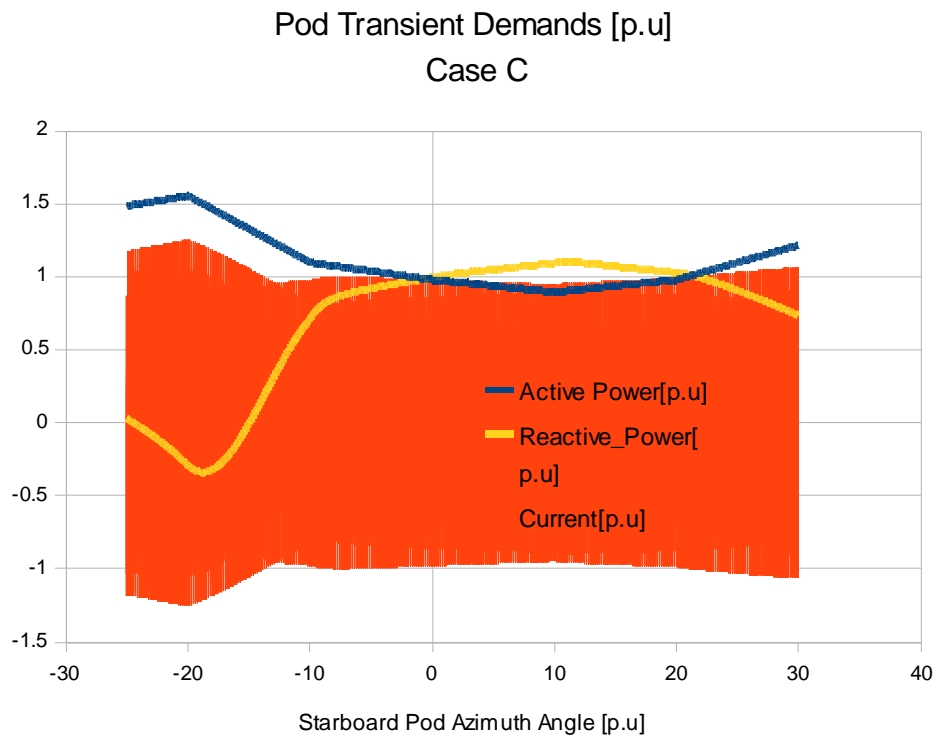


Figure 48

It can be noticed, that, as in case A, the active power curve strictly depends on the total propeller required torque, while the motor line current response is affected from both active and reactive power demand.

The azimuth degrees for each pod where the maximum or minimum total demand for active and reactive power have been recorded, are the same to that of study case A.

It also must be pointed out that like in case A, the pod requirements in azimuth angle 22.6 degrees are equal to those in zero azimuth angle.

■ Case Study D:

As in case A, this simulation involves only the use of starboard bow thruster. According to this case (figure 49), the starboard pod turns from the port side of the hull to the open sea (starboard). As in all examined study cases, the pod is powered by ideal electric power source.

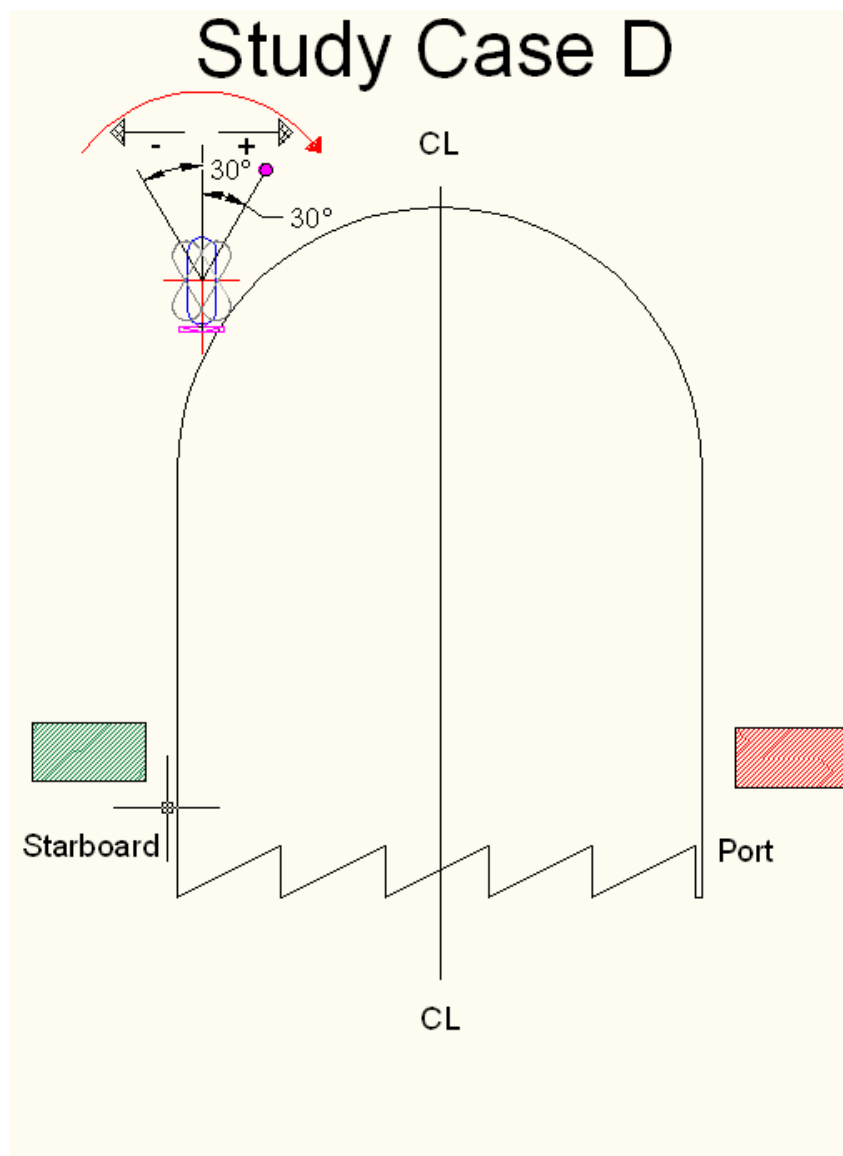


Figure 49

Diploma Thesis

The motor power demands in function to the starboard pod azimuth angle at each time point throughout the simulation (regarding active and reactive power as well as three phase current) are presented in the figure 50:

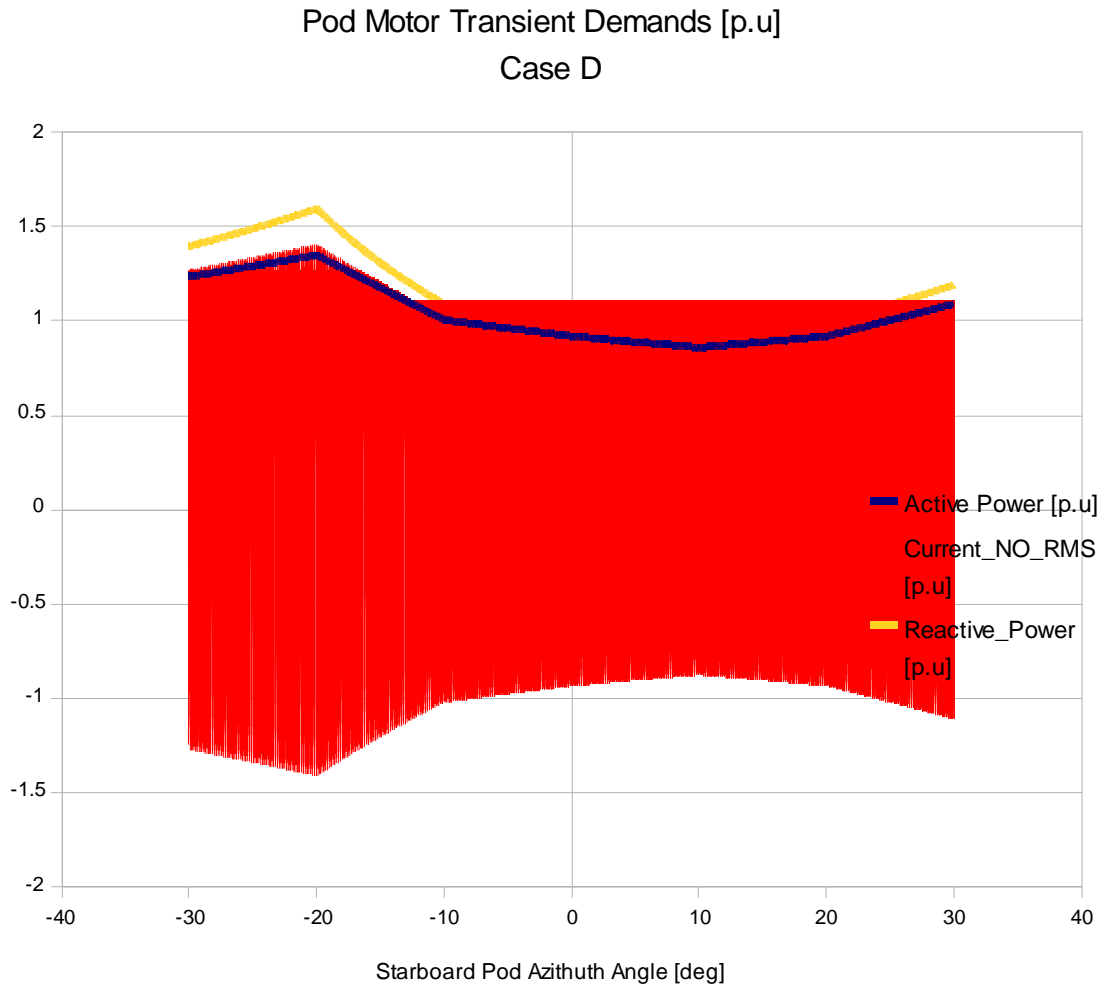


Figure 50

It can be noticed that all the examined magnitudes strictly depend on the applied torque (figure 39) provided that the angular speed of the motor remains constant.

As it can also be observed by the LRS diagram of the propeller required torque for various angles, the minimum required power is recorded ten degrees towards the open sea, while the maximum required power appears twenty degrees towards the hull of the ship referring to pod zero azimuth angle.

Diploma Thesis

■ Case Study E:

In this case (figure 52), two pods (port and starboard) are involved. Like in study case B, the starboard pod turns from the hull side to the open sea, while the port pod turns from the open sea to the hull side. As in all examined study cases, the pods are powered by ideal electric power source. This means that there is different loading between these two motors at the same time, as the first one turns from the hull side to the open sea, while the second one turns from the open sea to the hull side. In other words, both of them turn from port to starboard.

In this case, the required torque for different azimuth angles for each pod is presented in the figure 51.

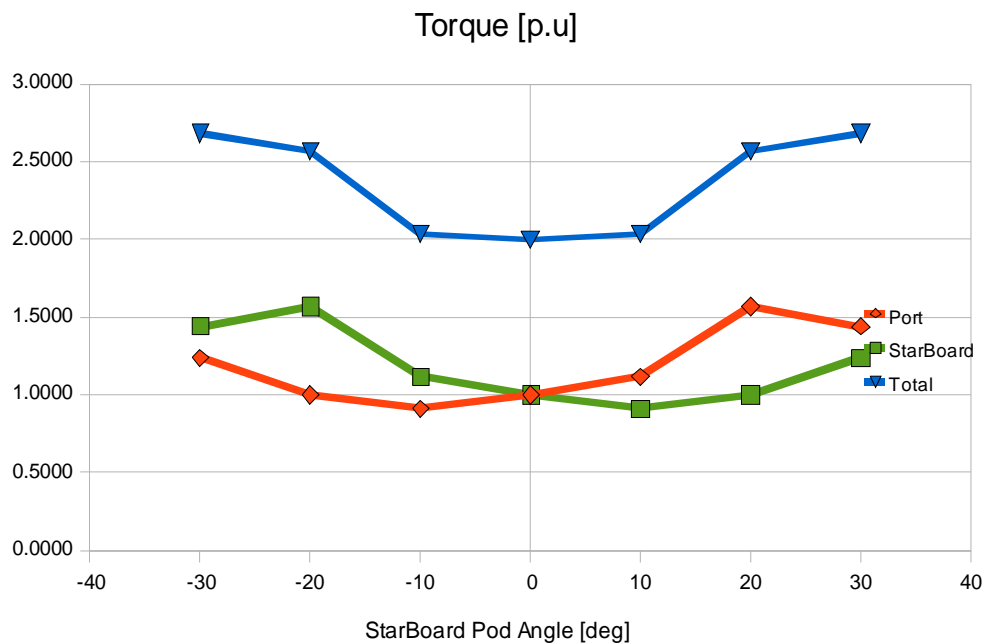


Figure 51

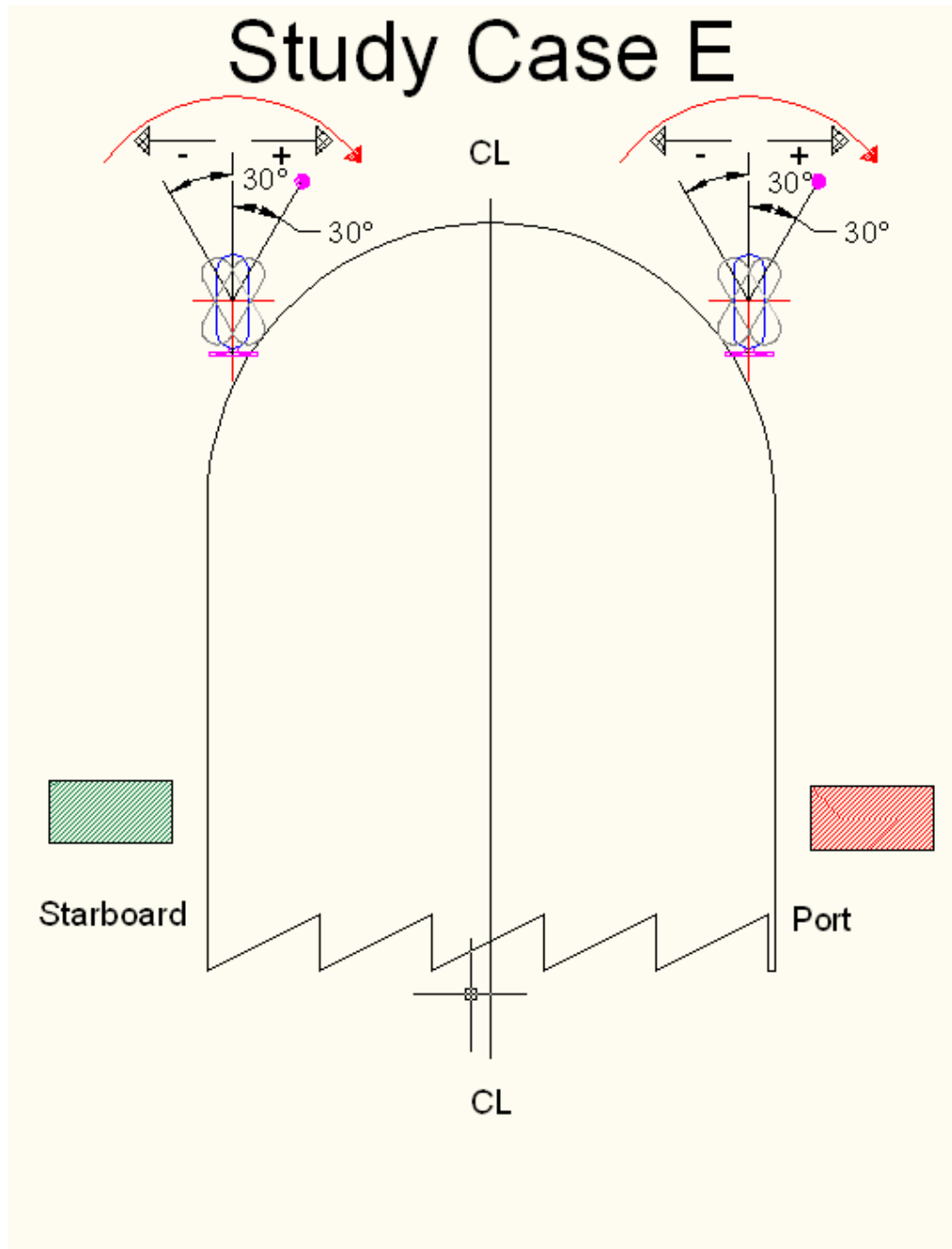


Figure 52

Diploma Thesis

The total motor power demands (regarding active and reactive power as well as three phase current) are presented in the figure 53:

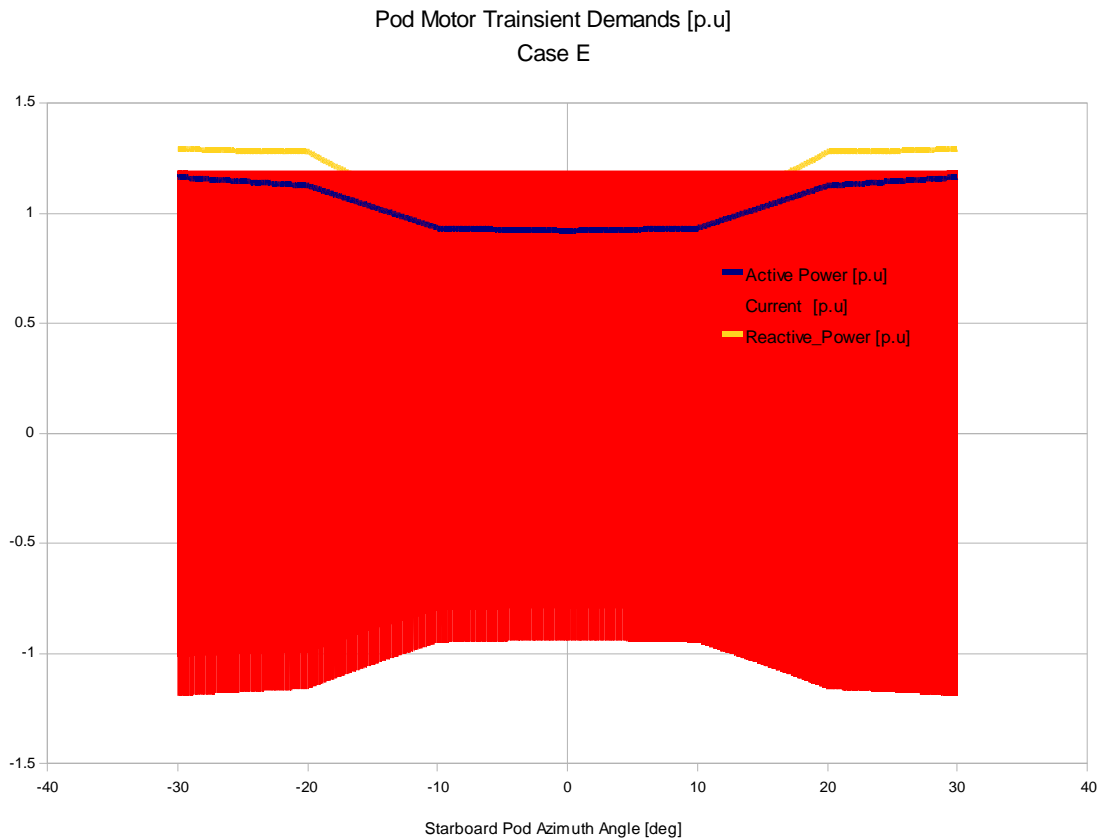


Figure 53

It can be noticed that, as in case A, the active power curve strictly depends on the total propeller required torque.

It must be also mentioned that at zero azimuthing angle for both pods, the total power requirements stand at their lowest ever rate.

Last but not least, the total pod requirements depend on the azimuth angle regardless the angle direction.

■ Case Study F:

In this case (figure 55), the simulation concerns the operation of the starboard and port pod. Both of them turn from the hull side to the open sea.

In detail, the starboard port turns from the port side to the starboard side, while, the port pod turns from the starboard side to the port side.

The pods are powered by ideal electric power source. It can be seen that there is no difference in loading between these two motors at the same time as both of them turn from the hull side to the sea.

In this case, the required torque for different azimuth angles for each pod is presented in the figure 54.

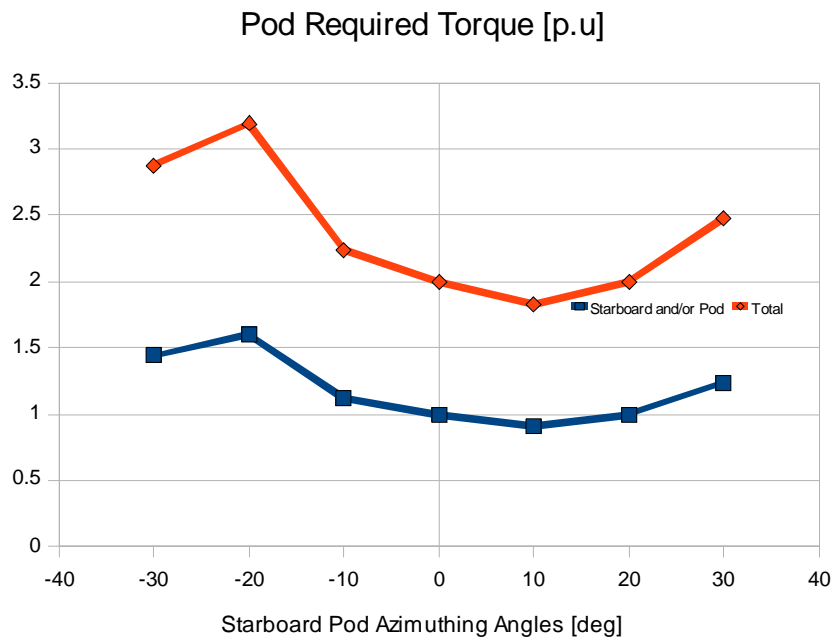


Figure 54

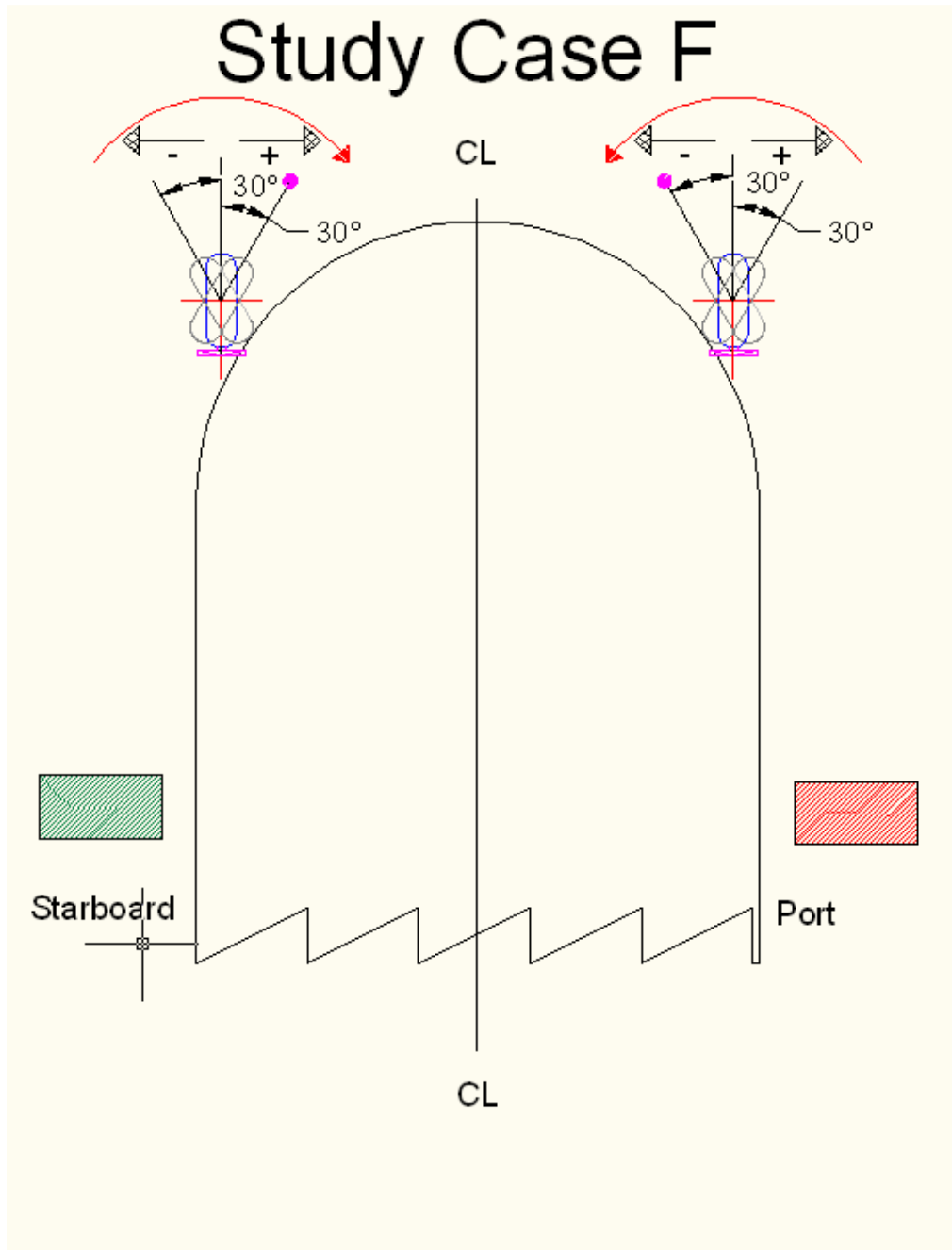


Figure 55

Diploma Thesis

The total motor power demands (regarding active and reactive power as well as three phase current) are presented in the figure 56:

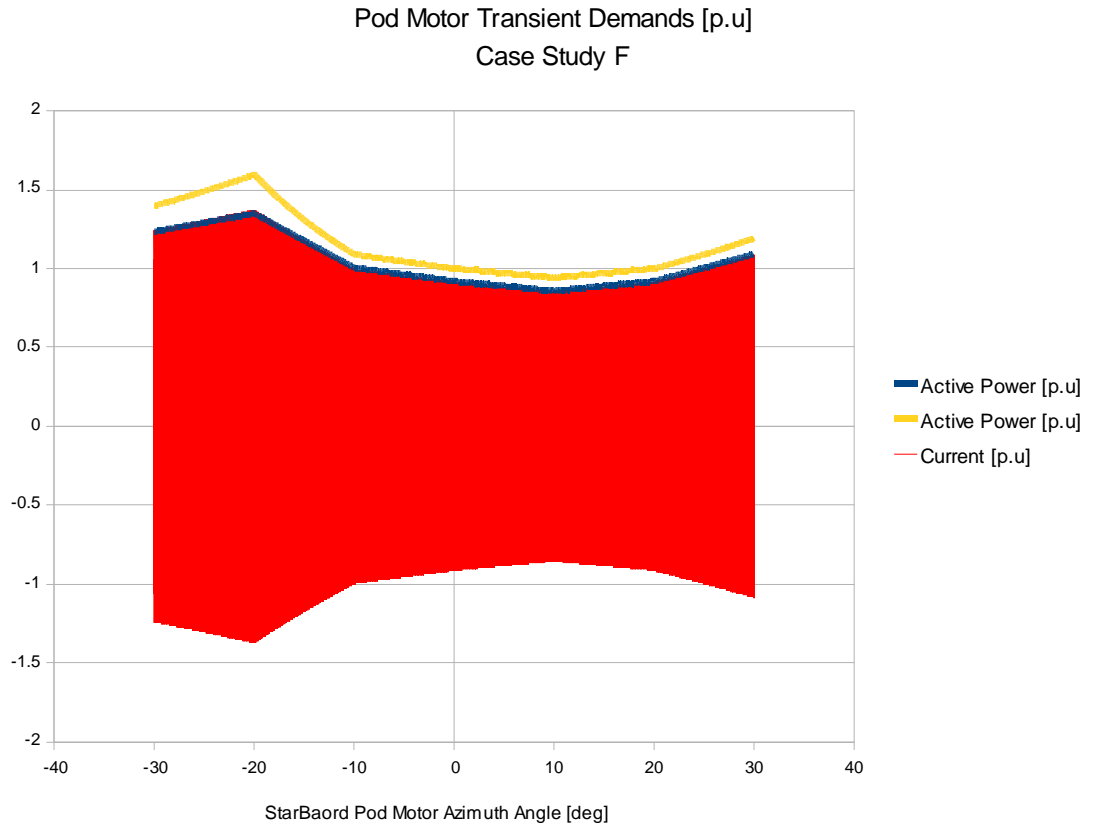





Figure 56

It can be noticed as in the case D that all the examined magnitudes (active and reactive power, as well as three phase current) strictly depend on the total propeller required torque (figure 39).

As it can also be observed by the LRS diagram of the propeller required torque for various angles, like in case D, the minimum required power appears ten degrees towards the open sea, while the maximum required power is noted twenty degrees towards the hull of the ship referring to pod zero azimuth angle.

In addition, the pod requirements in azimuth angle 22.6 degrees are equal to those in zero azimuth angle.

VI. Conclusions

-  Regarding the synchronous motor configuration, due to the presence of its exciter, according to the instantaneous propeller pod demand in active power, the power factor of the motor is adjusted on a continuous basis. According to starboard simulation results, the starboard pod for the azimuthing angle range [-25.0 -14.75] requires from the system a negative amount of reactive power. This means that the motor produces rather than consumes reactive power.
-  Regarding the asynchronous motor configuration, due to the lack of exciter effect on the asynchronous motor operation, the active and reactive power (thus the motor inrush current) behaves in the same way throughout the simulation time duration. This means that the motor operation cannot be adjusted to special motor needs (turning to port or to starboard). This is one of the most important reasons why this type of motor is not preferable for this kind of use.
-  Due to the fact that the hydrodynamic loading in case A is supposed to be the same to case C, at each point time throughout the simulation time duration and regardless the number of podded propulsors, the waveforms of active and reactive power as well as motor inrush currents are exactly the same. For the same reasons, regarding asynchronous motor configurations, the simulation results of case D are exactly the same to those in case F.

CHAPTER 05

Short Circuits

Diploma Thesis

Short Circuits:

I. Introduction

For the purposes of this degree dissertation, six different scenarios of short circuits are simulated involving no load condition, passive loading via R and L and bow thruster loading. In detail, three different types of short circuits are applied (single-, two- and three- phase faults). The fault is considered a connection of the phase, where fault is applied to neutral.

The waveforms groups 28,29 and the table16 represent the steam system response to the range of fault scenarios. All fault scenarios involve the use of two steam generators. Moreover, the fault application is equal to 4.0 msec.

The assumption of 4.0msec is based on the fact that it is the maximum allowable three phase fault time duration for (R-L and bow thruster loading condition) according to which the applied fault does not lead the system to limit cycle error.

It must also be noted that three phase faults are applied to all three phases (R, S & T), two phase faults are applied to R and S phases and single phase faults are applied to only R phase.

In wave graphs, instantaneous waveform values herring after called as NO_RMS values.

Diploma Thesis

II. Data Tables and Graphs

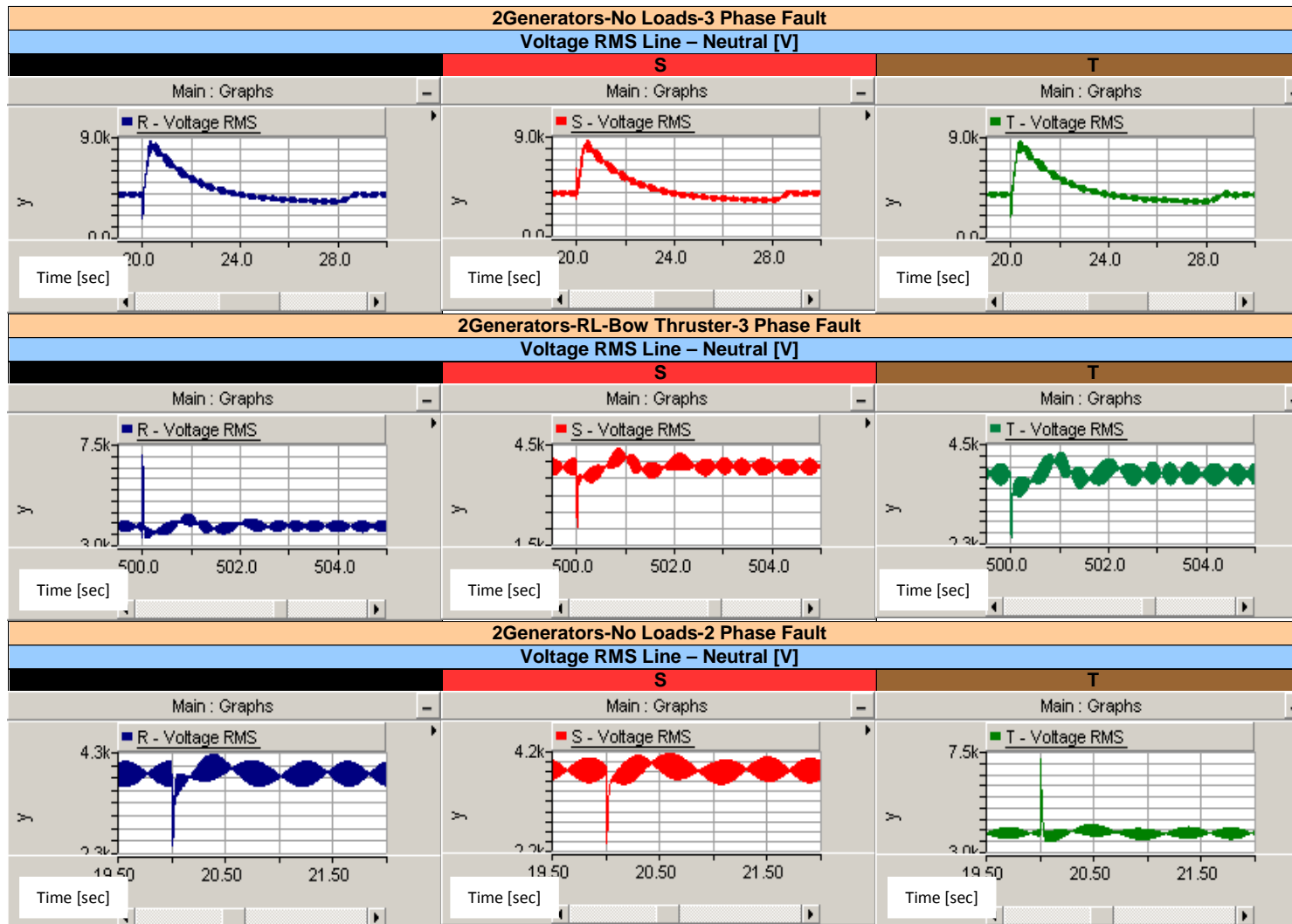
It must be pointed out that the voltage (phase to neutral) and current values which are tabulated to the following table refer to RMS values rather than to Instantaneous values.

	R		S		T		R	S	T	FREQUENCY	
	V_MIN RMS [V]	V_MAX RMS [V]	V_MIN RMS [V]	V_MAX RMS [V]	V_MIN RMS [V]	V_MAX RMS [V]	I_MAX RMS [kA]	I_MAX RMS [kA]	I_MAX RMS [kA]	MIN [Hz]	MAX [Hz]
2G-NO LOADS – 3PH	1612.00	8500.00	2967.00	8527.00	1837.00	8590.00	7.870	4.617	7.955	61.53 0.99 p.u	62.68 1.01 p.u
2G-RL- BOW THRUSTER – 3PH	3261.00	7008.00	1983.00	4350.00	2358.00	4289.00	1.047	4.533	5.317	44.55 0.72 p.u	62.31 1.005 p.u
2G-NO LOADS – 2PH	2382.70	4185.20	2340.40	4128.00	3415.00	7120.40	4.861	4.820	0.000	52.46 0.85 p.u	62.00 1.00 p.u
2G-RL- BOW THRUSTER – 2PH	2033.00	4389.40	1639.30	4323.00	3259.00	7668.20	8.436	8.118	0.263	55.24 0.92 p.u	62.96 1.015 p.u
2G-NO LOADS – 1PH	1859.00	4737.00	3557.60	6402.30	3560.00	6982.00	0.078	0.000	0.000	57.62 0.93 p.u	63.86 1.03 p.u
2G-RL- BOW THRUSTER – 1PH	2063.00	4046.50	3554.40	5512.40	3554.00	5762.17	0.556	0.443	0.262	53.90 0.87 p.u	64.33 1.038 p.u

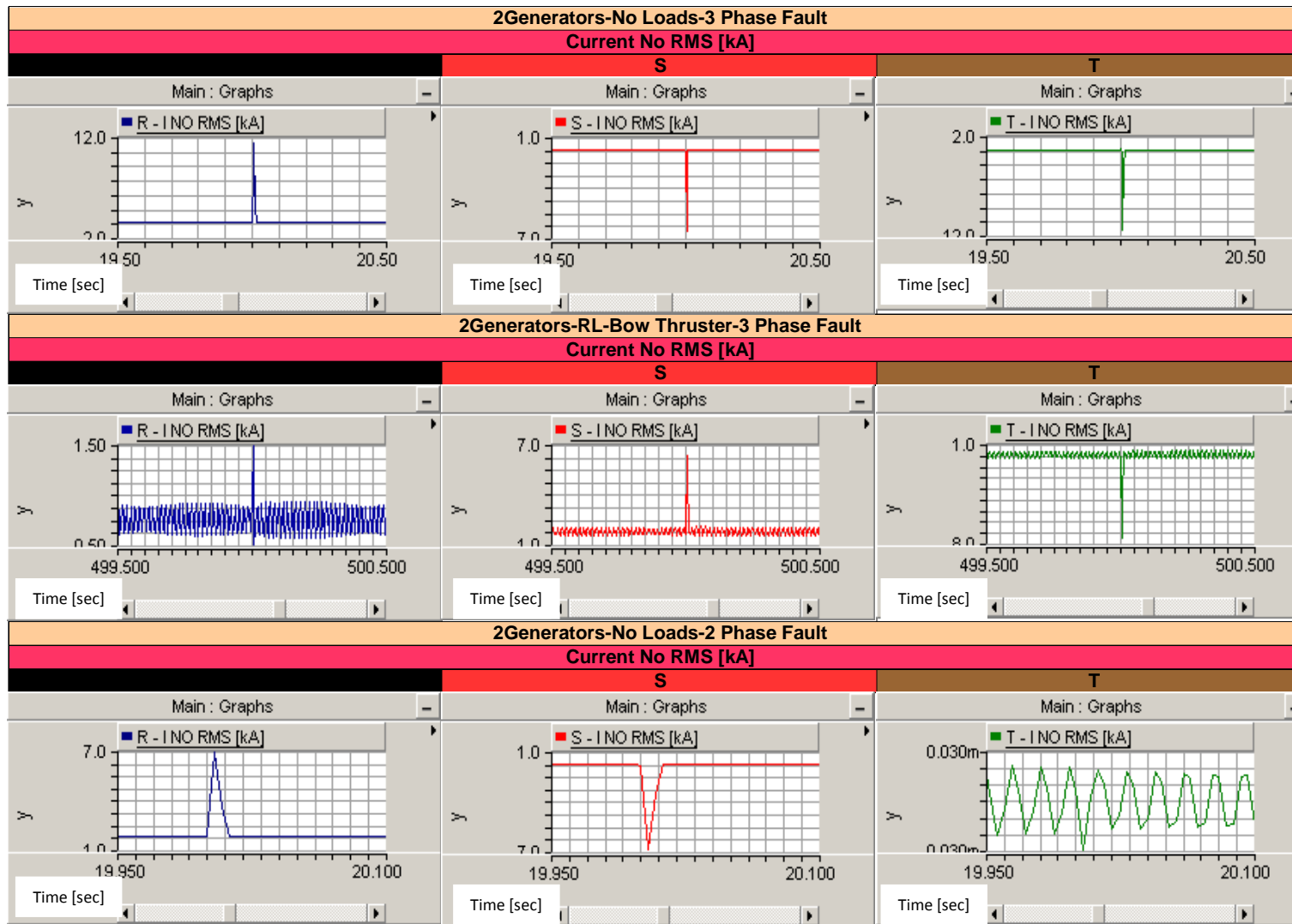
Table 16

Diploma Thesis

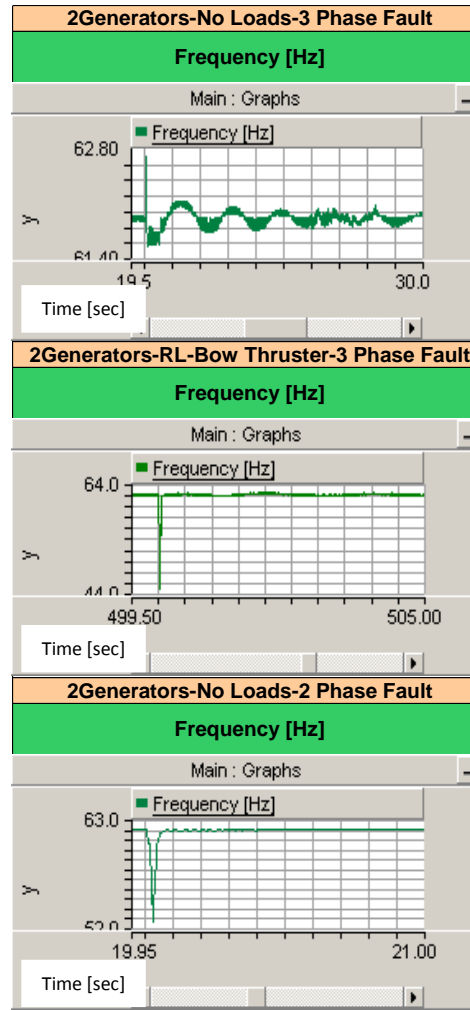
Waveform Group 28



Diploma Thesis

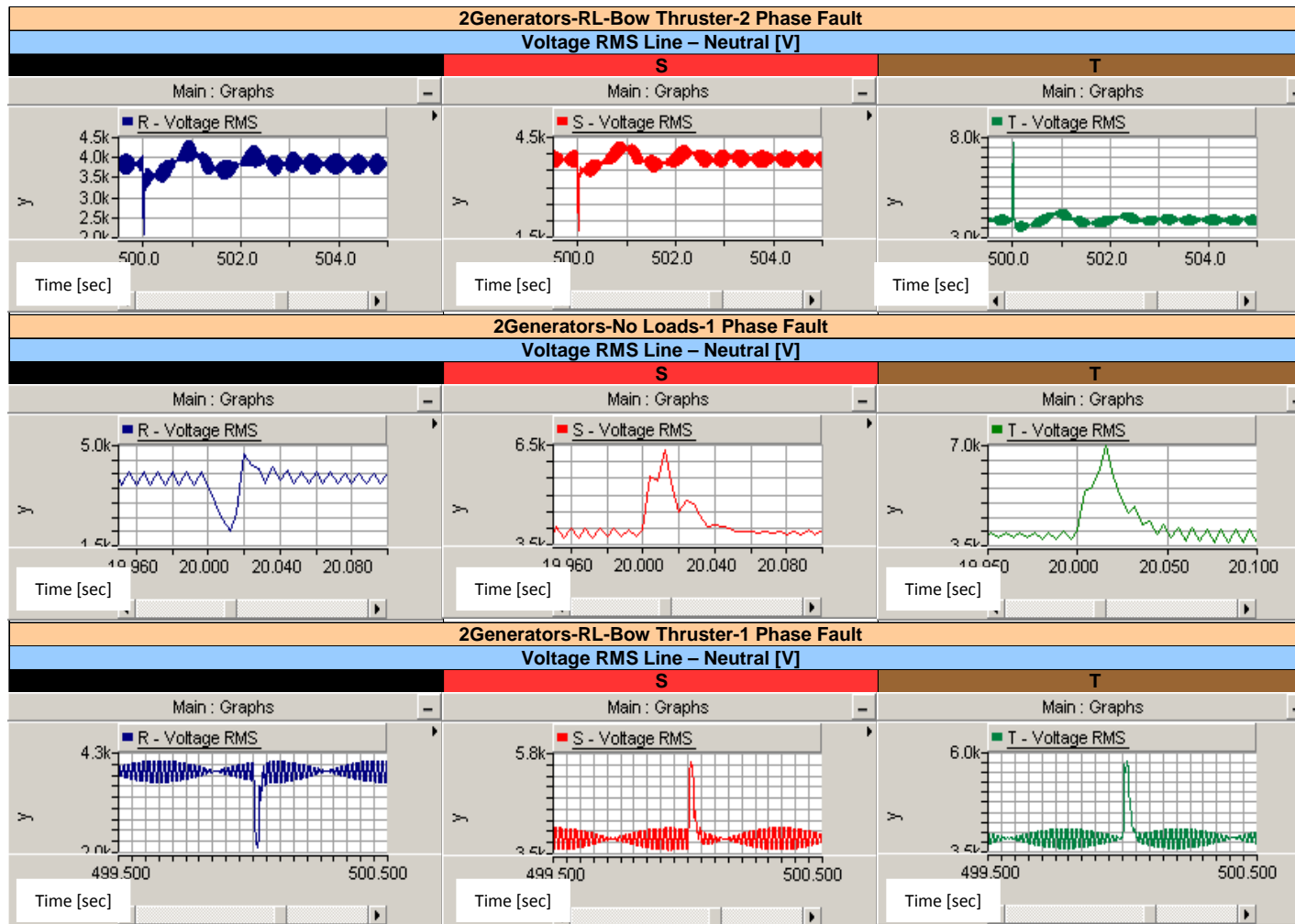


Diploma Thesis

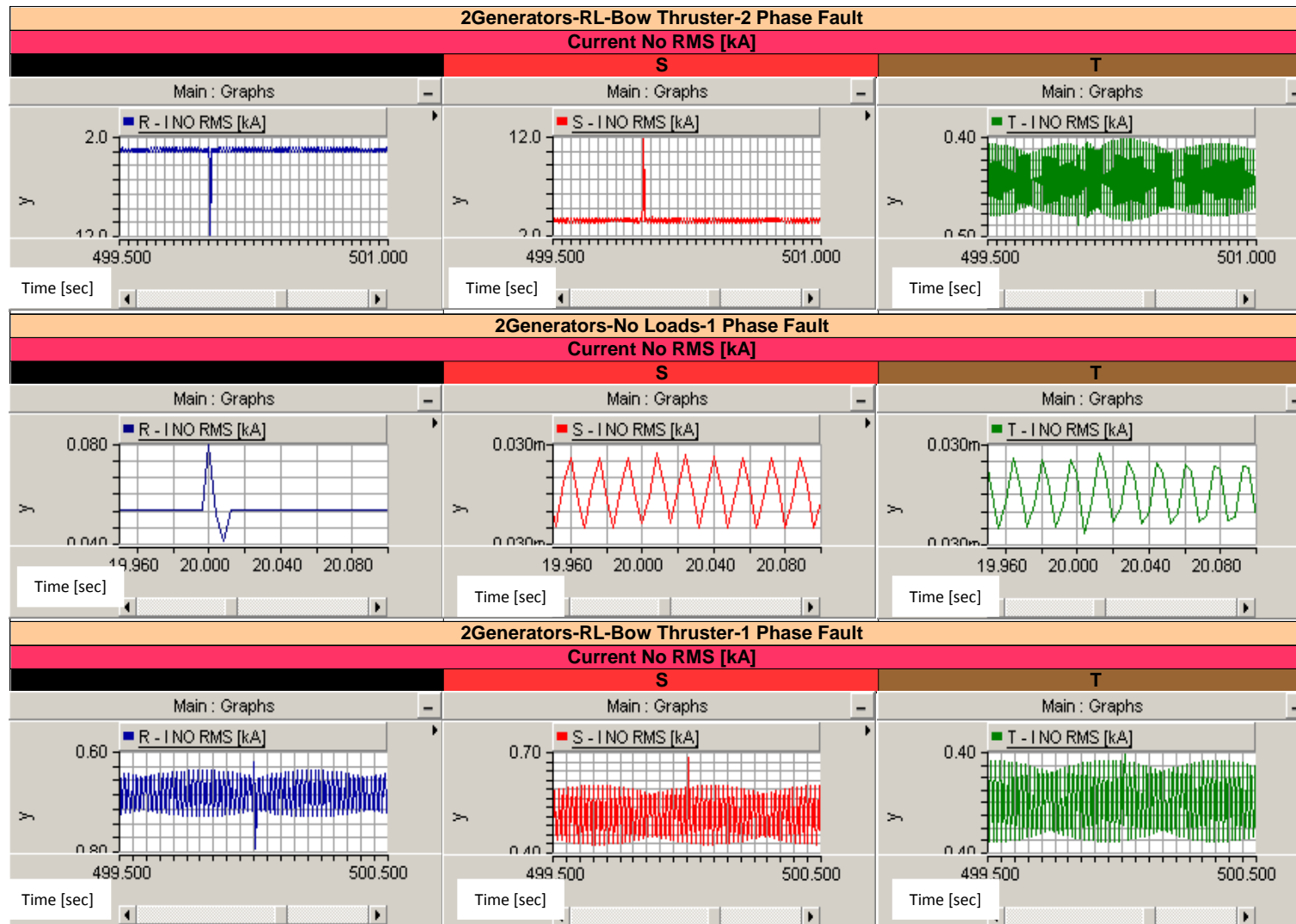


Diploma Thesis

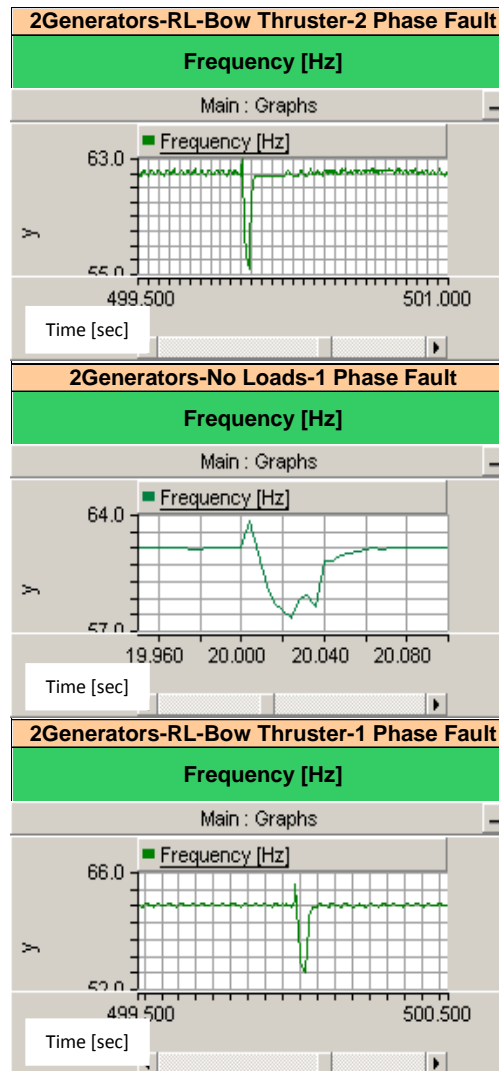
Waveform Group 29



Diploma Thesis



Diploma Thesis



Diploma Thesis

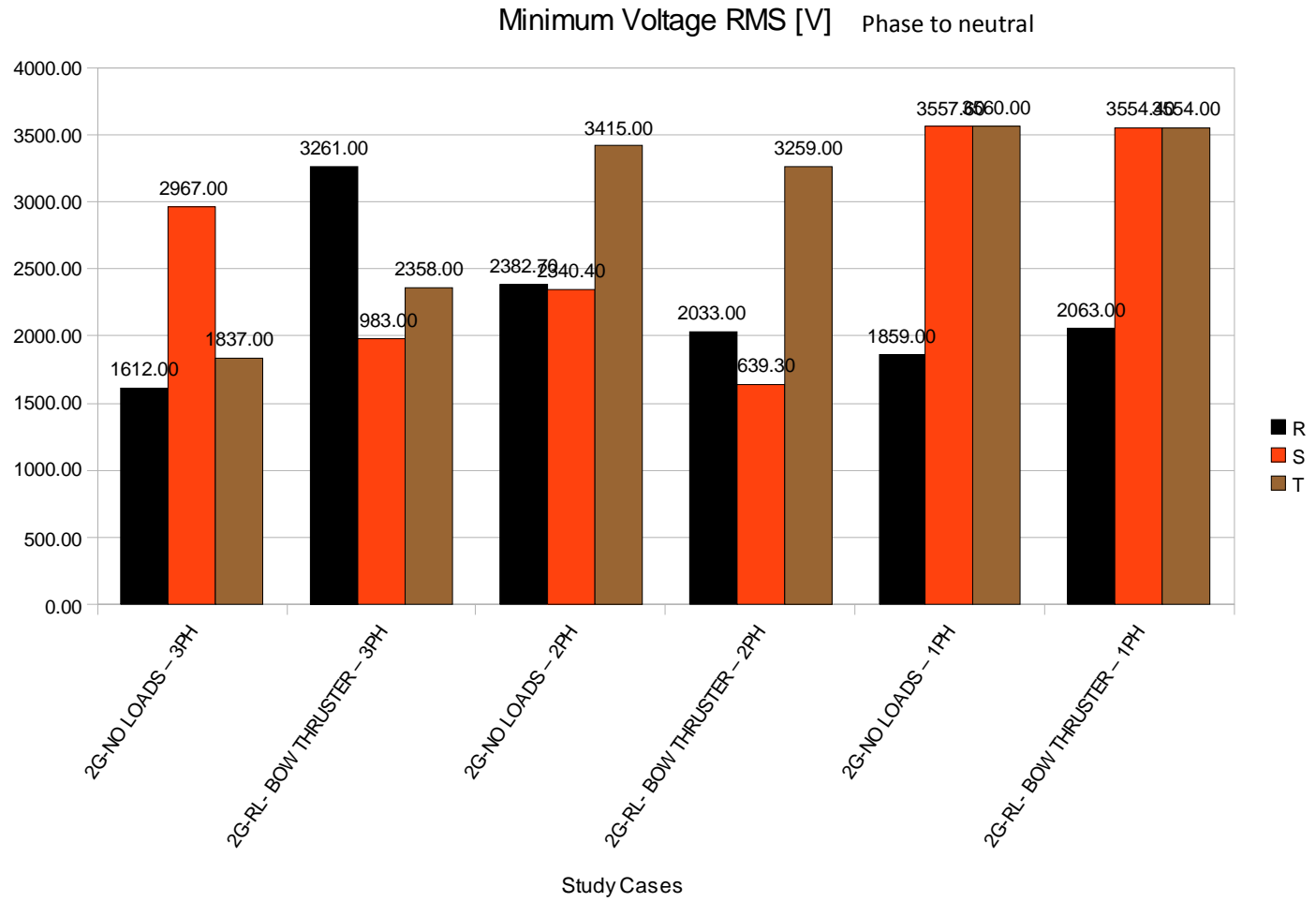


Figure 57

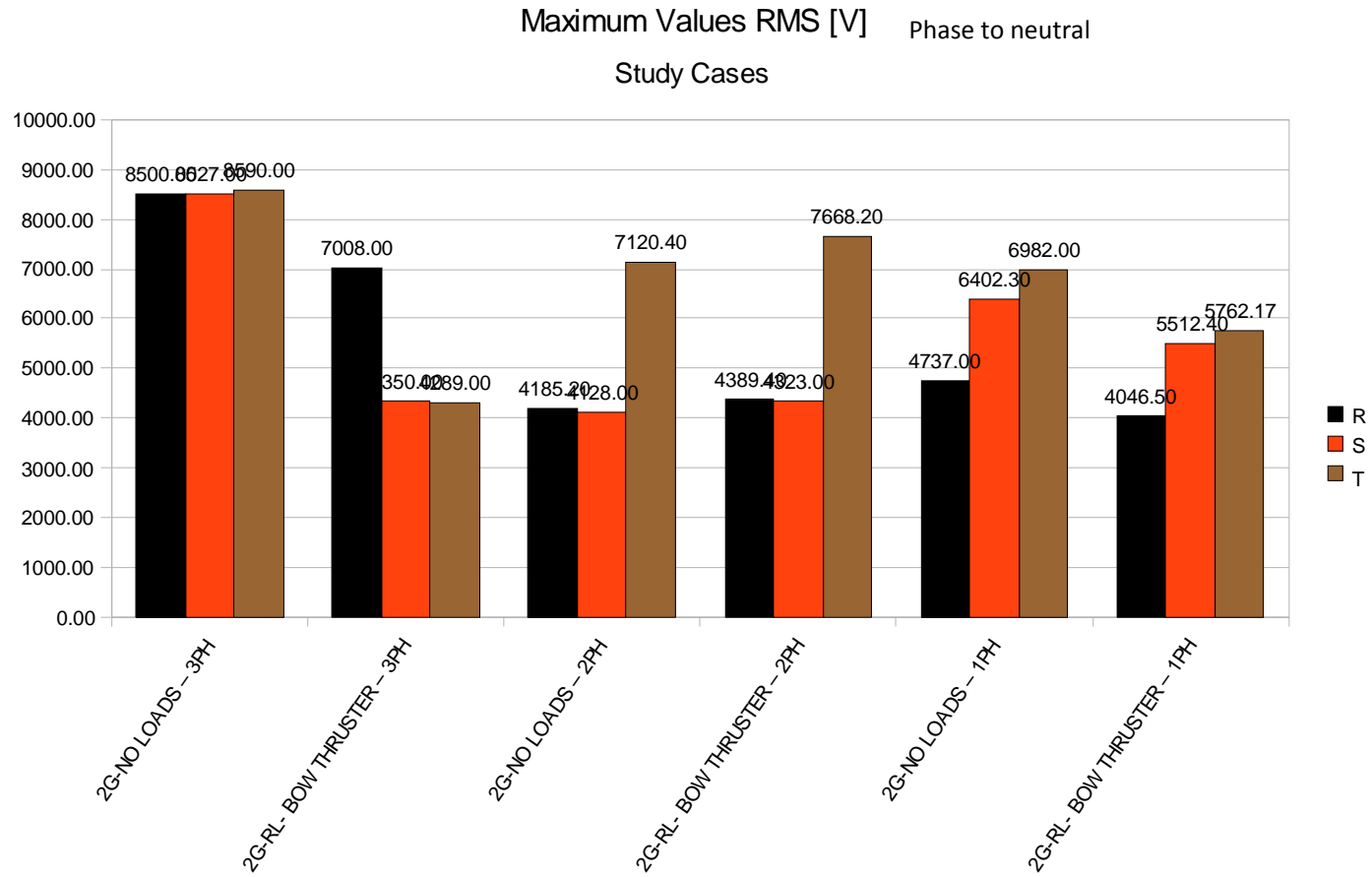


Figure 58

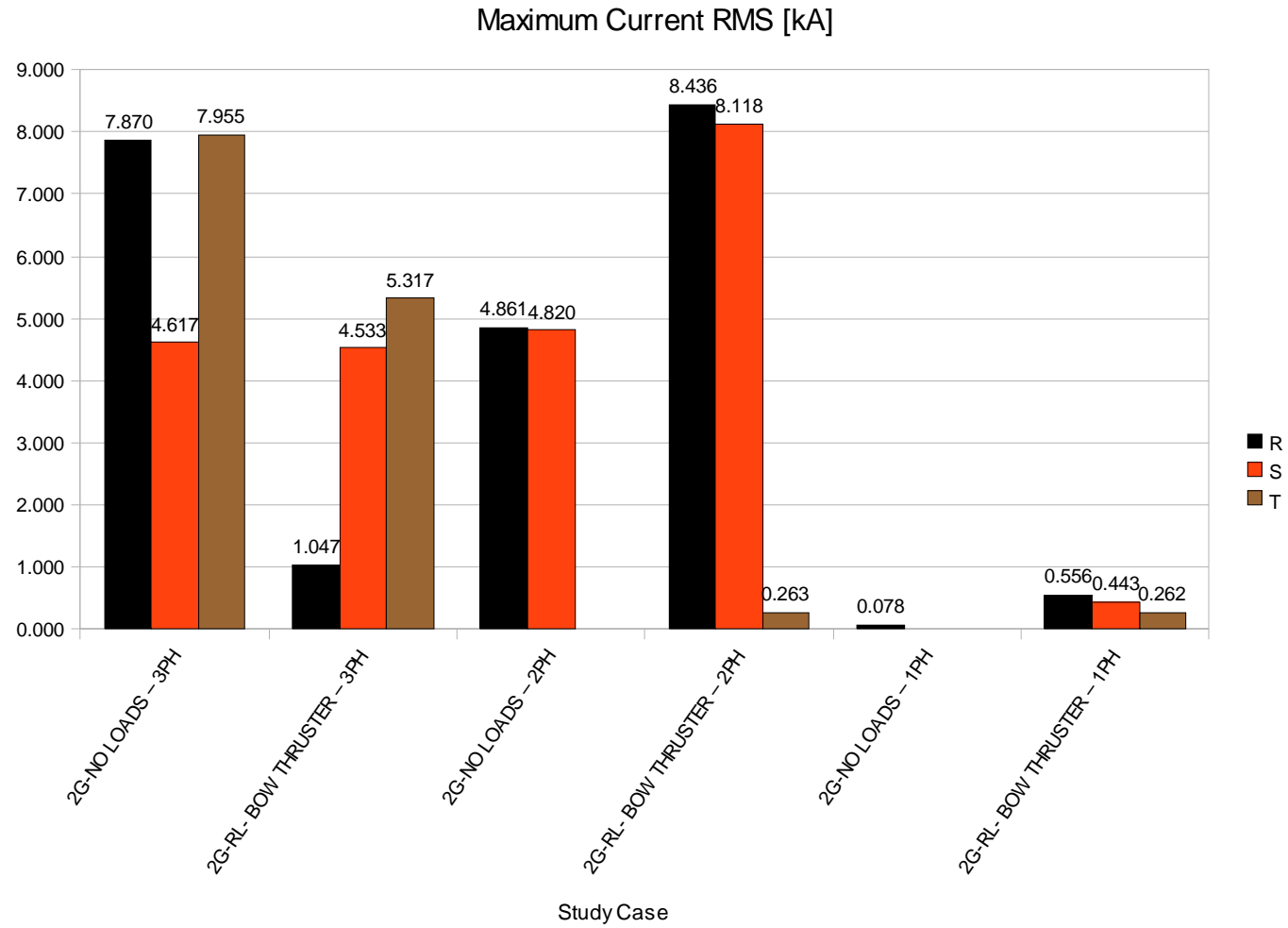


Figure 59

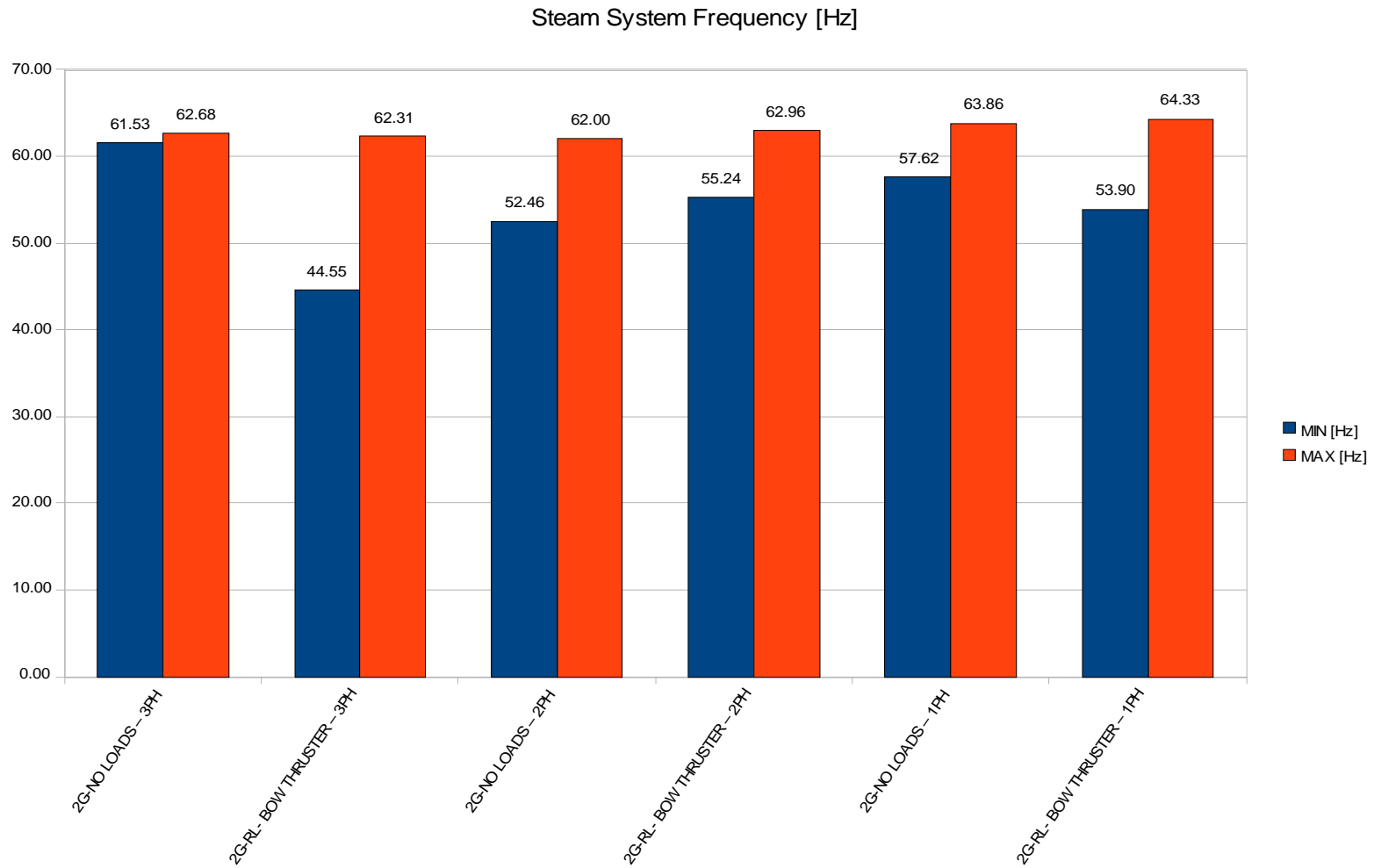


Figure 60

III. Conclusions

The purpose of this investigation is to study:

- The contribution of loading on the short circuit. Further, the distinction between a passive load and a dynamic one is made, namely an R-L and that of large power motor.
- The contribution of the synchronous generator along with its associated AVR and speed governor.

✚ Minimum Voltage Value Comments:

In the three phase application (symmetrical fault application), in the two of the three phases, the minimum voltage value increases and the third phase minimum voltage value decreases significantly compared with the two study cases of load and R-L & bow thruster loading. The motor contributes to the electrical grid as a source due to its pre-fault rotating inertia moment. This contribution of the motor is not that significant in the asymmetrical faults studied, namely the single and two-phase ones.

✚ Maximum Voltage Value Comments:

The bow thruster motor behaves in the same way as in minimum voltage investigation. In detail, the motor presence decreases the maximum voltage value in cases where it increases the minimum voltage value, while it increases the maximum voltage value in the same cases where it decreases the minimum voltage value.

✚ Minimum and Maximum Frequency Value Comments:

Considering that the recorded frequency overshoot values are of minor importance in comparison with the frequency dips, remarks focus only on the frequency drops. According to the recordings, in three and single fault phase (symmetrical and slight asymmetrical fault respectively) application, the motor contribution leads to decreasing even more the minimum frequency value while in two phase fault application (strong asymmetrical fault), the motor contribution leads to

Diploma Thesis

increasing the minimum frequency value in comparison with no load condition.

- ✚ It must be highlighted that comparing to the no load conditions, the study cases in which the motor action increases the minimum voltage value, decreases at the same time the minimum frequency value. On the other hand, the study cases in which the motor action decreases the minimum voltage value, increases at the same time the minimum frequency value.

CHAPTER 06

Dynamic Response Full Generator Model: Approximation Formula

Diploma Thesis

I. Voltage and Speed System Response Approximation Analysis

In this section a simplified mathematical model (transfer function) for the entire system of a synchronous generator along with its associated speed governor and AVR sub-systems is sought. Two types of synchronous generators are examined for the purposes of this degree dissertation, namely diesel and steam generators.

In detail, the system of the single synchronous generator accompanied by its exciter, speed governor, steam turbine or diesel engine is supposed to be represented with acceptable accuracy for this study case by the use of a second order polynomial transfer function. The examined quantities are the voltage and frequency at the bus bar of each generator for specific type of loading.

In both cases, it is supposed that the system excitation is the sudden connection of passive loads to the generator bus-bar.

Considering that the system studied is non-linear, the approximation analysis presented in the following, is valid only in certain operating conditions (i.e. loading is 29% of the nominal load, while the load is of a step-function profile, as well as the initial conditions are non-zero).

The mathematical representation of the excitation is the following (Equation 7):

$$u(t) = (S_{LOAD} / S_{GENERATOR}) u_{STEP} (t = 0) \quad \text{Equation 7}$$

Where:

$(S_{LOAD} / S_{GENERATOR})$: the nominal complex power of the loads to the nominal complex power of the examined generator.

In any case it is supposed that the power factor of the passive loads is equal to 0.8p.u i.e. equal to the nominal power factor of each generator.

For the purposes of this project the connected R-L load apparent power is $S=1.25\text{MVA}$ (0.8p.u).

Diploma Thesis

It is also supposed that at load connecting time ($t=0.0\text{sec.}$) the system operates at its no-load steady-state condition.

In accordance with the system response, the following equations seem to be the most accurate approach.

Taking into consideration the above assumptions, in any case the response of the system can be described by the Equation 8:

Response of the system in time domain:

$$y(t) = A_1 \left(1 - \frac{A_2}{\sqrt{1-J^2}} e^{-J\omega_n t} \sin(\omega_n \sqrt{1-J^2} t + \phi) \right) \quad \text{Equation 8}$$

or in the frequency domain:

$$Y(s) = A_1 \left(\frac{1}{s} - A_2 \frac{\left(\frac{\cos(\phi)\omega_n(1-J^2)^{1/2}}{(s+J\omega_n)^2 + \omega_n^2(1-J^2)} + \frac{\sin(\phi)(s+J\omega_n)}{(s+J\omega_n)^2 + \omega_n^2(1-J^2)} \right)}{\sqrt{(1-J^2)}} \right) \quad \text{Equation 9}$$

The capacity of each generator is equal to 4.3125 MVA.

The excitation of the system has been supposed to be the following (Equation 10):

$$x(t) = (1.25 / 4.3125)u_{STEP}(t=0) = 0.29u_{STEP}(t=0) \Rightarrow X(s) = 0.29 \frac{1}{s} \quad \text{Equation 10}$$

According to the excitation as well as the response of the system, the transfer function of the system is described by the equation 11:

$$G(s) = \frac{A_1 s}{0.29} \left(\frac{1}{s} - A_2 \frac{1}{\sqrt{1-J^2}} \left(\frac{\cos(\phi)\omega_n \sqrt{1-J^2}}{(s+J\omega_n)^2 + (\omega_n \sqrt{1-J^2})^2} + \frac{\sin(\phi)\omega_n \sqrt{1-J^2} (s+J\omega_n)}{(s+J\omega_n)^2 + (\omega_n \sqrt{1-J^2})^2} \right) \right) \quad \text{Equation 11}$$

Diploma Thesis

For the four different types of approximations corresponding to both of the generator types, the parameterization of the previous equations is presented in Table 17:

Steam Generator		
	Voltage Response Approximation	Frequency Response Approximation
J	0.24	0.09
ω_n[rad/sec]	4	1.5
ϕ[rad]	0	0
A_1	1.0013	0.993
A_2	0.135	0.035

Diesel Generator		
	Voltage Response Approximation	Frequency Response Approximation
J	0.24	0.12
ω_n[rad/sec]	4	1.9
ϕ[rad]	0	0
A_1	1.001	1
A_2	0.13	0.035

Table 17

Diploma Thesis

II. Steam Generator Response Approximation:

In accordance to the given parameters the transfer function for voltage and frequency response approximation is the following:

Voltage Response Problem:

$$G(s) = \frac{3.45s^2 + 4.76s + 55.2}{s^2 + 1.92s + 16.0} \quad \text{Equation 12}$$

Poles	Zeros
-0.96+3.8831j	-0.6899+3.94j
-0.96-3.8831j	-0.6899-3.94j

Speed Response Problem:

$$G(s) = \frac{3.424s^2 + 0.745s + 8.56}{s^2 + 0.27s + 2.50} \quad \text{Equation 13}$$

Poles	Zeros
-0.1350+1.5754j	-0.1088+1.5774j
-0.1350-1.5754j	-0.1088-1.5774j

Diploma Thesis

III. Diesel Generator Response Approximation:

In accordance with the given parameters the transfer function for voltage and frequency response approximations is the following:

Voltage Response Problem:

$$G(s) = \frac{3.452s^2 + 4.833s + 55.23}{s^2 + 1.92s + 16.0} \quad \text{Equation 14}$$

Poles	Zeros
-0.96+3.883j	-0.7+3.9382j
-0.96-3.883j	-0.7-3.9382j

Speed Response Problem:

$$G(s) = \frac{3.45s^2 + 1.344s + 12.54}{s^2 + 0.456s + 3.61} \quad \text{Equation 15}$$

Poles	Zeros
-0.228+1.8863j	-0.1948+1.8896j
-0.228+1.8863j	-0.1948 - 1.8896j

A better investigation of the characteristics of the four previous approximations regarding system stability as well as system response to harmonic excitation is root locus, Bode, and Nyquist diagram of the transfer function of the problem approximations.

Diploma Thesis

IV. Steam Generator Response Approximation Graphs and Steam System Stability:

The steam system voltage response and its approximation are both illustrated to the figure 61:

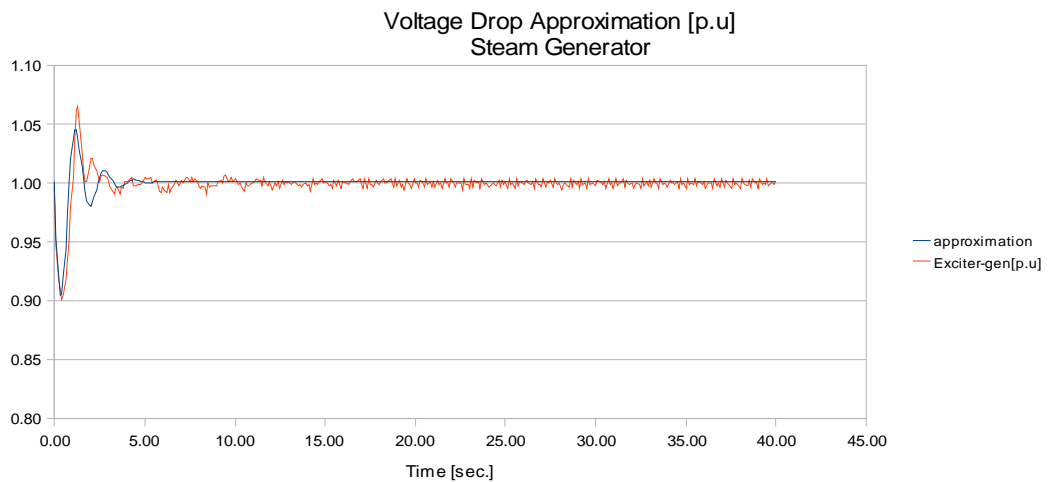


Figure 61

On the other hand, the approximation error [%] between the approximation and the simulation data is the following (figure 62):

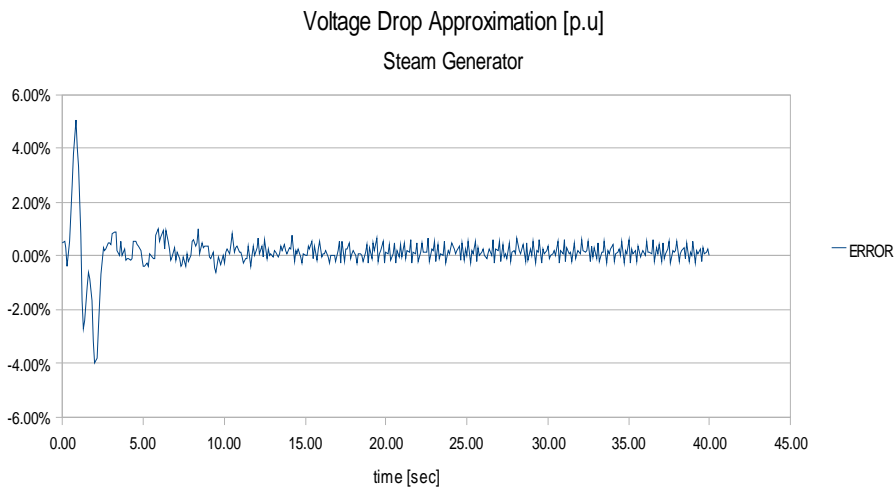


Figure 62

Diploma Thesis

The root movement by varying the gain of the transfer function is presented in the figure 63:

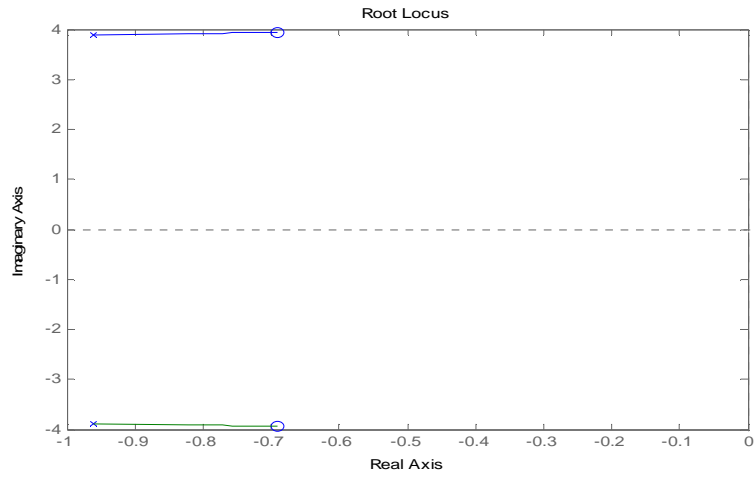


Figure 63

For harmonic excitation, the system response is presented in the figure 64:

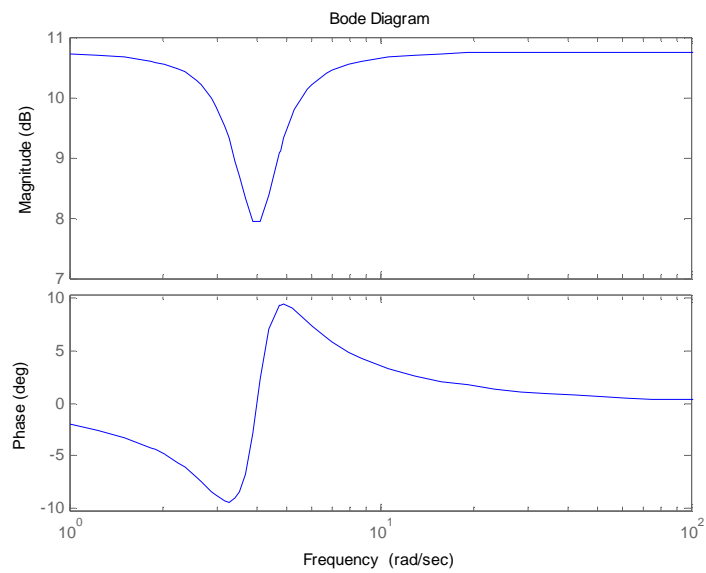


Figure 64

Diploma Thesis

Considering the system poles and zeros, the Nyquist diagram below presents the stable condition of the system:

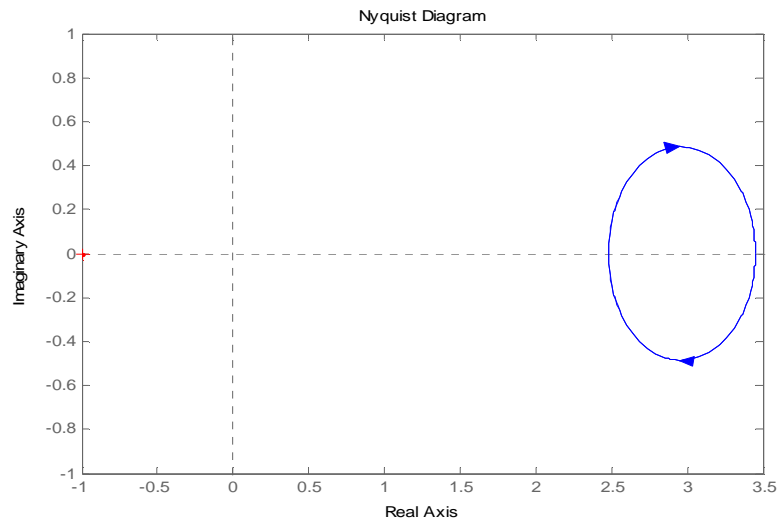


Figure 65

Specifically, according to this, provided that the system is stable, the equality below is valid.

$$Z = N + P$$

Where:

Z: the number of transfer function closed loop zeros located on the right complex field.

N: the number of cycling ($N > 0$ clockwise direction, $N < 0$ counter clock wise direction) of the point $(-1+0j)$ by the Nyquist curve.

P: the number of transfer function open loop poles located on the right complex field.

In accordance to the previous poles and zeros investigation, there are no poles and zeros located on the right complex field. On the top of that, there is also no cycling of the point $-1+0j$ of the Nyquist curve.

Diploma Thesis

The previous claim confirms that the Nyquist equation is valid, hence the system is stable. This can also be confirmed by the response graph. According to this graph, the step excitation (limited excitation) is followed by a limited response. In association with the definition of system stability, it can be also concluded that the system is stable.

The steam system frequency response and steam system stability are illustrated in the figure 66:

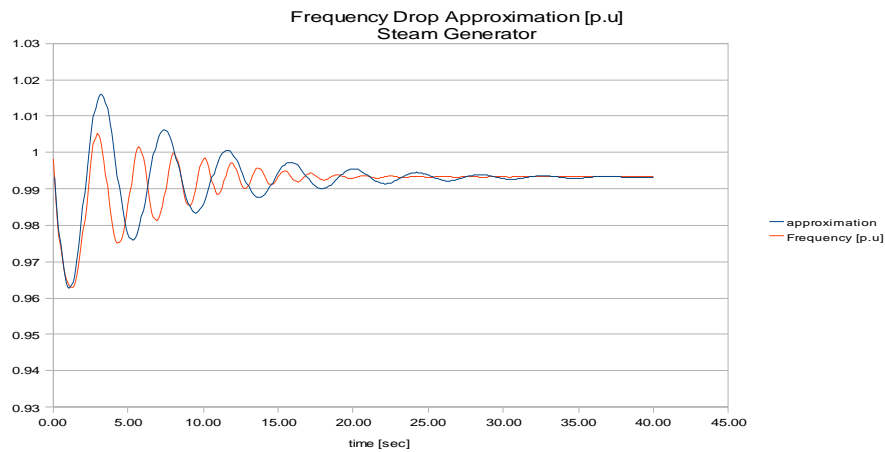


Figure 66

On the other hand, the approximation error [%] between the approximation and the simulation data are the following (figure 67):

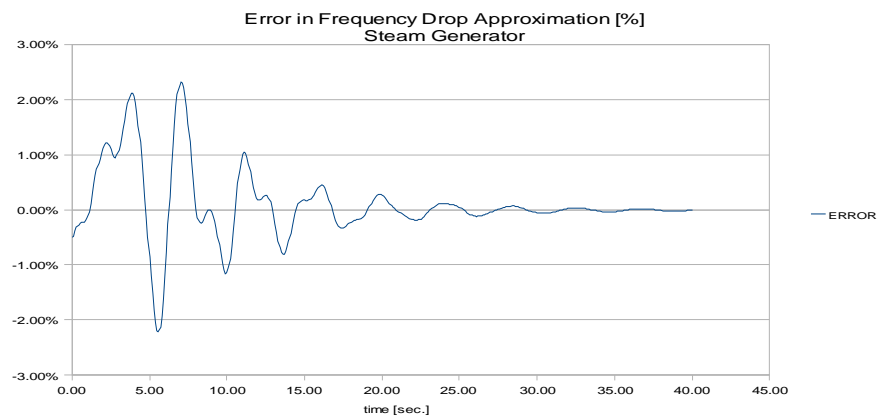


Figure 67

Diploma Thesis

The root movement by varying the gain of the transfer function is presented in the figure 68:

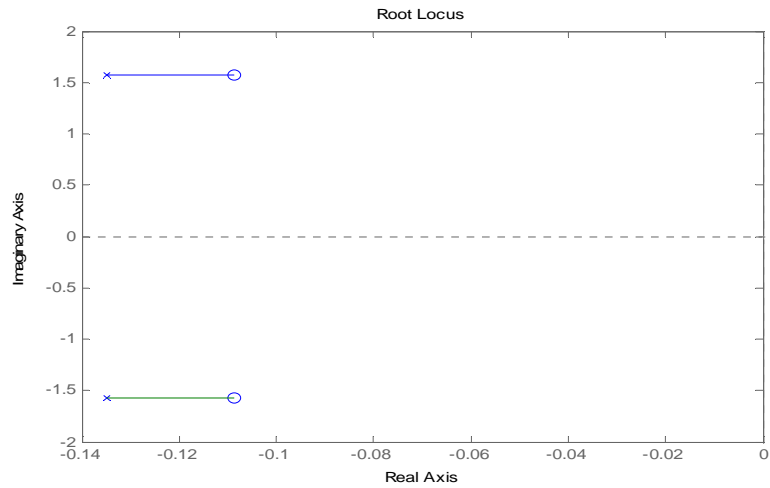


Figure 68

For harmonic excitation, the system response is presented in the figure 69:

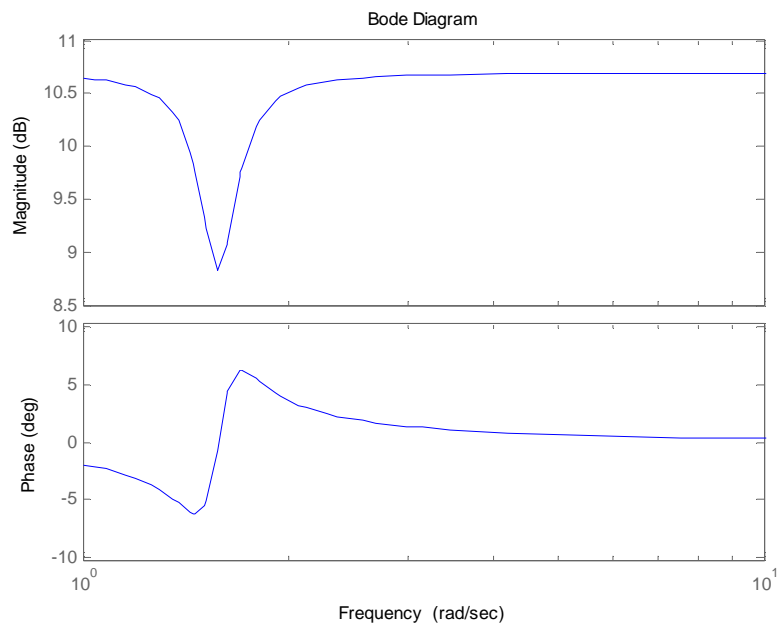


Figure 69

Diploma Thesis

Considering the system poles and zeros, the Nyquist diagram below shows the stable condition of the system:

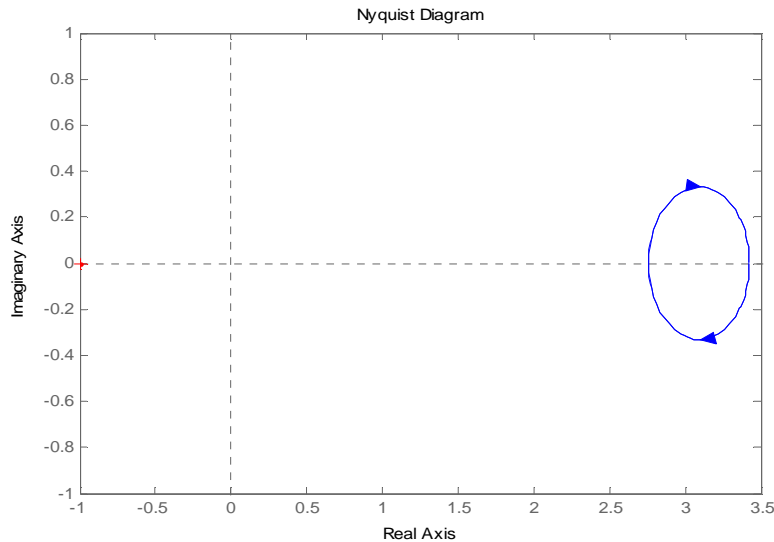


Figure 70

Specifically, according to this, provided that the system is stable, the equality below is valid.

$$Z = N + P$$

Where:

Z: the number of transfer function closed loop zeros located on the right complex field.

N: the number of cycling ($N > 0$ clockwise direction, $N < 0$ counter clock wise direction) of the point $(-1+0j)$ by the Nyquist curve.

P: the number of transfer function open loop poles located on the right complex field.

In accordance with the previous poles and zeros investigation, there are no poles and zeros located on the right complex field. On the top of that, there is also no cycling of the point $-1+0j$ of the Nyquist curve. Moreover, as in voltage level approximation for limited input, the system response is limited. This means that the system is valid.

Diploma Thesis

V. Diesel Generator Response Approximation Graphs and Diesel System Stability:

The diesel system voltage response and its approximation are illustrated to the graphs below (figure 71,72):

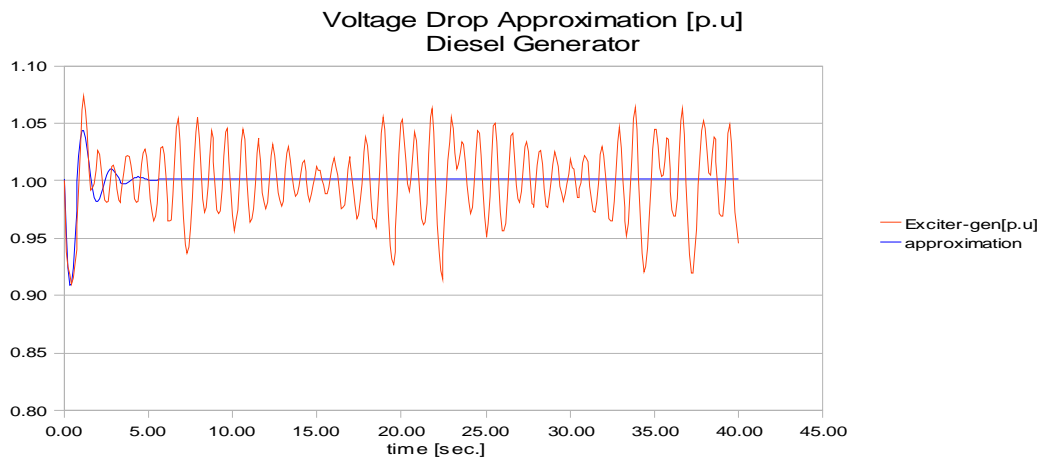


Figure 71

On the other hand, the approximation error [%] between the approximation and the simulation data should be the following:

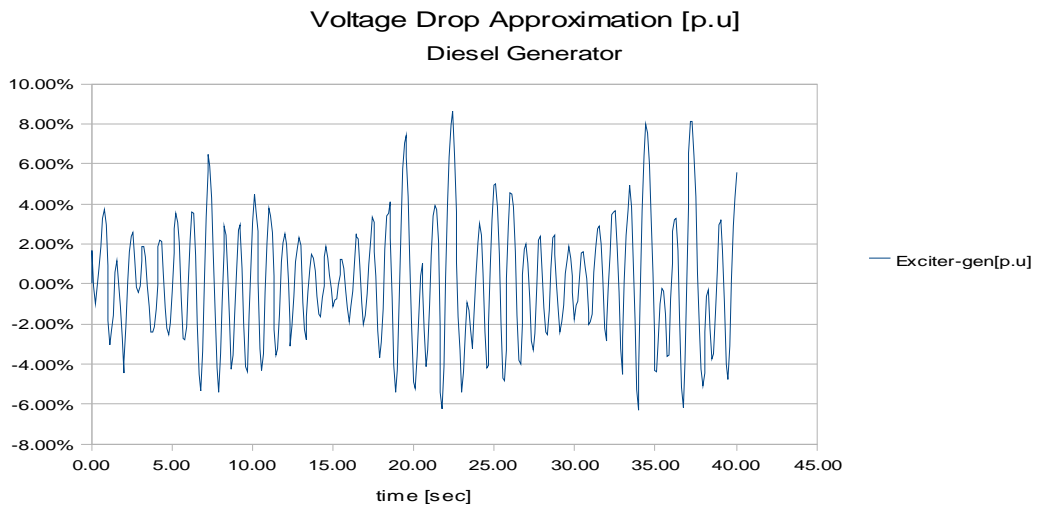


Figure 72

Diploma Thesis

The root movement by varying the gain of the transfer function is presented in the figure 73:

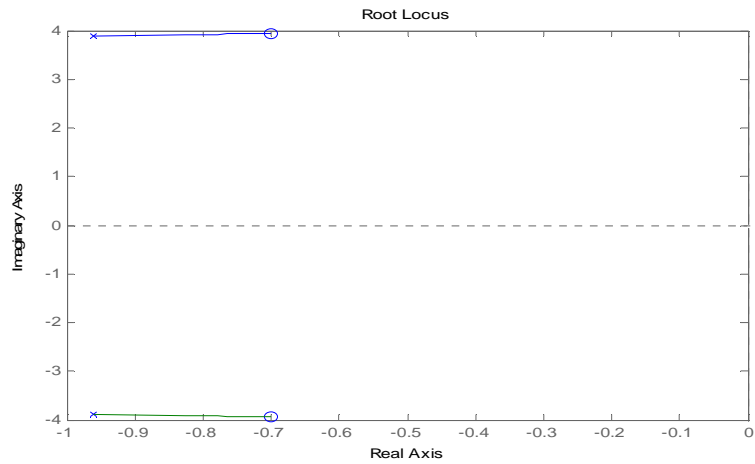


Figure 73

For harmonic excitation, the system response is represented in the figure 74:

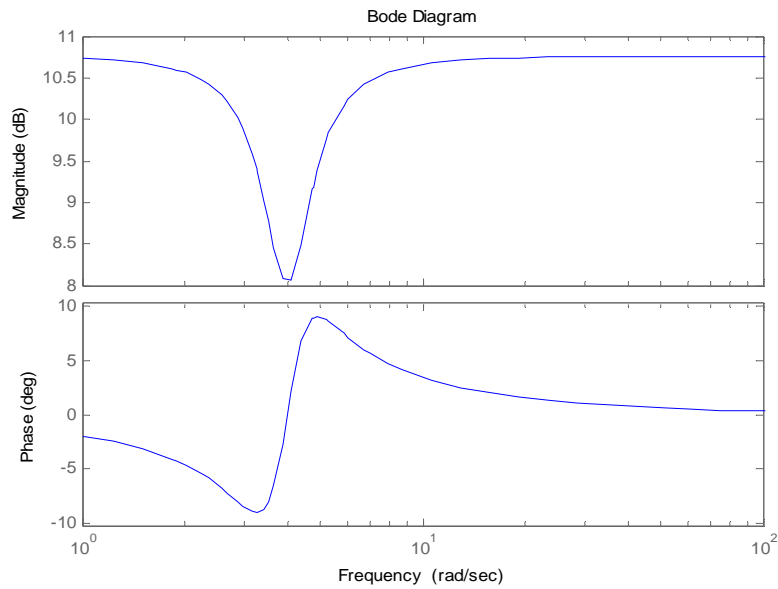


Figure 74

Diploma Thesis

Considering the root and zeros of the system, the Nyquist diagram below shows the stable condition of the system:

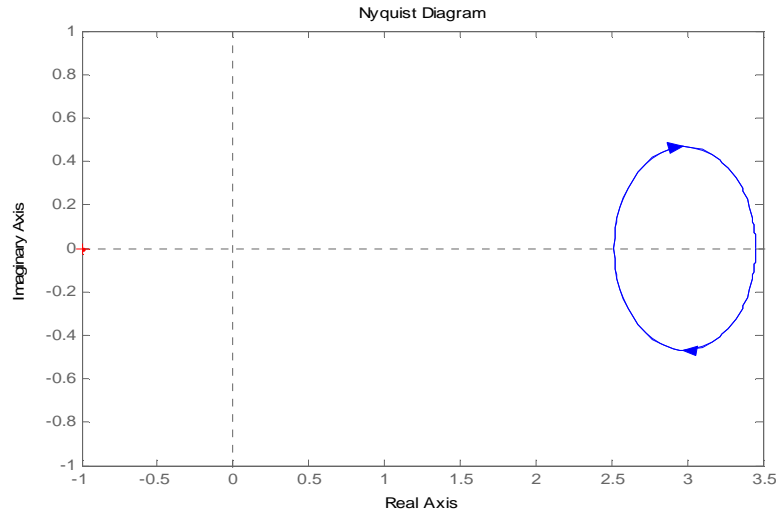


Figure 75

Specifically, according to this, provided that the system is stable, the equality below is valid.

$$Z = N + P$$

Where:

Z: the number of transfer function closed loop zeros located on the right complex field.

N: the number of cycling ($N > 0$ clockwise direction, $N < 0$ counter clock wise direction) of the point $(-1+0j)$ by the Nyquist curve.

P: the number of transfer function open loop poles located on the right complex field.

In accordance with the aforementioned poles and zeros investigation, there are no poles and zeros located on the right complex field. On the top of that, there is also no cycling of the point $-1+0j$ of the Nyquist curve.

The previous claim confirms that the Nyquist equation is valid. This means that the system is stable. As in previous cases, by using the stability definition it can be concluded that the system is stable.

Diploma Thesis

The diesel system frequency response and diesel system stability are illustrated in the graphs below (figure76):

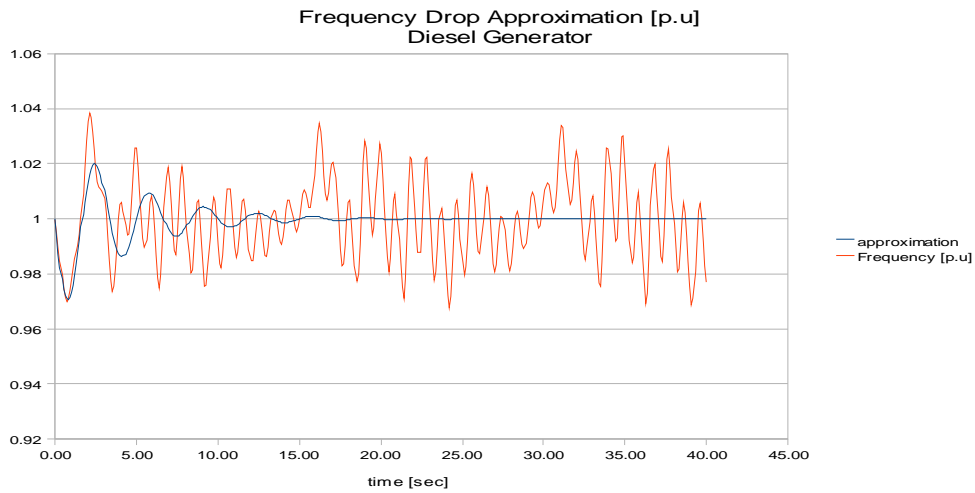


Figure 76

On the other hand, the approximation error [%] between the approximation and the simulation data is illustrated in the figure 77:

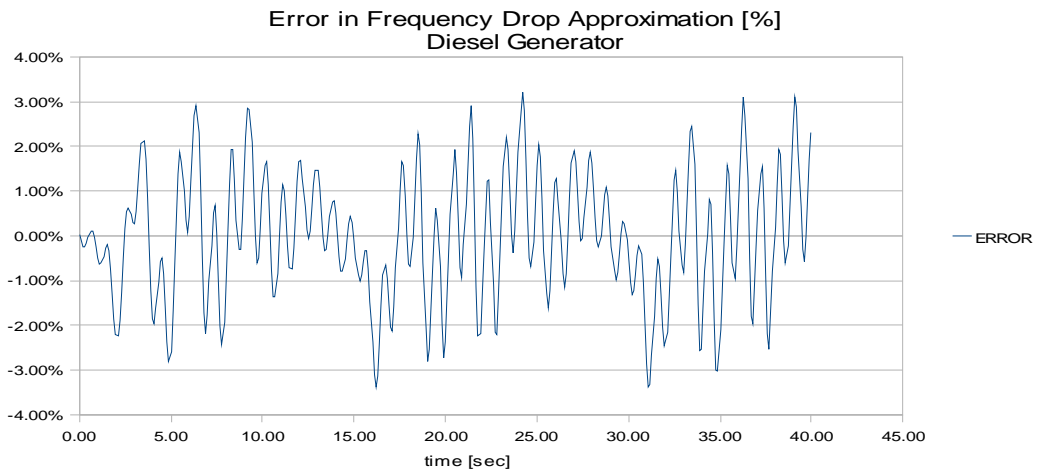


Figure 77

Diploma Thesis

The root movement by varying the gain of the transfer function is represented in the figure 78:

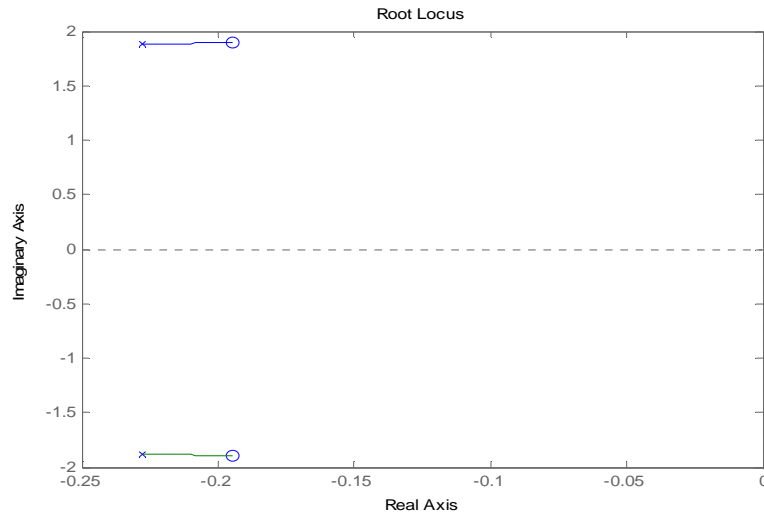


Figure 78

For harmonic excitation, the system response is presented in the figure 79:

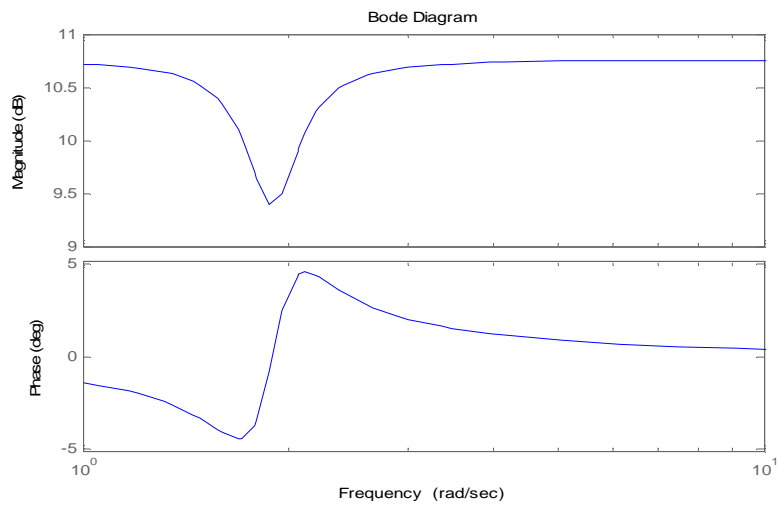


Figure 79

Diploma Thesis

Considering the system poles and zeros, the Nyquist diagram below express the stable condition of the system:

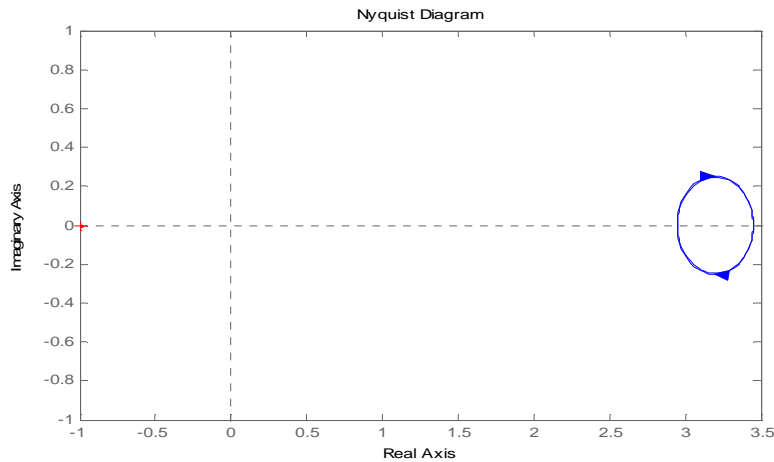


Figure 80

Specifically, according to this, provided that the system is stable, the equality below is valid.

$$Z = N + P$$

Where:

Z: the number of transfer function closed loop zeros located on the right complex field.

N: the number of cycling ($N > 0$ clockwise direction, $N < 0$ counter clock wise direction) of the point $(-1+0j)$ by the Nyquist curve.

P: the number of transfer function open loop poles located on the right complex field.

In accordance with the aforementioned poles and zeros investigation, there are no poles and zeros located on the right complex field. On the top of that, there is also no cycling of the point $-1+0j$ of the Nyquist curve.

The previous claim confirms that the Nyquist equation is valid. This means that the system is stable. As in all previous examined scenarios, according to stability systems definition, it can be concluded once again that the system is stable.

VI. Steam System Further Investigation:

The existing research work regarding steam generator response approximation efforts for the purposes of this project involves only the sudden connection of an R-L load to the generator bus-bar. In detail, the just used R- L load capacity was approximately equal to 29.0% of the generator nominal capacity. In addition, both of them were considered to have the same nominal power factor equal to 0.8 p.u.

Thus it was considered that it would be valuable to know what happens by involving R – L loads with the same power factor but for various capacities in association with generator nominal capacity.

The figures 81,82 present the time response of the steam system for various R – L load configurations regarding voltage and frequency level. Moreover, the figure 83 gives a more clear view regarding the association between the $S_{Load}/S_{Generator}$ and the generator (Maximum, Minimum) voltage and frequency response.

Steam Generator Voltage Response [p.u]
In function to S_Load/S_Generator , P.F=0.8

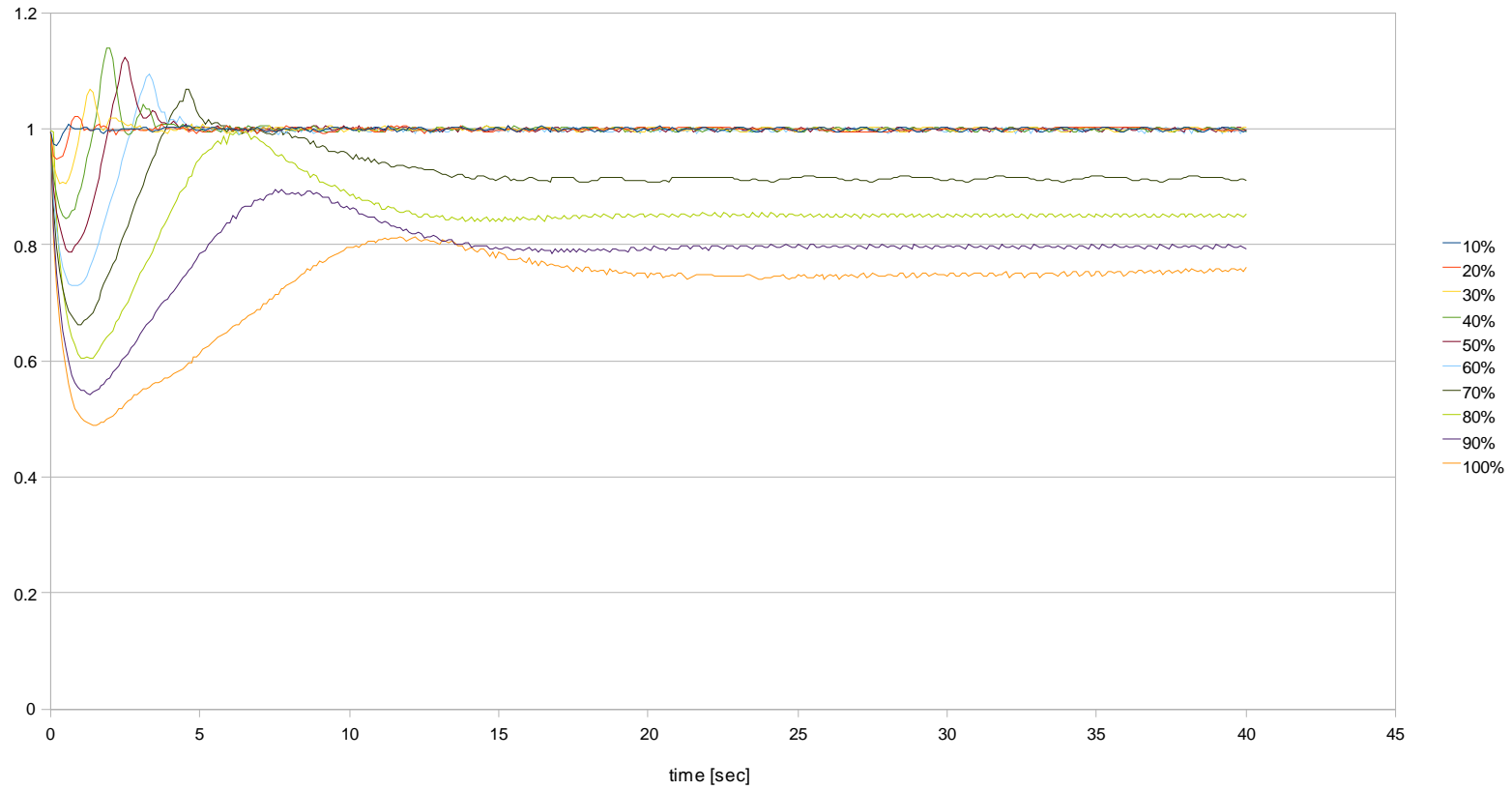


Figure 81

Steam Generator Frequency Response [p.u]
In function to S_Load/S_Generator , P.F=0.8

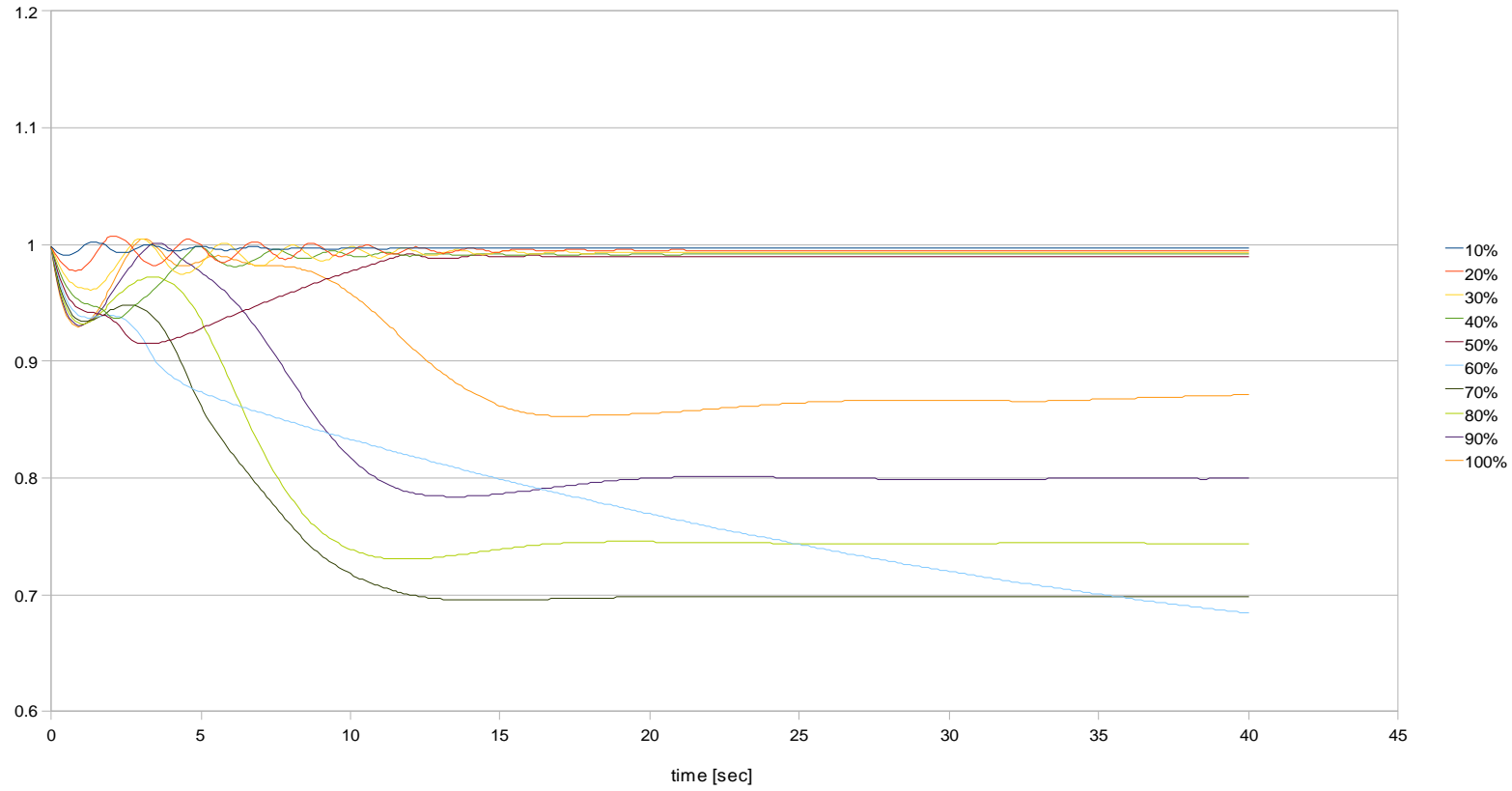


Figure 82

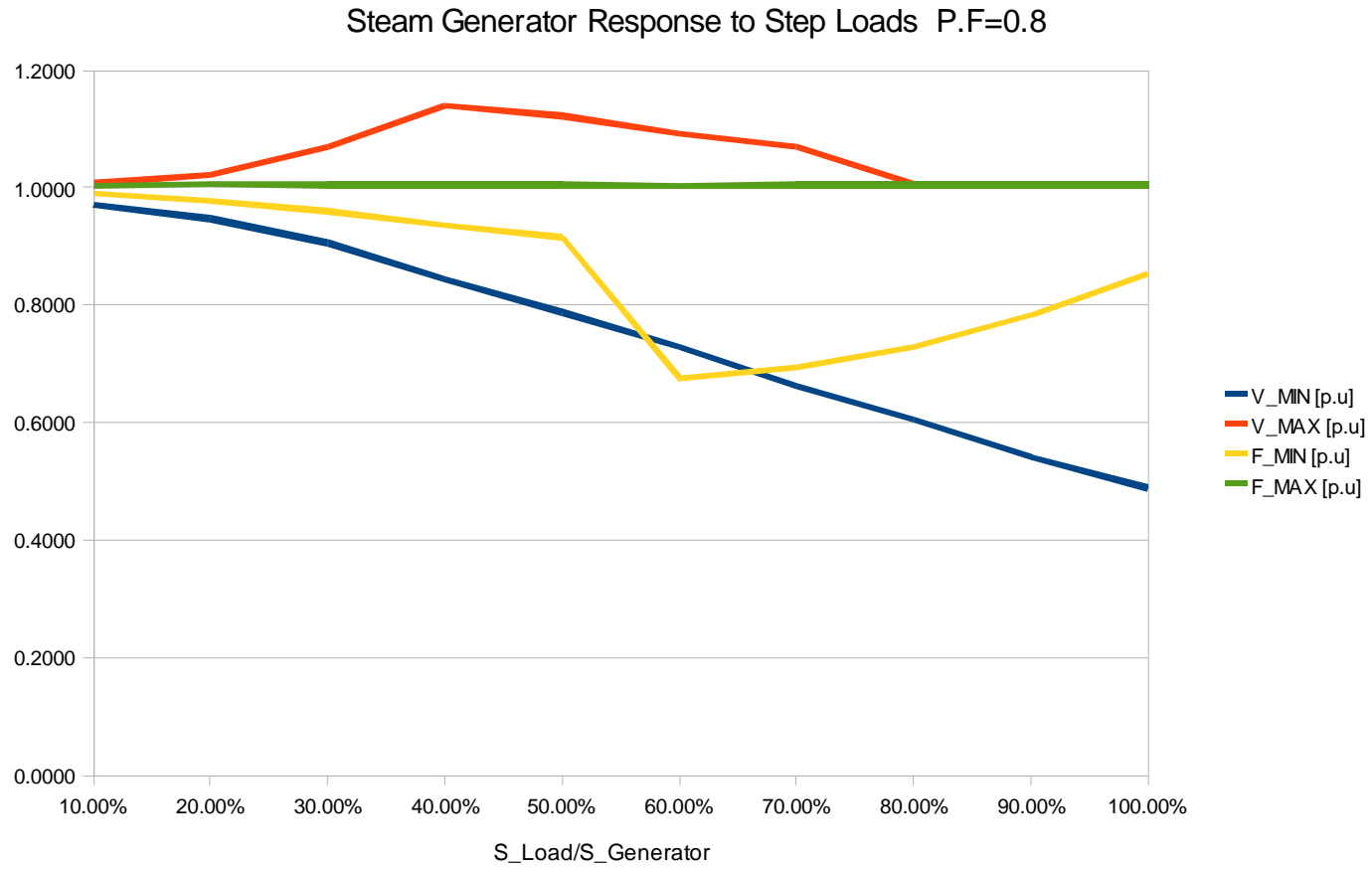


Figure 83

VII. Conclusions

From the graphs of this chapter it can be concluded that the voltage as well as the frequency response of not only steam systems but also diesel systems can be described via a second order transfer function with satisfactorily good accuracy. However, the steam generator response seems to be closer to approximation than the diesel generator. This may be due to a highly possible not proper diesel speed governor setting.

On the other hand, as it can be observed by the last graph, the voltage drop increases steadily by raising the capacity of the suddenly applied load. However, the behavior of the maximum voltage over shoot is not evident as it stand at its highest ever rate at load application capacity equal to the 40.0% of generators capacity.

Regarding the steam system frequency response, the frequency overshoot through the range of load scenarios is minimal while significant frequency dips are recorded. In detail, the frequency drop increases gradually in the mean time between no load condition and load capacity equal to 40.0%. This downward trend is followed by a further drop standing at its lowest ever rate at 60.0% loading. However this downward trend is accompanied by a significant increase standing at 0.85 p.u at 100% loading.

FUTURE POSSIBLE ISSUES

Diploma Thesis

Possible Issues to Investigate further in the Future:

- Investigation of Pod operation with the entire All Electric Ship system considered; this configuration is the so called Integrated Full Electric Propulsion (IFEP) and is expected to introduce significant compliancy in the network studied.
- Improvement in diesel engine models in PSCAD environment so that the actual behavior is better represented.
- Other types of electric motors should be also studied. The most promising novel motor types recently developed are:
 - Permanent Magnet Motors (of axial radial and transverse axis).
 - High Temperature Superconductive Motors
 - Complicated novel configurations such as Advanced Induction Motor.
 - Study of novel thruster configurations e.g. twin tunnel, rim-driver along with associated electric motor drives.

APPENDIX A (Paper)

On Studying the Power Supply Quality problems due to Thruster Start-ups

J.M. Prousalidis, P. Mouzakis, E. Sofras,
School Of Naval Architecture And Marine Engineering
National Technical University of Athens
Athens, Greece
jprousal@naval.ntua.gr

D. Muthumuni,
Manitoba HVDC Centre
Manitoba, Canada
Dharshana@hvdc.ca

O. Nayak
Nayak Corporation,
Princeton, NJ, U.S.A
om@nayakcorp.com

Abstract: The target of this paper is twofold: primarily to highlight the significant effect of certain power supply quality problems on the normal operation of the entire ship grid, namely inrush currents and voltage dips due to manoeuvring thruster motor starting-ups. At a second stage, the paper aims at recommending some amelioration of standardization status. Hence, the authors suggest the exploitation of existing experience on pulsed load standardizing, taking into account the resemblance between the systems. The study is enriched by actual case studies and simulations in PSCAD computer program.

Keywords: power quality, thruster, pulsed loads.

I. INTRODUCTION

It is more than two decades that auxiliary propulsion systems (the so-called thrusters) have been introduced in the aft or stern part of several ship types increasing their maneuverability and collision avoidance capabilities. Thus, nowadays, thruster systems installed especially in the bow of a ship, is an indispensable piece of equipment of hers, while it is a common practice that rotation is provided by an electric motor, often an asynchronous (induction) alternative current one.

This electric motor drive is of high power demands, in the order of 0.5 up to 2.5 MW, which increases considerably the electric power demands that the electric power generation set has to meet. Moreover, things are getting worse during starting-up of such huge electric power system, when -like any other motor- the thruster motor absorbs a transient “inrush current” of high values (varying, in general, between 4-7 times the rated current [1-3]). Consecutively, during the inrush phenomenon (i.e. for approximately up to 15-20 s after its time zero) the thruster motor power demands in terms of active and reactive power are high, too. During this interval, the “transient power factor” is fairly low, as the reactive power required is significantly higher than in steady-state.

J. Prousalidis is an Assistant Professor at the School of Naval and Marine Engineering of National Technical University of Athens, 9 Heroon Politechniou St, 15773 Athens, Greece (jprousal@naval.ntua.gr).

P. Mouzakis, is finishing his graduation studies in at the School of Naval and Marine Engineering of National Technical University of Athens.

E. Sofras is a PhD candidate at the School of Naval and Marine Engineering of National Technical University of Athens.

D. Muthumuni, PhD is with the Manitoba HVDC Center, Manitoba, Canada.

O. Nayak, is with Nayak Corporation.

This high energy demand at a low power factor cannot be easily covered by the vessel’s generator sets leading to their possible overloading or even tripping. Furthermore, as a result of the transient inrush current, large voltage drops take place in the entire network, introducing “symmetrical” voltage dips to all three-phases. More specifically, in the bow thruster cases, the motors are installed far away from the generator plant (perhaps farther away than any other large power equipment), therefore the distribution cable is fairly long resulting to a rather large valued cable impedance which is added upon any other intervening impedance like that of a starting-autotransformer. Hence, during motor starting-up there is an increased voltage drop on this impedance, while of course there is a thermal stress on the cable itself. This stress worsens further, in case of repetitive starting-up of the motor and has to be taken into account during cable sizing at the design stage.

In most large scale applications the thruster propeller is a controllable pitch one and during starting-up the blade pitch is set to 0° in order to minimize the electric power demands. However, even this closed propeller has a significant moment of inertia which is added upon the motor’s one deteriorating even further the starting-up phenomenon. Due to this large valued inertia, occasionally voltage and/or frequency stability problems might be noticed [4]. Coming back to the starting-up procedure, as soon as the transients have decayed, the actual ship maneuvering operating mode begins, via varying the thruster’s blade angle. In this way, it is ensured that motor starting-up with its adverse phenomena is not repeated during the rest of the maneuvering mode. Still considering the possible behaviour of the thruster unit during maneuvering, the variations in the propeller’s pitch can result to significant power fluctuations in the power demands. Therefore, it can be argued that the thruster unit operation resembles that of a pulsed load, i.e. load that has large power demand for a very short interval followed by small power demand for fairly longer intervals.

On the other hand, the transient phenomenon described above is not thoroughly covered by most standard rules, as the only relevant limitation is that of the permissible transient voltage fluctuations.

Hence, the target of this paper is twofold: primarily to

highlight the significance of the power supply quality problems due to thruster motor starting-ups, namely inrush currents and voltage dips. On the other hand, the paper aims at not only recommending alleviating measures, but also some possible improvement of the current status in standards towards facing the problem even at the design stage of the ship system. From this point of view, the authors suggest the exploitation of the standardization experience on pulsed loads, considering the similarities between the two loading systems, as highlighted in a specific section. Thus, following the approach of standards on pulsed loads, the thruster electric power demands in both steady- and transient state of operation are compared with the capacity of the generators-in-operation. Two sets of case studies obtained from actual ship systems are presented accompanied by simulations in PSCAD environment (the computer program of Manitoba HVDC Research Center) [5] are used for analysis purposes.

II. THRUSTER ELECTRIC ASYNCHRONOUS MOTOR STARTING-UP

As it is well known there are two major types of induction (or asynchronous) machines, the squirrel cage and the wound rotor ones. Their main difference consists in that in the wound rotor case, the rotor resistance, and hence the motor performance, can vary via externally connected variable resistor units. Focusing on starting-up, where the rotor resistance plays a substantial role, external resistors can be connected, so that the motor absorbs a transient inrush current as equal as its rated value. However, this advantage of the wound rotor types, is compensated by the significantly higher cost. Therefore, several starting-up methods have been developed for the squirrel cage induction motors, a brief overview of which follows.

A. Direct-On-Line (DOL) starting-up

Transient inrush current is mainly due to the low impedance of the motor during its starting-up and the slip rotor resistance, in particular. Due to the highly inductive character of this impedance, a DC offset is also introduced. The mathematical explanation of this offset consists in the initial conditions of the differential equations introduced.

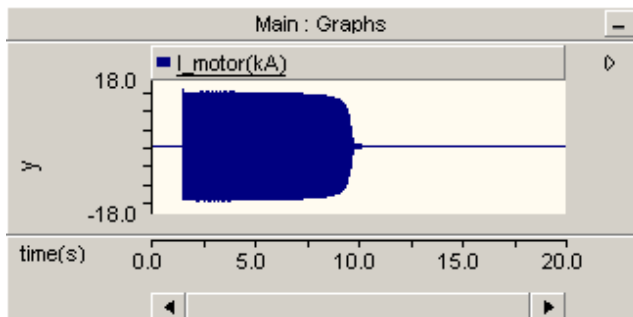


Figure 1. Transient inrush current of a 1.0 MW motor

Eventually, as speed grows-up close to its nominal value, slip decreases, slip rotor resistance, and hence total motor impedance increases to its steady-state value. Moreover, as the current is of high value, a voltage dip occurs in the entire electric system, of magnitude even up to 20%, see Fig. 2.

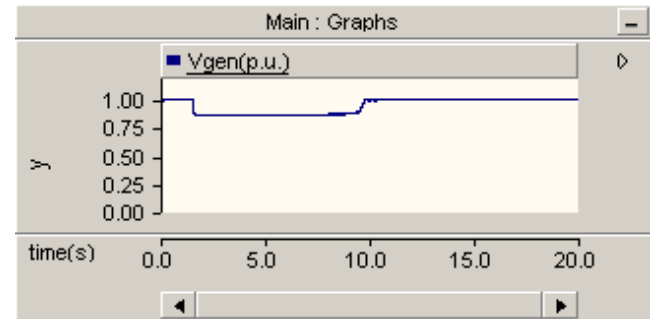


Figure 2. Voltage dip during starting-up of a 1.0 MW motor

Eventually, as speed grows-up close to its nominal value, slip decreases, rotor resistance and hence total motor impedance increases to its steady-state value. Due to the low impedance of highly inductive nature during this starting-up, the motor requires significantly larger amounts of active and especially reactive power, (i.e. a lot of energy at fairly low power factor) than in steady-state conditions. For all these reasons, DOL starting-up is not at all recommended for motors above 3 kW. An improved version of the DOL method, which is exploited in larger power motors, is that of the “Wye/Delta” (Y/D) starter. According to this method, initially the motor windings are connected in wye-connection resulting in smaller currents –but lower electromagnetic torque, too-, while as soon as steady-state speed has been reached, the winding connection changes into delta. It is worth noting that neither the Y/D starter, is not easily applicable to high power motors, either [1-3].

B. Starting-up via autotransformer

In this case, the motor starts-up via the intervention of an autotransformer connected in series to the motor with its power supply. The autotransformer ratio is adjusted by an on-load tap-changing mechanism offering, at starting-up a higher current capacity. This is achieved by connecting the motor on the auto-transformer secondary side, i.e. at a lower voltage level. As soon as the motor has reached its nominal operation speed, the tap changer resumes to the 1:1 ratio of the autotransformer, or alternatively a changeover switch completely by-passes the entire autotransformer. Anyhow, the main problem of this approach is that, the high-valued starting current entails a large voltage drop at the autotransformer impedance, worsening even further the voltage dip problem, which in turn delays even longer the motor to reach steady-state. Thus, for the same motor as before, starting-up time has increased by 450% compared to DOL (Fig. 3 and 4).

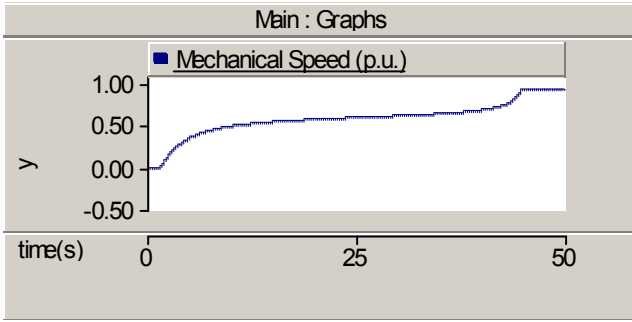


Figure 3. Speed building-up delay due to autotransformer (the tap changes at 50 s, i.e. when steady-state is reached)

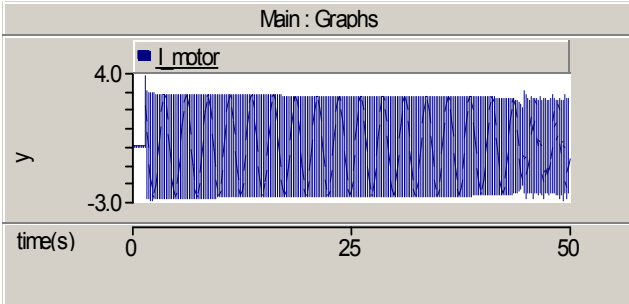


Figure 4. Inrush current during starting-up of a 1.0 MW motor via an autotransformer

C. Starting-up via Autotransformer and Capacitor

The problems during starting-up via-an-autotransformer can be alleviated by installing an additional reactive power source i.e. a capacitor bank close to the motor. It is recommended that the capacitor rating is approximately 30% of the motor rated power[1]. In this way, steady-state is reached at almost the same time as DOL method (Fig. 5 and 6). It is worth noting that when steady-state is reached, towards 12 s, see Fig. 6, a current spike is observed in current waveform, due to autotransformer tap changing.

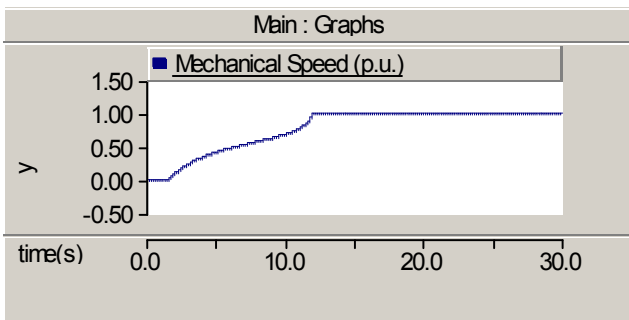


Figure 5. Speed building-up during starting-up via combination of autotransformer and capacitor (the tap changes at 12.5 s, i.e. when steady-state is reached)

However, this solution is not appealing in terms of both cost and space requirements considering the two auxiliary components (autotransformer and capacitor) needed only during the critical period of starting-up.

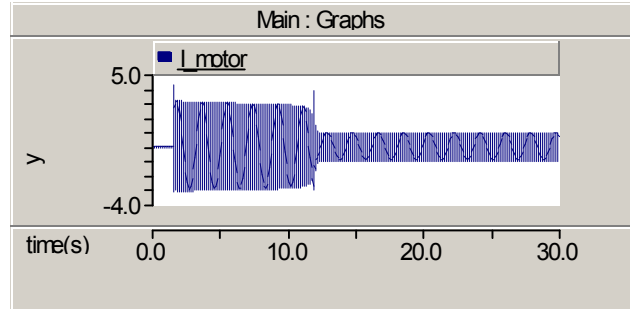


Figure 6. Inrush current during starting-up of a 1.0 MW motor via an autotransformer in series with a capacitor

It is worth noting that the large power capacitor installed can provoke other fast electromagnetic transients during switching on and off endangering the whole equipment. More specifically, during circuit breaker making, a capacitor absorbs large high frequency inrush currents, while during breaking voltage escalation problems with multiple circuit breaker restriking can occur [6].

D. Soft Starting via power electronic devices

This method, which is fairly new, is based on progressively increasing the output voltage of the generator in a linear manner by using power electronic devices – soft starters or power converters with soft starting capabilities. The proportional augmentation of the voltage applied to the motor input, can be explicitly expressed as:

$$\begin{aligned} V_{\text{rms}} &= 0, \text{ if } t < 0 \\ V_{\text{rms}} &= K_v \cdot t, \text{ if } t > 0 \end{aligned} \quad (1)$$

where

t: motor starting-up time

K_v : voltage increment gradient

However, up-to-date soft starting devices although not space demanding nor noisy, are pretty costly especially in the case of high power applications, while due to their power electronic switching, power supply quality problems due to harmonic pollution can be emerged [2].

E. AVR Soft- Starting

This method has been initially introduced in a previous paper [1] and can only be applied in cases of a motor supplied by a dedicated generator [2]. More specifically, the method is based on progressively increasing the output voltage of the dedicated generator, in a manner similar to the one soft starting devices do. This proportional augmentation of generator voltage is achieved by properly controlling its AVR. However, this procedure has to be carefully initiated, as two factors have to be taken into account:

- The voltage output has to start by a non-zero value, V_o , so that no voltage collapse occurs. V_o is recommended to be in the order of 30% of the rated voltage [1-2].
- A de-magnetisation procedure has to be done first, so that no remanence flux in the airgap spoils the initialisation of the AVR.

AVR technology, nowadays offers solutions readily available to both difficulties. Thus, the generator rms terminal voltage, V_{rms} can be set during the motor starting-up as a ramp-like time expression :

$$V_{rms} = \begin{cases} 0, & \text{if } t < 0 \\ V_o + K_v t, & \text{if } t > 0 \end{cases} \quad (2)$$

where

t: motor starting-up time

V_o : initial rms terminal voltage

K_v : voltage increment gradient

i.e. slightly different from (1), only in terms of V_o .

In contrast to the other methods, which focus on modifying the power supply to the motor, AVR-soft-starting refers to the power produced by the generator. In motor thruster case studies, the dedicated generator is often a shaft generator which can be programmed as described above [1-2]. In limited applications, though, the dedicated generator can be a conventional generator intentionally de-synchronized from the parallel operation of all the others, so that AVR soft starting is performed. AVR-soft-starting is also more favourable in terms of cost and space savings than using soft starters [2]. Regarding duration of starting-up, this can be adjusted to be within acceptable time limits, namely less than 50 sec, see Fig. 7.

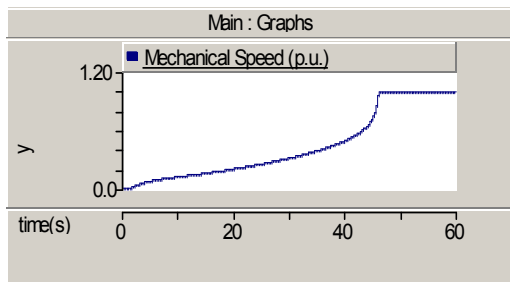


Figure 7. Speed building-up during starting-up of a 1.0 MW induction motor via AVR-soft starting-up

III. STARTING – UP OF THRUSTERS DRIVEN BY INDUCTION MOTORS

Taking into consideration the alternative starting-up methods of induction motors, two major alternative configurations are used for starting-up an electric driven thrusters unit.

On the one hand, the combination of a squirrel cage

induction motor along with controllable pitch propeller is used. Initially the pitch is set to 0, so that the total inertia and consequently the inrush phenomenon is as minimum as possible during starting-up. Moreover, manoeuvring is attained via varying only the propeller pitch, without resorting to repetitive starting-up, which, as a matter of fact is not easily allowed by the manufacturers, as it leads to temporary equipment over-heating.

On the other hand, the second configuration comprises a wound rotor induction motor along with variable resistors and a fixed pitch propeller. As already mentioned, in this case, the inrush phenomenon due to the transient current is mild (the current is controlled so that its rated value is not exceeded). Furthermore, in this case with fixed pitch, manoeuvring is performed via consecutive starting and stopping the motor; as starting current does not exceed its rated value, no over-heating is endangered.

IV. RELEVANT STANDARDS

Several Power Supply Quality related issues emerged with the extensive electrification of most ship systems and the advent of All Electric Ship concept have not been incorporated yet into standards, at least in a clear manner as pointed out in [7]. The problems during thruster starting-up can be included in this category, too as explained in the following.

More specifically, the phenomenon of large power motor starting-up, seen as a voltage dip, is partially covered by the standardized limits of transient voltage fluctuations, i.e. the maximum permissible voltage dip along its corresponding duration within a fundamental period, see Table I. Considering that the most significant problem caused by the thruster motor starting-up is the voltage dip, provoking malfunction to a series of other equipment, the related standards are a fairly good starting point of discussion. Almost all standards set limits on these transient voltage fluctuations (maximum tolerance with respect to the rated value as well as maximum duration).

Thus, according to [8] : “A voltage transient is a sudden but temporary change in the peak amplitude of the voltage, which exceeds the user voltage tolerance limits. Typical time duration for voltage transients is between a fraction of a cycle and 2 seconds for both 60Hz and 400Hz systems. Transients are usually the result of changes in load. The reaction of the prime mover, alternator and associated controls to that change defines the recovery time. Voltage recovery times can be shorter than the original disturbance that caused the transient. A typical example of this, is voltage recovery during the start of a large motor load.” According to this approach, no restrictions on the transient peak load current, neither on the corresponding power demands (in terms of active and reactive power) are cited.

On the other hand, compliance with these voltage norms is verified as described in the following [8]: “when the generator is running at no load, at nominal voltage, and the specified sudden load is switched on, the instantaneous voltage drop at the generator terminals shall not be more than 15% of the generators nominal voltage. The generator voltage shall be restored to within $\pm 3\%$ of the rated voltage within 1.5 sec. Concerning the sudden load applied, although not officially written it is 60% of the generator capacity”.

TABLE I: Comparison of shipboard Standards regarding transients and spikes

Standard/rule	VOLTAGE TRANSIENT*	VOLTAGE SPIKE
ABS (2005) BV(2003) DNV(2001) GL(2004) PRS (2002) RINA(2005)	$\pm 20\%$ (1,5s)	No
(LRS) (2001)	+20%, -15% (1,5s)	No
IEEE 45-1998	$\pm 12\%$ (2s)	$\pm 2500V$ (380V – 600V)
		1000V (120V-240V)
STANAG 1008 (Ed.9), USA MIL-Std-1399	$\pm 16\%$ (2s) [$\pm 22\%$ (2s)] 18-35V, 24Vdc	2.5kV, 440V 1kV, 115V 0.6kV, 24Vdc

* Permissible transient frequency variation is $\pm 10\%$ (5s) in all rules

After the authors’ suggestion, the best choice of “a sudden load” for assessing this generator set transient response would be the thruster electric motor, considering that in most cases, this is the largest motor installed onboard, being of equivalent capacity to that of the ship generators. Furthermore, taking also into account that the starting-up procedure (followed by a corresponding stopping) could be repeated more than once during manoeuvring operation,

it can be argued that this "thruster" operation has a behaviour resembling that of a pulsed load. This is further discussed in the following section.

B. The thruster as a pulsed – load. Standardization issues

A pulsed load is “a repetitive random or cyclic load that imposes time-varying power requirements on the system that result in amplitude modulation in voltage and frequency” [9,10]. Although, the term refers either to certain navigation systems (e.g. sonars or radars) or to sophisticated weapon systems, its definition as mentioned above does not exclude any other load with the features noted (i.e. “repetitive high power”). Hence, the occasionally repetitive starting-up procedure of a thruster motor, can be considered to be a specific-type pulsed load. Moreover, the resemblance is improved considering that like the other pulsed loads [9,10], thruster motors are supplied via auxiliary power interface units, see section II, so that the related power quality problems are minimized.

Nevertheless, what is important is that for this type of loads there are certain standards, which can be used as the grounds for further discussion. Therefore, a brief citation of the standards on pulsed loads is made, followed by a case study. Thus, it is stipulated that “**Pulsed loads should not exceed the limits specified in the equations below since that will cause voltage and frequency modulations exceeding the limits of this power supply standard. If such a load can not be avoided, the power supply design authority is to be consulted so corrective action can be determined.**” [9,10], see also Fig. 12:

$$Q_{pulse} < 0.065 * S_{supply} \text{ and } P_{pulse} < 0.25 * S_{supply} \quad (3)$$

,where P_{pulse} , Q_{pulse} = active, reactive power of the pulsed load respectively, while S_{supply} = full rated apparent power of the supply during pulsed load operation.

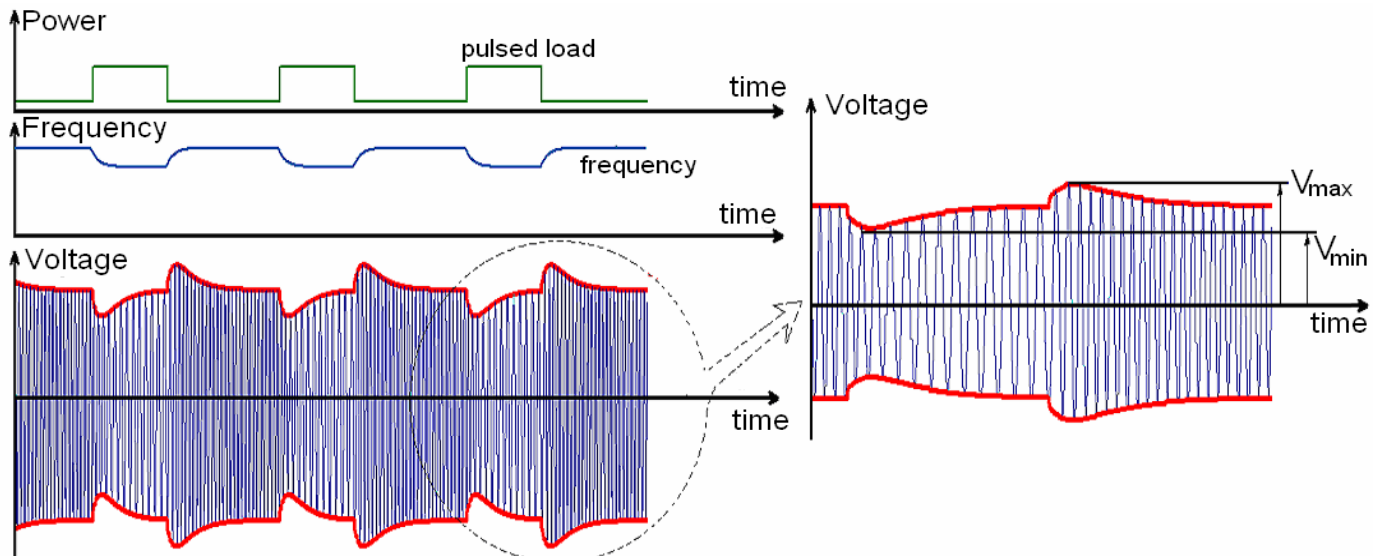


Figure 11. Voltage and frequency modulation due to pulsed load

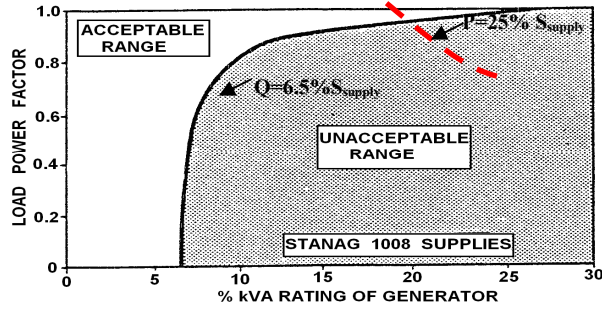


Figure 12 Limit-curve for pulsed load operation according to [9,10] (load power factor vs. % pulsed power w.r.t. supplying generator rated apparent power)

Limitations of equation (3) are set, so that the variations of voltage and frequency are well confined within the following modulation limits:

$$\Delta V/V_{\text{nominal}} \leq \pm 2.5\% \text{ and } \Delta f/f_{\text{nominal}} \leq \pm 0.5\% \quad (4)$$

,which, are stricter than the transient fluctuations tabulated in Table I, as they refer to the quasi- steady-state modulation phenomenon.

If the thruster motor is to be considered a pulsed load, it is more appropriate to consider P_{Pulse} and Q_{Pulse} equal to its transient power demands. Depending on the configuration discussed in section II, this could be either several times the rated values (in case of squirrel cage rotor with single starting-up followed by propeller pitch variations [3]) or almost equal to the rated thruster motor power (in case of the wound rotor, where repetitive starting-up during maneuvering occurs). From the power generation point of view, the generator sets must have the capacity to meet the motor demands withstanding any related problems e.g. frequency or voltage stability problems.

V. CASE STUDIES

The rules discussed above, regarding a thruster as a pulsed load, have been examined in two different case studies obtained from actual ship cases, namely:

A. A Car/passenger ferry with a bow-thruster motor of 1.0 MW/440V(power factor=0.9 inductive), of squirrel cage type, supplied by a dedicated shaft generator 1.4 MVA/440V.

B. An LNG carrier with a bow-thruster motor of 1875 kW/6.6 kV (power factor=0.8 inductive), of squirrel cage type, supplied by two synchronized steam- and one stand-by generator of 4312.5 kVA /6.6 kV each.

In both study cases, power quality problems during starting-up have been noticed and alternative schemes have been investigated. These alternatives include combinations of power generators, supplying the thruster motors, as well as the auxiliary starting-up interfaces, so that the adversity of the related power quality problems is alleviated. In all

cases, the criteria set in equation (3) for both the transient and steady-state (i.e. rated) power demands of the thruster motors have been used. All simulations are performed in PSCAD computer program.

More specifically, concerning case study A, in Figure 13, a representative comparison among several starting methods is made.

In this case study, four alternative power starting-up interfaces have been considered for investigation, namely:

- A1.** Direct On Line case, which evidently could not be applied considering the motor rated power,
- A2.** Power Supply via an autotransformer with two-step tap changer,
- A3.** Power supply via the combination of an autotransformer with a capacitor bank,
- A4.** The dedicated shaft generator operates in AVR-soft starting mode.

In Table II the thruster power demands with respect to the operating generators rated capacity, are presented in two different columns. In the first column, the worst power demands at (nominal) steady-state conditions, i.e. rated motor power along with any interface power supply (i.e. capacitor) is compared to the rated generator power. In the second column, the corresponding transient power demands of the thruster, as obtained from the simulations, are presented. The inappropriate selection of the generator capacity is emerged in all sub-cases, regardless if interest is focused on steady-state rated values of the thruster or transient-state ones. The limits of equation (3) are exceeded; hence the grid suffers from a significant voltage dip, which the generator can not compensate. On the other hand, the motor succeeds in starting up only in sub-cases A3 and A4. In particular, sub-case A2 is proven marginally unsuccessful, as the motor reaches its nominal speed slightly after 48 s, see Figure 13f, i.e. when its thermal limits have been exceeded and the over-current relay should trip [1]. In contrast, sub-case A4, is marginally successful from the motor thermal limits point of view.

Regarding case study B, seven alternative combinations of synchronized generators (modeled with their complete dynamic model along with their speed governors and AVR's), as well as starting-up interfaces have been considered:

B1: One steam turbine generator 4312.5 kVA, along with an autotransformer with two-step tap changer,

B2: Two steam turbine generators (2x4312.5 kVA), along with an autotransformer with two-step tap changer,

B3i: Two steam turbine generators (2x4312.5 kVA), along with an autotransformer with three-scale tap changer,

B3ii: Two steam turbine generators, along with autotransformer with two-step tap changer and a capacitor of 500 kVAr,

B3iii: Two steam turbine generators 2x4312.5 kVA, along with an autotransformer with three-step tap changer and a capacitor of 300 KVAR,

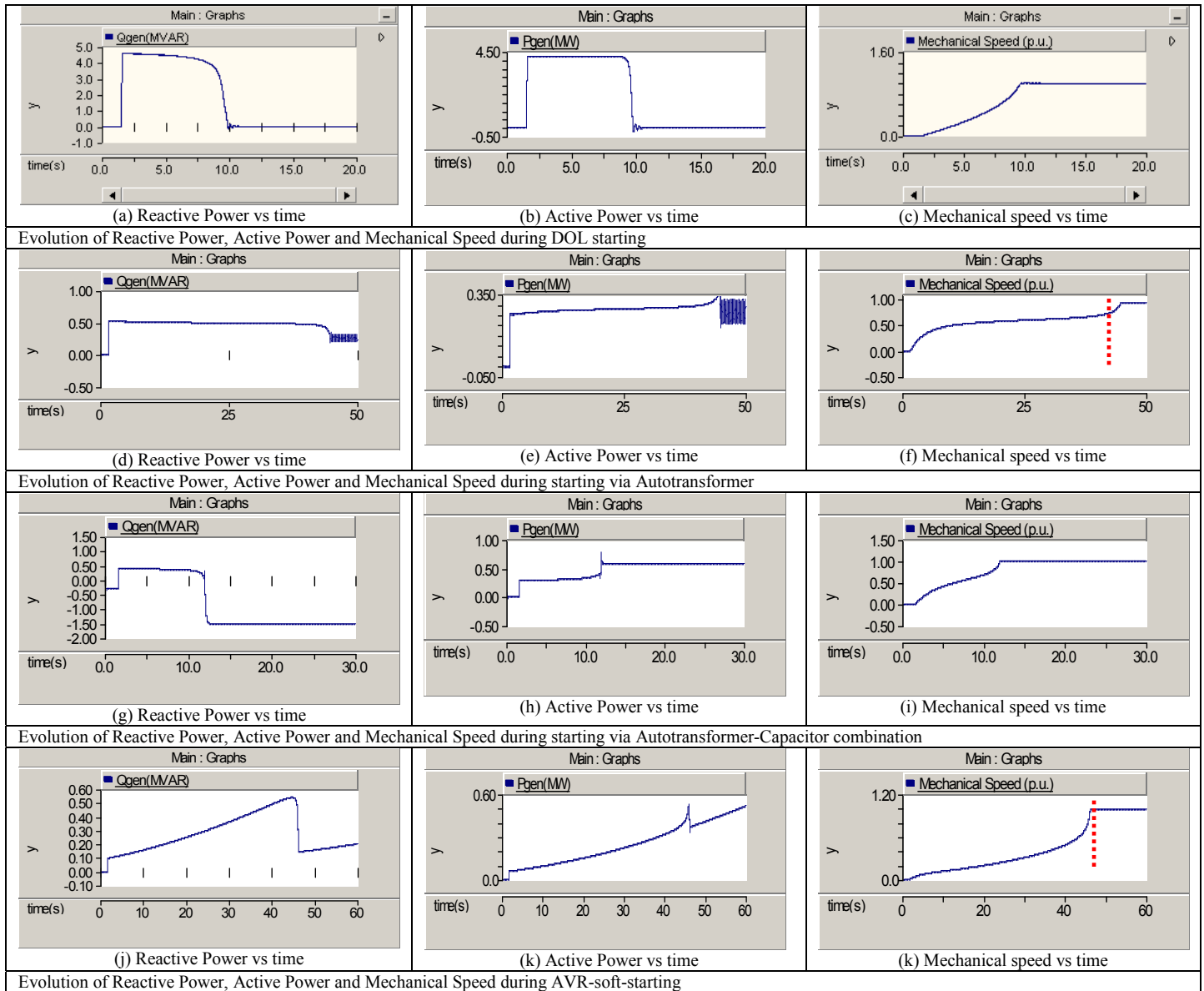


Figure 13. Comparison among several starting-up methods for case study A

TABLE II. Case study A (car/passenger ferry) (figures underlined exceed the limits of equation (3))

	Nominal power demands from the generator (motor rated values 1000 KW, 436 kVAr)		Transient State power demands from the generator (motor maximum demands during starting-up: 0,35 MW, 0,5 MVAR)	
	Active Power $P_{\text{thrust}} / S_{\text{supply}}$	Reactive power $Q_{\text{thrust}} / S_{\text{supply}}$	Active Power $P_{\text{thrust}} / S_{\text{supply}}$	Reactive power $Q_{\text{thrust}} / S_{\text{supply}}$
A1:Single-dedicated shaft generator (unsuccessful)	<u>71.43</u> >25%	<u>31.14</u> %>6.5%	<u>314.29</u> %>25% *	<u>547.6</u> %>6.5% *
A2:Shaft generator and autotransformer (marginally unsuccessful)	<u>71.43</u> >25%	<u>31.14</u> %>6.5%	25% *	<u>59.5</u> %>6.5% *
A3:Shaft generator, autotransformer and capacitor banks 300 kVAr	<u>71.43</u> >25%	<u>9.71</u> %>6.5%	25%	<u>53.57</u> %>6.5%
A4. AVR-soft-starting and shaft generator (marginally successful)	<u>71.43</u> >25%	<u>31.14</u> %>6.5%	25%	<u>53.00</u> %>6.5%

* The electric motor does not succeed in starting rotating as the generator is not capable of providing the energy required. The exact power demands of the motor are determined by considering the generator to be ideal sources in the simulations

TABLE III. Case study B (LNG-carrier)) (figures underlined exceed the limits of equation (3))

	Nominal power demands from the generator(s) (motor rated values: 1875 kW, 1406.25 kVAr)		Transient State demands from the generator(s) (starting-up motor demands: 3.45 MW, 2.588 MVAr)		Minimum Voltage and Voltage Dip at generator terminals (in % of rated value)	Minimum frequency and Maximum frequency Dip (in % of rated value)
	Active Power $P_{thruster}/S_{supply}$	Reactive power $Q_{thruster}/S_{supply}$	Active Power $P_{thruster}/S_{supply}$	Reactive power $Q_{thruster}/S_{supply}$		
B1: 1 steam-turbine generator 4312.5 kVA +autotransformer with 2-step tap changer (unsuccessful)	<u>43.48%</u> >25%	<u>32.61%</u> >6.5%	<u>80%</u> >25%*	<u>60%</u> >6.5%*	-	-
B2: 2 steam-turbine generators 2x4312.5 kVA+autotransformer with 2-step tap changer	21.73%	<u>16.30%</u> >6.5%	7.54%	<u>20.29%</u> >6.5%	88.48% (Dip DV=11.52%)	96.18% (Dip Df=3.82%)
B3i: 2 steam-turbine generators 2x4312.5 kVA+autotransformer with 3-step tap changer	21.73%	<u>16.30%</u> >6.5%	5.10%	<u>14.26%</u> >6.5%	94.39% (Dip DV=5.61%)	98.61% (Dip Df=1.39%)
B3ii: 2 steam-turbine generators 2x4312.5 kVA+autotransformer with 2-step tap changer+capacitor 500 KVA	21.73%	<u>10.50%</u> >6.5%	8.12%	<u>18.55%</u> >6.5%	89.63% (Dip DV=10.37%)	97.45% (Dip Df=2.55%)
B3iii: 2 steam-turbine generators 2x4312.5 kVA+autotransformer with 3-step tap changer+capacitor 300 KVA	21.73%	<u>12.80%</u> >6.5%	5.22%	<u>13.33%</u> >6.5%	94.70% (Dip DV=5.30%)	98.61% (Dip Df=1.39%)
B3iv: 2 steam-turbine generators 2x4312.5 kVA+autotransformer with 2-step tap changer+capacitor 300 KVA	21.73%	<u>12.80%</u> >6.5%	8.12%	<u>19.36%</u> >6.5%	89.34% (Dip DV=10.66%)	97.37% (Dip Df=2.63%)
B4:2-steam-turbine generators + 1 stand-by generator (3x4312.5 kVA)+autotransformer with 2-step tap changer	14.49%	<u>10.86%</u> >6.5%	5.02%	<u>15.30%</u> >6.5%	94.09% (Dip DV=5.91%)	97.71% (Dip Df=2.29%)

* The electric motor does not succeed in starting rotating as the generator is not capable of providing the energy required. The exact power demands of the motor are determined by considering the generators to be ideal sources in the simulations

B3iv:Two steam turbine generators 2x4312.5 kVA, along with an autotransformer with two-step tap changer and a capacitor of 300 KVA,

B4: Two steam turbine generators synchronized and one stand-by generator (3x4312.5 kVA) along with an autotransformer with two-step tap changer. The stand-by unit, is to be synchronized prior to thruster starting-up.

The corresponding simulation results are tabulated in Table III. Like in case A, the first column includes the comparison of rated power demands of the thruster system along with any capacitor power supply with respect to the operating generator apparent power. The second column presents the corresponding transient power demands of the thruster motor, as provided by the simulations. The last two

columns correspond to the worst voltage and frequency dips occurred during the starting-up procedure; they are measured at the main generator bus-bar.

It can be seen, that like in case A, even if the rated power of the thruster is used, the problematic operation is deduced. Therefore, in all cases, where divergences of power demands from the limits of equation (3) are noticed, significant voltage and frequency dips occur. With the exception of sub-case B1, where the thruster motor fails to start-up due to insufficient power redundancy on behalf of the (only in this sub-case) generator, the active power restriction is met in all cases, whereas the reactive power one is not. Hence, it is plausible to argue that numerical

limits in equation (3) need some reconsideration. Further, the limits of voltage and frequency dips in (4) are, in certain cases, but not the limits of Table I. It is also noted that the ratios of thruster power demands over the supplying generator rated capacity, can be used as classification indices, indicating how effective each alternative solution is. Considering that the optimum solution is the one resulting in minimum values of voltage and frequency dips, several combinations between the transient power demands are sought, see Table IV. Thus, in Table IV, it is proven that ranking according to the “sum” or the “product” of transient power demands coincides with that of the dips. It is underlined, that while these transient power demands of the thruster motors are provided by their manufacturer [3], the dips are assessed via simulations of the entire ship grid operation.

Regarding the alternatives investigated, further conclusions can be drawn. Thus, power redundancy does not necessarily lead to the optimum solution. More specifically, synchronizing an extra generator (sub-case B4) can be less favorable solution than that of the combination of two generators along with an auto-transformer with 3-step tap changer (sub-cases B3i and B3iii). Similarly, an alternative with a large capacitor bank, besides being more expensive and more space demanding, can be less appealing than a combination of an autotransformer with increased step number in its tap changer along with a smaller capacitor unit (sub-case B3iii versus B3ii).

VI. CONCLUSIONS

This paper deals with highlighting the significance of the maneuvering thruster start-ups in the electric power quality of the entire ship grid. It is further shown, that the existing standardization status is not sufficient and has to be improved. This argumentation is enriched by presenting the analysis results of two actual ship case studies with troublesome thruster operation, namely a car-passenger ferry and an LNG carrier.

Thus, the authors, on the one hand, recommend that the voltage-transient recovery test of the generators is performed by considering a thruster start-up to be the sudden-load specified by the standards.

On the other hand, it is recommended to exploit the experience on pulsed loads standardization, where numerical limits of the load power demands with respect to supplying generator capacity exist. These power ratios compared to the corresponding limits can be used as a means of qualitative assessment that a problematic operation of the entire grid is expected. Although, it is shown that thruster units and pulsed loads have similarities, and, hence these limits could be the same, still their numerical values could be modified to thruster units.

Moreover, the ratios of the load power demands with respect to supplying generator capacity could be used as an index for quantitative evaluation of the adverse effect the thruster load provokes on the normal operating condition of the ship grid. Through this approach, alternative power supplying schemes could be evaluated and compared, too.

VII. ACKNOWLEDGEMENTS

The authors wish to express their gratitude towards MARANGAS MARITIME Inc. and its personnel for their valuable assistance offered during this work in many ways. But for their help, this work would not have been accomplished.

VIII. REFERENCES

- [1] P. Vallianatos, J. Prousalidis, E. Styvaktakis, "On starting-up large power motors rotating high inertia loads in autonomous systems", Proceedings of International Conference on Electric Machines (ICEM-2006), Chania (Crete), September 2006.
- [2] J. Prousalidis, P. Vallianatos: "The merits of thruster start-up using a shaft generator - A Ready Solution?", Marine Engineering Review (MER), July – August 2006.
- [3] H. Gremmel, "Switchgear Manual", 10th edition, Asea Brown Boveri's Publications June 2001.
- [4] J. Mindikowsky, "Assessment of electric power quality in ship systems fitted with converter subsystems", Shipbuilding and Shipping, 2003.
- [5] Manitoba HVDC Research Center: "PSCAD User's Guide", 2006.
- [6] A Greenwood, 'Electrical Transients in Power Systems', John Wiley & sons, New York (USA), (1990).
- [7] I.K. Hatzilau, J. Prousalidis, E. Styvaktakis, F. Kanellos, S. Perros, E. Sofras, "Electric power supply quality concepts for the All Electric Ship (AES)", 2006 World Marine Transport Technology Conference, London (UK), March 2006.
- [8] IEEE Standard 45-1998, "IEEE Recommended Practice for Electrical Installations on Shipboard".
- [9] STANAG 1008, "Characteristics of Shipboard Electrical Power Systems in Warships of the North Atlantic Treaty.
- [10] USA MIL-STD-1399(NAVY), "Interface standard for Shipboard systems – Section 300A – Electric Power, Alternating Current"

Table IV. Classification of alternative starting-up methods

Ranking	Cases	Active Power $P_{thruster}/S_{supply}$	Reactive power $Q_{thruster}/S_{supply}$	$(P_{thruster}/S_{supply}) +$ $(Q_{thruster}/S_{supply})$	$(P_{thruster}/S_{supply})^*$ $(Q_{thruster}/S_{supply})$	Voltage Dip DV	Frequency Dip Df
1	B3iii	5,22%	13,33%	18,55%	0,70%	5,30%	1,39%
2	B3i	5,10%	14,26%	19,36%	0,73%	5,61%	1,39%
3	B4	5,02%	15,30%	20,32%	0,77%	5,91%	2,29%
4	B3ii	8,12%	18,55%	26,67%	1,51%	10,37%	2,55%
5	B3iv	8,12%	19,36%	27,48%	1,57%	10,66%	2,63%
6	B2	7,54%	20,29%	27,83%	1,53%	11,52%	3,82%
7	B1	80,00%	60,00%	140,00%	48,00%		

APPENDIX B (Technical Manuals)

Diploma Thesis

Steam Turbine Manual:

PLAN RECORD		REVISIONS		AP- PROVED	CHECK- ED
ISO METRIC SCREW THREADS	No.	DESCRIPTION (DATE)			
本図はオート K3538 (大宇 H GOLAR) 向用として調製した。	1	<ul style="list-style-type: none"> • Added the Hull Number • Delete the item 7 & 8 in chapter 7 according to design progress • Revised LO supply condition of Generator according to design progress. 		Y.T	I.H
	2	• Added the Hull Number (S.S.)		T.H.	S.U.

A4

DRAWING No.

大字	12
	4
率工	1
機品-1	1
機品-2	1
長崎設	1
長巻	1
船体計	1
計	20
出図先	R C

DRAWINGS FOR SUBMISSION

REVISED PLAN

A4 x 22 + A3 x - SHEET(S) WITH COVER

MARINE TURBINE DESIGNING SEC.	
APPROVED	3,450kW GENERATOR TURBINE MANUFACTURING SPECIFICATION
CHECKED	
DRAWN	
CONFERRED	
SCALE	~

ORDER	ITEM	DRAWING No.	REV. No.
			2

DRAWN

ISSUED

②

CONTENTS

1. GENERAL
2. TECHNICAL DATA
3. WEIGHT TABLE (DRY)
4. MATERIALS
5. SCOPE OF SUPPLY
6. SPARE TOOL LIST
7. EQUIPMENT SUPPLIED
8. WARRANTY AND GUARANTEE
9. CONSTRUCTION

△

Diploma Thesis

1. GENERAL

- 1) Classification :
- 2) Standard : JIS, ISO
- 3) Unit : Metric , °C
- 4) Language : Drawings / English
Name plate / English
Caution plate / English
Instruction book / English
- 5) Test and inspection : To be carried out in accordance with DNV refer to "List of inspection and test", "Shop test plan", "Hydraulic test pressure table"
- 6) Insulation : Exposed surface being 55°C and over shall be insulated.
Material / Silica powder, glass cloth with aluminum leaf.
- 7) Painting : Turbine / Silver
Others / 7.5GY7/4 (Green yellow)
- 8) Electric source : AC 440V × 60Hz × φ3
AC 220V × 60Hz × φ1
DC 24V
- 9) No. of sets : Two (2) sets / ship

2. TECHNICAL DATA

a)	Main steam turbine	Horizontal Multi-stages impulse condensing turbine
	Rated Output (Generator)	: 3,450 kW (Generator output)
	Steam inlet condition (Rated)	: 58.8bar(g) (60 kg/cm ² g) × 510 °C
	Turbine exhaust vacuum	: 0.067bar(A) (710 mmHg.v.)
→	Speed (Turbine / Generator)	: Abt. 10,000 / 1,800 rpm →
	Direction of generator rotation looking from turbine side	: Clockwise
1/0.18		
b)	Reduction gear	Single helical single reduction gear
	Output at reduction gear end	: Abt. 3,632 kW (Assumed generator efficiency 95.0%)
c)	Oil tank (Epoxy coating)	1,600 litter (Initial charge capacity)
d)	Main oil pump (Shaft driven)	6.0 bar(g) (6.0 kg/cm ² g) × 400 l/min
e)	Aux. oil pump (Motor driven)	2.0 bar(g) (2.0 kg/cm ² g) × 150 l/min
	Motor capacity	: 3.7 kW × 1,800 rpm
f)	Oil cooler / Shell and tube type	Shell and tube type
	Cooling water (Fresh water)	: Max. 3 kg/cm ² (g) × 30 m ³ /h × 36°C
	Oil temperature (Inlet / Outlet)	: 60 / 45 °C
	Tube	: Low fin tube
	Cooling surface	: Abt. 29.5 m ²
g)	L O / Governor oil	Turbine oil (ISO VG32)
	LO setting pressure	: 1.0 bar(g) (1.0 kg/cm ² g)
	GO setting pressure	: 5.0 bar(g) (5.0 kg/cm ² g)
h)	Governor / WOODWARD UG-8D	(with APM – motor control)
	Adjustable speed range (no-load / full-load)	: +15 % ~ -5 % / +4 % ~ -2 %
	Speed variation (Momentary / Permanent)	: Max. 10 % / Max. 5 %

Diploma Thesis

i) Gland packing steam control device	/ Air operated valve & controller
Max. steam quantity supplied	: 150 kg/h × 17 bar (abs) It is preferable that temperature of supplied packing steam is more than 230°C.
Max. steam quantity spilled	: 300 kg/h
Required dry air	: 5 N l / min
j) Gland leakage steam and air to gland condenser	
Steam quantity (200mmAq vac.)	: 50 kg / h × abt. 785 kcal/kg
Air quantity (200mmAq vac.)	: 35 kg / h
k) Overspeed trip (Mechanical)	: 1962 ~ 1998 rpm
l) LO pressure low trip	: 0.4 bar(g) (0.4 kg/cm ² g)
m) Turbine exhaust pressure high trip / (alarm)	: -0.27 / (-0.53) bar(g) (vac. condition) (200 / (400) mmHg vac.) 0.5 / (0.3) bar(g) (atmos. condition) (0.5 / (0.3) kg/cm ² g)
n) Sentinel valve setting pressure	: 0.3 bar(g) (0.3 kg/cm ² g)
o) Aux. oil pump auto- start / stop pressure	: Start; LO 0.6 bar(g) (0.6kg/cm ² g) Stop; LO 0.85 bar(g) (0.85 kg/cm ² g) and MSV full open
p) Turbine rotor excess vibration trip / (alarm)	: 80 / (50) μ m p-p
q) Turbine rotor excess displacement trip / (alarm)	: ±0.7mm / (±0.55) mm (+: To turbine exh. side)
r) Gland packing steam press. low alarm & high alarm	: Low alarm; 0.03 bar(g) (0.03 kg/cm ² g) High alarm; 0.2 bar(g) (0.2 kg/cm ² g)

3. WEIGHT TABLE (DRY) (1 T/G set)

Turbine and reduction gear common bed	:	16,450 kg
Attached equipment	:	2,000 kg
Oil cooler	:	600 kg
Spare parts and tools	:	250 kg
Total (without Generator)	:	19,300 kg

Diploma Thesis

Steam/Diesel Generator Manual:

TEST REPORT OF BRUSHLESS A.C. GENERATOR

P.- /

CERTIFICATE NO
MACHINE NO. :

MESSRS :

S. NO.:

SURVEYOR :

RULE :

INSPECTOR :

DATE :

MODEL :		OUTPUT: 4312.5 kVA	RATING : CONT.	VOLTAGE : 6600 V						
LOAD CURRENT :	377.0 A	NO. OF POLES : 10 P	Ex. FIELD VOLTAGE : 52.0 V	Ex. FIELD CURRENT : 11.8 A						
FREQUENCY :	60.0 Hz	SPEED : 720 min ⁻¹	P. F. : 0.80	NO. OF PHASES : 3						
(A.C. EXCITER)		OUTPUT : 36.7 kVA	VOLTAGE : 98.4 V	CURRENT : 215.0 A						
NO. OF POLES :	14 P	FREQUENCY : 84 Hz	NO. OF PHASES : 3	P. F. : 0.95						
ORDER NO. :	WORKING NO. : 92358	G	INSULATION CLASS : F	TEST NO. : G 21936						
ROTATION :	CLOCK-WISE (VIEW ANTL COUP-SIDE)			SPACE HEATER : 220 V 726 W						
				AMBIENT TEMP. : 50 °C						
WINDING RESISTANCE (AT 115 °C)		STATOR COIL : 0.1664 Ω	Ex. FIELD (J-K) COIL : 5.881 Ω							
		ROTOR COIL : 0.5666 Ω	Ex. FIELD (Jc-Kc) COIL : - Ω							
		Ex. ARM. COIL : 0.0301 Ω								
RESULT:GOOD										
NO-LOAD SATURATION TEST RESULT:GOOD										
ASCENDING		DESCENDING		AIR-GAP RESULT:GOOD						
VOLTAGE (V)	Ex. FIELD CURRENT(A)	VOLTAGE (V)	Ex. FIELD CURRENT(A)	5.7 5.7 2.7						
2400	1.39	7200	5.78	5.5 5.6 2.5 2.5						
3600	2.18	6600	4.72	3 PHASE SHORT CIRCUIT CHARACTERISTICS TEST RESULT:GOOD						
4800	3.09	6000	4.03	SHORT CURRENT (A)	Ex. FIELD CURRENT(A)					
5400	3.66	5400	3.40	377.0	6.63					
6000	4.32	4800	2.87	188.5	3.31					
6600	5.10	3600	1.98	94.3	1.65					
7200	5.97	2400	1.24							
7800	7.37	447	0.00							
TEMPERATURE RISE TEST () IN : WATER TEMP RESULT:GOOD										
(DNV TYPE TEST MACHINE : KOB-04-922) (BY THERMOMETER METHOD. * = RESISTANCE METHOD. # = E.T.D. METHOD.)										
LOAD (%)	RUN (Hr)	AMBIENT TEMP.	STATOR		ROTOR		BEARING			
100	3.5	34 (32) °C	FRAME	CORE	* COIL	# COIL	COIL	* COIL	COUP. SIDE	OTHER SIDE
			37 K	- K	72.5 K	55 K	33 K	69 K	18 K	13 K
OVER CURRENT TEST: 150 % CURRENT 1 MIN.					OVER SPEED TEST 120 % SPEED 2 MIN. RESULT:GOOD					
OVER LOAD TEST : - % LOAD - MIN. RESULT:GOOD					HIGH VOLTAGE TEST					
					STATOR : 14200 V 1MIN.		ROTOR GD2 : 4447.7 Kg·m ² RESULT:GOOD			
					ROTOR : 1500 V 1MIN.		APPROVED BY :			
					EXCITER : 1500 V 1MIN.		REVIEWED BY :			
					SPACE HEATER : 1500 V 1MIN.		PREPARED BY :			
RESULT:GOOD					INSULATION RESISTANCE (BY 2500V & 500V MEGGER)					
					STATOR : 10000 MΩ					
					ROTOR : 1000 MΩ					
					EXCITER : 1000 MΩ					
					TOTAL : 1000 MΩ					
					SPACE HEATER : 1000 MΩ					
RESULT:GOOD										

Diploma Thesis

BRUSHLESS A.C. GENERATOR

P.- 2

LOAD CHARACTERISTICS TEST										RESULT: GOOD
LOAD (%)	FREQUENCY (Hz)	L O A D		P.F.	OUTPUT (kW)	A.C. EXCITER FIELD				EFF (%)
		VOLTAGE (V)	CURRENT (A)			V F 1 (V)	I f 1 (A)	V f 2 (V)	I f 2 (A)	
AUTO : USE NO.1 A.V.R. (NO. 138936B)										
100	60.0	6600	377.3	0.8	3450.0	52.0	11.80			95.2
75	60.5	6594	283.2	0.8	2587.5	42.0	9.50			94.9
50	61.0	6591	188.9	0.8	1725.0	33.0	7.50			93.9
25	61.5	6581	94.6	0.8	862.5	26.0	5.80			90.0
0	62.0	6628	0.0	-	0.0	20.0	4.60			-
AUTO : USE NO.2 A.V.R. (NO. 138937B)										
100	60.0	6600	377.3	0.8	3450.0	52.0	11.70			
75	60.5	6599	283.0	0.8	2587.5	42.0	9.40			
50	61.0	6580	189.2	0.8	1725.0	33.0	7.40			
25	61.5	6582	94.6	0.8	862.5	25.0	5.70			
0	62.0	6628	0.0	-	0.0	20.0	4.60			
VOLTAGE-SPEED CHARACTERISTICS TEST										
0	60.0	6600				22.0	5.00			
0	62.0	6600				20.0	4.60			
0	64.0	6600				19.0	4.20			
0	58.0	6600				24.0	5.40			
0	54.0	6600				29.0	6.50			
0	50.0	6540				36.0	8.20			
CURRENT OF SELF EXCITER		L O A D			SILICON (I1)	REACTOR (I10)	C. T. (I100)			
		P.F. 0.8	FULL-LOAD		13.5 A	6.2 A	5.8 A			
		P.F. -	FULL-LOAD		- A	- A	- A			
		NO-LOAD			5.7 A	7.2 A	0.0 A			
VOLTAGE ADJUSTABLE RANGE		NO-LOAD	NO.1 AVR : 5872 V ~ 7315 V 60 Hz							
		"	NO.2 AVR : 5880 V ~ 7320 V 60 Hz							
		"	NO.1 MVR : 5150 V ~ 8000 V 60 Hz							
		"	NO.2 MVR : 5100 V ~ 8000 V 60 Hz							
MORE THAN ±5% OF THE RATED VOLTAGE AT THE RATED SPEED										
RESULT: GOOD										
SELF EXCITER TAP POSITION		CURRENT TRANS PRIMARY : K-L			CURRENT TRANS SECONDARY : k-l-2-1-6-5					
		REACTOR : K-L-2-1-4-3			M.V.R REACTOR TAP : K-L-4-3 AVR : EXU-61A					

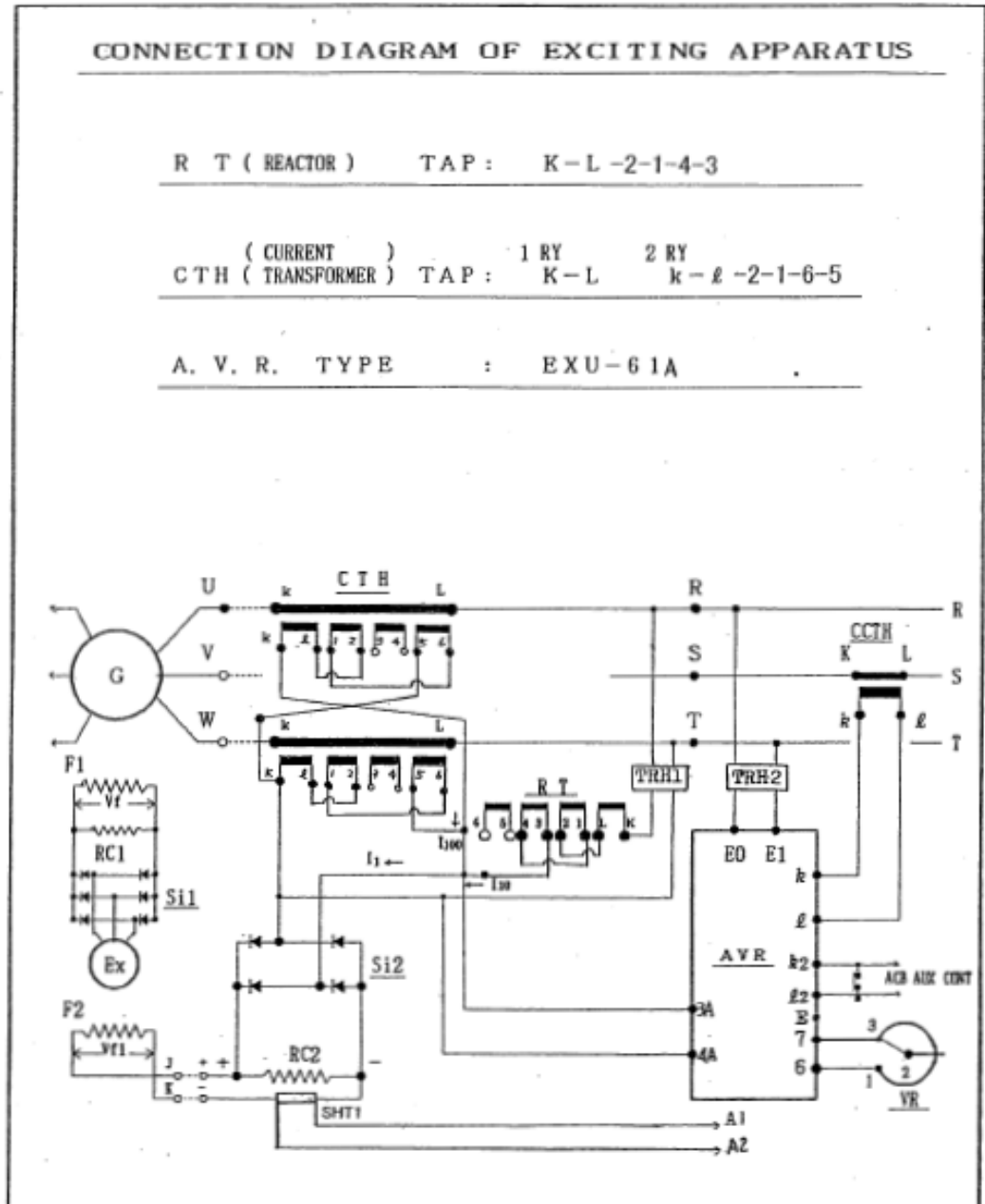
MACHINE NO. :

CONNECTION DIAGRAM OF EXCITING APPARATUS

R T (REACTOR) TAP : K-L-2-1-4-3

(CURRENT) 1 RY 2 RY
 CTH (TRANSFORMER) TAP : K-L k-l-2-1-6-5

A. V. R. TYPE : EXU-61A



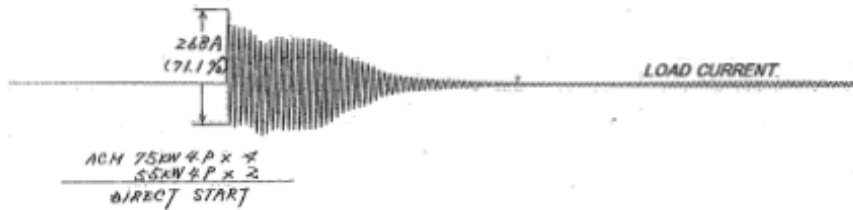
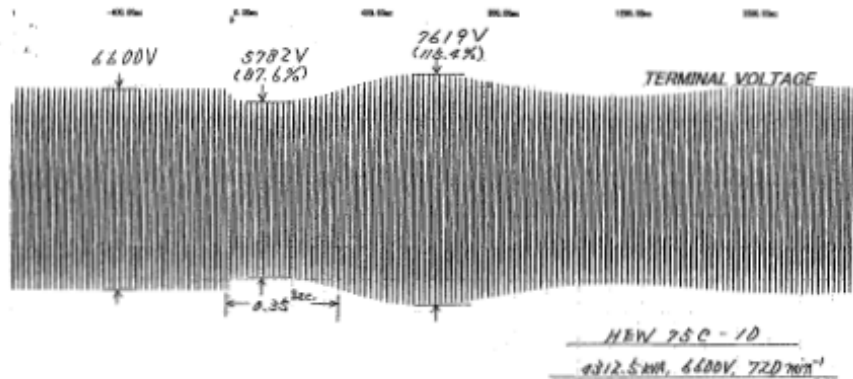
TRANSIENT MAXIMUM VOLTAGE DROP TEST

MESSRS : _____
 TYPE : _____
 OUTPUT : 4312.5KVA, 6600V, 720min⁻¹, 60Hz
 CONDITION : NO-LOAD, RATED VOLTAGE, RATED FREQUENCY
 MACHINE NO. : _____

60%KVA CONVERSION	MEASURED VALUE	CRITERIA	RESULT
MAXIMUM VOLTAGE DROP	9.47 %	LESS THAN 15 %	Good.
RECOVERY TIME	0.35 sec.	WITHIN 1.5 sec	Good.

$$\Delta V = \frac{V - V_{min}}{V - V_{min} + (X_e \times I_s / 100)} \times 100 (\%)$$

* V = 100.0 %
 X_e = 166.7 %
 V_{min} = 87.6 %
 I_s = 71.1 %



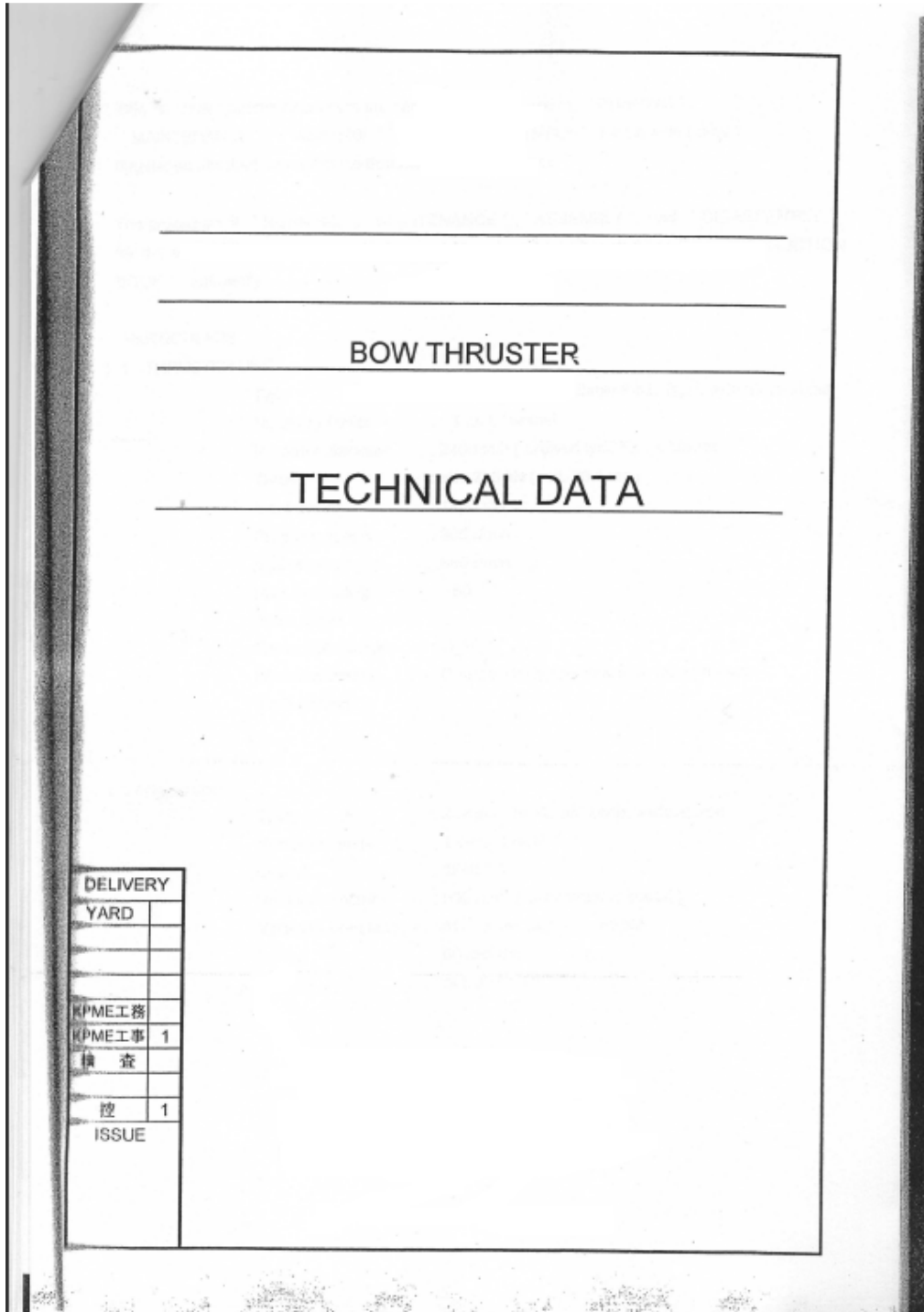
Diploma Thesis

Transformer Manual:

STARTING AUTO TRANSFORMER TEST REPORT					
CUSTOMER		ORDER NO.		SERIES NO.	
TYPE		CIRCUIT VOLTAGE	6600 V	FREQUENCY	60 Hz
CAPACITY	2000 kW	NO. OF PHASE	3 Φ	USE TIME RATING	1 MIN.
INSULATION LEVEL	6B	INSULATION CLASS	B	TAP %	% % % 50 - 65 - 80
MOTOR RATING	MOTOR CAPACITY	2000 kW	RATING VOLTAGE	6600 V	
	RATING CURRENT	215.5 A	PULL VOLTAGE STARTING CURRENT	1730 A	
TESTING RESULT					
1.	STRUCTURE INSPECTION	STRUCTURE FITTING MEASUREMENTS GOOD			
2.	INSULATION RESISTANCE MEASUREMENT	CHARGING PARTS TO EARTH & BETWEEN EACH PHASE OVER 500M Ω (BY 1000V MEGGER)			
3.	DIELECTRIC TEST	CHARGING PARTS TO EARTH & BETWEEN EACH PHASE 16 kV 60Hz 1MINUTE GOOD			
4.	RESISTANCE MEASUREMENT	TEMPERATURE 18 $^{\circ}$ C UNIT : Ω			
	NO.	20077			
TERMINAL					
	U ₀ - U	0.118			
	U ₀ - 80%	0.106			
	U ₀ - 65%	0.0942			
	U ₀ - 50%	0.0712			
	V ₀ - V	0.118			
	V ₀ - 80%	0.106			
	V ₀ - 65%	0.0943			
	V ₀ - 50%	0.0712			
	W ₀ - W	0.118			
	W ₀ - 80%	0.106			
	W ₀ - 65%	0.0942			
	W ₀ - 50%	0.0713			
5.	RATIO TEST (AT NO LOAD)				
	U	GOOD			
	V	GOOD			
	W	GOOD			
6.	NO LOAD CURRENT TEST (UNIT-A) at 60Hz				
	U	7.88			
	V	7.70			
	W	8.40			
EXTRA	THERMAL PROTECTOR				
TEST DATE	ROOM TEMPERATURE	18 $^{\circ}$ C	RELATIVE HUMIDITY	50 %	CHECKED BY / TESTED BY

Diploma Thesis

Bow Thruster Motor:



Diploma Thesis

This list shows various data which are necessary in the case of 'RUNNING', 'MAINTENANCE', 'ASSEMBLY' and 'DISASSEMBLY' for the side (bow) thruster as attached manual of the thruster's instruction book.

The procedure of 'RUNNING', 'MAINTENANCE', 'ASSEMBLY' and 'DISASSEMBLY' for the side (bow) thruster should be operated and worked after studying the 'INSTRUCTION BOOK' sufficiently.

I. PARTICULARS

I.1 THRUSTER UNIT

Type	: KT-187B3 Controllable Pitch Type, with Motor Base
Number of units	: 1 unit/vessel
Propeller diameter	: 2400 mm (skewed type) x 4 blades
Thrust	: abt. 256 kN { abt. 26.1 ton }
Input power	: 1800 kW
Propeller speed	: 300 r/min
Input shaft speed	: 880 r/min
Max. controlling blade angle	: 50 °
Rated blade angle	: ±19.4 °
Direction of input shaft rotation	: Counter clockwise view from prime mover

I.2 Prime mover

Type	: 3 phase, Totally enclosed, vertical type
Number of units	: 1 unit/vessel
Output	: 1800 kW
Revolution number	: 900 r/min (Synchronous speed)
Voltage x Frequency	: AC 3 φ 3300 V 60 Hz
Rating	: 60 minutes
Current	: abt. 207 Amp

Handwritten notes:
I_{flor} = 207 Amp
(E=600)

Diploma Thesis

I.3 AUX. MACHINERY

(1) Hydraulic unit

Oil service pump

Type : Vertical screw type x 1 set/unit 25-6N8D
41 lit/min x 4.5 MPa { 46 kgf/cm² } x 3440 r/min

Driving motor

Type : Totally enclosed induction motor x 1 set/unit
AC 3 ϕ 440 V 60 Hz 5.5 kW x 3600 r/min

DC solenoid valve

Type : DE6P-20-208-WD24AL DC 24 V

Pressure switch [For alarm] [For interlock]
ON Pressure : 0.36 MPa { 3.5 kgf/cm² } 0.5 Mpa { 4.9 kgf/cm² }
OFF Pressure : 0.3 Mpa { 2.9 kgf/cm² } 0.44 Mpa { 4.3 kgf/cm² }
[For pump motor auto change]
ON Pressure : 0.46 MPa { 4.5 kgf/cm² }
OFF Pressure : 0.4 Mpa { 3.9 kgf/cm² }

Relief valve

Set pressure : 5.5 MPa { 56 kgf/cm² }
Strainer : 150 Mesh

(2) Flexible coupling

Type : SF coupling 1140T-10

(3) Gravity tank

Capacity : 80 lit.
Alarm level : 32 lit.

(4) Hand pump

Type : ROTARY PUMP
Delivery volume : 0.2 lit/ rotation

I.4 Mass (WEIGHT)

Thruster : abt. 11000 kg
Prime mover : abt. 7000 kg
Hydraulic unit : abt. 260 kg
Flexible coupling : abt. 138 kg
Accessary : abt. 50 kg

Diploma Thesis

II. OPERATION

II.1 Interlock for prime mover

- (1) Gravity tank oil level : Normal (checking by float switch)
- (2) Control oil pressure : Normal (checking by press. switch)
- (3) Blade angle : Neutral($AB = 0^\circ$)
Allowable range : ± 3 degree

II.2 Rated draft

The draft should be kept shown in "fig.- 1" at running.

$$\text{Fore draft} : df \geq D + Dh \quad M$$

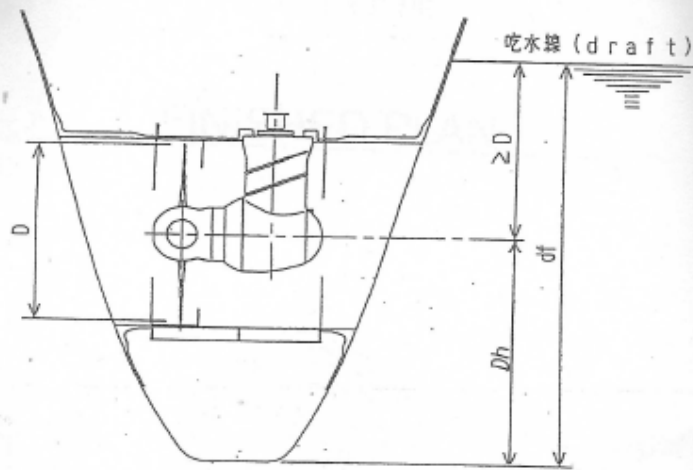


fig.- 1

II.3 Oil temperature of the thruster

The kinematic coefficient of viscosity for thruster should be kept the range of $40 \sim 500 \text{ mm}^2/\text{s}$ (cSt) at running.

The corresponding temperature to the forementioned viscosity is at about $10 \sim 60^\circ\text{C}$ for the gear oil ISO VG 100

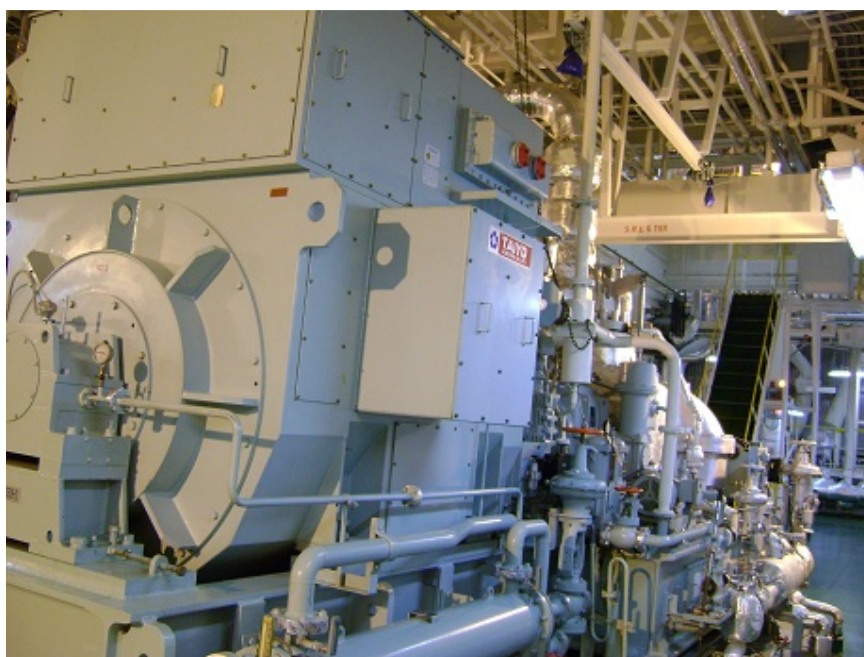
APPENDIX C

Diploma Thesis

The pictures below represent parts of the examined LNG vessel.



One of the main electric power distributors.



One of the two installed steam generators.

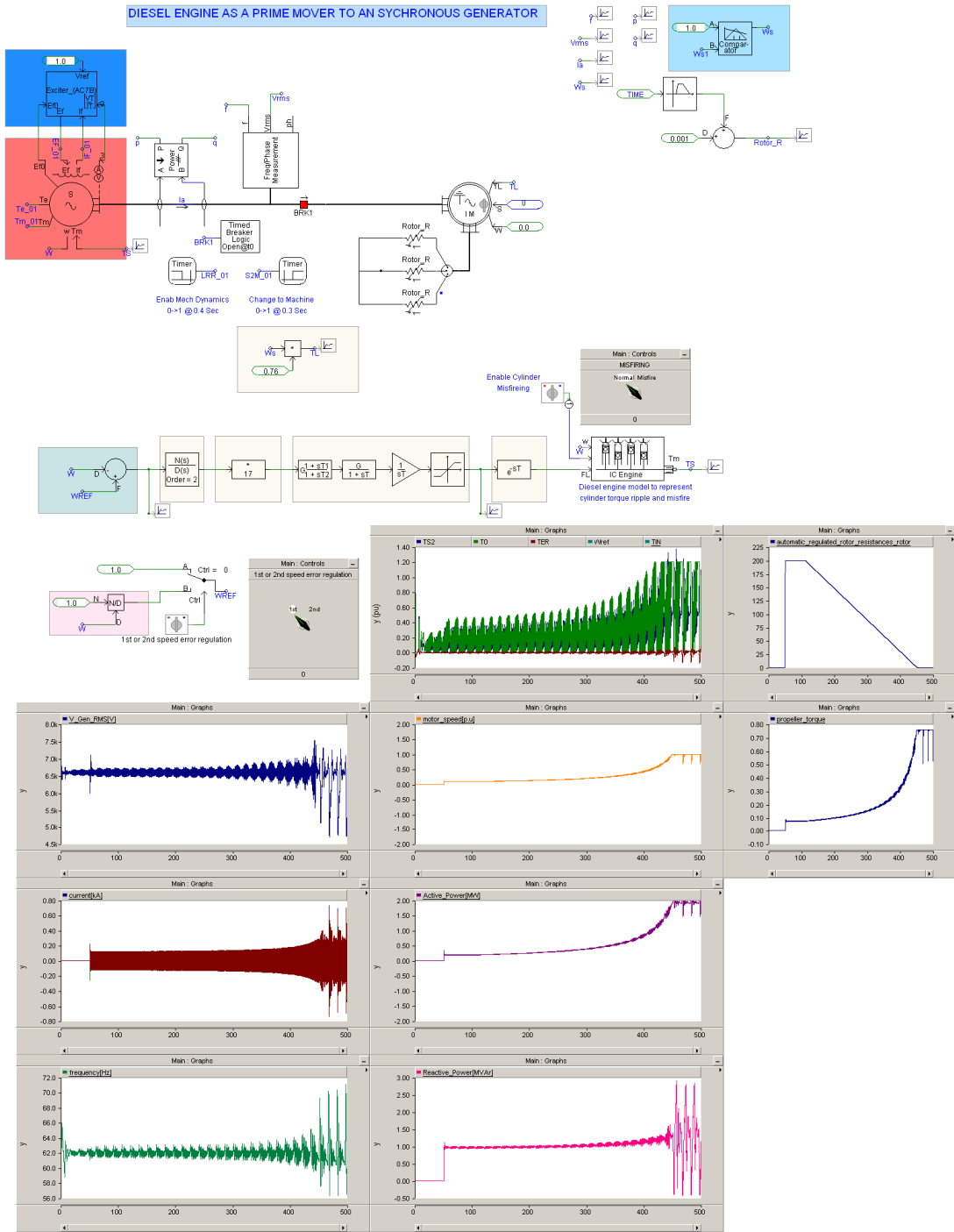
Diploma Thesis



Mr. Panagiotis Mouzakis (Author) on board.

APPENDIX D

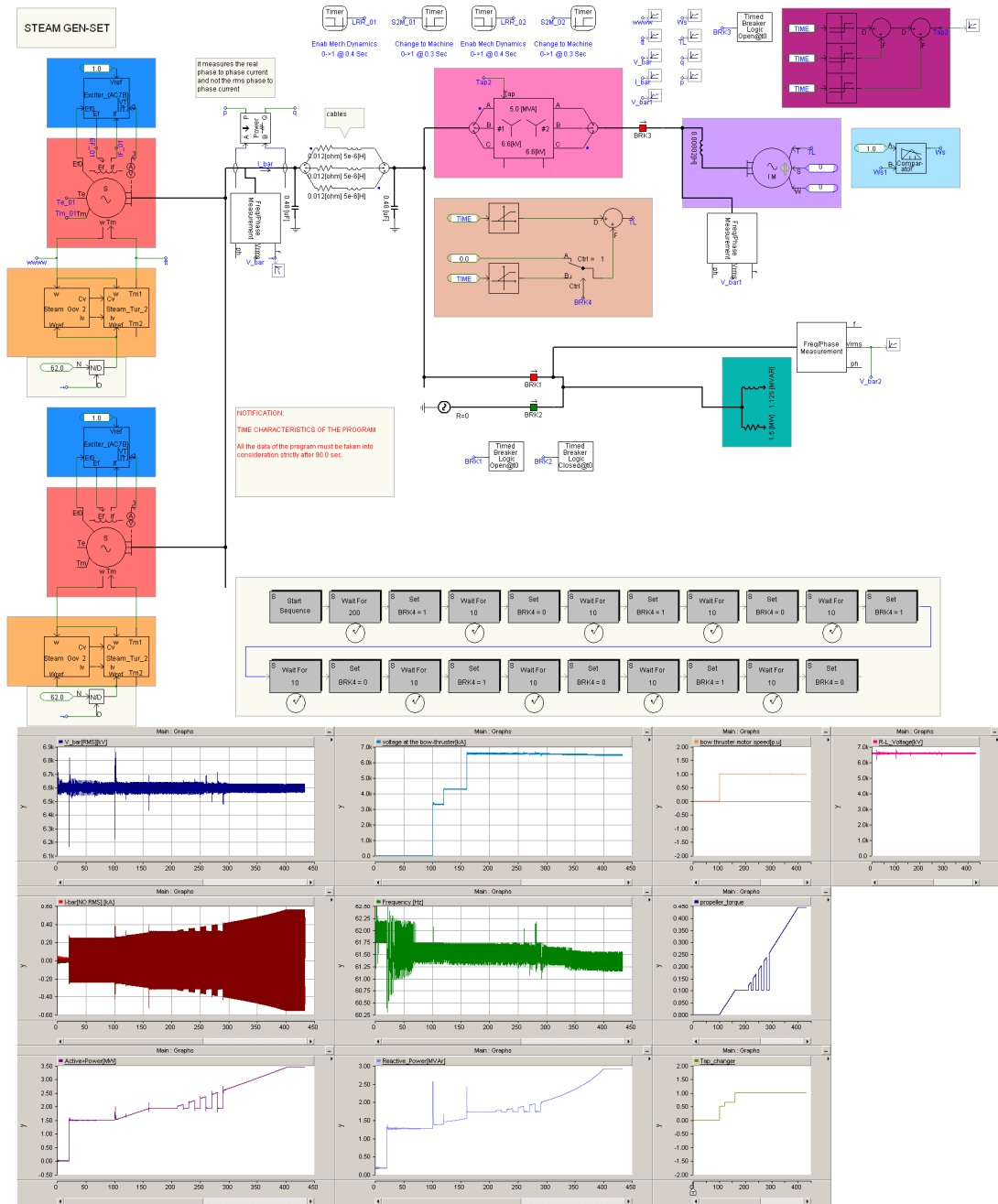
Diploma Thesis



Typical diesel generator configuration

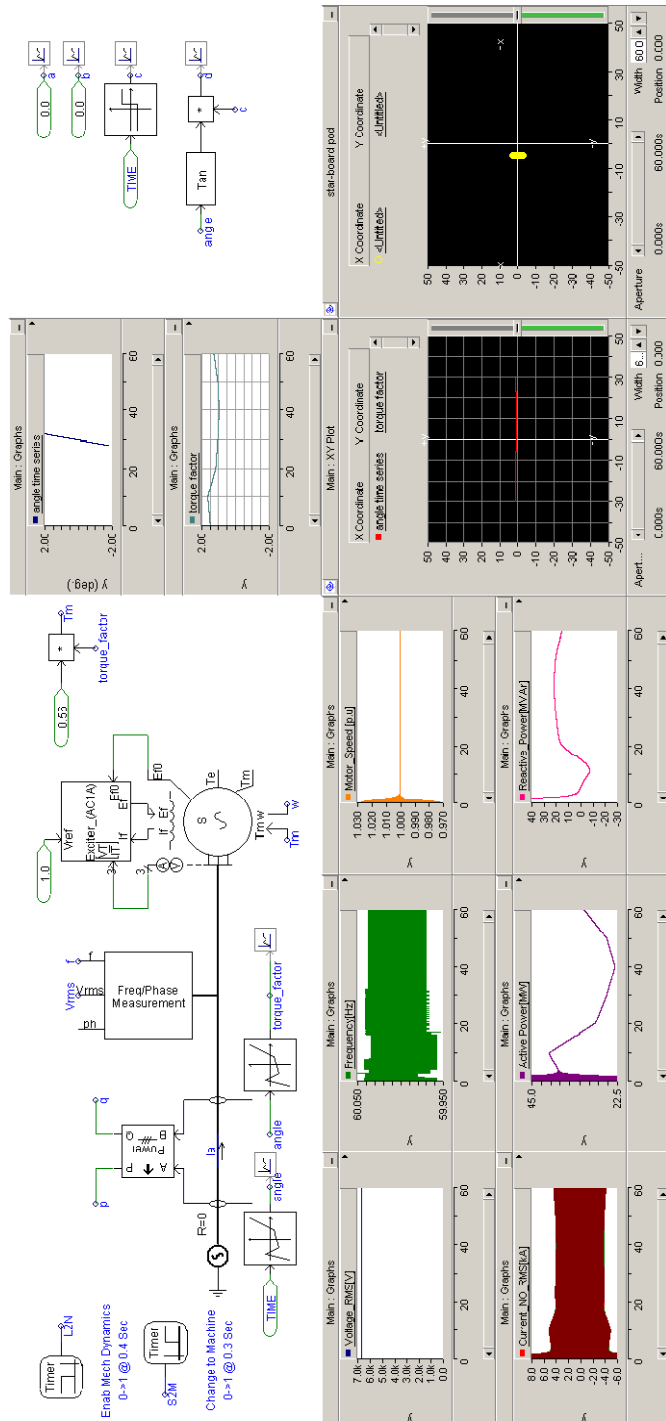
APPENDIX E

Diploma Thesis



Typical steam generator configuration

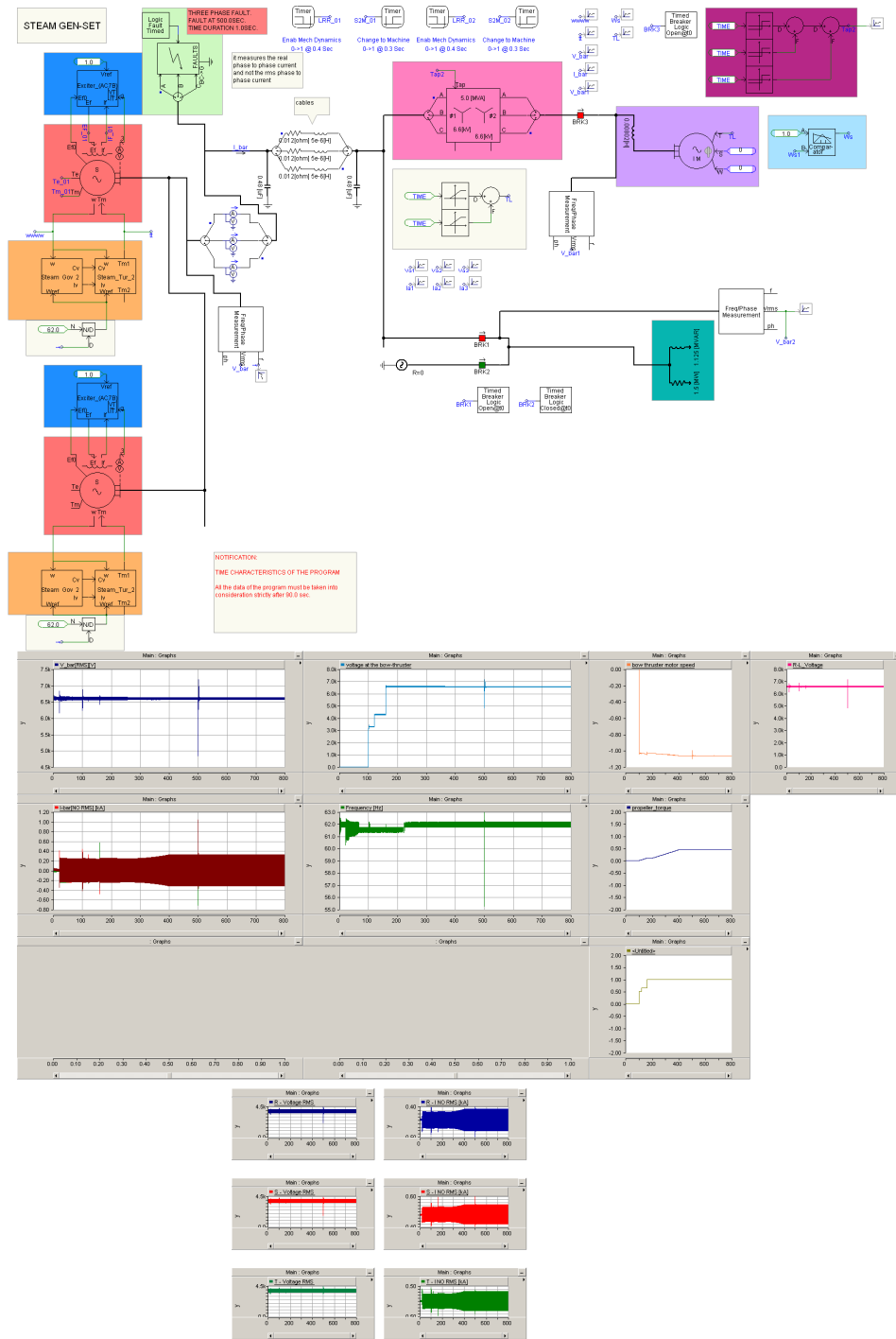
APPENDIX F



Typical Podded propulsor configuration

APPENDIX G

Diploma Thesis



Typical short circuit configuration

APPENDIX H

BIBLIOGRAPHY

Diploma Thesis

REFERENCES

- [1] P. Vallianatos, J. Prousalidis, E. Styvaktakis, *"On starting-up large power motors rotating high inertia loads in autonomous systems"*, Proceedings of International Conference on Electric Machines (ICEM-2006), Chania (Crete), September 2006
- [2] J. Prousalidis, P. Vallianatos: " The merits of thruster start-up using a shaft generator - A Ready Solution?", Marine Engineering Review (MER) , July – August 2006.
- [3] J. Mindikowsky, "Assessment of electric power quality in ship systems fitted with converter subsystems", Shipbuilding and Shipping, 2003.
- [4] Manitoba HVDC Research Center:" PSCAD-EMTDC User's Guide", 2006.
- [5] A Greenwood, 'Electrical Transients in Power Systems', John Wiley & sons, New York (USA), (1990).
- [6]H. Gremmel, "Switchgear Manual", 10th edition , Asea Brown Boveri's Publications June 2001
- [7] I.K. Hatzilau, J. Prousalidis, E. Styvaktakis, F. Kanellos, S. Perros, E. Sofras, *"Electric power supply quality concepts for the All Electric Ship (AES)"*, 2006 World Marine Transport Technology Conference, London (UK), March 2006.
- [8] IEEE Standard 45-1998, *"IEEE Recommended Practice for Electrical Installations on Shipboard"*.
- [9] STANAG 1008, *"Characteristics of Shipboard Electrical Power Systems in Warships of the North Atlantic Treaty"*.
- [10] USA MIL-STD-1399(NAVY), *"Interface standard for Shipboard systems – Section 300A – Electric Power, Alternating Current"*.
- [11] JS Carlton, Lloyd's Register, London, "Podded propulsors: some results of recent research and full scale experience".
- [12] J Prousalidis, "A ready solution? ", MER 2006
- [13] ABB Pod Brochures
- [14] Principles of Naval Architecture , SNAME 1988
- [15] Gerasimos Politis, "Ship Propulsion", 2006
- [16] John Prousalidis "All Electric Ship-The State of the Art",2009

